



UNIVERSITÀ DEGLI STUDI DI CAMERINO

School of Advanced Studies

DOCTORAL COURSE IN

Chemical Science

XXXIV^o cycle

**STRUCTURAL IMPLEMENTATION OF UNSATURATED
SYSTEMS DRIVEN BY ELECTROPHILIC
NITROGEN-CONTAINING FUNCTIONAL GROUPS**

PhD Student

Dr. Lixia Yuan

Supervisors

Prof. Alessandro Palmieri

Prof. Xianxi Zhang

Co-supervisors

Prof. Marino Petrini

Prof. Yanlan Wang

CONTENTS

ACKNOWLEDGEMENTS	i
ABSTRACT	ii
ABBREVIATIONS	vi
LIST OF PUBLICATIONS	viii
PREFACE	ix
CHAPTER ONE Efficient Synthesis of Conjugated Nitrotrienes and Benzothiaziones	1
1.1 Synthesis and applications of β-nitroenones	2
1.1.1 Synthesis of β -nitroenones	2
1.1.2 Synthetic applications of β -nitroenones	4
1.2 Synthesis of β-nitroacrylates and their applications	8
1.2.1 Synthetic routes for β -nitroacrylates	9
1.2.2 Synthetic applications of β -nitroacrylates	10
1.3 Conjugated nitroalkenes	18
1.3.1 Synthesis of nitroalkenes.....	18
1.3.2 Synthetic routes for nitrodienes and their applications	20
1.4 Preparation and synthetic investigations of a new class of conjugated nitrotrienes	25
1.4.1 State of the art	25
1.4.2 Results and discussion.....	27
1.4.3 Conclusion	32
1.4.4 Experimental section.....	32
1.5 Mild and economical one-pot synthesis of benzothiaziones from β-nitroacrylates	38
1.5.1 State of the art	38
1.5.2 Results and discussion.....	39
1.5.3 Conclusion	42
1.5.4 Experimental section.....	42
CHAPTER TWO Synthesis of Unsymmetrical Bisindolymethanes and Their Anti-cancer Activity Test	44
2.1 Synthesis of 3-(1-arylsulfonylalkyl) indoles and their applications	45
2.1.1 Synthetic routes for sulfonyl indoles.....	45
2.1.2 Applications of sulfonyl indoles.....	47
2.2 Synthetic routes to bisindolymethanes	55
2.2.1 Synthesis of symmetrical bisindolymethanes	55
2.2.2 Synthesis of unsymmetrical bisindolymethanes	59
2.3 The combination of organic synthesis and biological testing	63
2.3.1 Necessity of combining organic synthesis and biological testing	63
2.3.2 Commonly used biological testing methods	64
2.4 Synthesis of unsymmetrical bisindolymethanes by reaction of indolymagnesium bromides with sulfonyl indoles and their anti-cancer activity test	68
2.4.1 State of the art	68
2.4.2 Results and discussion.....	69
2.4.3 Conclusion	74
2.4.4 Experimental section.....	74
CHAPTER THREE Effect of the Binding of Piceatannol and Oxyresveratrol to Soybean Protein Isolate on the Structural and Functional Properties	83
3.1 Synthesis of stilbene representatives and their functions	84
3.1.1 Synthesis of resveratrol	84

3.1.2 Synthesis of piceatannol and oxyresveratrol	86
3.2 Effect of the binding of piceatannol and oxyresveratrol to soybean protein isolate on the structural and functional properties.....	91
3.2.1 State of the art	91
3.2.2 Results and discussion.....	92
3.2.3 Conclusion	102
3.2.4 Experimental section.....	103
CHAPTER FOUR References and ¹H NMR & ¹³C NMR Spectra	109
4.1 References	110
4.2 ¹H NMR & ¹³C NMR Spectra.....	120

ACKNOWLEDGEMENTS

I would like to show my gratitude to the people who gave me a lot of help and support during the writing process of my dissertation.

First of all, I would like to express my sincere gratitude to my supervisors, Professors Alessandro Palmieri and Marino Petrini. During my doctoral studies, they patiently gave me many valuable opinions and suggestions and also encouraged me a lot. This dissertation would not have been possible without their diligent teaching and insightful advice.

Second, I am very grateful to my supervisors in China, Professors Xianxi Zhang and Yanlan Wang. They have always pointed the direction of my research and contributed a lot to my work and life at Liaocheng University. Here I also owe thanks to my advisor Prof. Min Liu, who has always taken into account my work in China and my life in Italy. The benefits I receive from them will have a lasting impact on my future research.

In addition to my supervisors, I have benefited from many other lab friends. Dr. Lupidi, Dr. Elena, Elenora, Benedetta, Jenny, Dario, and Martina have helped me a lot and taken away the loneliness of coming to Italy alone to study. Some Chinese friends, Chuanpan, Fenghe, Jing Tao, Yue Sun, made me happy and comfortable.

Here, my special thanks go to the cooperation between the University of Camerino and Liaocheng University. They have given me the opportunity to study abroad, to discover the fun of the world and to enjoy life.

Last but not least, there are no words that can express the feelings towards my parents and husband who helped me and shared my problems, frustrations and joys.

ABSTRACT

The present thesis can be divided into four chapters. The first chapter reports an efficient synthesis of conjugated nitrotrienes and benzothiaziones. The second chapter describes a new simple synthesis of unsymmetrical bisindoylmethanes and their anti-cancer activity test. The third chapter reports the biological tests between soy protein isolate and stilbene representatives. The fourth chapter lists the references and ^1H NMR & ^{13}C NMR spectra.

CHAPTER ONE: Efficient Synthesis of Conjugated Nitrotrienes and Benzothiaziones

Nitro-containing compounds are excellent scaffolds for synthesizing small molecules and heterocyclic systems that can be used in pharmaceuticals, agrochemicals, and materials science. β -Nitroenones (**1**, Figure 1) and β -nitroacrylates (**2**, Figure 1) can be considered as good starting materials for various targets.

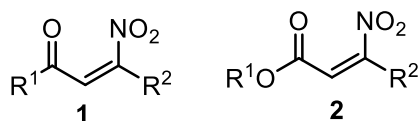
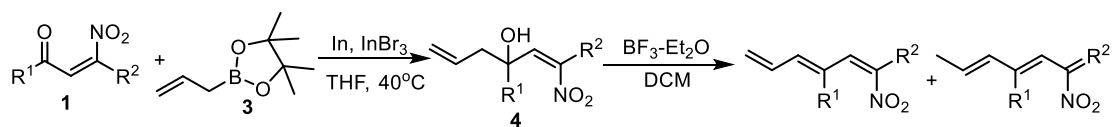


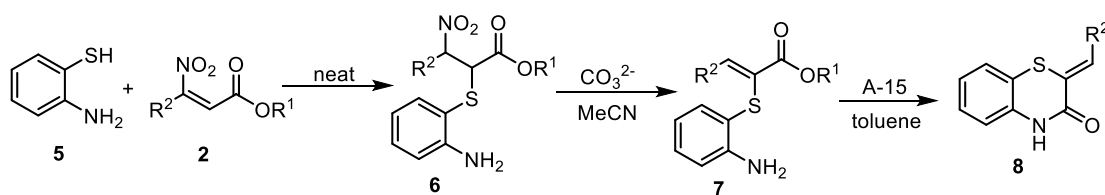
Figure 1. Structures of β -nitroenones and β -nitroacrylates.

This chapter reports a brief overview of the chemistry of nitro-containing compounds and the efficient synthesis of conjugated nitrotrienes and benzothiaziones. For the synthesis of conjugated nitrotrienes, β -nitroenones **1** can be allylated with allylboronic pinacol ester **3** to give tertiary homoallylic alcohols **4**. Subsequently, **4** can eliminate water to generate the corresponding conjugated nitrotrienes in the presence of the Lewis acid boron trifluoride etherate (Scheme 1). The successful application of this route with a wide range of substituents and the excellent yield obtained demonstrate its versatility. The nitrotrienes are obtained as a mixture of two isomers. However, this procedure can prevent the elimination of the nitro group which is retained in the triene molecule.



Scheme 1. Synthesis of conjugated nitrotrienes from β -nitroenones.

The critical situation caused by the increasing number of tuberculosis and the synergetic effect between tuberculosis and human immunodeficiency virus or multidrug-resistance makes the discovery of a drug with the structure of benzothiazinone an emergency. Considering the drawbacks of previous studies, such as long reaction times, limited substituents or pretreatment before reaction, a sustainable, convenient one-pot synthesis of benzothiazinones was proposed. The synthesis can be carried out in three steps: (i) Michael addition of β -nitroacrylates **2** and aminothiophenols **5** to form adducts **6** under neat condition; (ii) elimination of nitrous acid to afford **7**; (iii) intramolecular cyclization to obtain benzothiazinones **8** (Scheme 2). Since solid promoters (carbonate on polymer and Amberlyst-15) were used in the last two steps, the whole three steps can be combined in one-pot procedure by simple filtration and final flash column chromatography. This synthetic method can produce a series of benzothiazinones with good overall yields, in addition, products with different substituents can be prepared.



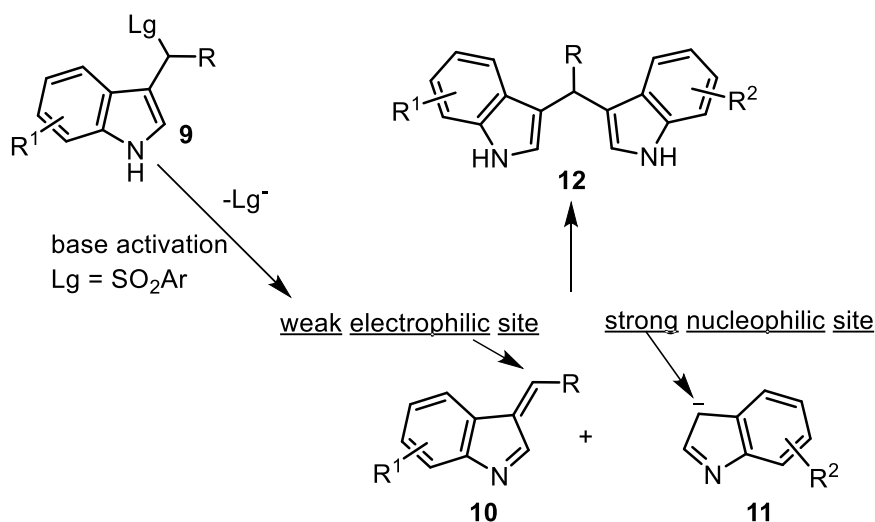
Scheme 2. One-pot synthesis of benzothiazinones.

CHAPTER TWO: Synthesis of Unsymmetrical Bisindolylmethanes and Their Anti-cancer Activity Test

Bisindolylmethanes, widely distributed in various vegetables, have the ability to regulate plant growth and prevent cancer. Several studies on the synthesis of symmetrical bisindolylmethanes are currently available. However, the development of synthetic protocols for unsymmetrical bisindolylmethanes is limited by the use of harmful Lewis acid or Brønsted acid catalysts and plagued by the formation of by-products or low yield of targets. In this chapter, a new, mild procedure was proposed to obtain unsymmetrical bisindolylmethanes from sulfonyl indoles.

Sulfonyl indoles ($\text{Lg} = \text{SO}_2\text{Ar}$) **9** can afford a weakly electrophilic alkylideneindolenine **10** upon basic promoted elimination of arylsulfonic acids. Reaction of intermediate **10** with a rather strong, stabilized nucleophilic indole **11**,

obtained by metalation of indoles with Grignard reagents, can generate the unsymmetrical bisindolymethanes **12** by a Michael-type process (Scheme 3). The target products with different substituents can be prepared in moderate to excellent yields, and the reaction of pyrrolylmagnesium bromides with sulfonyl indoles under un-optimized conditions showed the wide boundaries of this route.



Scheme 3. Synthetic route to unsymmetrical bisindolymethanes.

In addition, the anti-cancer activity of five selected compounds was tested and compared with cisplatin. The results indicate that unsymmetrical bisindolymethanes have anti-cancer activity and can be considered as good anti-cancer reagents.

CHAPTER THREE: Effect of the Binding of Piceatannol and Oxyresveratrol to Soybean Protein Isolate on the Structural and Functional Properties

Piceatannol (PIC, **13**, Figure 2), oxyresveratrol (OXY, **14**, Figure 2), and soy protein isolate (SPI) are essential nutritional molecules for a human's daily life. In this chapter, the interaction between PIC/OXY and SPI was investigated using multiple spectroscopic techniques and molecular docking simulations. Steady-state fluorescence, Förster resonance energy transfer and time-resolved fluorescence spectroscopy confirmed the static quenching mechanism. In addition, the binding affinity of PIC to SPI was stronger than that of OXY, and the interactions were spontaneous and exothermic. The surface hydrophobicity, sulfhydryl group content, particle size, zeta potential, and α -helical contents can determine the subtle change in

the secondary structure of SPI after binding. The emulsifying and foaming properties of SPI were improved after complexing with PIC or OXY. The molecular docking results and thermodynamic parameters showed that PIC and OXY were bound to SPI at the same sites, van der Waals forces and hydrogen bonds were the main interaction forces. The results also showed that the encapsulation of SPI can enhance the antioxidant activity of PIC and OXY. The *in vitro* gastrointestinal digestion of PIC and OXY in the presence of SPI helps patients with stomach problems.

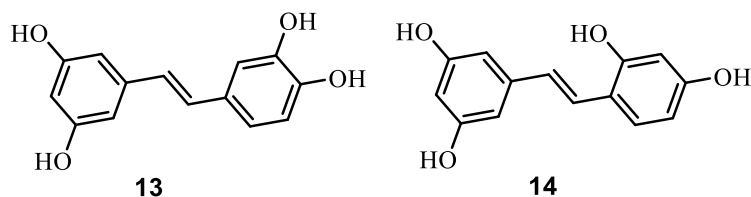


Figure 2. Structures of piceatannol and oxyresveratrol.

CHAPTER FOUR: References and ^1H NMR & ^{13}C NMR Spectra

This chapter displays the references and ^1H NMR & ^{13}C NMR Spectra.

ABBREVIATIONS

PCC	pyridinium chlorochromate
<i>m</i> CPBA	<i>m</i> -chloroperoxybenzoic acid
EWGs	electron-withdrawing groups
DBU	1,8-diazabicyclo[5.4.0]undec-7-ene
DCM	dichloromethane
TBAF	tetrabutylammonium fluoride
MeOH	methanol
2-MeTHF	2-methyl tetrahydrofuran
A-21	Amberlyst 21
MsCl	methanesulfonyl chloride
SolFC	solvent-free conditions
A-15	Amberlyst 15
EtOAc	ethyl acetate
THF	tetrahydrofuran
DME	1,2-dimethoxyethane
BEMP	2- <i>tert</i> -Butylimino-2-diethylamino-1,3-dimethylperhydro-1,3,2-diazaphosphorine
DMAP	4-dimethylaminopyridine
MS	molecular sieves
TEMPO	2,2,6,6-tetramethylpiperidine-1-oxyl
DMF	<i>N,N</i> -dimethylformamide
MeCN	acetonitrile
TB	tuberculosis
HIV	human immunodeficiency virus
DHP	3,4-dihydro-2 <i>H</i> -pyran
[bupy]BF ₄	1-butylpyridinium tetrafluoroborate
DCE	dichloroethane
CAN	ceric ammonium nitrate
PDE-5	phosphodiesterase 5
DLS	dynamic light scattering
CD	circular dichroism

TRF	time resolved fluorescence
DAPG	2,4-diacetylphloroglucinol
MTT	3-(4,5-dimethylthiazol-2-yl)-2,5-diphenyl tetrazolium bromide
IC ₅₀	half maximal inhibitory concentration
PIC	piceatannol
OXY	oxyresveratrol
SPI	soy protein isolate
FRET	Förster resonance energy transfer
RSFQ	ratio of synchronous fluorescence quenching
<i>H</i> ₀	surface hydrophobicity
SH	sulfhydryl group contents
FE	foam expansion
FS	foam stability
EAI	emulsifying activity index
ESI	emulsifying stability index
ESC	experimental scavenging capacity
TSC	theoretical scavenging capacity
SE	synergistic effect

LIST OF PUBLICATIONS

- [1] L.X. Yuan, A. Palmieri, M. Petrini, Synthesis of unsymmetrical bisindolylmethanes by reaction of indolylmagnesium bromides with sulfonyl indoles, *Advanced Synthesis & Catalysis* 362 (2020) 1509-1513.
- [2] L.X. Yuan, H. Liu, M. Liu, Y.F. Ren, Y.H. Zhu, Effect of the binding of piceatannol and oxyresveratrol to soybean protein isolate on the structural and functional properties, *Journal of Food Science* submit.

PREFACE

Nitrogen-containing compounds including amines, nitriles, nitrogen-containing heterocycles, and compounds with nitro group are diffusely found in natural products and pharmaceutical molecules, such as penicillin, vitamin B₂, cephalosporin, and so on. More than 90% of the drug molecules approved by the U.S. FDA contain nitrogen atoms.^[1] Owing to their pharmaceutical value, nitrogen-containing compounds have attracted extensive attention in recent years in the development and pharmacological studies. Moreover, they can be used as agrochemicals, dyes, fluorescent materials, and more.

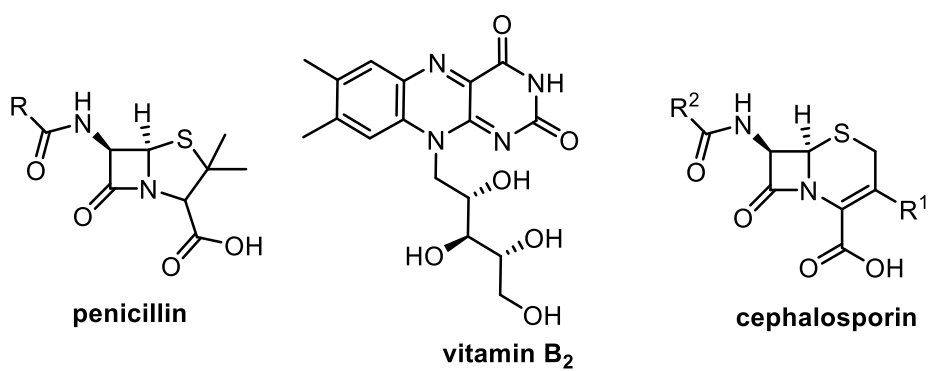


Figure 3. Structures of penicillin, vitamin B₂ and cephalosporin. R is variable group.

Unsaturated systems are an important part in organic synthesis, bioorganic chemistry, and materials science. The possession of π electrons make them can be attacked by electrophiles, or activated by transition metals. The activated unsaturated systems can be easily attacked by different kinds of nucleophiles.^[2]

The unsaturated systems driven by electrophilic nitrogen-containing functional groups can combine the advantages of nitrogen-containing compounds and unsaturated systems. The most successful case is nitrogen-containing heterocycles, such as indole, pyrrole, carbazole, benzimidazole, benzothiazoles, oxadiazole, imidazole, isoxazole, etc. Taking pyrrole as an example, the presence of nitrogen causes its reactivity is similar to that of benzene, which can easily alkylated and acylated with electrophiles. In addition, pyrrole can be involved in reduction, cyclization, and deprotonation processes. Most importantly, compounds with a pyrrole skeleton often show pharmaceutical activity, such as atorvastatin, ketorolac, and sunitinib.^[3]

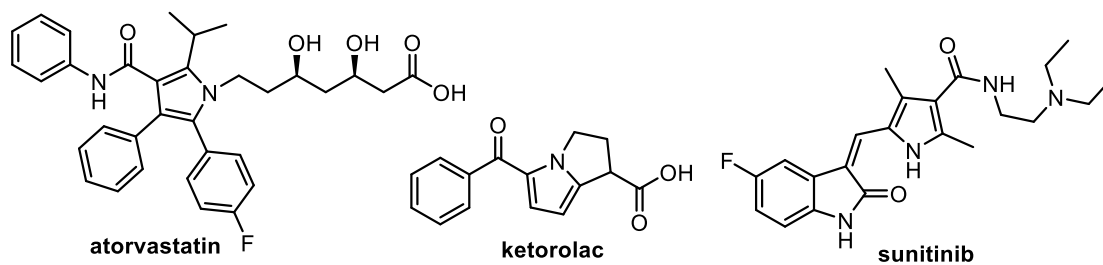


Figure 4. Structures of atorvastatin, ketorolac, and sunitinib.

Over the past few decades, great efforts have been made in nitrogen-containing unsaturated systems and many interesting results have been obtained. This thesis describes the efficient synthesis of conjugated nitrotrienes, benzothiaziones, and unsymmetrical bisindoylmethanes using nitrogen-containing unsaturated systems β -nitroenones, β -nitroacrylates, and alkylideneindolenine. In addition, biological studies were also conducted involving unsymmetrical bisindoylmethanes and the interaction between stilbene representatives and soy protein isolate.

Note: The numbers of compounds, schemes, and figures preceding the main body are not the same as those in the thesis.

CHAPTER ONE

Efficient Synthesis of Conjugated Nitrotrienes and Benzothiaziones

Based on the high electron-withdrawing ability of nitro groups and their synthetic versatility, nitro-containing compounds can be employed as nucleophiles (nitroalkanes) or electrophiles (nitroalkenes) to generate new carbon-carbon and carbon-heteroatom bonds.^[4] They can also be used as precursors for highly functionalized materials with biological activity. β -Nitroenones (**1**, Figure 1) and β -nitroacrylates (**2**, Figure 1) deserve special attention for their application in the synthesis of heterocyclic systems and biologically active targets.

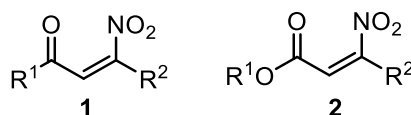


Figure 1. Structures of β -nitroenones **1** and β -nitroacrylates **2**.

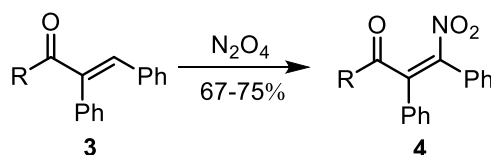
1.1 Synthesis and applications of β -nitroenones

β -Nitroenones, a class of enones with the nitro group at β position, are used as precursors for the preparation of small molecules and heterocyclic systems. They can be synthesized in the following ways: (i) nitration of α , β -unsaturated ketones; (ii) oxidation of oximes; (iii) oxidation of allyl alcohols; (iv) dehydration of β -nitroalcohols.

1.1.1 Synthesis of β -nitroenones

1.1.1.1 Nitration of α , β -unsaturated ketones

The first synthesis of β -nitroenones was performed by Bellec et al. in 1979.^[5] In this approach, aromatic β -nitroenones **4** can be prepared with moderate yields by reacting α -acyl stilbenes **3** with the nitrating agent nitrogen tetroxide (Scheme 1).

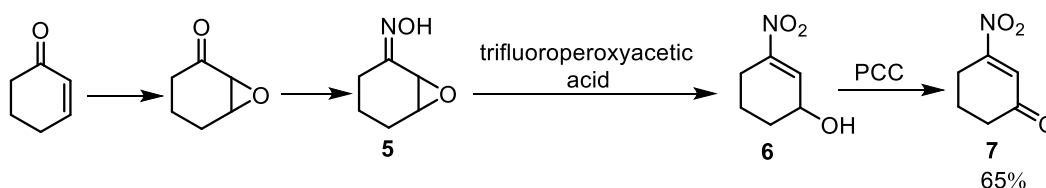


Scheme 1. Synthesis of aromatic β -nitroenones from nitrogen tetroxide.

1.1.1.2 Oxidation of oximes

Corey and Estreicher^[6] synthesized 3-nitro-2-cyclohexenone **7** in 65% overall yield by utilizing 2-cyclohexenone. The actual reaction was performed by the oxidation of epoxyoxime **5** with trifluoroperoxyacetic acid to afford nitroalcohol **6**,

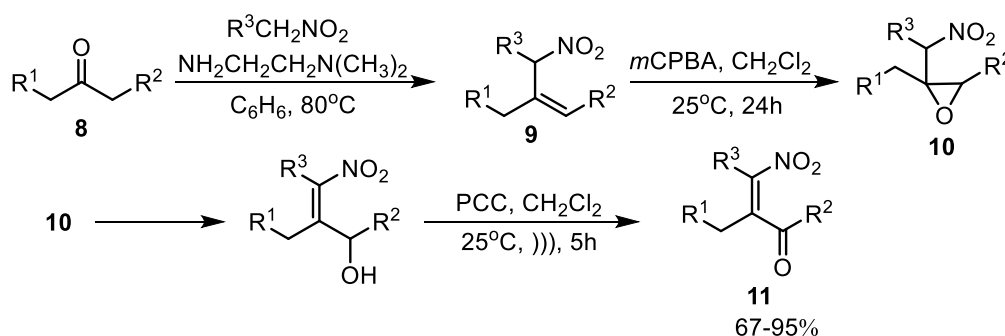
followed by oxidation either with pyridinium chlorochromate (PCC) or chromic acid-sulfuric acid (Scheme 2).



Scheme 2. Synthetic route for 3-nitro-2-cyclohexenone.

1.1.1.3 Oxidation of allyl alcohols

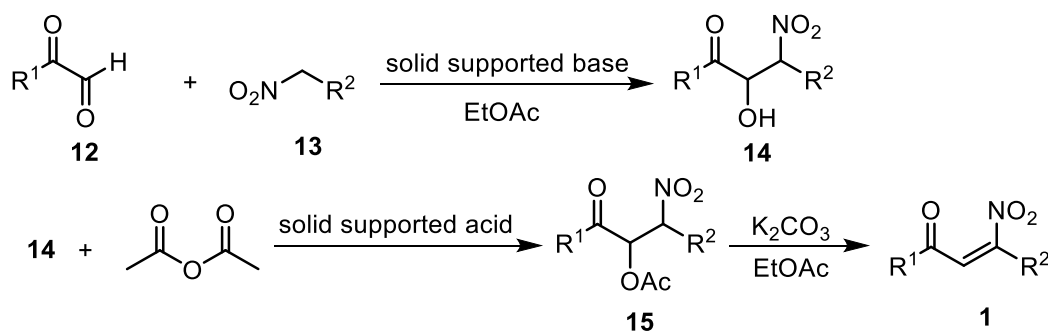
Loubinoux et al.^[7] proposed a new route with good yields for the synthesis of β -nitroenones. Allylnitroolefin **9**, synthesized from ketone **8**, can react with *m*-chloroperoxybenzoic acid (*m*CPBA) to form nitroepoxide **10**. The nitroepoxide **10** can be converted to β -nitroenones **11** by a ring-opening reaction and subsequent oxidation by PCC (Scheme 3).



Scheme 3. Synthesis of β -nitroenones from aliphatic ketones.

1.1.1.4 Dehydration of β -nitro alcohols

In our laboratory, a convenient and sustainable approach was devised to synthesize β -nitroenones **1** following this strategy: (i) base-catalyzed Henry reaction between arylglyoxal **12** and nitroalkane **13**, (ii) acetylation of β -nitro- α -hydroxyketone **14**, (iii) elimination of acetic acid from **15** (Scheme 4).



Scheme 4. Synthesis of β -nitroenones from β -nitro alcohols.

The previous methods always have drawbacks like the use of hazardous solvents or dangerous reagents, and the limited scope of β -nitroenones. Therefore, we would like to continue the use of this route, which is a more efficient and sustainable protocol for the synthesis of a variety of β -nitroenones.

1.1.2 Synthetic applications of β -nitroenones

β -Nitroenones play an important role in the synthesis of several small molecules and heterocyclic systems, such as 1,4-diketones, β -nitroketones, polyfunctionalized furans, pyrrole and indole derivatives, β -nitro- β,γ -unsaturated ketones and in the α -alkenylation reaction of β -ketoesters.

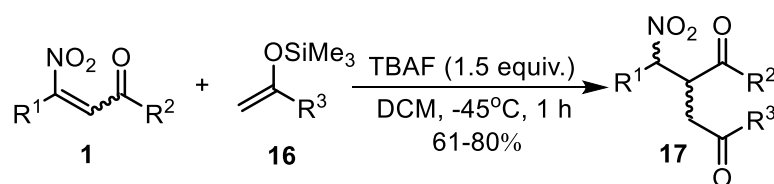
1.1.2.1 Synthesis of polyfunctionalized diketones

Functionalized 1,4-dicarbonyl frameworks are of practical interest owing to their importance in the synthesis of heterocycles and biologically active molecules.^[8]

Ballini and Rinaldi^[9] proposed a route based on the chemical reactivity of nitroalkanes with electron-poor alkenes bearing two electron-withdrawing groups (EWGs) in α - and β -position (mainly ketones and esters). The reaction was promoted by 1,8-diazabicyclo[5.4.0]undec-7-ene (DBU), and Michael adducts can be obtained via spontaneous elimination of nitrous acid in a one-pot synthesis.

However, some important limitations reduce its synthetic potential, such as the impossibility to preserve the nitro group in the final product, and the formation of regioisomers for unsymmetrical electron-poor alkenes.

To overcome these limitations and find a new efficient way to synthesize **17**, the reaction between silyl enol ethers **16** and β -nitroenones **1** was carried out (Scheme 5).^[10] After the process optimization, the best conversion was achieved operating at -45°C in dichloromethane (DCM) as solvent, with a slight excess of silyl enol ethers (1.3 equiv.) and tetrabutylammonium fluoride (TBAF, 1.5 equiv.) as silyl enol ethers activator.



Scheme 5. Synthesis of polyfunctionalized diketones from β -nitroenones.

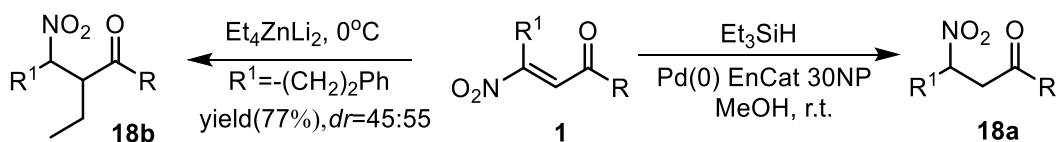
1.1.2.2 Synthesis of β -nitro ketones

Despite the wide application of β -nitro ketones, only a few synthetic routes for their preparation have been reported. Meanwhile, they still have some limitations like the elimination of nitrous acid from the title compounds in the purification step (chromatography), the use of dangerous solvents and harmful reactants.^[11]

To overcome these limitations and find a better way to synthesize β -nitro ketones, β -nitroenones **1** can be used as a source. Moreover, the routes can be divided into two kinds (C=C chemoselective reduction and nucleophilic addition) depending on the reaction type.

In the C=C chemoselective reduction process for **18a**, solid heterogeneous palladium catalyst and triethylsilane are employed (Scheme 6).^[12] The route has advantages like: (1) use of green solvent (MeOH or MeOH/2-MeTHF); (2) room temperature; (3) easy filtration of the solid-supported catalyst; (4) recycle of the catalyst.

For nucleophilic addition of tetraorganozincate to β -nitroenones, β -nitro ketones **18b** can be obtained in good yield and moderate chemoselectivity. Solvent-free and mild conditions make the process satisfactory.^[13] However, drawbacks like spontaneous hydrolysis of the nitro group (Nef reaction) may take place during the work-up procedure limiting the viability of this method.

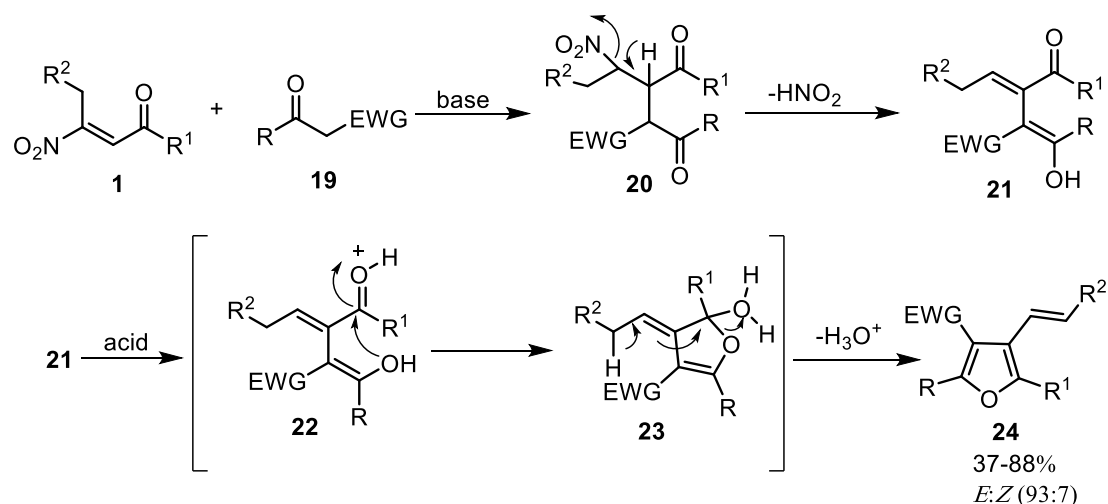


Scheme 6. Synthesis of β -nitro ketones.

1.1.2.3 Synthesis of polyfunctionalized furans starting from β -nitroenones and active methylene compounds

Furan ring is a useful component of many biologically active targets. It is the core of some natural compounds and important polymers, and several furan-containing scaffolds are privileged structures in medicinal chemistry.^[14] β -Nitroenones **1** and α -functionalized ketones **19** can be used to synthesize 3-alkylidene furans **24** in good overall yields and excellent diastereoselectivity (Scheme 7).^[15] The protocol consists of two steps: (i) base-promoted addition of **19** to

1 to give the adduct **20**, which eliminates a molecule of nitrous acid to provide the intermediate **21**; and (ii) acid-catalyzed cyclization of **21** (via the adducts **22** and **23**) leading to the title targets **24**.



Scheme 7. Two-step synthesis of tetrasubstituted furans.

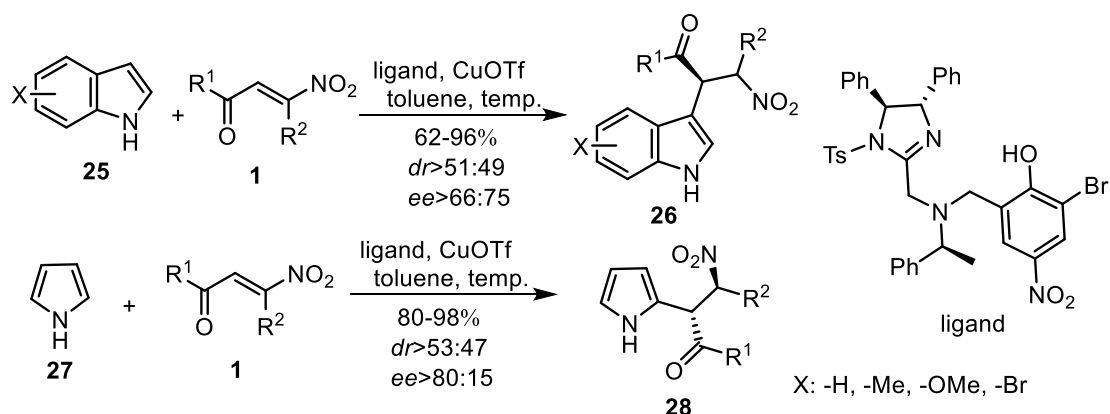
Due to the mild reaction conditions, a variety of functional groups, such as ketones, esters, nitriles, and sulfones, can be installed on the furan ring. Moreover, the use of solid support in these two steps can avoid the use of the typical wasteful aqueous work-up, reduce the operation to a simple filtration, with evident advantages from the sustainability viewpoint.

1.1.2.4 Catalytic asymmetric Friedel-Crafts/protonation of nitroalkenes and *N*-heteroaromatics

α -Substituted β -indolylalkylamine is a common structure observed in drugs acting as receptor agonists. The corresponding biological activity strongly depends on stereochemistry, therefore, much effort has been devoted to the stereoselective synthesis of α -substituted β -indolylalkylamines.^[16] The straightforward approach for the synthesis of chiral α -substituted tryptamines would be the Friedel-Crafts reaction of indoles and nitroalkenes. However, the catalytic asymmetric Friedel-Crafts reaction of indoles and α -substituted nitroalkenes is poorly developed.^[17]

To explore new asymmetric catalysts and their application in the synthesis of nitrogen-containing chiral molecules, Arai et al.^[18] successfully developed chiral imidazoline-aminophenol-Cu complex for the catalytic asymmetric Friedel-Crafts reaction of nitroalkenes with indoles and pyrroles (Scheme 8).

Under the optimized conditions, β -nitroenones **1** were also effective in the diastereoselective Friedel-Crafts/protonation and maintained a high enantiomeric excess. Various substituted indoles **25** were able to be used to give products **26** with good diastereoselectivity, and high enantioselectivity was recorded for the major products. In addition, Friedel-Crafts/protonation using pyrrole **27** was smoothly catalyzed under similar reaction conditions and afforded adducts **28** in a highly enantioselective manner.



Scheme 8. Catalytic asymmetric Friedel-Crafts reaction of β -nitroenones with indoles and pyrroles.

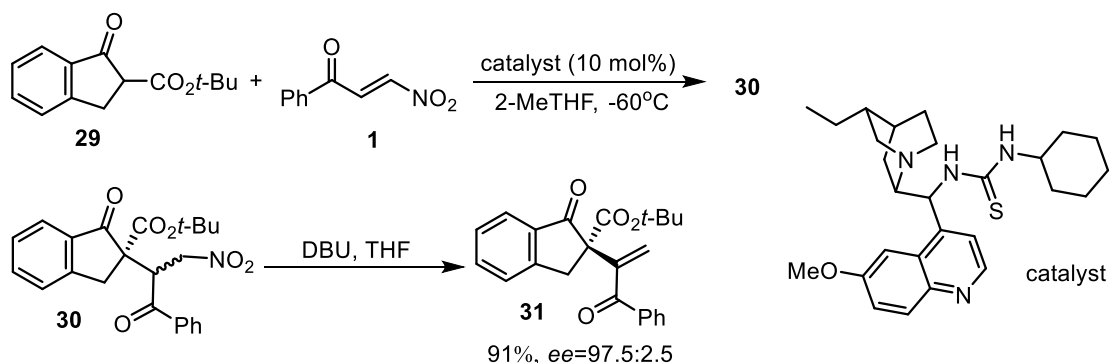
1.1.2.5 Catalytic enantioselective alkenylation of β -ketoesters

All-carbon quaternary stereocenters with alkenyl substituents are structural motifs found in various natural products and bioactive molecules.^[19] However, the enantioselective construction of this kind of compounds presents an additional level of difficulty due to the lack of available synthetic methods for the installation of alkenyl groups at sterically hindered positions.

The nitro functional group can be used as a powerful directing and leaving group. Mukherjee et al.^[20] reasoned that β -nitroenone **1** would reverse its naturally nucleophilic α -position to an electrophilic center. The formation of the desired C–C bond between **1** and β -ketoester **29** would be electronically feasible. In fact, due to the hydrogen bonding acceptor ability of the nitro group, the conjugate addition can be catalyzed regioselectively using a suitable H-bond donor.

This reaction proceeds via a one-pot two-step sequence, involving catalytic regio-, diastereo- and enantioselective conjugate addition of **29** to β -nitroenones **1**, followed by a base mediated nitrous acid elimination of **30** (Scheme 9). This process provides synthetically versatile product **31** bearing an all-carbon quaternary

stereocenter including an alkenyl substituent with a terminal double bond in high yield and excellent enantioselectivity.

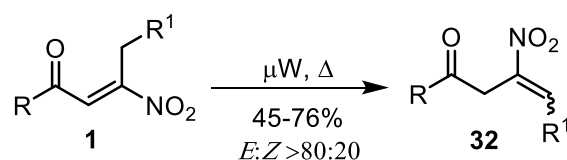


Scheme 9. Addition of indanone β -ketoester to β -nitroenone.

1.1.2.6 Diastereoselective isomerization of (*E*)- β -nitroenones into β -nitro- β,γ -unsaturated ketones

Our laboratory proposed a new general and practical method for converting β -nitroenones **1** into β -nitro- β,γ -unsaturated ketones **32** under microwave conditions (Scheme 10).^[21] In particular, the method enables the preparation of the title compounds in very good overall yields with excellent diastereoselectivity. Moreover, the adopted reaction conditions simplify the work-up operations to an easy solvent evaporation, thereby minimizing waste generation and energy consumption, with apparent benefits from a sustainable viewpoint.

Simultaneously, Protti et al.^[22] pointed out the unique and unprecedented photoreactivity of **1**, making it possible to obtain **32** upon visible light exposition under mild conditions. The route should be helpful to elucidate the multifaceted reactivity of such substrates characterized by an emerging synthetic potential.



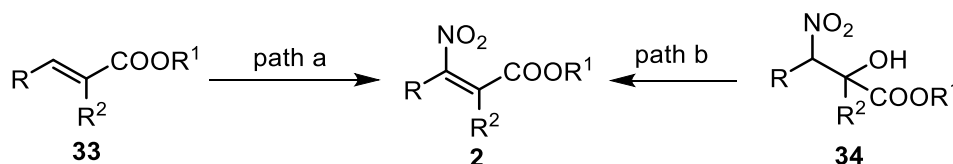
Scheme 10. Isomerization of *E*-derivatives of β -nitroenones.

1.2 Synthesis of β -nitroacrylates and their applications

β -Nitroacrylates are an emerging class of conjugated nitroalkenes with two EWGs at α - and β -positions, making these molecules versatile key building blocks for the synthesis of various highly functionalized materials.^[23]

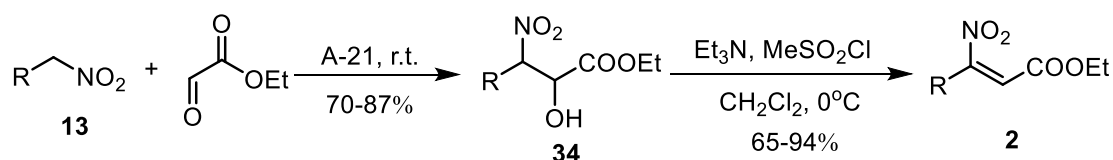
1.2.1 Synthetic routes for β -nitroacrylates

The synthetic approaches to β -nitroacrylates **2** involve either the direct nitration of acrylates **33** (path a, Scheme 11), or the dehydration of nitroalcohols **34** (path b, Scheme 11).^[24] Due to the harsh reaction conditions needed, poor yields and low selectivity, path a is of little practical use.



Scheme 11. The main synthetic approaches for preparing β -nitroacrylates.

Ballini et al.^[25] reported a synthetic protocol featured by few steps, good yields, and with the possibility to retain several other functionalities (Scheme 12). The first step in the sequence is a nitroaldol (Henry) reaction between nitroalkane **13** and ethyl glyoxalate, carried out under heterogeneous catalysis, using Amberlyst 21 (A-21) as solid base. The resulting β -nitro alcohols **34** (yields: 70-87%) were dehydrated to (*E*)- β -nitroacrylates **2** by mesylation of the hydroxy group, followed by basic elimination of methanesulfonic acid. The dehydration reaction is very fast (about 1.5h) and the yields are good (65–94%).

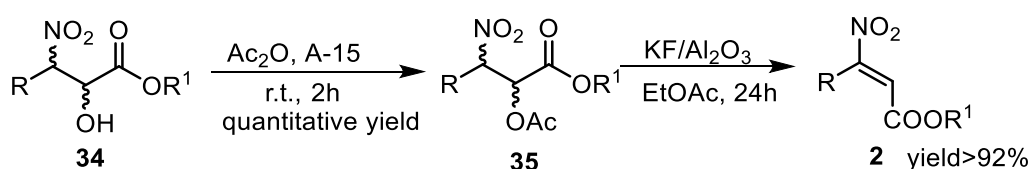


Scheme 12. Synthesis of β -nitroacrylates from nitroalkane and ethyl glyoxalate.

However, the conversion of **34** into **2** requires: (i) the highly toxic and corrosive reagent methanesulfonyl chloride (MsCl, 1–4 equiv.); (ii) a large excess of trialkylamine (usually Et₃N, 4 equiv.); (iii) dry DCM as the solvent; (iv) an inert atmosphere; (v) careful control of the temperature (approximately -10 to -20 °C, due to the exothermic reaction); (vi) complicated aqueous work-up (HCl, DCM, brine, Na₂SO₄). The harsh conditions and the large amount of waste produced do not fit with the requirements for a sustainable development.

To minimize the waste generation and energy consumption, a new, efficient and eco-friendly procedure for the conversion of β -nitro alcohols **34** into β -nitroacrylates

2 was developed in our laboratory.^[26] The method involves an acidic esterification of the hydroxyl group followed by a base-induced elimination of acetic acid. After a series of trials, **35** was isolated in quantitative yield under solvent-free conditions (SolFC) and a catalytic amounts of Amberlyst 15 (A-15) at room temperature using a slight excess of Ac₂O (Scheme 13). Since adduct **35** was found to be extremely pure, it can be used for further manipulation without any purification process. The best elimination conditions were obtained using 1 equivalent of KF–Al₂O₃ and ethyl acetate (EtOAc, as a green solvent) at room temperature. Following these results and with the aim of minimizing the waste generation and energy consumption, an overall protocol for the conversion of **34** to **2** was investigated. In the following studies, we continued to use this route for synthesizing functionalized β-nitroacrylates.



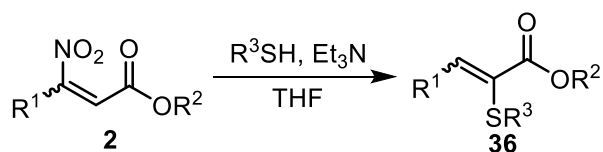
Scheme 13. Investigation of the overall protocol to convert β-nitro alcohols into β-nitroacrylates.

1.2.2 Synthetic applications of β-nitroacrylates

β-Nitroacrylates have been shown to be a highly versatile class of nitroalkenes, and due to the presence of both nitro and ester groups in their structure, they are prone to provide access to a large variety of polyfunctionalized molecules.

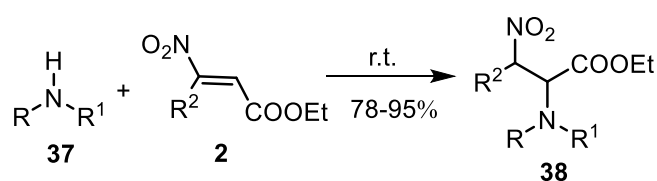
1.2.2.1 Anti-Michael addition of thiols and amines to β-nitroacrylates

α-Thioacrylates have been used as Michael acceptors and as dienophiles in Diels-Alder reactions. However, the synthetic processes usually require harsh conditions and always produce products with low selectivity. Lewandowska^[27] proposed an efficient route for α-thioacrylates **36** by treating β-nitroacrylates **2** with propanethiol in the presence of a catalytic amount of triethylamine in THF at ambient temperature (Scheme 14).



Scheme 14. α-Addition of thiolate nucleophiles to β-nitroacrylates.

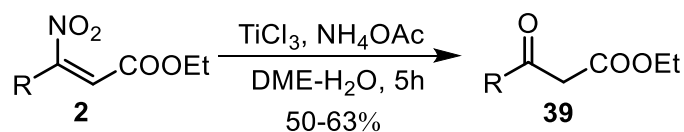
β -Nitro- α -amino esters are essential components for the synthesis of several important targets, such as (i) α,β -dehydro- α -amino acids, which are common components of naturally occurring peptides, and (ii) β -nitro- α -amino acids that have been studied as enzyme inhibitors and as precursors for the synthesis of various α -amino acids and diamino acids.^[28, 29] However, only a few methods have been reported for the synthesis of β -nitro- α -amino esters. Palmieri et al.^[30] found that the reaction of 1 equiv. of amines **37** with 1 equiv. of β -nitroacrylates **2**, proceeded under solvent-free and catalyst-free conditions via an anti-Michael reaction at room temperature to give β -nitro- α -amino esters **38** with good yields (Scheme 15).



Scheme 15. Anti-Michael addition of β -nitroacrylates and amines.

1.2.2.2 Efficient preparation of β - or α - keto esters

β -Keto esters are multi-coupling reagents with electrophilic carbonyl and nucleophilic carbons, which make them valuable tools for the synthesis of complex molecules.^[31] The treatment of a 1,2-dimethoxyethane (DME)/water solution of β -nitroacrylates **2** with titanium trichloride, in the presence of ammonium acetate, gives the direct conversion into β -keto esters **39** with satisfactory yield (Scheme 16).^[25] The method also tolerates various functionalities such as esters, carbonyls, ketals and heteroaromatic structures.

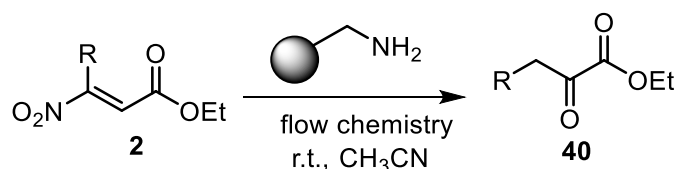


Scheme 16. Synthesis of β -keto esters.

α -Keto esters are essential natural products and important starting materials for various synthetic processes. Common methods for preparing α -keto esters include the modified Dakin-West reaction and the addition of a Grignard reagent to oxalates or oxalyl chlorides as well as with some alternative syntheses. These procedures are often hampered by harsh conditions, restricted selectivity and low yields.^[32]

Ley et al.^[33] presented a combination of commercially available mesofluidic

flow device and tubes filled with immobilized reagents and scavengers, a novel method for the synthesis of α -keto esters (Scheme 17). The entire reaction was carried out in the flow apparatus with β -nitroacrylates **2** as substrates, which are captured by benzylamine polymer, the released α -keto ester products **40** can be acquired through flowing 4 steps in-line column.

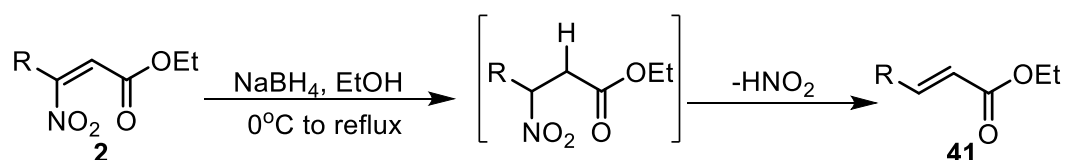


Scheme 17. General procedure for the flow synthesis of α -keto ester.

1.2.2.3 Michael addition synthesis of α,β -unsaturated esters

α,β -Unsaturated esters are useful chemical entities that can be obtained by condensation reactions involving aldehydes, i.e. (i) Knoevenagel condensation of active methylene esters with aldehydes; (ii) condensation of alkyl acetates with aldehydes followed by dehydration; (iii) Reformatsky reaction with aldehydes followed by elimination of the subsequent hydroxyl esters; (iv) Wadsworth-Emmons olefination of carbonyl compounds. The methods of synthesizing α,β -unsaturated esters have been reported for a long time, but there are disadvantages such as drastic conditions, poor yields and low selectivity.

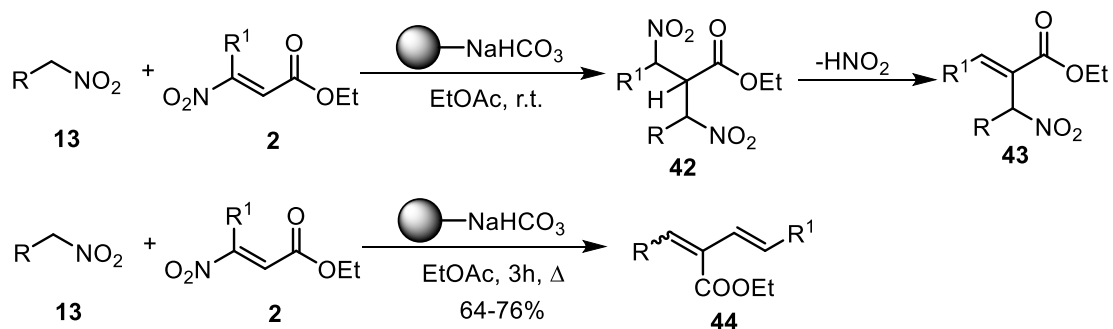
Ballini et al.^[25] reported that the conversion of β -nitroacrylates **2** to α,β -unsaturated esters **41** can be carried out directly via a NaBH_4 promoted tandem Michael addition-elimination process in EtOH. In fact, sodium borohydride first acts as a reducing agent, converting β -nitroacrylates **2** to nitroalkanes then, under reflux, causes nitrous acid elimination, working as a base towards an acidic hydrogen in α -position to the carbonyl. The conversion **2** to **41** can be formally considered as the substitution of α vinylic nitro group with hydrogen (Scheme 18).



Scheme 18. Synthetic routes for α,β -unsaturated esters.

Our laboratory investigated the Michael addition of nitroalkanes **13** to

β -nitroacrylates **2** for the production of a new class of nitro-functionalized α,β -unsaturated esters, promoted by carbonate on polymer (Scheme 19).^[34] This reaction allows the formation of nitro α,β -unsaturated ester **43** by elimination of nitrous acid from the adduct **42**. In addition, under refluxing EtOAc and in the presence of an excess (2.5 equiv.) of carbonate on polymer, the conjugate addition of **13** to **2** allows a double elimination of nitrous acid with the formation of the dienes **44** in satisfactory to good overall yields (64–76%).

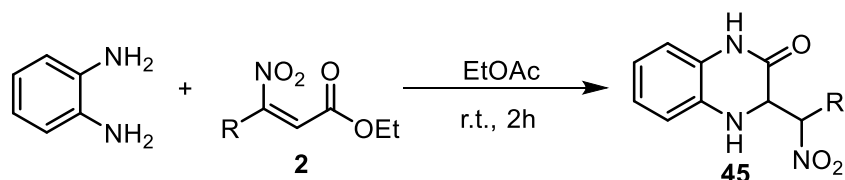


Scheme 19. Michael addition of nitroalkanes to β -nitroacrylates.

1.2.2.4 β -Nitroacrylates as strategic building blocks for the synthesis of nitrogen-containing heterocyclic compounds

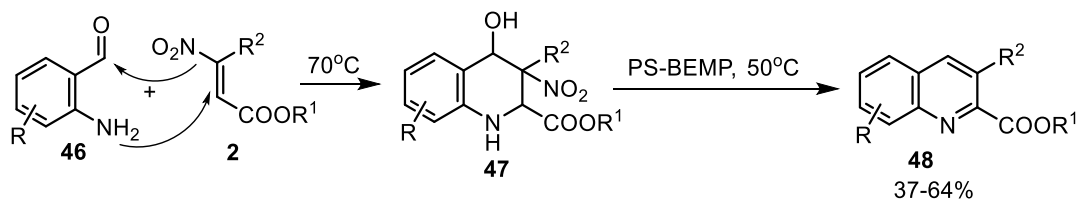
Pyrroles, indoles, quinolones and quinoxalinones derivatives are important *N*-heterocyclic compounds. They are used as important frameworks in organic synthesis and also in other important fields such as material science and medicinal chemistry. Therefore, the development of efficient, convenient and sustainable synthetic methods is crucial for practical purposes. Due to the simultaneous presence of two different EWGs at α - and β -positions on a double bond, β -nitroacrylates can play an important role in the synthesis of these heterocyclic systems.

Ballini et al.^[35] performed an uncatalysed one-pot synthesis of polyfunctionalized dihydroquinoxalinone derivatives via an anti-Michael reaction using β -nitroacrylates as key starting materials. Starting from *o*-phenylenediamine and **2**, the best yield of compounds **45** was obtained after two hours at room temperature by using 1.25 equiv. of *o*-phenylenediamine and EtOAc as solvent (Scheme 20).



Scheme 20. The preparation of dihydroquinoxalinones.

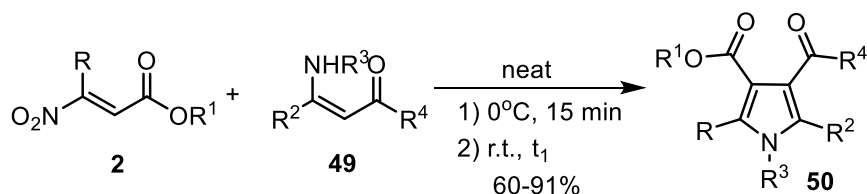
The quinolinic cores are mainly found in natural compounds and have been intensively studied as building blocks for the synthesis of highly functionalized materials.^[36] In particular, quinoline-2-carboxylates play an important role as precursor of bioactive molecules and as useful ligands in metal-catalyzed reactions.^[37, 38] Palmieri et al.^[39] developed a new general and valuable one-pot method for synthesizing quinoline-2-carboxylates by using 2-aminobenzaldehydes **46** and β -nitroacrylates **2**. The strategy involves four different reactions: (i) an aza-Michael addition between **46** and **2**; followed by (ii) an intramolecular Henry reaction to give benzopiperidines **47**; (iii) elimination of water; (iv) removal of nitrous acid to provide the aromatization of the piperidine core, then form the title targets **48** (Scheme 21). With this method, products with various substituents at 3-position as well as in the benzene ring can be prepared in good overall yield. Furthermore, the mildness of the conditions allowed the preservation of some functional groups like ester, cyano, chlorine, fluorine and carbon-carbon double bond. Additionally, the use of supported 2-*tert*-butylimino-2-diethylamino-1,3-dimethylperhydro-1,3,2-diazaphosphorine (BEMP) minimizes the use of materials, and avoids any complex aqueous work-up, with evident advantages from a sustainable point of view.



Scheme 21. Synthetic approach for synthesizing quinoline-2-carboxylate derivatives.

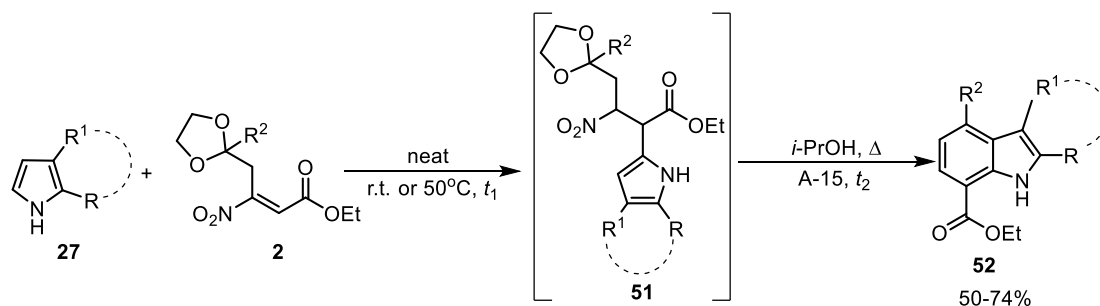
During pyrrole synthesis, the high catalyst loading leads to important disadvantages like high costs and potential pollution.^[40] Our laboratory found that the reaction of β -nitroacrylates **2** with β -enaminones **49** represents a highly improved, one-pot synthesis of pyrroles **50** (Scheme 22).^[41] Contrary to standard nitroalkenes, β -nitroacrylates work well without any solvent and promoter, just using

stoichiometric amount of the reactants **2** and **49**, in short reaction times and avoiding the need for high temperatures. In fact, this approach is general, provides good to excellent yields of the products and tolerates the presence of various functionalities. Furthermore, β -nitroacrylates can also be used to efficiently synthesize alkyl pyrrole-2-carboxylates^[42] and pyrrole-2-acetic acid^[43] under mild conditions.



Scheme 22. Eco-friendly preparation of polyfunctionalized pyrroles.

Indoles can be prepared either by benzannulation of pyrroles or assembling the indole core to benzene derivatives. However, these approaches often show important drawbacks, such as limited generality, modest scalability and the need for harsh conditions. Our laboratory presented a one-pot synthesis of polysubstituted indoles starting from pyrroles **27** and ketal-functionalized β -nitroacrylates **2** with innovative, mild and efficient features.^[44] As described in Scheme 23, the starting compounds **27** and **2** react rapidly to afford the intermediate **51** via a Friedel-Crafts reaction under solvent- and catalyst-free conditions. The formed adduct **51** gives indoles **52** in satisfactory overall yields (50–74%) under heterogeneous conditions (A-15) in refluxing 2-propanol as sustainable solvent.^[45] The reaction can be performed in a one-pot synthesis without the need of isolating the intermediate **51** generated in the first step.



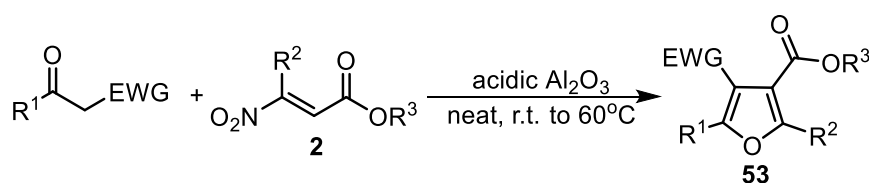
Scheme 23. General pathway to the synthesis of indole derivatives.

1.2.2.5 β -Nitroacrylates as precursors of oxygen-containing heterocyclic compounds

Highly substituted furans are found to be key structural elements for many biologically active natural products and important pharmaceuticals.^[46] They also

represent general building blocks for the synthesis of more complex heterocyclic compounds. Although some methods have proven to be very useful for the synthesis of furan derivatives, there are some limitations, including the difficulty in obtaining furans with sensitive functional groups, and limited flexibility in their substitution pattern.

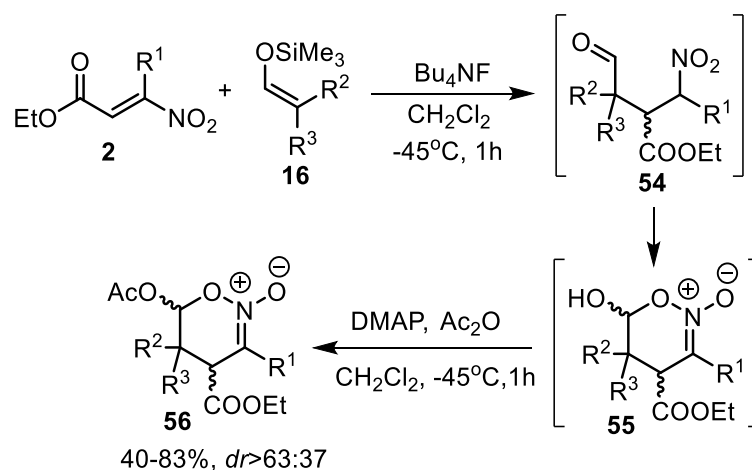
Palmieri et al.^[47] proposed acidic alumina as the most efficient solid acid to obtain tetrasubstituted furans **53** from α -functionalized carbonyl derivatives and β -nitroacrylates **2** (Scheme 24). The procedure works well without the need for any solvent and quenching or extraction, as the reaction mixture can be charged directly into a chromatography column for immediate purification. This method can be considered as simple, mild, and of general use.



Scheme 24. Synthesis of tetrasubstituted furans.

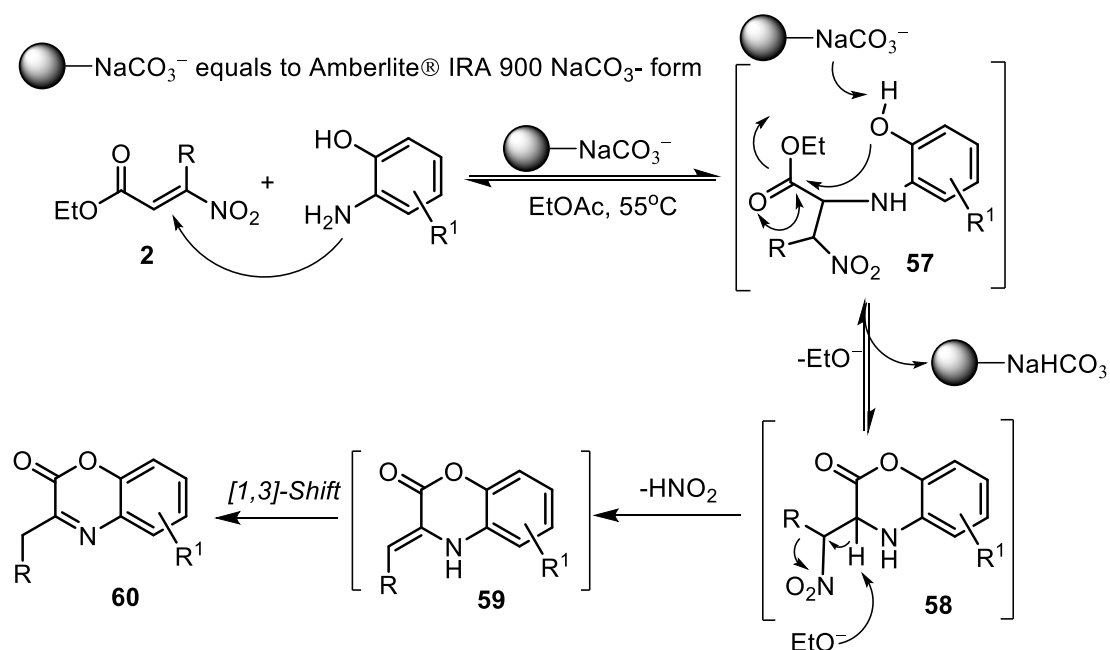
1.2.2.6 Synthesis of *N,O*- heterocyclic compounds

1,2-Oxazine-2-oxides are an important class of key building blocks for the synthesis of a large number of useful products like pyrrolizidine, pyrrolidines, β -lactam-*N*-oxides, oxazine, γ -nitroketones, etc.^[48] Ballini et al.^[49] devised a procedure for the preparation of 1,2-oxazine-2-oxides, starting from β -nitroacrylates and silyl enol ethers. The Michael addition of **16** to **2**, as portrayed in Scheme 25, followed by the in situ acetylation of the resulting hydroxyl group (**54** to **55**), gave the target compounds **56** directly. Although compounds **55** can be isolated by chromatography, they were proved rather unstable. The in situ acetylation of the hydroxyl group in the presence of 4-dimethylaminopyridine (DMAP) and acetic anhydride provides more stable derivatives **56**. The procedure is featured by good yields and chemoselectivity, and furthermore, represents an extension of the chemical versatility of an emerging class of key building blocks such as β -nitroacrylates.



Scheme 25. The preparation of 1,2-oxazine-2-oxides.

At the same time, a new, chemoselective, environmentally friendly synthetic process for 2H-1,4-benzoxazin-2-ones, has been realized accounting for different transformations, in a single synthetic operation starting from β -nitroacrylates **2** and 2-aminophenols.^[50] The possible mechanism of the reaction includes a domino process involving four different transformations: (i) hetero-Michael addition between the amine functionality and **2** to give the intermediates **57**; (ii) intramolecular transesterification and the formation of **58**; (iii) elimination of a molecule of nitrous acid to yield the intermediates **59**; and (iv) [1,3]-proton shift to form the target products **60**, as previously reported in the literature (Scheme 26).^[51]



Scheme 26. Plausible mechanism of the formation of 2H-1,4-benzoxazin-2-ones.

1.3 Conjugated nitroalkenes

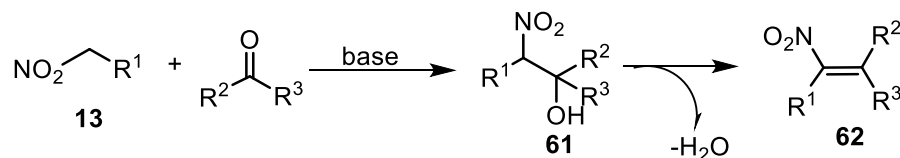
Nitroalkenes, or nitro-olefins, are compounds that incorporate the functional groups of their constituents (i.e. alkenes and nitro group). They are widely used in different carbon-carbon bond forming reactions, such as Michael reaction,^[52] cycloadditions, and Morita-Baylis-Hillman reaction,^[53] as well as for the generation of oximes, hydroxylamines, nitroalkanes, aliphatic amines, and nitroso compounds.^[54] Furthermore, conjugated nitroalkenes are important because of their biological use as insecticides, fungicides and pharmacologically active substances.^[55]

1.3.1 Synthesis of nitroalkenes

Nitroolefins are typically synthesized via Henry reaction, which relies on the base-mediated condensation of aldehydes or ketones with nitroalkanes.^[56] Another approach is to synthesize nitroolefins by directly incorporating nitro group into olefin. However, the second method is rarely practiced due to the lack of selectivity and low yield.

1.3.1.1 Henry reaction

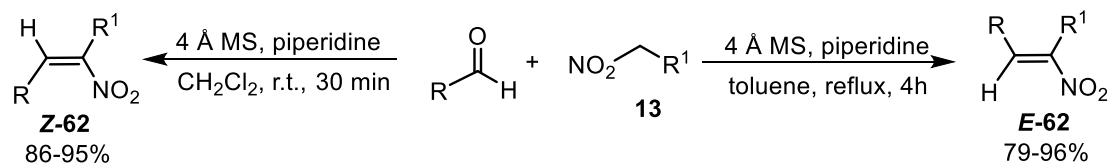
The reaction between nitroalkanes **13** and carbonyl compounds can be carried out under different conditions, such as ultrasound, microwave, or ionic liquid-accelerated conditions, and heterogeneous condensation.^[57] After the following step of dehydration of β -nitro alcohol **61**, nitroalkenes **62** can be prepared successfully (Scheme 27).^[58] In a Knoevenagel-type process, arylaldehydes and nitroalkanes can generate nitroalkenes directly under base-promoted conditions.^[59]



Scheme 27. Henry reaction between nitroalkanes and carbonyl compounds.

Fioravanti and colleagues^[60] proposed a method to control the stereochemical outcome of the reaction by simply changing the reaction conditions (solvent and temperature). As shown in Scheme 28, aliphatic aldehydes react with nitroalkanes **13** in the presence of catalytic amounts of piperidine over 4 Å molecular sieves (MS),

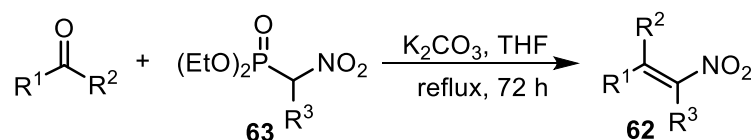
using toluene at reflux or DCM at room temperature under anhydrous conditions and inert atmosphere. Under these conditions, only (*E*)-nitroalkenes or (*Z*)-nitro alkenes **62** were obtained in high to excellent yields.



Scheme 28. Stereoselective one-pot synthesis of (*Z*)- or (*E*)-nitroalkenes.

1.3.1.2 Horner-Wadsworth-Emmons reaction

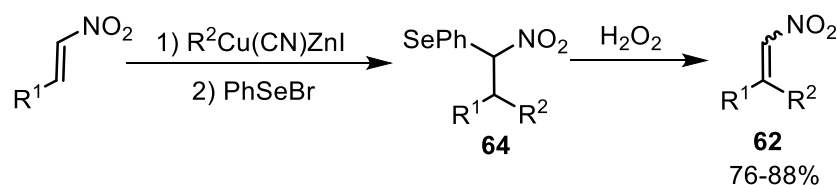
Fujii^[61] described the preparation of nitroalkenes by the condensation of 1-nitroalkanephosphonates **63** and carbonyl compounds using potassium *tert*-butoxide, THF as solvent at 0-60°C. Later, Franklin^[62] attempted to obtain nitroalkenes **62** in the presence of potassium carbonate, THF as solvent, at reflux (Scheme 29).



Scheme 29. Horner-Wadsworth-Emmons synthesis of nitroalkenes.

1.3.1.3 Conjugate addition

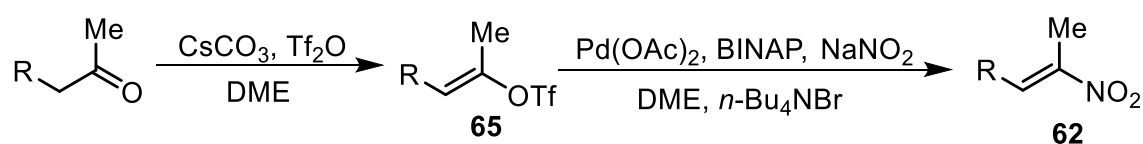
Jubert and Knochel^[63] described the preparation of β,β -disubstituted nitroalkenes by the addition/elimination of copper-zinc organometallic reagents to nitroalkenes. Sakakibara et al.^[64] reported the synthesis of nitroalkenes from nitroalkanes using phenylselenenyl bromide. By combining Knochel's and Sakakibara's work, Denmark and Marcin^[65] reported a general and high productive route for the synthesis of nitroalkenes. The process includes the conjugate addition of copper-zinc reagents to nitroalkenes and phenylselenation to form the intermediate **64**, followed by oxidative elimination. Thus, α, β -unsaturated nitroalkenes **62** were obtained in good yield (Scheme 30).



Scheme 30. Synthesis of α, β -unsaturated nitroalkenes.

1.3.1.4 Cross-coupling synthesis of nitroolefins

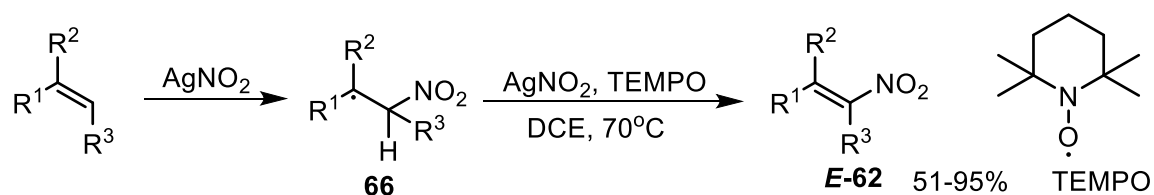
Chang et al.^[66] explored a one-pot palladium-catalyzed method for the preparation of substituted nitroolefins using ketones. Ketones can form (*E*)-enol triflates **65** via the reaction with triflic anhydride (Tf₂O) and Cs₂CO₃. Then nitroolefins **62** can be prepared by an intermolecular Pd(II)-catalyzed cross-coupling of triflate **65** with NaNO₂ in the presence of phase-transfer agents (Scheme 31). Screening different catalysts (Pd(OAc)₂, PdCl(MeCN)₂, PdCl₂, and Pd₂(dba)₃), ligands (BINAP, Ph₃P, and JohnPhos) and phase-transfer reagents (*n*-Bu₄NBr, *n*-Bu₄NF), the combination of Pd(OAc)₂, BINAP and *n*-Bu₄NBr provided the optimized condition and better yields.



Scheme 31. Palladium-catalyzed synthesis of nitroolefins.

1.3.1.5 Stereoselective nitration of olefins with AgNO₂ and TEMPO

Maiti et al.^[67] reported that silver nitrite and 2,2,6,6-tetramethylpiperidine-1-oxyl (TEMPO) can promote the regio- and stereoselective nitration of various olefins. Alkenes can react with silver nitrite to form nitro radical **66**, which would generate a carbon-centered radical that can be further oxidized to give the corresponding nitroolefins **62** (Scheme 32). This method is practical, allowing nitration of a wide array of substrates, including aromatic, aliphatic, and heteroaromatic olefins.

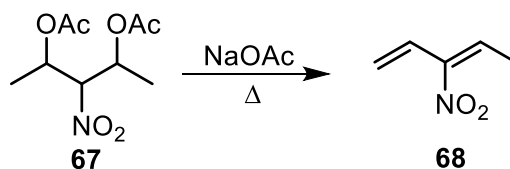


Scheme 32. Synthesis of nitroolefin by AgNO₂ and TEMPO.

1.3.2 Synthetic routes for nitrodienes and their applications

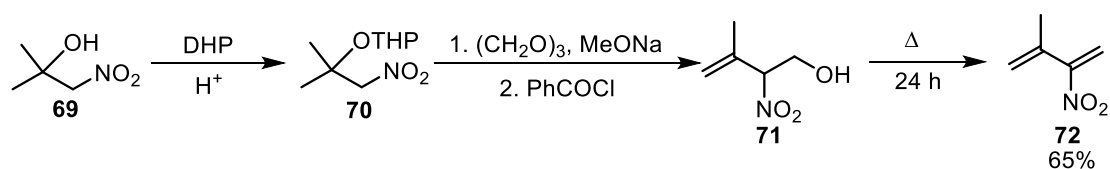
The synthesis and reaction of conjugated electron-deficient dienes, especially their applications in Diels-Alder reaction, remains a challenge in synthetic organic chemistry.

Buckley and Charlish^[68] described the synthesis of 3-nitropenta-1,3-diene **68** by heating 2,4-diacetoxy-3-nitropentane **67** with a small amount of sodium acetate (Scheme 33).



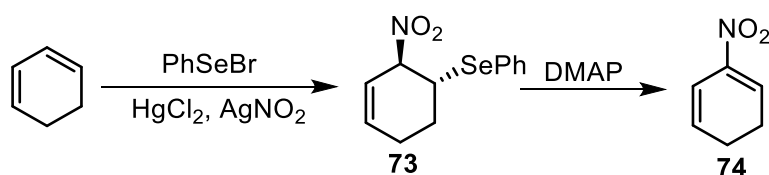
Scheme 33. Synthesis of 3-nitropenta-1,3-diene.

Barco et al.^[69] reported a three-step sequence for the preparation of **72**. The commercially available nitro-alcohol **69** was first converted to tetrahydropyranyl ether **70**, which was reacted with paraformaldehyde in the presence of sodium methoxide to give allylic nitro alcohol **71**, and then transformed into **72** in a 65% overall yield by using benzoyl chloride in refluxing benzene (Scheme 34).



Scheme 34. Three-step preparation of substituted nitrodiene.

Bäckvall and co-workers^[70] reported the synthesis of 2-nitro-1,3-dienes **74** by a sequence that involves the nitroselenation of the corresponding conjugated dienes followed by a base-catalyzed elimination of the phenylseleno group. As shown in Scheme 35, when the nitroselenation adducts **73** from conjugated dienes were treated with a catalytic amount of a base such as DMAP, the phenylseleno group was eliminated under a mild condition.



Scheme 35. Synthesis of nitrodiene by nitroselenation and elimination of the phenylseleno group.

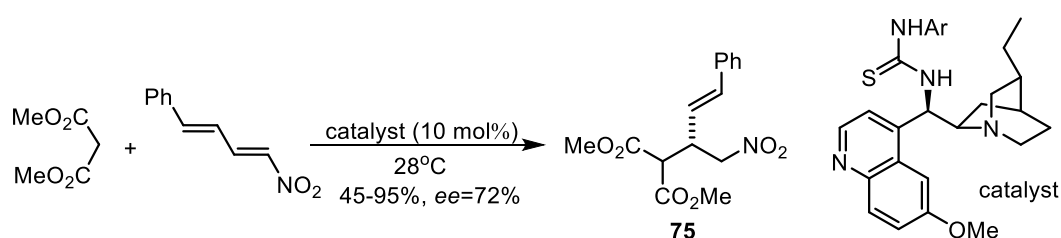
The applications of nitrodienes have received increasing attention in recent years. They are used to develop preparative methods for synthesizing different classes of complicated polyfunctional products, some of which are biologically important.

1.3.2.1 Michael addition of malonates to nitrodienes

Nitroalkenes have been well studied as Michael acceptors in the field of organocatalytic reactions due to their high electrophilicity, strong

electron-withdrawing properties and hydrogen bonding ability derived from the nitro group. Moreover, the enantioenriched nitroalkene adducts are valuable synthons for various chiral heterocyclic skeletons found in bioactive molecules.^[71]

Ghosh et al.^[72] reported an efficient, highly regio-, and enantioselective protocol in which the Michael addition of malonates, β -ketoesters, and β -diketones to nitrodienes, promoted by cinchona alkaloid-based thiourea catalysts (Scheme 36). The addition reactions are highly regioselective, yielding products **75** in good to excellent yields and enantioselectivities. The addition products are useful to build up stereo- and regiochemically diverse heterocyclic frameworks consisting of flexible rings and containing embedded functionalities.

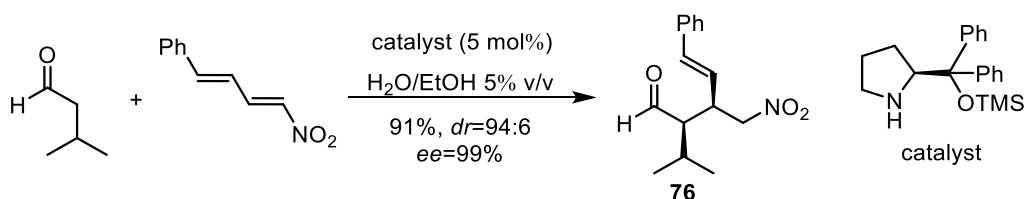


Scheme 36. Asymmetric Michael addition of dimethyl malonate to nitrodiene.

1.3.2.2 Michael addition of carbonyl compounds to nitrodienes

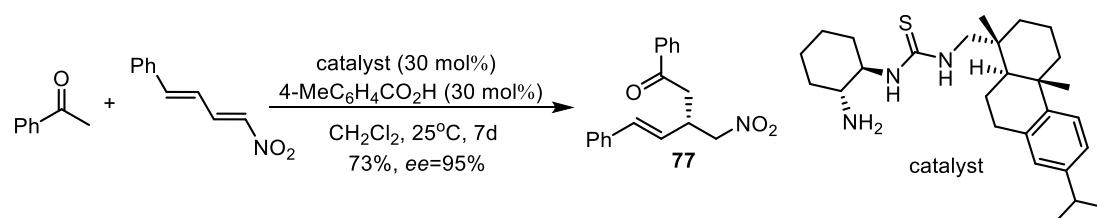
As one of the most efficient, atom-economical and robust methods, the direct Michael reaction of carbonyl compounds to nitrodienes has attracted widespread interest because the enantioenriched adducts serve as versatile intermediates for the preparation of complex organic targets and thus extensive attention has been given to developing efficient catalytic systems for various carbonyl compounds as carbon nucleophiles.

Alexakis and co-workers^[73] performed the asymmetric conjugate addition of aldehydes to nitrodienes in the presence of chiral prolinol catalyst. Under optimized conditions, adduct **76** can be obtained in good yield and enantioselectivity (Scheme 37). It is important to note that only 1,4-addition was observed during the preliminary optimization study without any trace of 1,6-addition adducts.



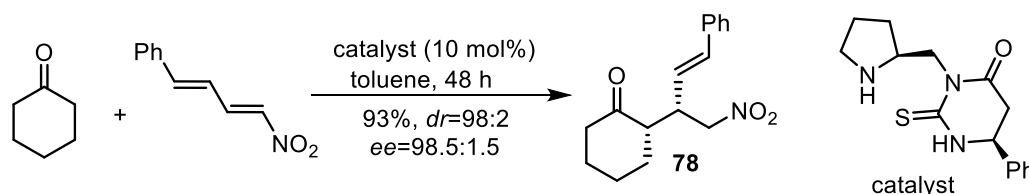
Scheme 37. Michael addition of aldehydes to nitrodienes.

Chiral γ -nitro ketones are synthetic precursors for many biologically active molecules. In Wu's study, a highly enantioselective Michael addition of aromatic ketones to nitrodienes was developed using dehydroabietic amine-based chiral primary aminethiourea (Scheme 38).^[74] In this process, a variety of aromatic ketones and nitrodienes could be used for the reaction, and the obtained chiral γ -nitro ketones **77** have excellent enantioselectivity with 73% yield.



Scheme 38. Enantioselective Michael addition between aromatic ketones and nitrodienes.

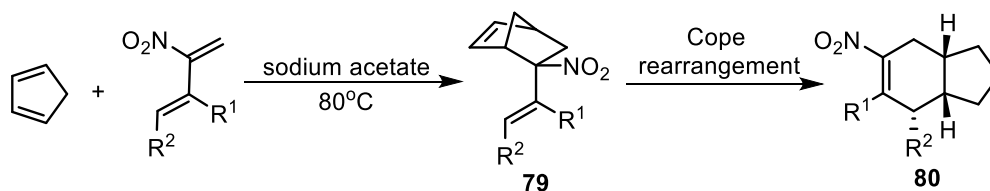
Among various Michael additions, the enantioselective reaction between cyclic ketones and nitrodienes has received little attention compared to the corresponding reaction with nitroolefins. Kokotos and co-workers^[75] found that pyrrolidine-thioxotetrahydropyrimidinone was an excellent catalyst for the less-studied reaction between cyclic ketones and substituted nitrodienes. The product **78** of the reaction between ketone and nitrodiene was obtained in high yield (93%) with excellent diastereo- and enantioselectivity (Scheme 39).



Scheme 39. Enantioselective Michael addition between cyclic ketone and nitrodiene.

1.3.2.3 Diels-Alder cycloaddition

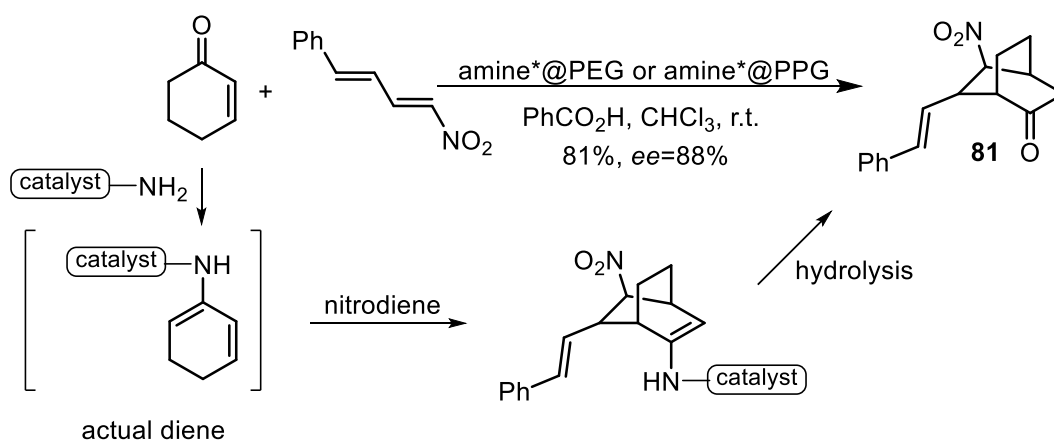
Barco et al.^[76] explored the reactions between nitrodienes and cyclopentadiene, resulting in a mixture of products **79** and **80**, the latter one resulting from a Cope rearrangement of the exo-nitro adducts **79** (Scheme 40).



Scheme 40. Asymmetric Diels-Alder reaction between cyclopentadiene and nitrodiene.

Through in situ enamine activation, an effective asymmetric organocatalytic Diels-Alder reaction of α,β -unsaturated cyclohexenones with aromatic nitroolefins in solutions of aqueous salts can be developed, but using nitrodiene instead of nitroolefins as dienophiles results in a dramatic decrease in reactivity.^[77] Surprisingly, it was found that the unusual Diels-Alder reaction could be promoted effectively by supramolecular catalysts self-assembled from chiral amines and poly(ethylene glycol)s (PEGs) or poly(propylene glycol)s (PPGs; amine*@PEG and amine*@PPG) in the presence of an acid.

At first, the asymmetric Diels-Alder reaction between cyclohex-2-enone and phenylnitrodiene in CHCl_3 was investigated (Scheme 41). In terms of stereoselectivity, the applied chiral amines provided the desired Diels-Alder products **81** with excellent diastereo and enantioselectivities.^[78] This is the first application of a novel chiral supramolecular catalysts that self-assembles from chiral amines with readily available achiral poly(alkene glycol)s via weak non-covalent interactions. The obtained results will open new opportunities and alternatives for the design of functional supramolecular catalysts and their fascinating prospects as catalysts in asymmetric transformations.

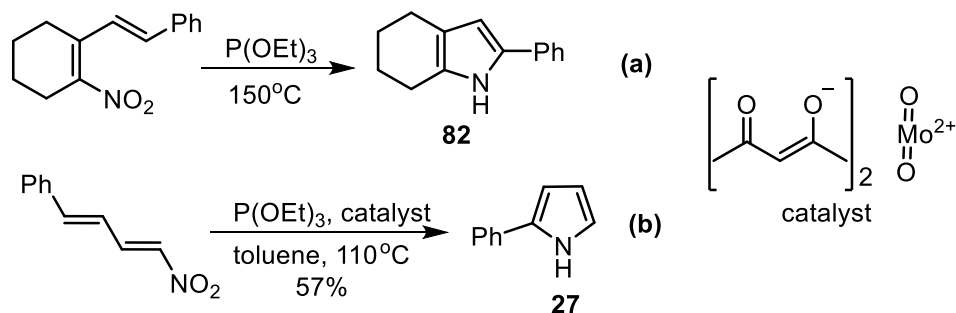


Scheme 41. Supramolecular catalyst promoted Diels-Alder reactions.

1.3.2.4 Substituted pyrrole synthesis from nitrodiene

Although the Cadogan-Sundberg method has been widely used for the synthesis of indoles and carbazoles, to date, only one example to convert a simple non-arene nitrodiene to a pyrrole derivative **82** was found in the literature (Scheme 42a). With the traditional use of triethylphosphite as the reducing agent, pyrrole derivatives **27**

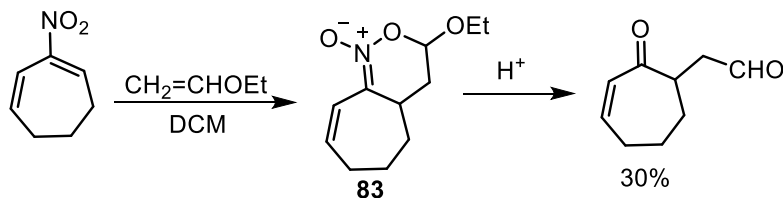
were obtained in unacceptably low yield from the corresponding nitrodiene.^[79] However, with triphenylphosphine in the presence of bis-(acetylacetonato)dioxo-molybdenum (VI) catalyst, several pyrrole derivatives were prepared from the corresponding nitrodiene, and in higher yields (Scheme 42b).



Scheme 42. Synthesis of pyrrole derivatives from the corresponding nitrodiene.

1.3.2.5 Synthesis of 1,4-dicarbonyl compounds from nitrodiene

The reaction of 1,6-nitrocycloheptadiene with ethyl vinyl ether in DCM gave nitronate **83** in almost quantitative yield. Then hydrolysis of **83** under hydrolytic Nef conditions afforded aldehyde in moderate yield (Scheme 43).^[70] Other dicarbonyl compounds can also be obtained in excellent yields using the same procedure.



Scheme 43. Synthesis of 1,4-dicarbonyl compounds.

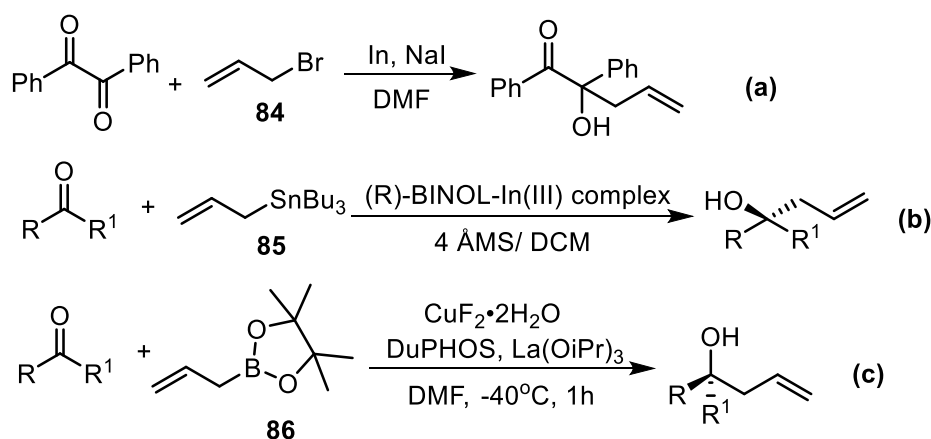
1.4 Preparation and synthetic investigations of a new class of conjugated nitrotrienes

1.4.1 State of the art

In synthetic organic chemistry, the allylation of carbonyl groups to supply homoallylic alcohols is an essential transformation.^[80] Several catalysts can promote the allylation of aldehydes to afford secondary homoallylic alcohols with excellent enantioselectivities.^[81, 82] However, the catalytic allylation of ketones has proven to be a more difficult transformation due to the significant distinction in reactivity between aldehydes and ketones. Furthermore, the formation of quaternary stereocenters,

formed during the allylation of ketones, is rather challenging.

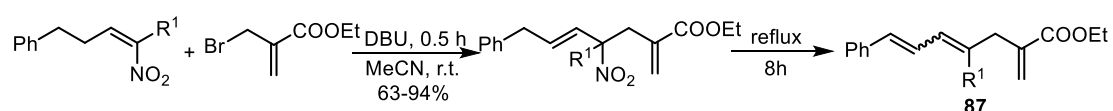
Typical protocols for the allylation of ketones involve the use of Barbier-type allylindium species, produced in situ from allyl halides **84** and a stoichiometric amount of In(0) or In(I) (Scheme 44a).^[83, 84] Catalytic methods involving allyltributylstannane **85** as reagent employ In(III)^[85, 86] or other Lewis acids^[87] (Scheme 44b). Considering the toxicity of stannanes, significant progress has been made using allylsilane derivatives under transition metal catalysts.^[88] Recently, allylations by allylboronic acid pinacol ester **86** using transition metal catalysts^[89, 90] or metal-free conditions^[91, 92] have been reported (Scheme 44c). However, with few exceptions, the versatility of usable substrates is rather limited. Furthermore, to our knowledge, a catalytic synthetic method involving β -nitroenones is not yet known. Therefore, there is a need to develop a truly universal catalytic allylation method from β -nitroenones.



Scheme 44. Routes for allylations of ketones.

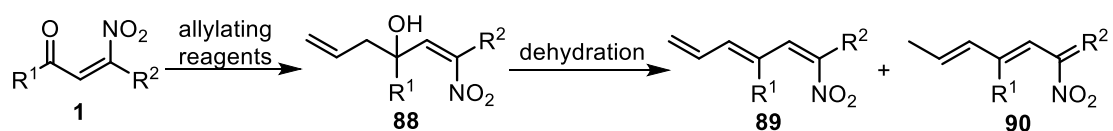
Considering the purpose of using non-toxic reagents and catalysts, indium is actually a good choice. Unlike most other metals, indium is stable to air and moisture, which offers potential for catalyst recovery and recycling, while the fact that it is non-toxic enables its reactions to be handled very easily.^[93] The low first ionization potential makes it an effective catalyst or reagent for C-C bond formation reactions as it can readily tolerate other functional groups containing N, O, S, etc. The conventional inorganic In(III) Lewis acids [for example, In(III)Cl₃ and In(III)(OTf)₃] are commonly used as catalysts for various C-C bond formation reactions.^[94] In addition, non-toxic boronates also require activation by a Lewis acid or base due to their much lower reactivity.^[95]

Triene compounds, which are always present in natural seed oils, have various beneficial effects, such as anti-carcinogenic, anti-obesity, anti-allergic and anti-cancer.^[96] Moreover, they can also be considered^[96] as building blocks for other functional materials. Although they are highly valued in organic chemistry and biological sciences, related synthetic methods for their preparation are still limited. Ballini and co-workers^[97] performed the Baylis-Hillman reaction using nitroalkenes as activated alkenes, ethyl-2-bromomethylacrylate as electrophilic acceptor and DBU as catalyst base. The nitrodienes are obtained in good yield and very short reaction time. Meanwhile, it is possible to realize one-pot synthesis of trienic systems **87** starting from suitable nitroalkenes (Scheme 45). However, the elimination of nitrous acid limits the applications of the nitro group.



Scheme 45. Synthesis of triene by Baylis-Hillman reaction.

In this section, we would like to present a mild, efficient way to synthesize homoallylic alcohols from β -nitroenones and also prepare nitrotrienes with moderate yields after dehydration. Therefore, the work can be divided into two main steps: (i) allylation of β -nitroenones **1** to form **88** using allylating reagents; (ii) synthesis of conjugated triene compounds **89** or **90** by elimination of water from **88** (Scheme 46).



Scheme 46. The synthetic approach from β -nitroenones.

1.4.2 Results and discussion

Parameters such as temperature, stoichiometry, solvent, reagents and reaction times were measured for each trial to find the optimized conditions.

1.4.2.1 Allylation reaction between β -nitroenones and allylating reagents

The first step involves the allylation of β -nitroenones using allylating reagents. The initial experiments were carried out with the reaction of **1a** and allyl bromide **84** catalyzed by indium metal in MeOH (Table 1). At a temperature of 0°C, the corresponding allyl alcohol **88a** was afforded in modest yield (49%, Table 1, entry 1).

Better performance in shorter time was obtained for the same reaction at 25°C (50%, Table 1, entry 2). Improvement over the short reaction time and higher yield was obtained by sonication (59%, Table 1, entry 3). After changing the solvent to ethanol, the yield is almost the same (60%). In addition, solvents such as DMF and THF or β -nitroenone **1b** were also attempted, but no improvement was obtained. The general results could not satisfy us, so we moved to other allylating reagents.

Table 1. Optimization of reaction conditions for allylation with allyl bromide.^[a]

Entry	R ^[b]	T°C	Sonication	Time (h)	Yield ^[c] (%)
1	Ph	0	No	6.5	49
2	Ph	25	No	5	50
3	Ph	25	Yes	2.5	59
4	4-MeOC ₆ H ₄	25	Yes	5.5	58

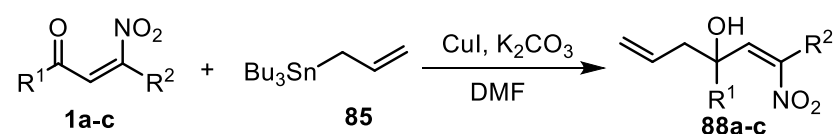
[a] Conditions: β -nitroenone **1a** (1 mmol), allyl bromide **84** (3 mmol), indium (2 mmol), MeOH (5.0 mL).

[b] β -Nitroenones **1a** (R=Ph), **1b** (R=4-MeOC₆H₄). [c] Isolated yield after chromatography on silica gel.

Grignard reagents were also tried, but without any effect.

Allyltributylstannane **85** was also used as an allylating agent in the presence of copper(I) iodide and potassium carbonate (Table 2). After optimization of the conditions, the best result was found in DMF at 25°C (55%, Table 2, entry 1). The utilization of γ -valerolactone was always accompanied by low yield, and acetonitrile (MeCN) did not work at all. Furthermore, changing the substituents resulted in longer reaction time and lower yield. Therefore, we tried allylboronic pinacol ester, which can allylate ketones with excellent yield.^[98, 99]

Table 2. Allylation with allyltributylstannane.^[a]



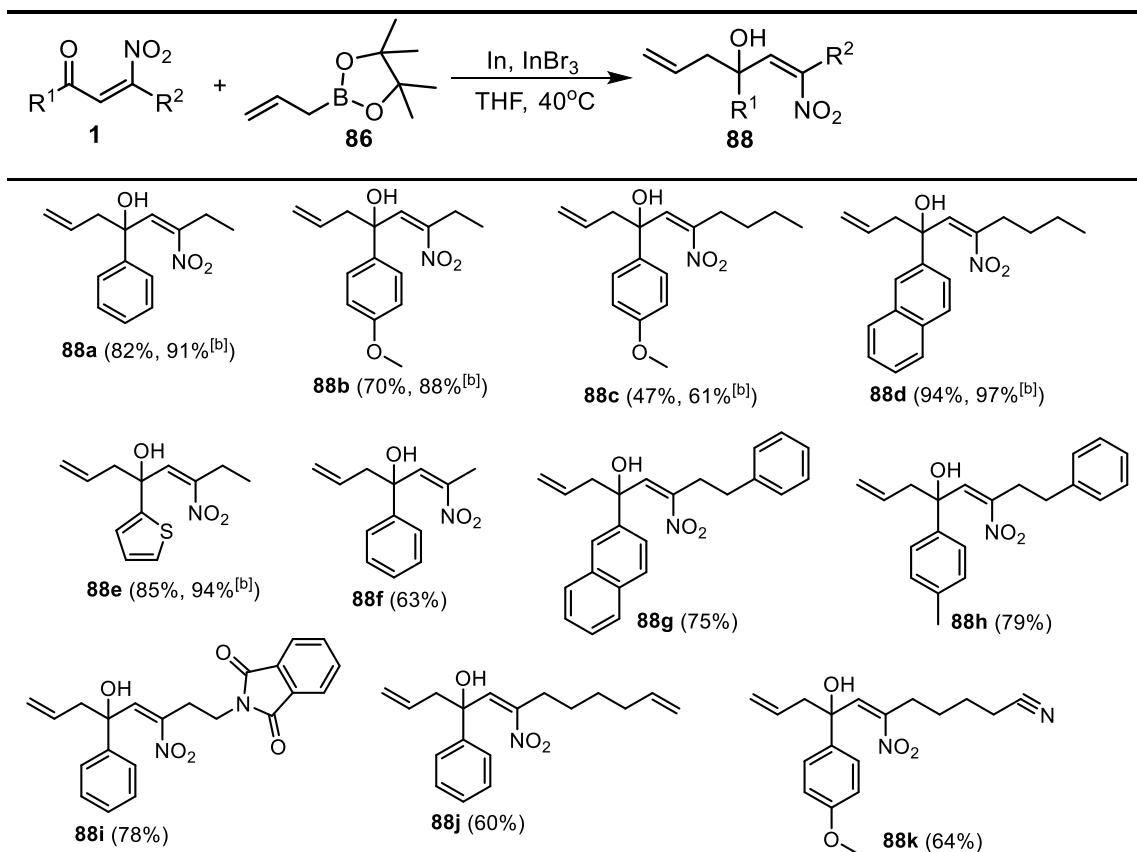
Entry	R ¹	R ²	Time (h)	Yield ^[b] (%)
1	Ph	Et	4	55
2	4-MeOC ₆ H ₄	Et	24	20
3	4-MeOC ₆ H ₄	<i>n</i> -Bu	24	47

[a] Conditions: β -nitroenones **1a-c** (1 mmol), allyltributylstannane **85** (1.2 mmol), copper(I) iodide (0.25 mmol), potassium carbonate (1 mmol), DMF (3 mL). [b] Isolated yield after chromatography on silica gel.

The conversion of β -nitroenones **1** to the corresponding alcohols **88** by allylboronic pinacol ester **86** can be successfully carried out under the conditions of indium(0) and indium(III) bromide as catalyst, THF as solvent at 40°C. During the optimized process, indium(III) chloride was also used to promote the reaction. However, its reactivity is relatively weak compared to indium(III) bromide. The reaction time is around 30 hours and gives a series of **88** with satisfactory and excellent yield (Table 3). The allylboronic pinacol ester route is an efficient, convenient and sustainable method for the conversion of β -nitroenones to the corresponding **88**. Moreover, it can tolerate a wide array of substituents, such as common alkyl, unsaturated double bonds, cyano and aromatic structures. In addition, we also performed the reaction using In(I)I to give **88a-e** with higher yield. Compared with the combination of In(0) and In(III)Br₃, In(I)I shows higher efficiency.

We have also tried to perform the cyclisation of the above compounds under microwave activation (180°C). Unfortunately, the yield is too low and not enough satisfactory to extend the application. Therefore, the next step of dehydration was carried out directly.

Table 3. Allylation with allylboronic pinacol ester.^[a]



^[a] Reaction conditions: β -nitroenones **1** (1 mmol), allylboronic pinacol ester **86** (1.5 mmol), indium (0.3 mmol), indium bromide (0.15 mmol), THF (10 mL).

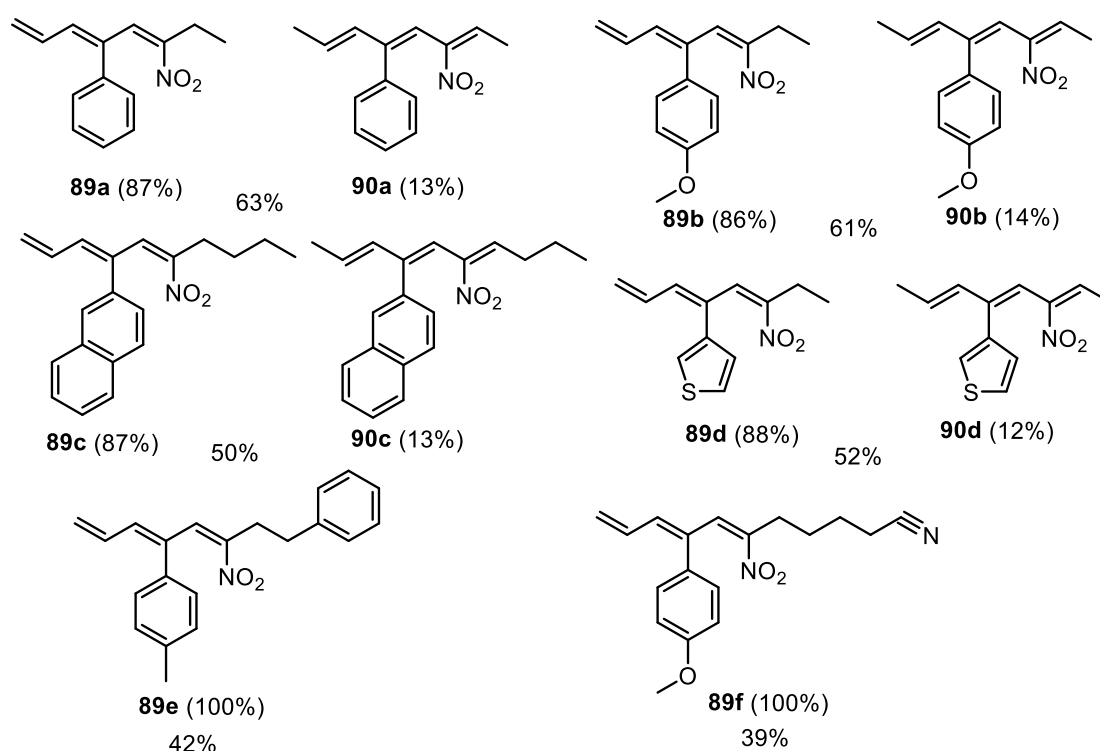
^[b] Reaction conditions: β -nitroenones **1** (1 mmol), allylboronic pinacol ester **86** (1.5 mmol), indium iodide (0.05 mmol), dry THF (5 mL).

1.4.2.2 Synthesis of nitro-trienes by the elimination of water

The second step involves the preparation of nitrotriene compounds from the dehydration of the above allylated alcohols, and **88a** was used as a model for the optimization studies. We primarily tried silica supported aluminium chloride and anhydrous aluminium chloride, since Lewis acids and solid catalysts can be used for the dehydration of alcohols with considerable advantages due to their economical and environmentally friendly.^[100] Unfortunately, the yields are too low even upon addition of another equivalent of acid. However, with silica supported boron trifluoride in DCM, we obtained the final product with a yield of 30%, which is a significant improvement, but not enough to be fully satisfying. Based on the above results, boron trifluoride etherate was used for another attempt, and finally gave the pleasing result with 63% yields of mixtures of the two isomers **89a** and **90a** under the condition of

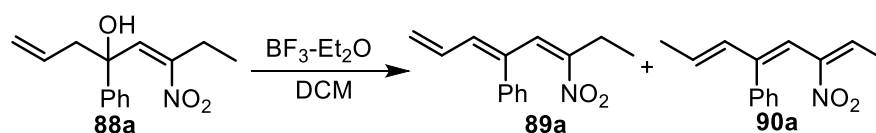
-10°C, DCM as solvent.

The regioisomeric composition of the mixture has been determined by ¹H-NMR. As shown in Table 4, a lower temperature has a positive effect on the yield and also on the ratio of **89a**, although a longer reaction time is required. On the other hand, dehydration was tried at -25°C and no product was obtained under this condition. A variety of allylated alcohols **88** were employed to demonstrate the generality of the optimized reaction conditions and to provide the mixtures with good overall yields (Scheme 47). The products **89e** and **89f** have been obtained as single regioisomers.



Scheme 47. A series of conjugated nitro-trienes. In parentheses the relative regioisomeric percentage.

Table 4. Elimination of water with boron trifluoride etherate.^[a]



Entry	T°C	Time (h)	Yield ^[b] (%)	Percentage of 89a
1	25	1.5	53	75
2	0	2.5	53	83
3	-10	5	63	87
4	-25		-	

[a] Conditions: allylated alcohol **88a** (0.3 mmol), boron trifluoride etherate (0.45 mmol), DCM (4.5 mL).

[b] Isolated yield after chromatography on silica gel.

1.4.3 Conclusion

In summary, a very convenient In-InBr₃-catalyzed allylation of β -nitroenones has been developed to give tertiary homoallylic alcohols. Homoallylic alcohols are versatile materials in organic synthesis and can be converted to conjugated nitrotrienes when the Lewis acid boron trifluoride etherate is present. As far as we know, this whole procedure represents the first synthesis of triene compounds embedding the nitro group. This method can provide practical guidelines for the subsequent synthesis of nitrotriene compounds and also demonstrate the practical value of using tertiary homoallylic alcohols.

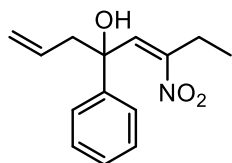
1.4.4 Experimental section

¹H NMR analyses were recorded at 400 MHz on a VarianMercury Plus 400. ¹³C NMR analyses were recorded at 100 MHz. IR spectra were recorded with a PerkinElmer FTIR spectrometer Spectrum Two UATR. Microanalyses were performed with a CHNS-O analyzer Model EA 1108 from Fisons Instruments. GS-MS analyses were obtained on a Hewlett-Packard GC/MS 6890 N that works with the EI technique (70 eV).

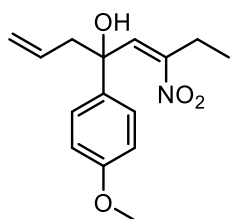
Homoallylic nitro alcohols (**88**): Allylboronic pinacol ester **86** (1.5 mmol) was added to a mixture of β -nitroenones **1** (1 mmol), indium (0.3 mmol) and indium(III) bromide (0.15 mmol) in THF (10 mL) at 40°C until the starting material was completely consumed (by TLC). The reaction mixture was acidified with HCl (10 mL) and then it was extracted with DCM (3×20 mL). The organic layer was dried over Na₂SO₄, concentrated and dried in vacuo. Silica gel column chromatographic purification of the residue using hexane-EtOAc (95:5) gave pure **88**.

Conjugated nitro-trienes (**89** and **90**): To a stirred solution of homoallylic nitro alcohols **88** (1 mmol) in DCM (15 mL) was added boron trifluoride etherate (1.5 mmol) at -10°C under nitrogen. After the completion of the reaction was monitored by TLC, the residue was acidified with HCl (10 mL) and extracted by DCM (3×20 mL). The organic phase was dried over Na₂SO₄, concentrated at reduced pressure and followed by silica gel column chromatographic purification using a mixture of hexane and EtOAc (98:2).

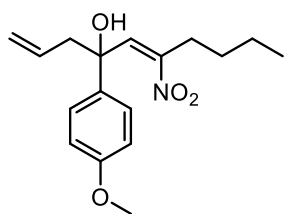
Spectroscopic data for compounds **88**, **89** and **90**:



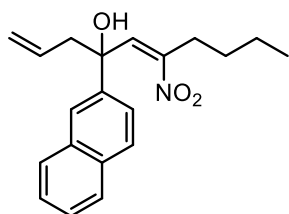
88a. Yield 0.203 g (82%). Pale yellow oil. IR (neat) ν : 703, 924, 1335, 1520, 3392 cm^{-1} . $^1\text{H-NMR}$ (DMSO- d_6 , 400MHz) δ : 0.92 (t, 3H, $J = 7.4$ Hz), 2.50 (s, 1H), 2.72-2.80 (m, 4H), 5.25-5.31 (m, 2H), 5.61-5.72 (m, 1H), 7.25-7.32 (m, 1H), 7.35-7.40 (m, 3H), 7.43-7.46 (m, 2H). $^{13}\text{C-NMR}$ (DMSO- d_6 , 100MHz) δ : 12.5, 20.8, 49.1, 74.5, 122.3, 125.3, 127.9, 128.9, 131.7, 138.2, 144.2, 155.8. GC-MS (70 eV): m/z : 206 (59), 159 (100), 131 (12), 105 (37), 77 (32). Anal. Calcd. For $\text{C}_{14}\text{H}_{17}\text{NO}_3$ (247.29): C: 68.00; H: 6.93; N: 5.66; O: 19.41. Found: C: 68.07; H: 6.82; N: 5.57; O: 19.54.



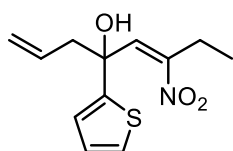
88b. Yield 0.194 g (70%). Clear yellow oil. IR (neat) ν : 832, 1176, 1248, 1513, 2939, 3499 cm^{-1} . $^1\text{H-NMR}$ (DMSO- d_6 , 400MHz) δ : 0.95 (t, 3H, $J = 7.4$ Hz), 2.38 (s, 1H), 2.73-2.81 (m, 4H), 3.81 (s, 3H), 5.23-5.31 (m, 2H), 5.61-5.75 (m, 1H), 6.90 (d, 2H, $J = 8.8$ Hz), 7.32-7.39 (m, 3H). $^{13}\text{C-NMR}$ (DMSO- d_6 , 100MHz) δ : 12.6, 20.7, 48.9, 55.6, 74.3, 114.2, 122.1, 126.6, 131.9, 136.2, 138.3, 155.4, 159.2. GC-MS (70 eV): m/z : 236 (73), 189 (100), 135 (41), 81 (15). Anal. Calcd. For $\text{C}_{15}\text{H}_{19}\text{NO}_4$ (277.32): C: 64.97; H: 6.91; N: 5.05; O: 23.08. Found: C: 65.01; H: 7.07; N: 4.85; O: 23.07.



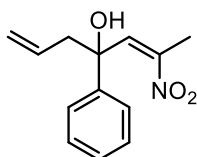
88c. Yield 0.144 g (47%). Pale yellow oil. IR (neat) ν : 739, 1252, 1508, 2959, 3539 cm^{-1} . $^1\text{H-NMR}$ (DMSO- d_6 , 400MHz) δ : 0.83 (t, 3H, $J = 7.0$ Hz), 1.18-1.29 (m, 4H), 2.37 (s, 1H), 2.70-2.78 (m, 4H), 3.81 (s, 3H), 5.24-5.30 (m, 2H), 5.61-5.73 (m, 1H), 6.87-6.92 (m, 2H), 7.32-7.37 (m, 3H). $^{13}\text{C-NMR}$ (DMSO- d_6 , 100MHz) δ : 13.9, 22.9, 26.9, 30.2, 48.9, 55.5, 74.3, 114.2, 122.1, 126.6, 131.9, 136.3, 138.3, 154.5, 159.2. GC-MS (70 eV): m/z : 264 (67), 243 (12), 217 (100), 175 (13), 135 (91), 77 (21). Anal. Calcd. For $\text{C}_{17}\text{H}_{23}\text{NO}_4$ (305.37): C: 66.86; H: 7.59; N: 4.59; O: 20.96. Found: C: 66.74; H: 7.62; N: 4.63; O: 21.01.



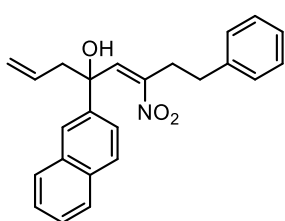
88d. Yield 0.306 g (94%). Pale yellow oil. IR (neat) ν : 475, 749, 1331, 1517, 2958, 3555 cm^{-1} . $^1\text{H-NMR}$ (DMSO- d_6 , 400MHz) δ : 0.74 (t, 3H, $J = 7.1$ Hz), 1.10-1.35 (m, 4H), 2.54 (s, 1H), 2.74 (t, 2H, $J = 7.5$ Hz), 2.88 (d, 2H, $J = 7.6$ Hz), 5.28-5.35 (m, 2H), 5.62-5.74 (m, 1H), 7.47 (s, 1H), 7.48-7.54 (m, 3H), 7.82-7.88 (m, 3H), 7.94 (d, 1H, $J = 1.9$ Hz). $^{13}\text{C-NMR}$ (DMSO- d_6 , 100MHz) δ : 13.8, 22.8, 27.0, 30.1, 49.0, 74.6, 122.4, 123.5, 124.1, 126.6, 126.8, 127.8, 128.4, 128.8, 131.7, 132.8, 133.3, 137.9, 141.5, 155.2. GC-MS (70 eV): m/z : 278 (15), 263 (64), 237 (17), 207 (17), 155 (100), 127 (76). Anal. Calcd. For $\text{C}_{20}\text{H}_{23}\text{NO}_3$ (325.40): C: 73.82; H: 7.12; N: 4.30; O: 14.75. Found: C: 73.88; H: 7.21; N: 4.27; O: 14.64.



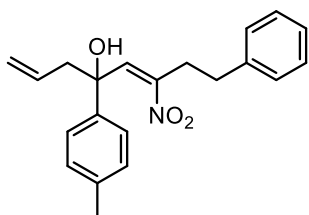
88e. Yield 0.215 g (85%). Pale yellow oil. IR (neat) ν : 709, 1331, 1525, 2978, 3529 cm^{-1} . $^1\text{H-NMR}$ (DMSO- d_6 , 400MHz) δ : 1.04 (t, 3H, $J = 7.3$ Hz), 2.65 (s, 1H), 2.77-2.92 (m, 4H), 5.27-5.34 (m, 2H), 5.69-5.81 (m, 1H), 6.97-7.00 (m, 2H), 7.24 (s, 1H), 7.26-7.29 (m, 1H). $^{13}\text{C-NMR}$ (DMSO- d_6 , 100MHz) δ : 12.9, 20.7, 49.2, 73.9, 122.4, 124.0, 125.6, 127.4, 131.4, 136.8, 148.7, 155.3. GC-MS (70 eV): m/z : 206 (59), 159 (100), 131 (12), 105 (37), 77 (32). Anal. Calcd. For $\text{C}_{12}\text{H}_{15}\text{NO}_3\text{S}$ (253.32): C: 56.90; H: 5.97; N: 5.53; O: 18.95; S: 12.66. Found: C: 56.78; H: 5.94; N: 5.61; O: 19.03; S: 12.64.



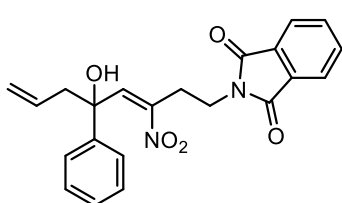
88f. Yield 0.147 g (63%). Pale yellow oil. IR (neat) ν : 698, 724, 1326, 1519, 3537 cm^{-1} . $^1\text{H-NMR}$ (DMSO- d_6 , 400MHz) δ : 2.26 (s, 3H), 2.48 (s, 1H), 2.81 (d, 2H, $J = 7.4$ Hz), 5.31 (d, 2H, $J = 11.7$ Hz), 5.64-5.77 (m, 1H), 7.26-7.35 (m, 1H), 7.39 (t, 2H, $J = 7.6$ Hz), 7.45-7.50 (m, 3H). $^{13}\text{C-NMR}$ (DMSO- d_6 , 100MHz) δ : 13.6, 48.7, 74.3, 122.0, 125.1, 127.7, 128.7, 131.5, 138.4, 143.8, 150.3. GC-MS (70 eV): m/z : 192 (60), 145 (100), 105 (29), 78 (30), 67 (30). Anal. Calcd. For $\text{C}_{13}\text{H}_{15}\text{NO}_3$ (233.26): C: 66.94; H: 6.48; N: 6.00; O: 20.58. Found: C: 67.03; H: 6.51; N: 5.77; O: 20.69.



88g. Yield 0.280 g (75%). Pale yellow oil. IR (neat) ν : 476, 699, 749, 1326, 1520, 3026, 3537 cm^{-1} . $^1\text{H-NMR}$ (DMSO- d_6 , 400MHz) δ : 2.13(s, 1H), 2.53-2.86 (m, 4H), 3.03-3.19 (m, 2H), 5.19-5.28 (m, 2H), 5.51-5.64 (m, 1H), 7.02 (d, 2H, $J = 7.5$ Hz), 7.14-7.27 (m, 3H), 7.43-7.58 (m, 4H), 7.81-7.91 (m, 4H). $^{13}\text{C-NMR}$ (DMSO- d_6 , 100MHz) δ : 29.1, 33.7, 48.5, 74.5, 121.9, 123.2, 123.9, 126.3, 126.4, 126.6, 127.6, 128.2, 128.5, 128.6, 128.7, 131.2, 132.6, 133.1, 139.2, 140.5, 141.0, 152.9. GC-MS (70 eV): m/z : 327 (34), 311 (34), 284 (50), 207 (29), 155 (100), 127 (90), 91 (35). Anal. Calcd. For $\text{C}_{24}\text{H}_{23}\text{NO}_3$ (373.44): C: 77.19; H: 6.21; N: 3.75; O: 12.85. Found: C: 76.98; H: 6.32; N: 3.54; O: 13.16.

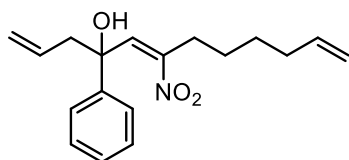


88h. Yield 0.267 g (79%). Pale yellow oil. IR (neat) ν : 699, 734, 1326, 1520, 3027, 3540 cm^{-1} . $^1\text{H-NMR}$ (DMSO- d_6 , 400MHz) δ : 2.05 (s, 1H), 2.38 (s, 3H), 2.61-2.79 (m, 4H), 3.06-3.20 (m, 2H), 5.20-5.27 (m, 2H), 5.55-5.65 (m, 1H), 7.15 (d, 2H, $J = 6.9$ Hz), 7.19-7.26 (m, 3H), 7.28-7.34 (m, 4H), 7.46 (s, 1H). $^{13}\text{C-NMR}$ (DMSO- d_6 , 100MHz) δ : 21.0, 29.1, 33.9, 48.5, 74.4, 121.6, 125.0, 126.3, 128.5, 128.7, 129.4, 131.5, 137.5, 139.5, 140.7, 140.8, 152.5. GC-MS (70 eV): m/z : 290 (19), 275 (48), 119 (100), 91 (82), 65 (24). Anal. Calcd. For $\text{C}_{21}\text{H}_{23}\text{NO}_3$ (337.41): C: 74.75; H: 6.87; N: 4.15; O: 14.23. Found: C: 74.66; H: 6.95; N: 4.33; O: 14.06.

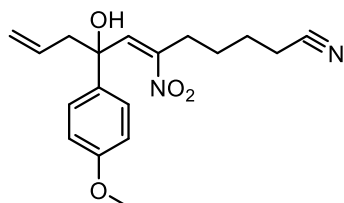


88i. Yield 0.306 g (78%). Pale yellow solid, mp: 134-136 $^{\circ}\text{C}$. IR (neat) ν : 717, 1331, 1398, 1703, 2927, 3513 cm^{-1} . $^1\text{H-NMR}$ (DMSO- d_6 , 400MHz) δ : 2.48-2.55 (m, 1H), 2.67 (s, 1H),

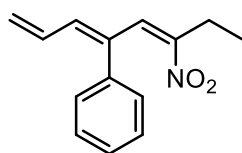
2.70-2.77 (m, 1H), 3.26 (t, 2H, $J = 6.2$ Hz), 3.85-3.99 (m, 2H), 4.91-5.10 (m, 2H), 5.38-5.50 (m, 1H), 7.12-7.23 (m, 3H), 7.24-7.28 (m, 2H), 7.50 (s, 1H), 7.68-7.73 (m, 2H), 7.76-7.81 (m, 2H). ^{13}C -NMR (DMSO- d_6 , 100MHz) δ : 26.5, 36.0, 48.5, 74.8, 122.2, 123.5, 125.0, 127.9, 128.9, 131.3, 132.4, 134.1, 141.2, 143.4, 149.4, 168.5. GC-MS (70 eV): m/z : 330 (38), 183 (99), 171 (47), 159 (65), 105 (100), 77 (79). Anal. Calcd. For $\text{C}_{22}\text{H}_{20}\text{N}_2\text{O}_5$ (392.40): C: 67.34; H: 5.14; N: 7.14; O: 20.39. Found: C: 67.45; H: 5.09; N: 7.33; O: 20.13.



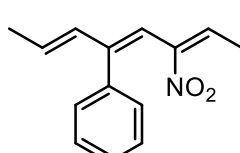
88j. Yield 0.181 g (60%). Pale yellow oil. IR (neat) ν : 699, 912, 1331, 1521, 2933, 3540 cm^{-1} . ^1H -NMR (DMSO- d_6 , 400MHz) δ : 1.16-1.41 (m, 4H), 1.92-2.00 (m, 2H), 2.41 (s, 1H), 2.69-2.81 (m, 4H), 4.89-5.00 (m, 2H), 5.25-5.32 (m, 2H), 5.60-5.78 (m, 2H), 7.25-7.33 (m, 1H), 7.34-7.41 (m, 3H), 7.42-7.47 (m, 2H). ^{13}C -NMR (DMSO- d_6 , 100MHz) δ : 26.8, 27.2, 28.6, 33.3, 48.8, 74.2, 114.5, 122.1, 125.1, 127.7, 128.6, 131.5, 138.1, 138.5, 144.0, 154.4. GC-MS (70 eV): m/z : 213 (11), 186 (17), 105 (100), 77 (26), 41 (14). Anal. Calcd. For $\text{C}_{18}\text{H}_{23}\text{NO}_3$ (301.38): C: 71.73; H: 7.69; N: 4.65; O: 15.93. Found: C: 71.88; H: 7.43; N: 4.72; O: 15.97.



88k. Yield 0.211 g (64%). Pale yellow oil. IR (neat) ν : 1043, 1248, 1328, 1521, 2941, 3461 cm^{-1} . ^1H -NMR (DMSO- d_6 , 400MHz) δ : 1.37-1.63 (m, 4H), 2.27 (t, 2H, $J = 7.0$ Hz), 2.52 (s, 1H), 2.71-2.84 (m, 4H), 3.82 (s, 3H), 5.26-5.34 (m, 2H), 5.58-5.70 (m, 1H), 6.81-6.87 (m, 1H), 6.96-7.03 (m, 2H), 7.26-7.33 (m, 1H), 7.40 (s, 1H). ^{13}C -NMR (DMSO- d_6 , 100MHz) δ : 16.7, 25.0, 26.0, 26.9, 48.7, 55.3, 74.2, 111.4, 112.5, 117.4, 119.5, 122.4, 129.9, 131.2, 138.9, 145.5, 152.9, 159.8. GC-MS (70 eV): m/z : 284 (25), 268 (93), 229 (30), 135 (100), 107 (27), 77 (34). Anal. Calcd. For $\text{C}_{18}\text{H}_{22}\text{N}_2\text{O}_4$ (330.38): C: 65.44; H: 6.71; N: 8.48; O: 19.37. Found: C: 65.56; H: 6.82; N: 8.23; O: 19.39.

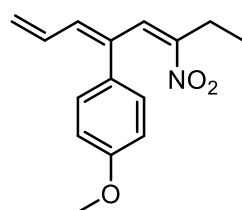


89a



90a

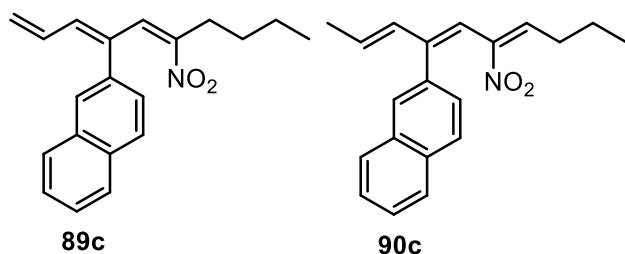
89a:90a (87:13). Yield 0.144 g (63%). Pale yellow oil. IR (neat) ν : 698, 764, 1334, 1520, 2939 cm^{-1} . ^1H -NMR (DMSO- d_6 , 400MHz) δ : 0.96 (t, 3H, $J = 7.3$ Hz), 1.41 (d, 0.8H, $J = 6.9$ Hz, **90a**), 1.84 (d, 0.8H, $J = 7.5$ Hz, **90a**), 2.38-2.45 (m, 2H), 5.39 (d, 1H, $J = 9.8$ Hz), 5.48 (s, 0.5H), 5.53 (s, 0.5H), 6.48-6.61 (m, 1H), 6.67 (d, 1H, $J = 11.3$ Hz), 7.32-7.39 (m, 5H), 7.81 (s, 1H). ^{13}C -NMR (DMSO- d_6 , 100MHz) δ : 11.5, 12.4, 14.9, 21.1, 116.1, 122.1, 126.7, 126.9, 127.2, 128.4, 128.5, 128.8, 129.0, 130.2, 130.9, 132.7, 133.1, 133.7, 138.7, 155.6. GC-MS (70 eV): m/z : 229 (63), 168 (100), 152 (59), 128 (32), 115 (36). Anal. Calcd. For $\text{C}_{14}\text{H}_{15}\text{NO}_2$ (229.28): C: 73.34; H: 6.59; N: 6.11; O: 13.96. Found: C: 73.58; H: 6.45; N: 5.94; O: 14.03.



89b

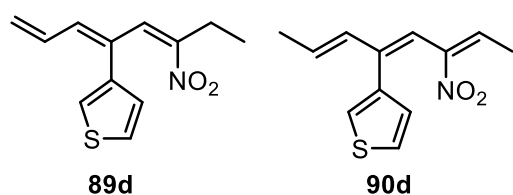
89b. Yield 0.158 g (61%). Pale yellow oil. IR (neat) ν : 832, 1176, 1244, 1511, 2937 cm^{-1} . ^1H -NMR (DMSO- d_6 , 400MHz) δ : 0.97 (t, 3H, $J = 7.4$ Hz), 2.40-2.46 (m, 2H), 3.82 (s, 3H), 5.33 (d, 1H, $J = 9.5$ Hz), 5.43 (s,

0.5H), 5.47 (s, 0.5H), 6.44-6.63 (m, 2H), 6.87-6.91 (m, 2H), 7.26-7.31 (m, 2H), 7.76 (s, 1H). ^{13}C -NMR (DMSO- d_6 , 100MHz) δ : 11.8, 21.3, 55.6, 114.0, 114.4, 121.3, 128.1, 128.7, 130.7, 131.1, 131.2, 133.5, 160.0. GC-MS (70 eV): m/z : 259 (84), 215 (51), 198 (100), 183 (47), 153 (31). Anal. Calcd. For $\text{C}_{15}\text{H}_{17}\text{NO}_3$ (259.31): C: 69.48; H: 6.61; N: 5.40; O: 18.51. Found: C: 69.31; H: 6.32; N: 5.77; O: 18.60.



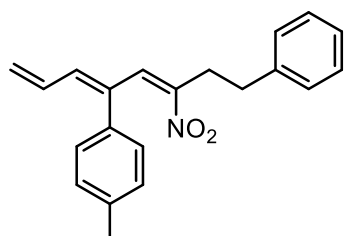
89c:90c (87:13). Yield 0.154 g (50%). Pale yellow oil. IR (neat) ν : 469, 747, 816, 1329, 1519, 2958 cm^{-1} . ^1H -NMR (DMSO- d_6 , 400MHz) δ : 0.47 (t, 0.3H, $J = 7.4$ Hz, **90c**), 0.67 (t, 3H, $J = 7.3$ Hz), 1.03-1.11 (m, 2H), 1.30-1.40 (m, 2H),

1.81 (d, 0.4H, $J = 6.9$ Hz, **90c**), 2.38 (t, 2H, $J = 7.8$ Hz), 5.38-5.60 (m, 2H), 6.54-6.68 (m, 1H), 6.81 (d, 1H, $J = 11.2$ Hz), 7.48-7.55 (m, 3H), 7.73 (s, 1H), 7.81-7.86 (m, 3H), 7.93 (s, 1H). ^{13}C -NMR (DMSO- d_6 , 100MHz) δ : 12.0, 13.5, 18.3, 21.1, 21.9, 27.0, 28.6, 30.5, 115.4, 121.8, 123.7, 125.7, 125.9, 126.1, 126.2, 126.5, 127.1, 127.2, 127.6, 127.7, 128.1, 128.2, 130.0, 132.6, 132.7, 134.1, 135.5, 138.1, 147.0, 154.4. GC-MS (70 eV): m/z : 263 (38), 249 (26), 207 (27), 155 (100), 127 (68). Anal. Calcd. For $\text{C}_{20}\text{H}_{21}\text{NO}_2$ (307.39): C: 78.15; H: 6.89; N: 4.56; O: 10.41. Found: C: 78.33; H: 6.94; N: 4.31; O: 10.42.



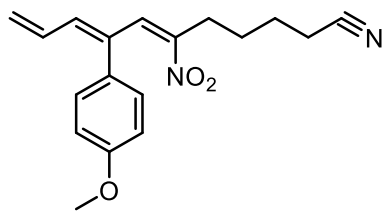
89d:90d (88:12). Yield 0.122 g (52%). Pale yellow oil. IR (neat) ν : 695, 828, 1329, 1523, 2978 cm^{-1} . ^1H -NMR (DMSO- d_6 , 400MHz) δ : 1.05 (t, 3H, $J = 7.4$ Hz), 1.49 (d, 0.5H, $J = 6.9$ Hz, **90d**), 1.84 (d, 0.5H, $J = 7.5$ Hz, **90d**), 2.48-2.58

(m, 2H), 5.33 (d, 1H, $J = 10.1$ Hz), 5.46 (s, 0.5H), 5.50 (s, 0.5H), 6.35-6.47 (m, 1H), 6.68 (d, 1H, $J = 11.3$ Hz), 6.92-7.02 (m, 2H), 7.24-7.26 (m, 1H), 7.65 (s, 1H). ^{13}C -NMR (DMSO- d_6 , 100MHz) δ : 12.0, 14.9, 15.2, 21.4, 114.0, 121.7, 125.7, 125.8, 126.2, 126.6, 128.0, 128.1, 129.3, 129.5, 131.4, 133.0, 133.4, 141.6, 142.4, 156.5. GC-MS (70 eV): m/z : 235 (76), 174 (100), 147 (26), 128 (35), 115 (33). Anal. Calcd. For $\text{C}_{12}\text{H}_{13}\text{NO}_2\text{S}$ (235.30): C: 61.25; H: 5.57; N: 5.95; O: 13.60; S: 13.63. Found: C: 61.17; H: 5.74; N: 5.58; O: 13.80; S: 13.71.



89e. Yield 0.134 g (42%). Clear yellow oil. IR (neat) ν : 700, 822, 1331, 1520, 2933 cm^{-1} . ^1H -NMR (DMSO- d_6 , 400MHz) δ : 2.37 (s, 3H), 2.66 (s, 4H), 5.37 (d, 1H, $J = 9.1$ Hz), 5.45 (s, 0.5H), 5.49 (s, 0.5H), 6.46-6.61 (m, 2H), 6.89-6.94 (m, 2H), 7.21-7.10 (m, 7H), 7.89 (s, 1H). ^{13}C -NMR (DMSO- d_6 , 100MHz) δ : 21.2,

29.9, 33.0, 122.0, 126.3, 126.8, 128.3, 128.4, 129.4, 129.5, 131.8, 132.9, 133.0, 136.0, 138.4, 140.1, 153.1. GC-MS (70 eV): m/z : 227 (100), 182 (92), 165 (50), 152 (17), 91 (58). Anal. Calcd. For $\text{C}_{21}\text{H}_{21}\text{NO}_2$ (319.40): C: 78.97; H: 6.63; N: 4.39; O: 10.02. Found: C: 79.11; H: 6.78; N: 4.15; O: 9.96.



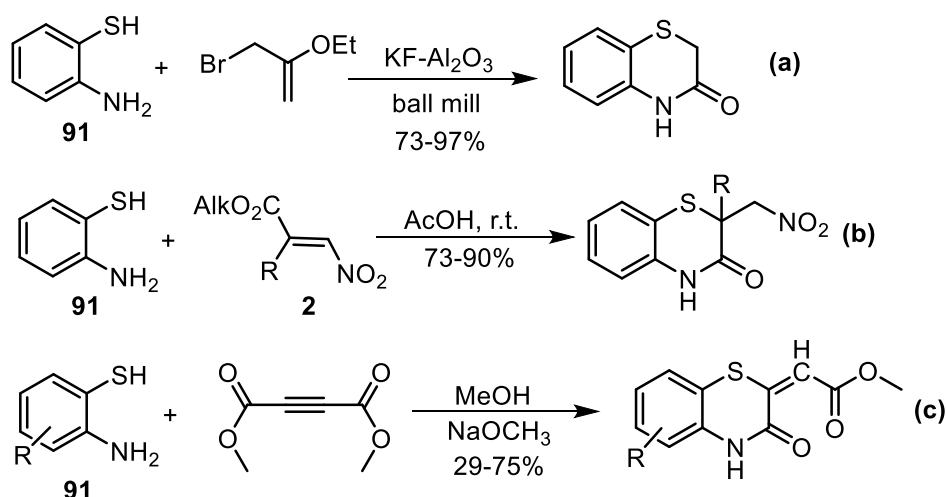
89f. Yield 0.122 g (39%). Yellow oil. IR (neat) ν : 787, 1083, 1287, 1522, 2938 cm^{-1} . $^1\text{H-NMR}$ (DMSO- d_6 , 400MHz) δ : 1.39-1.54 (m, 4H), 2.11-2.21 (m, 2H), 2.37 (t, 2H, $J = 7.5$ Hz), 3.83 (s, 3H), 5.45 (d, 1H, $J = 9.8$ Hz), 5.54 (d, 1H, $J = 15.8$ Hz), 6.52-6.72 (m, 2H), 6.82-6.97 (m, 3H), 7.29-7.40 (m, 1H), 7.97 (s, 1H). $^{13}\text{C-NMR}$ (DMSO- d_6 , 100MHz) δ : 16.7, 25.0, 26.2, 26.8, 55.4, 112.8, 113.6, 119.4, 121.4, 123.1, 130.0, 131.3, 132.5, 133.3, 134.5, 140.3, 153.0, 159.9. GC-MS (70 eV): m/z : 280 (100), 239 (58), 227 (56), 207 (94), 135 (67). Anal. Calcd. For $\text{C}_{18}\text{H}_{20}\text{N}_2\text{O}_3$ (312.37): C: 69.21; H: 6.45; N: 8.97; O: 15.37. Found: C: 69.37; H: 6.58; N: 8.70; O: 15.35.

1.5 Mild and economical one-pot synthesis of benzothiaziones from β -nitroacrylates

1.5.1 State of the art

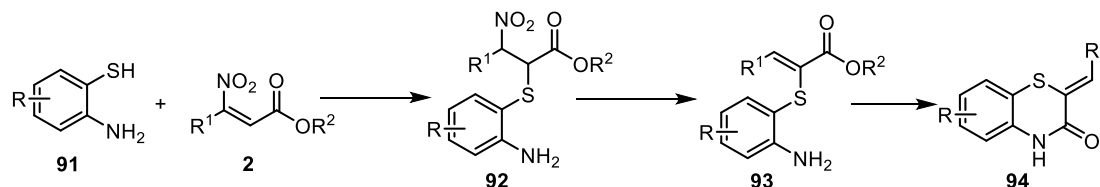
Tuberculosis (TB) is a leading cause of death in developing countries and a resurgent disease in developed countries.^[101] The synergetic effect between TB and human immunodeficiency virus (HIV) is frightening. In 2013, 1.5 million people died from TB, and 0.36 million of them were infected with both HIV and TB, according to the World Health Organization.^[102] In addition, an even more dangerous and completely incurable form of TB, known as totally drug-resistant TB, has been reported in Italy, Iran and India.^[103-105] Even though there are some drugs against TB such as isoniazid and rifampicin, the spread of multidrug-resistant and extensively drug-resistant strains of *Mycobacterium* TB worsens the situation.^[106] Based on the practical requirements, various studies have been conducted to find an anti-TB drug that works well against *Mycobacterium* TB. However, effective drug synthesis and subsequent clinical trials slow down the search for solutions. Previous studies have shown that compounds with benzothiazinone structure can inhibit *Mycobacterium* TB well *in vitro* and *in ex vivo* models of TB. In addition, benzothiazinones can be used as aldose reductase inhibitors, Ca^{2+} ion antagonists, K^{+} channel activators, anticonvulsants, anticancer agents, and immunostimulants.^[107, 108] Therefore, there is an urgent need for the development of new benzothiazinone compounds.

Now there are some related studies on the synthesis of benzothiazinones. Sharifi et al.^[109] developed a green and efficient reaction of 2-aminothiophenols **91** with 2-bromoalkanoates to obtain benzothiazinone. During the process, KF- Al_2O_3 support and ball milling can promote the reaction without the need of any solvent (Scheme 48a). Makarenko and co-workers^[110] proposed an efficient, sustainable one-pot synthesis of benzothiazinone using β -nitroacrylates **2** and **91**. The reaction takes only a few hours and gives excellent yields (Scheme 48b). Heindel and Reid^[111] propose **91** and dimethyl acetylenedicarboxylate as starting materials for benzothiazinones in moderate yield (Scheme 48c). The above reactions can generate benzothiazinones, but they also have drawbacks, such as long reaction time, limited substituents, or pretreatment before reaction, suggesting that the route to synthesize benzothiazinones needs further improvement.



Scheme 48. Typical routes for the synthesis of benzothiazinone derivatives.

Inspired by Makarenko et al.^[110], it was hoped to find a mild synthetic route for benzothiazinones by reaction of β -nitroacrylates with aminothiophenols. Since β -nitroacrylates **2** are conjugated olefins bearing two EWGs in α - and β -positions, it is straightforward to form adduct **92** by Michael addition with aminothiophenols **91**. After elimination of nitrous acid and intramolecular cyclization, benzothiazinones **94** can be successfully obtained via intermediate **93** (Scheme 49).



Scheme 49. Synthesis of benzothiazinones using β -nitroacrylates and aminothiophenols.

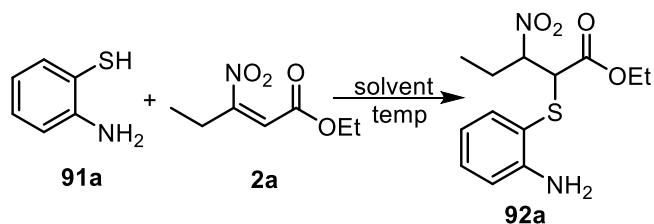
In this section, an economical and mild route for the synthesis of benzothiazinones via β -nitroacrylates and aminothiophenols is proposed inspired by the successful conversion of 2,5-disubstituted thiophenes from ketal-functionalized β -nitroacrylates and thioacetic acid.^[112] A variety of compounds with different substituents can be obtained in good overall yields under mild conditions.

1.5.2 Results and discussion

In order to find the optimized conditions, **2a** and **91a** were selected as models. The synthesis can be carried out in three steps: (i) Michael addition of β -nitroacrylate **2a** with aminothiophenol **91a** to afford adduct **92a**, (ii) elimination of nitrous acid to

generate **93a**, and (iii) intramolecular cyclization to form benzothiazinone **94a**. The flow chemistry approach using carbonate on polymer and A-15 has been attempted. Following the flow chemistry protocol in step i, **92a** was obtained with excellent yield in MeCN (84%, Table 5, entry 1). Unfortunately, the change of temperature and equivalent of carbonate on polymer caused the second step to give only 29% of the corresponding intermediate **93a** (Table 6, entries 1-3). We then proceeded to experiments in batch. Equimolar amounts of **2a** and **91a** can produce **92a** in moderate yield under neat condition (72%, Table 5, entry 2). And increasing the stoichiometry from 1 to 1.2 and 1.3 leads to the increasing and decreasing yields, respectively (Table 5, entries 3, 4). Higher temperature didn't show any improvement (Table 5, entry 5). Different solvents such as MeCN, toluene, EtOAc, DCM, 2-MeTHF were also tried to increase the yield. However, the reaction using the above solvents didn't work well. The most optimized condition for the first step was neat and the molar ratio between **2a** and **91a** is 1.2:1.

Table 5. The optimization of Michael addition conditions.



Entry	Ratio ^[a]	T °C	Yield ^[b] (%)
1	1:1	25	84 ^[c]
2	1:1	25	72
3	1.2:1	25	83
4	1.3:1	25	60
5	1.2:1	35	56

[a] Ratio was shown as **2a:91a**.

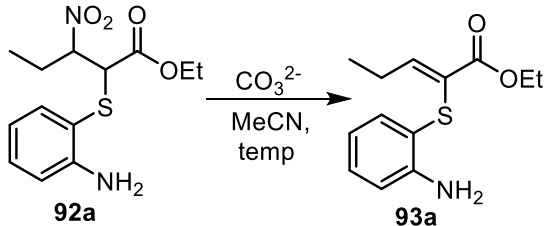
[b] Isolated yield after chromatography on silica gel.

[c] Flow chemistry.

In the second step, continued use of 2 equiv. of carbonate on polymer resulted in moderate yield (Table 6, entry 4). We then attempted to optimize the third step to convert **93a** to the target product **94a**. After several trials, the best yield was recorded in toluene at 100 °C and using 8 equivalents of A-15 (Table 7, entry 1). Considering

that the reaction was carried out under the conditions of neat, carbonate on polymer, A-15, the work-up only consists in a filtration and purification of the crude product by flash column chromatography.^[113] In order to further increase the efficiency of the protocol, the three steps can be combined into a one-pot process thus meeting the sustainability requirements of green chemistry processes.^[114] The total yield of **94a** calculated from the individual steps is 18%, but a yield of 38% was obtained after the one-pot synthesis. The result indicates that the one-pot synthesis can reduce the unnecessary losses. Moreover, changing R² from -Et to -Me led to a worse result (yield: 21%), so R² with -Et can be used for the next process of extending the substituents. A rapid and simple one-pot procedure was used to obtain a series of benzothiazinones with different substituents were obtained in moderate yield (Scheme 50). Moreover, trails with other substituents are also underway.

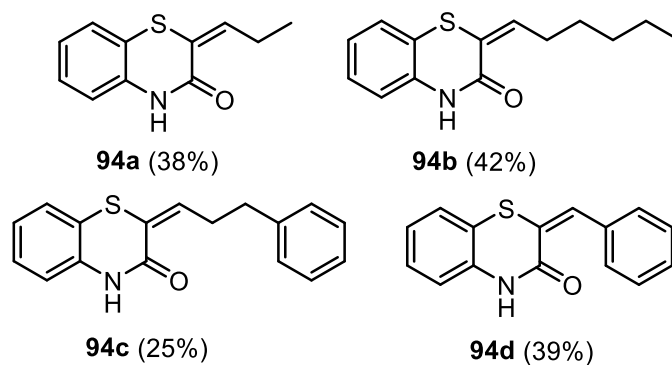
Table 6. The optimization of elimination of nitrous acid.



Entry	Amount of CO ₃ ²⁻	T °C	Yield ^[a] (%)
1	2 eq.	70	25 ^[b]
2	4 eq.	70	18 ^[b]
3	4 eq.	85	29 ^[b]
4	2 eq.	70	69

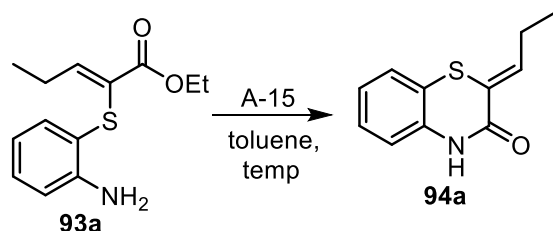
[a] Isolated yield after chromatography on silica gel.

[b] Flow chemistry.



Scheme 50. Obtained structures of benzothiazinones.

Table 7. The optimization of intramolecular cyclization.



Entry	Amount of A-15	T °C	Yield ^[a] (%)
1	8 eq.	100	32
2	10 eq.	100	29
3	10 eq.	90	22

[a] Isolated yield after chromatography on silica gel.

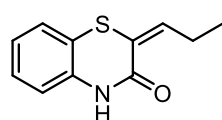
1.5.3 Conclusion

In general, the synthesis of the anti-TB agent benzothiazinones can be carried out with a one-pot procedure by reaction of β -nitroacrylates and aminothiophenols. The reaction involves a preliminary Michael addition between β -nitroacrylates and aminothiophenols, followed by the elimination of nitrous acid and intramolecular cyclization. A series of benzothiazinone derivatives can be obtained in moderate yield, and further trials will be undertaken in the future.

1.5.4 Experimental section

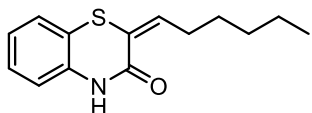
One pot synthesis of benzothiazinones (**94**): A mixture of β -nitroacrylates **2** (1.2 mmol) with aminothiophenols **91** (1 mmol) was stirred at r.t. for 7 hours to prepare **92**. To this mixture was added carbonate on polymer (2 mmol) in MeCN (15 mL) and the reaction was stirred at 70°C for another 2.5 hours. Accompanied with a simple filtration and removing solvent, A-15 (8 mmol) in toluene (15 mL) was added and reacted at 100°C for 16 hours. The residue was purified by silica gel column chromatographic (toluene:EtOAc, 95:5) after filtering and concentrating in vacuo.

Spectroscopic data for compounds **94**:

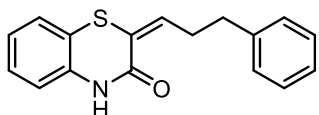


94a. Yield 0.078 g (38%). Yellow solid, mp: 119-122°C. IR (neat) ν : 680, 749, 1591, 1662, 2928 cm^{-1} . $^1\text{H-NMR}$ (DMSO- d_6 , 400MHz) δ : 1.17 (t, 3H,

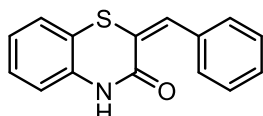
$J = 7.5$ Hz), 2.28-2.36 (m, 2H), 6.94 (d, 1H, $J = 7.9$ Hz), 6.98-7.05 (m, 2H), 7.12-7.22 (m, 2H), 9.53 (s, 1H). $^{13}\text{C-NMR}$ (DMSO- d_6 , 100MHz) δ : 12.6, 22.8, 117.0, 117.7, 120.5, 123.6, 125.5, 126.5, 134.0, 138.6, 161.2. GC-MS (70 eV): m/z : 205 ($[\text{M}^+]$, 100), 190 (25), 162 (27), 135 (18), 109 (8). Anal. Calcd. For $\text{C}_{11}\text{H}_{11}\text{NOS}$ (205.28): C: 64.36; H: 5.40; N: 6.82; O: 7.79; S: 15.62. Found: C: 64.77; H: 5.32; N: 6.99; O: 7.34; S: 15.58.



94b. Yield 0.104 g (42%). Yellow solid, mp: 67-70°C. IR (neat) ν : 680, 743, 1593, 1662, 2921 cm^{-1} . $^1\text{H-NMR}$ (DMSO- d_6 , 400MHz) δ : 0.93 (t, 3H, $J = 7.1$ Hz), 1.32-1.42 (m, 4H), 1.50-1.61 (m, 2H), 2.25-2.34 (m, 2H), 6.91 (d, 1H, $J = 8.0$ Hz), 6.98-7.06 (m, 2H), 7.11-7.23 (m, 2H), 9.32 (s, 1H). $^{13}\text{C-NMR}$ (DMSO- d_6 , 100MHz) δ : 14.0, 22.5, 27.8, 29.4, 31.6, 116.9, 117.8, 120.9, 123.6, 125.5, 126.4, 134.0, 137.7, 160.9. GC-MS (70 eV): m/z : 247 ($[\text{M}^+]$, 86), 185 (42), 177 (100), 164 (44), 109 (22). Anal. Calcd. For $\text{C}_{14}\text{H}_{17}\text{NOS}$ (247.36): C: 67.98; H: 6.93; N: 5.66; O: 6.47; S: 12.96. Found: C: 68.12; H: 6.77; N: 5.81; O: 6.28; S: 13.02.



94c. Yield 0.070 g (25%). Yellow solid, mp: 109-111°C. IR (neat) ν : 694, 741, 1591, 1660, 2979 cm^{-1} . $^1\text{H-NMR}$ (DMSO- d_6 , 400MHz) δ : 2.59-2.66 (m, 2H), 2.88 (t, 2H, $J = 7.7$ Hz), 6.92 (d, 1H, $J = 8.0$ Hz), 7.02 (t, 1H, $J = 7.6$ Hz), 7.08 (t, 1H, $J = 7.3$ Hz), 7.12-7.25 (m, 3H), 7.27-7.37 (m, 4H), 9.40 (s, 1H). $^{13}\text{C-NMR}$ (DMSO- d_6 , 100MHz) δ : 31.4, 34.4, 117.2, 117.8, 121.9, 123.9, 125.7, 126.4, 126.7, 128.6, 128.8, 134.1, 136.2, 141.1, 160.9. GC-MS (70 eV): m/z : 281 ($[\text{M}^+]$, 48), 190 (100), 162 (28), 91 (15). Anal. Calcd. For $\text{C}_{17}\text{H}_{15}\text{NOS}$ (281.37): C: 72.57; H: 5.37; N: 4.98; O: 5.69; S: 11.40. Found: C: 72.46; H: 5.18; N: 4.78; O: 5.97; S: 11.61.



94d. Yield 0.099 g (39%). Yellow solid, mp: 57-60°C. IR (neat) ν : 685, 744, 1368, 1661, 2916 cm^{-1} . $^1\text{H-NMR}$ (DMSO- d_6 , 400MHz) δ : 6.94 (d, 1H, $J = 7.9$ Hz), 7.04 (t, 1H, $J = 7.7$ Hz), 7.16-7.25 (m, 2H), 7.34-7.54 (m, 3H), 7.70 (d, 2H, $J = 7.6$ Hz), 7.98 (s, 1H), 9.23 (s, 1H). $^{13}\text{C-NMR}$ (DMSO- d_6 , 100MHz) δ : 116.8, 117.1, 120.2, 124.0, 125.7, 127.0, 128.7, 129.1, 130.4, 132.9, 134.9, 139.9, 160.8. GC-MS (70 eV): m/z : 253 ($[\text{M}^+]$, 100), 225 (30), 220 (46), 129 (18). Anal. Calcd. For $\text{C}_{15}\text{H}_{11}\text{NOS}$ (253.32): C: 71.12; H: 4.38; N: 5.53; O: 6.32; S: 12.66. Found: C: 71.45; H: 4.49; N: 5.28; O: 6.08; S: 12.70.

CHAPTER TWO

Synthesis of Unsymmetrical Bisindolylmethanes and Their Anti-cancer Activity Test

2.1 Synthesis of 3-(1-arylsulfonylalkyl) indoles and their applications

The indole skeleton is present in a large variety of compounds endowed of practical interest in the field of natural products, pharmaceuticals, agrochemicals, and material chemistry.^[115] Furthermore, the introduction of functionalized alkyl backbones at the 3-position of indole systems is a common practice for the synthesis of biologically active compounds. 3-(1-Arylsulfonylalkyl) indoles (sulfonyl indoles, **95**, Figure 2) are a typical class of 3-position indoles that can be used as starting materials for a variety of compounds.

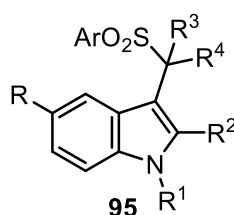
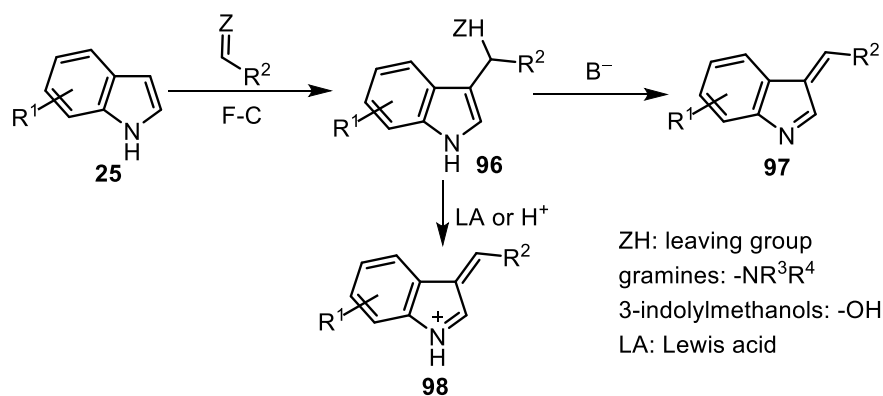


Figure 2. The structure of 3-(1-arylsulfonylalkyl) indoles.

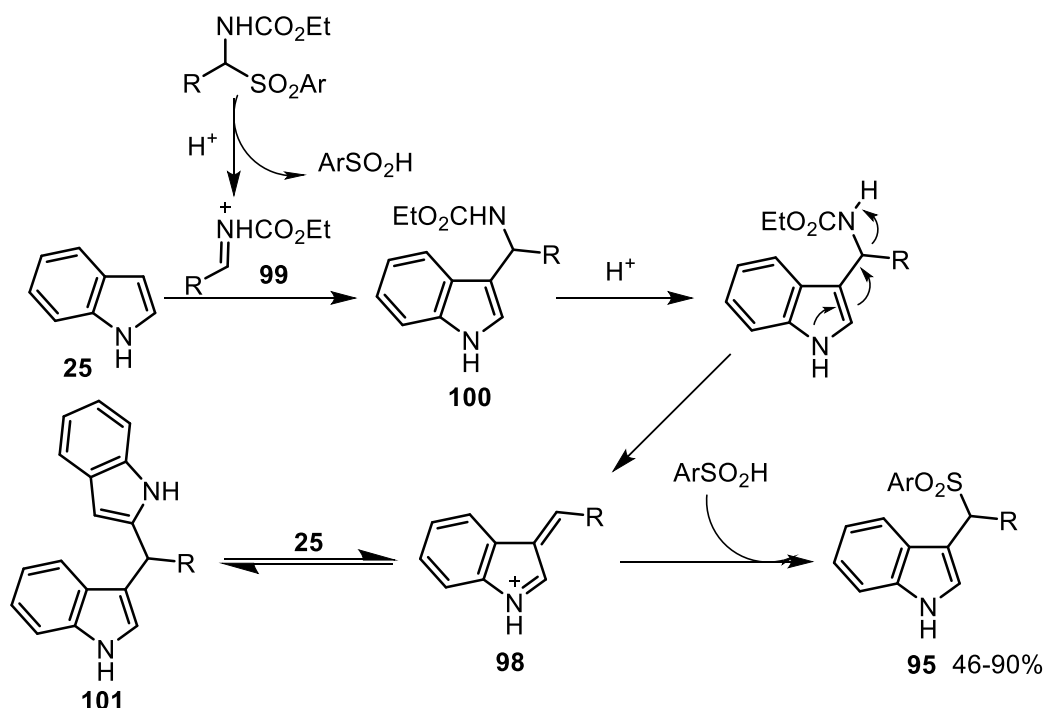
2.1.1 Synthetic routes for sulfonyl indoles

Derivatives of type **96**, which possess a good leaving group at the benzylic position, can be easily synthesized from indoles **25** and electrophilic reagents. They can be used as good precursors for introducing carbon frameworks at position 3. Under basic conditions, **96** can eliminate the leaving group and form an indolenine intermediate **97** that behaves like a vinylogous imine. Furthermore, **96** can also generate the indoleninium ion **98** in the presence of acid (Scheme 51). Compared to other related derivatives (*e.g.* gramines and indolylmethanols), sulfonyl indoles can readily and efficiently eliminate the leaving group under mild and controlled conditions. Therefore, sulfonyl indoles have a wider range of applications, and it is very important to discover an efficient and simple synthetic route for sulfonyl indoles.



Scheme 51. General reactivity of indole functionalization.

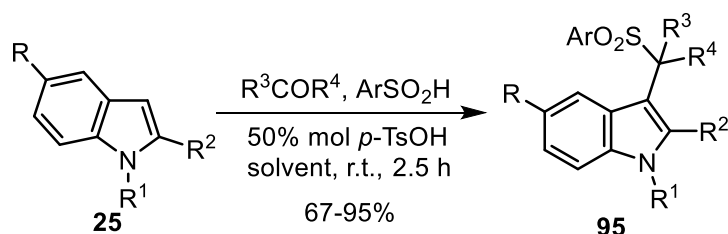
Petrini et al.^[116] aimed to use α -amido sulfone and indole **25** to prepare gramine derivative **100** in the presence of an acid-promoter. However, sulfonyl indoles **95** were obtained instead of the expected **100**. The presumed mechanism would involve: (i) acid-promoted elimination of arylsulfonic acid to form the *N*-acyliminium ion intermediate **99**, which can react with indole **25** to afford gramine derivative **100** (not isolated); (ii) protonation and elimination of ethyl carbamate to generate the indoleninium ion **98**; (iii) **98** can react with another molecule of **25** to form bisindoles **101**, or intercept the previously released sulfonic acid to produce sulfonyl indoles **95** (Scheme 52). If the reaction is stopped after 0.5 h, a great amount of bisindoles **101** can be isolated; however, sulfonyl indole is the only product if the reaction time is extended to 3 h. During the process, the best result was recorded at 55°C, montmorillonite K-10 as acid, and SolFC. In addition, a wide range of sulfonyl indoles can also be prepared with excellent yields. Later, Thirupathi and Kim^[117] also performed the synthesis of sulfonyl indoles using the same starting materials and under the conditions of 10% indium bromide as acid, DCM as solvent and at room temperature.



Scheme 52. A plausible mechanism for the formation of sulfonyl indoles.

Considering the existence of bisindole and the conclusion that aldehydes can

react with indole to form bisindolyl derivatives under acidic conditions,^[118] Palmieri and Petrini^[119] attempted to synthesize sulfonyl indoles from indoles and carbonyl compounds. Under F-C conditions, carbonyl compounds can react with indoles **25** to give bisindoles **101** as the main products. The formation of **101** is possible because the vinylogous iminium ion **98** reacts with a second molecule of indole. Therefore, arylsulfonic acids act as promoters and nucleophiles that effectively capture the intermediate iminium ion **98**. Moreover, the acidity provided by arylsulfonic acids generally cannot efficiently decompose the intermediate bisindoles **101**. To ensure a better yield of product **95**, *p*-toluenesulfonic acid must be added. Finally, after mixing indoles **25** with an appropriate carbonyl derivative and arylsulfonic acids in the presence of *p*-toluenesulfonic acid (50% mol), the formation of sulfonyl indoles **95** can be observed in good yield after 2.5 hours (Scheme 53).



Scheme 53. Synthesis of sulfonyl indoles by condensation of carbonyl derivatives and indoles.

In this thesis, we continued to use the above procedures to prepare sulfonyl indoles due to its convenience, simplicity and efficiency.

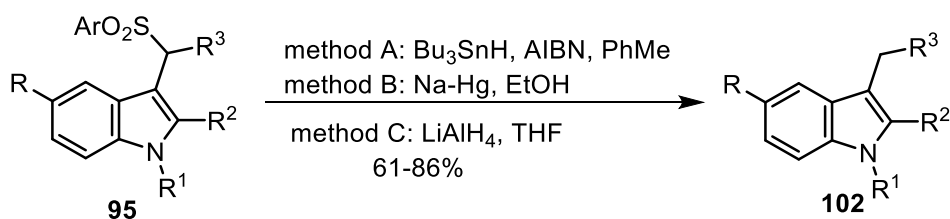
2.1.2 Applications of sulfonyl indoles

Gramine (ZH: -NR³R⁴, Scheme 51) and 3-indoylmethanol (ZH: -OH, Scheme 51) are good precursors of indolenine intermediate **97** and indoleninium ion **98**. However, the leaving group aptitude of secondary amines is too low to form **97** under mild conditions. Therefore, nucleophilic substitution on gramines always requires high temperatures or activating procedures to convert the tertiary amino group to an ammonium salt.^[120] Moreover, 3-indoylmethanol always needs to introduce aryl substituents into the side chain or use tertiary alkanols to generate indoleninium ion **98**. In comparison, sulfonyl indoles have the well-known ability of the arenesulfonyl moiety to serve as a good leaving group under both acidic and basic conditions. After elimination, sulfonyl indoles can lead to vinylogous *N*-acilimino species, which can be advantageously used for reaction with various nucleophilic systems. Therefore,

sulfonyl indoles can be regarded as excellent materials for 3-alkylindoles, 3-indolyesters, indolylalkylphosphonates, carbazoles, etc.

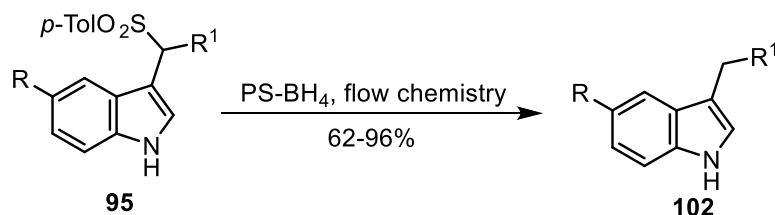
2.1.2.1 Synthesis of 3-alkyl and 3-aryl indoles

The first synthetic application of sulfonyl indoles **95** was performed with reducing agents in an attempt to replace the sulfonyl group with a hydrogen atom.^[121] Desulfonylation reactions can be carried out under different conditions, including radical-induced processes with Bu_3SnH or Na-Hg amalgam or using complex hydrides. All of these methods are effective, yielding desulfonylated compounds **102** (Scheme 54). Clearly, LiAlH_4 is preferable for practical reasons because of its low toxicity relative to other tested reactants.^[116]



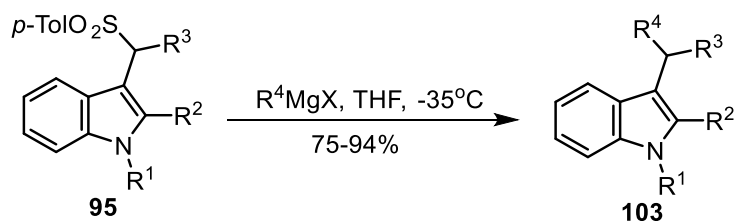
Scheme 54. Reductive desulfonylation of sulfonyl indoles under various conditions.

Our laboratory found that the reduction of sulfonyl indoles **95** was more suitable using polymer-supported sodium borohydride and flow chemical conditions (Scheme 55).^[122] Under optimized reaction conditions, various 3-alkylindoles **102** can be obtained in good yield by solvent evaporation and column chromatography if necessary. This procedure increases the sustainability of the process to suppress the solvent consumption and work up operations.



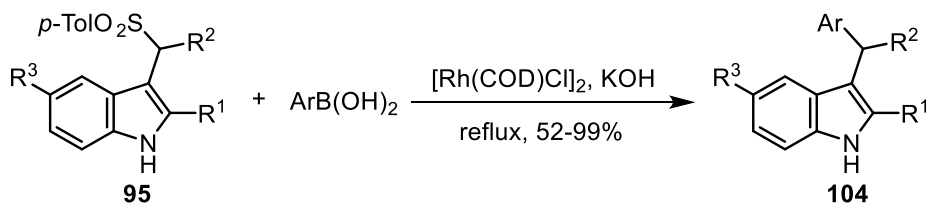
Scheme 55. Reduction of various sulfonyl indoles under flow conditions.

As shown in Scheme 56, Grignard reagent acts both as a base, providing the elimination of arylsulfonic acid, and as a nucleophile, leading to the efficient formation 3-allylindoles **103**.^[116]



Scheme 56. Reaction of sulfonyl indoles with Grignard reagents.

Zhou et al.^[123] developed an efficient rhodium-catalyzed addition reaction of arylboronic acids to novel electrophiles generated in situ from sulfonyl indoles. This strategy provided a readily access to the relevant C-3 *sec*-alkyl-substituted indoles **104** in moderate to high yields with various substrates (Scheme 57). The asymmetric version of this process has been attempted with slightly different catalyst, use of Pd(II)-based catalysts in this process is also effective if a phosphine ligand is applied in the reaction.^[124]



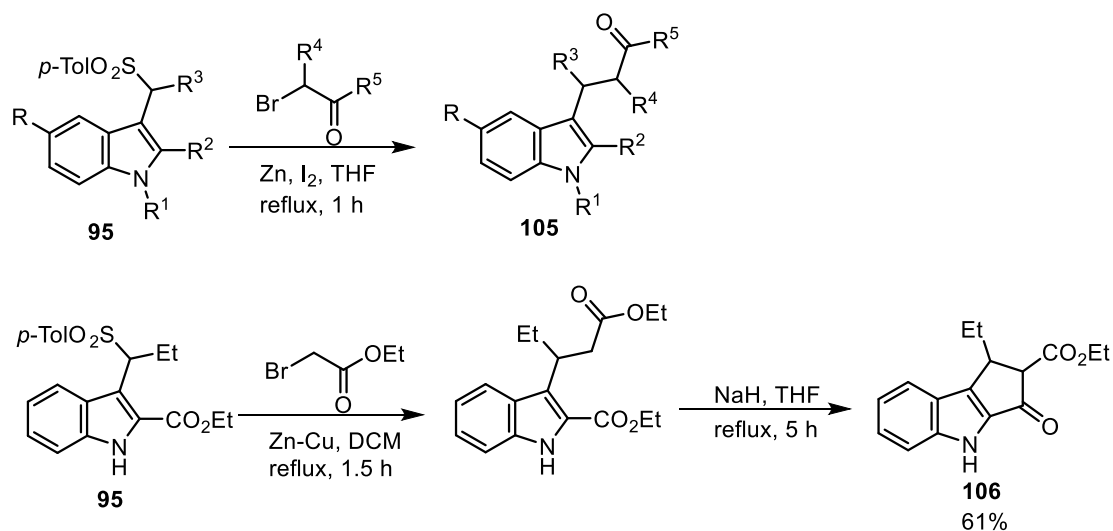
Scheme 57. Rhodium-catalyzed asymmetric addition of arylboronic acids to sulfonylindoles.

2.1.2.2 Reaction with Reformatsky reagents and the preparation of Tryptophols

Reformatsky reaction, an organic reaction involving α -halo esters and aldehydes or ketones, can form β -hydroxy esters in the presence of metallic zinc.^[125] The essence of this reaction is the promotion of Reformatsky enolates, which are formed from a α -halo ester with zinc dust. Compared to lithium enolates and Grignard reagents, Reformatsky enolates are less reactive, so nucleophilic addition to the ester group does not occur in the Reformatsky reaction.

A THF solution of sulfonyl indoles **95** was refluxed with 2-bromo carbonyl compounds for 1 h in the presence of zinc metal and a catalytic amount of iodine ensures a complete conversion of indoles **95** to the corresponding **105**.^[119] However, 3-sulfonyl indoles with $-\text{CO}_2\text{Et}$ at position 2 were less reactive under the above Reformatsky reaction conditions. To obtain the desired diesters, another form of activated zinc is required, as the zinc copper couple refluxed in DCM (Scheme 58).^[126] These 1,6-difunctionalized derivatives are ideal substrates for the Dieckmann

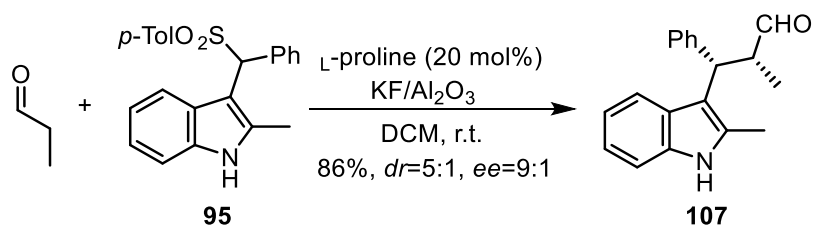
condensation that can be performed using sodium hydride in THF at reflux to generate β -keto ester **106**. They are key intermediates for the synthesis of tetracyclic lactam compounds that are of potential interest as neurotransmitters.^[127]



Scheme 58. Reformatsky reaction of sulfonyl indoles with 2-bromo carbonyl derivatives.

2.1.2.3 Reaction with enolate systems

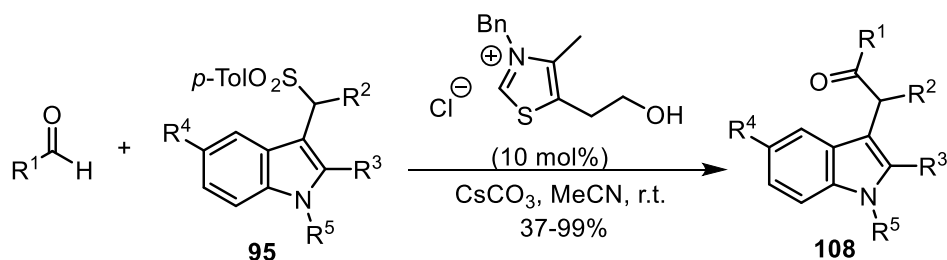
Petrini et al.^[128] tested the behavior of sulfonyl indoles **95** in the reaction with aldehydes under enantioselective enamine catalysis. Preliminary results show that among the organic or inorganic bases tested, only KF basic alumina can promote the in situ formation of the electrophilic compound from **95**. Concerning the organocatalyst used, *L*-proline can readily give the related 3-indolyl derivatives **107** with high diastereo- and enantio-control, giving these compounds an easy alternative to the classical Friede-Crafts route (Scheme 59).



Scheme 59. Enantioselective addition of aldehydes to sulfonyl indoles catalyzed by *L*-proline.

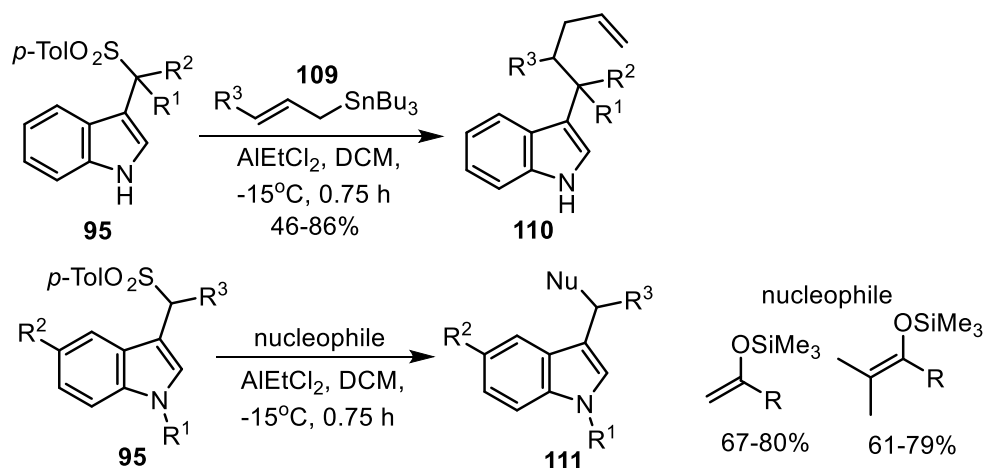
Subsequently, You and co-workers^[129] developed a highly efficient NHC-catalyzed intermolecular Stetter-type reaction with aldehydes and a novel electrophile generated from sulfonyl indoles **95**, providing a convenient route to the related 3-indolyl derivatives. This reaction provides α -(3-indolyl) ketone derivatives **108** in high yields for a variety of substrates using commercially available catalysts

and mild reaction conditions (Scheme 60).



Scheme 60. Enantioselective reaction of aldehydes with sulfonyl indoles.

In the presence of Lewis acids, sulfonyl indoles **95** are able to generate reactive vinylogous iminium ions, which can react with allylating reagents **109** to form indole derivatives **110**.^[130] Among the classical Lewis acids tested, AlCl₃ gave a promising result at -40°C, and increasing the temperature or prolonging the reaction time was ineffective to improve the chemical yield. It is known that the strength of aluminium-based Lewis acids can be appropriately adjusted by introducing alkyl substituents on the metal. The process was consistently improved using two equivalents of AlEtCl₂ when performed at -15°C. The generality of this method is demonstrated by the large number of substituted sulfonyl derivatives available for this reaction. In addition, a more direct introduction of useful functional groups was also sought by using silyl enol ethers that are compatible with the Lewis acid used, and the reaction were effective, yielding valuable functionalized indole derivatives **111** in satisfactory yields (Scheme 61).

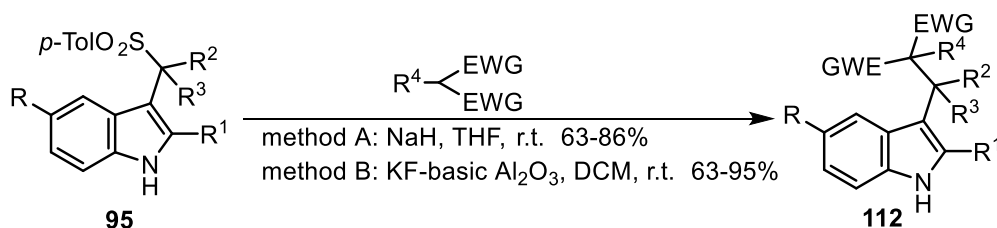


Scheme 61. The reaction of sulfonyl indoles with allylating reagents and silyl enol ethers.

2.1.2.4 Reaction with malonates and related derivatives

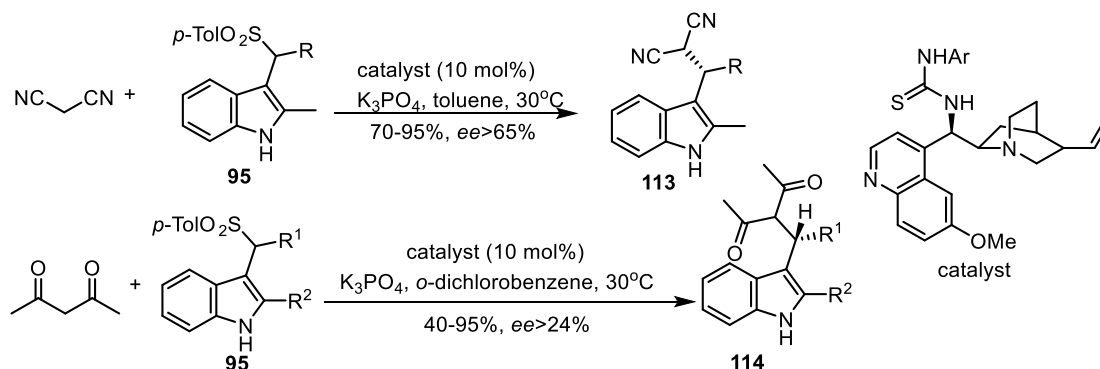
The effectiveness of KF-basic alumina as a promoter for the nucleophilic

additions of sulfonyl indoles **95** was subsequently tested using active methylene reagents.^[131] The results obtained using heterogeneous basic promoter (KF-basic alumina, DCM at room temperature, method B, Scheme 62) were compared with those acquired using NaH in THF at room temperature (method A, Scheme 62), show higher activity of the previous system for the production of adducts. The resulting 3-indolyl derivatives **112** are key intermediates in the synthesis of indole-based alkaloids and amino acids.



Scheme 62. Base-promoted additions of active methylene compounds to sulfonyl indoles.

Chiral thiourea derivative catalyzed the first highly enantioselective Michael addition of malononitrile to vinylogous imine intermediates which are generated in situ from arylsulfonyl indoles **95**. This organocatalytic route provides a simple and convenient way for 3-indolyl derivatives **113** with high yields and enantioselectivities.^[132] Under the similar reaction conditions (except solvent), a pair of β -diketones were added to **95** (Scheme 63).^[133] A series of optically active C3-alkyl-substituted indole derivatives **114** were obtained, and the resulting adducts can be easily converted into 3-*sec*-alkyl-substituted indoles containing a pyrazole skeleton, with direct connection between the α - and 4-positions, without affecting the enantioselectivity.

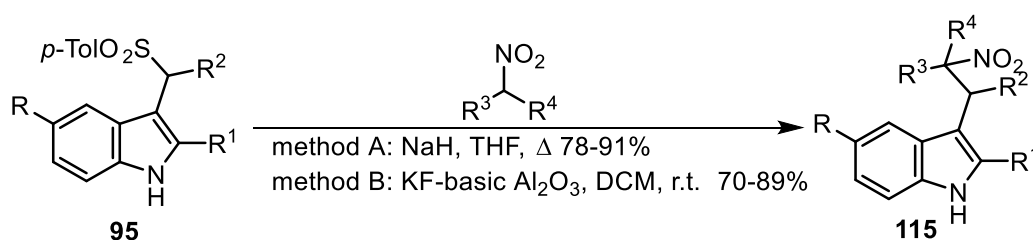


Scheme 63. Enantioselective addition of malononitrile or β -diketones to sulfonyl indoles.

2.1.2.5 Reaction with nitroalkanes

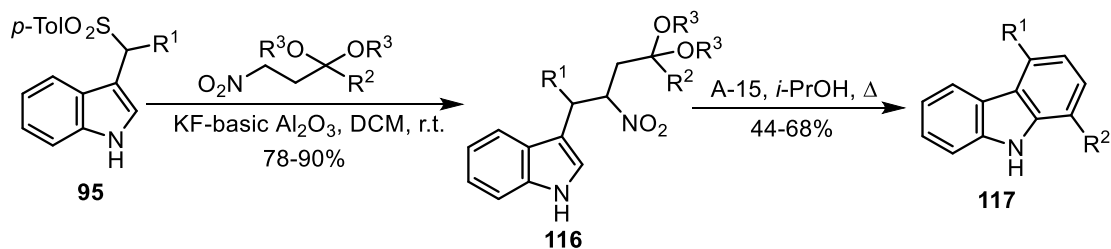
Using a wide range of bases, nitroalkanes can be easily converted to the

corresponding nitronate anions, which are then used as efficient nucleophiles with carbonyl groups, Michael acceptors and other electrophilic substrates.^[134] Furthermore, once the nitro group is introduced into a molecular backbone, it can undergo various synthetic transformations, including reduction, conversion to carbonyls and reductive removal. As shown in Scheme 64, nitroalkanes can be added to sulfonyl indoles **95** to form nitroindole derivatives **115** in the presence of sodium hydride or KF-basic alumina.^[131, 135] The obtained nitroindole derivatives **115** are key intermediates for the synthesis of tryptamines, β -carbolines, and other biologically active compounds, which can be obtained by preliminary reduction of the nitro group to a primary amine.^[136]



Scheme 64. Addition of nitroalkanes to sulfonyl indoles.

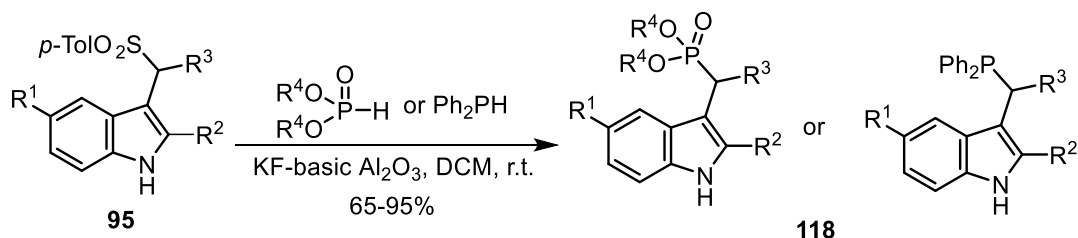
Carbazoles are tricyclic heteroaromatic compounds with a central pyrrole ring, which have considerable practical applications. Following the common strategy, symmetrical carbazole derivatives can be prepared in good yields; however, the synthesis of unsymmetrical carbazoles is still facing challenges. Petrini et al.^[137] proposed an efficient way to prepare carbazoles **117** from sulfonyl indoles **95** and nitro acetals which can protect the carbonyl group in β -nitro ketones and avoid initial *retro*-Michael reaction of β -nitro ketones under basic conditions.^[138] As shown in Scheme 65, nitro acetals can be reacted with sulfonyl indoles **95** in the presence of KF-basic alumina to afford adducts **116** in good yield. After acetal cleavage, Friedel-Crafts reaction, and final aromatization, carbazoles **117** was obtained by refluxing in isopropanol using A-15 as the proton source with satisfactory results. Therefore, unsymmetrical 1,4-disubstituted carbazoles can be easily prepared in moderate yields by a two-step procedure starting from sulfonylindoles **95**. Each step is performed under heterogeneous conditions, so that work-up would be minimized and isolation is only required to obtain the target carbazole.



Scheme 65. Synthesis of carbazoles from sulfonyl indoles.

2.1.2.6 Reaction with heteronucleophiles

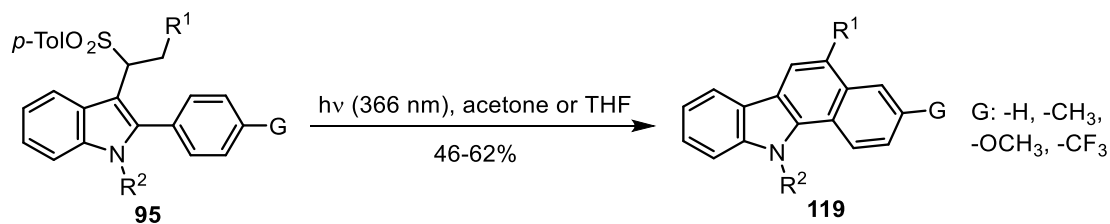
The base-promoted hydrophosphonylation of electrophilic compounds represents a viable approach to introducing a phosphonyl group into a wide range of functionalized substrates. Indoles bearing an alkylphosphonyl substituent at the 3-position have consistent pharmacological activity. In addition, these derivatives are also key intermediates in the synthesis of biologically active compounds. The use of dialkyl phosphites or diphenylphosphine as heteronucleophiles in the reaction with sulfonyl indoles **95** also successfully provided the corresponding indolylalkylphosphonates **118** (Scheme 66).^[139] KF-basic alumina at room temperature acts as an efficient basic promoter in this process, yielding good to excellent results.



Scheme 66. Addition of dialkyl phosphites or diphenylphosphine to sulfonyl indoles.

2.1.2.7 Photochemical reactions

Palmieri and co-workers^[140] discovered a general photochemical synthesis of benzo[*a*]-carbazoles **119** from the easily synthesized 2-aryl sulfonyl indoles **95**. The reaction is a one-pot process involving photochemical (initial C-S bond homolysis and $6\pi\epsilon$ electrocyclicization) as well as thermal steps. Irradiation of **95** in polar aprotic solvents (acetone or THF) selectively afforded the target products **119** in satisfactory yields (Scheme 67). This versatile and efficient procedure promises to be a useful alternative to the multi-step strategies reported in the literature.



Scheme 67. Photochemical synthesis of benzo[*a*]carbazole.

2.2 Synthetic routes to bisindolymethanes

As indole derivatives, bisindolymethanes consist of two indole units that can be linked by a simple or a substituted methylene bridge.^[141] Bisindolymethanes have the ability to regulate plant growth. Furthermore, they can protect and cure cancer in various organs such as breast, uterus, forestomach and liver, by inducing apoptosis.^[142] Therefore, research on bisindolymethanes has gradually increased in recent years.

The most common bisindolymethanes are 3,3'-bisindolymethanes, although 3,2'-bisindolymethanes are also available. In addition, bisindolymethanes can be divided into symmetrical and unsymmetrical depending on their structure. They can be prepared from aldehydes, ketones, alcohols, amines, alkynes, alkenes and other materials.

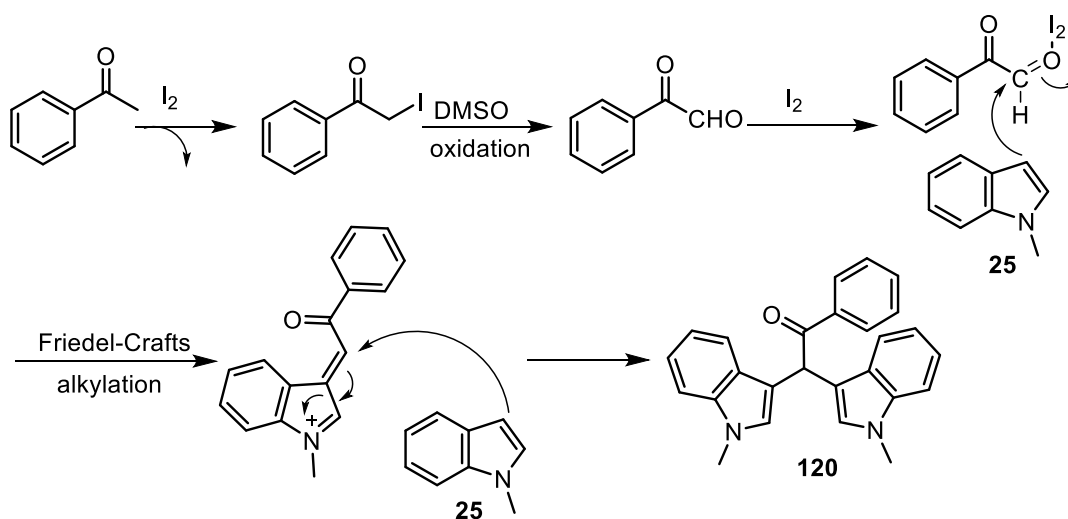
2.2.1 Synthesis of symmetrical bisindolymethanes

2.2.1.1 Synthesis from aldehydes or ketones and indoles

Fischer first prepared bisindolymethane in 1886. The standard method for the synthesis of bisindolymethane is the Friedel-Crafts reaction of indoles and carbonyl compounds in the presence of acid or base. In the presence of an acid catalyst, indoles can react with aliphatic or aromatic aldehydes or ketones to form vinylogous iminium ion **98**. Then **98** can be further added to a second indole molecule to generate bisindolymethanes **101**.^[143]

Wu et al.^[144] developed a protocol for the synthesis of bisindolymethanes **120** via I₂-promoted sp³ C-H dual-(het)arylation of simple and readily available aryl methyl ketones and indole derivative **25**. During the transformation, three mechanistically distinct reactions (iodination, Kornblum oxidation and Friedel-Crafts alkylation) are operative in the reacting system (Scheme 68). Notably, the reaction works well in the absence of any metals, bases or ligands. Due to the above characteristics of this

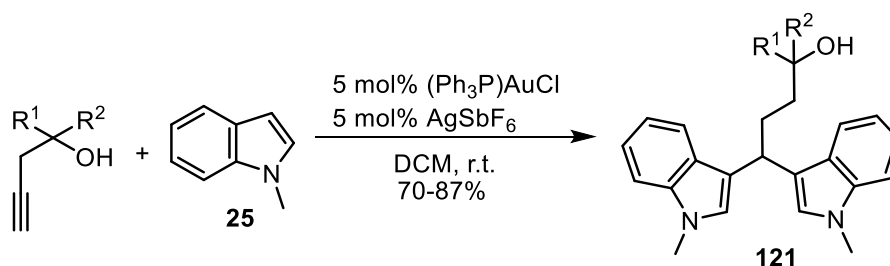
reaction, it should be of great use in organic chemistry.



Scheme 68. Synthetic routes for bisindoylmethane.

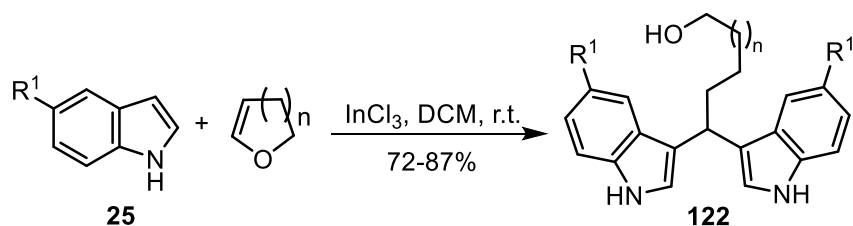
2.2.1.2 Synthesis from indoles and alkynes or alkenes

The reaction of indoles with π -bonds opens up a new route for the synthesis of various indole compounds. Barluenga's group^[145] explored the reaction of 3-butyn-1-ol derivatives with *N*-methylindole **25** to form **121** via a catalytic amount of in situ formed cationic gold complex. When terminal alkynes are used, the double addition of indoles occurs at the terminal carbon of the triple bond. When using an internal alkyne, a double addition occurs to the carbon at the end of the free hydroxyl group (Scheme 69).



Scheme 69. Gold(I)-catalyzed reaction of alkynol derivatives and indole.

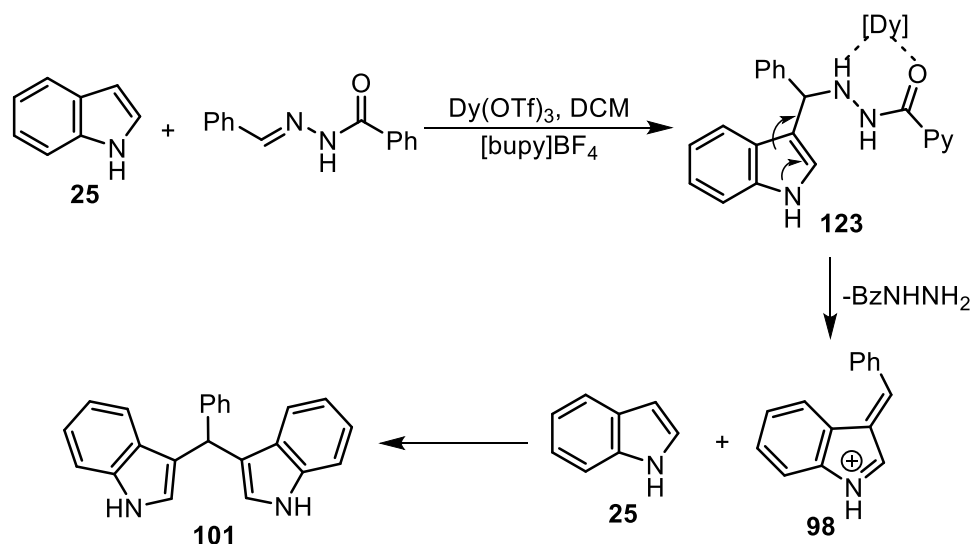
Indole and 5-substituted indoles such as 5-bromo and 5-methoxy derivatives have been reported to react with 3,4-dihydro-2*H*-pyran (DHP) or 2,3-dihydrofuran in the presence of InCl_3 . The corresponding bisindoylmethanes **122** were obtained in 72-87% yield (Scheme 70).^[146]



Scheme 70. Synthesis of bisindolmethanes.

2.2.1.3 Synthesis from imino derivatives and indoles

Benzoylhydrazone easily reacts with indole to generate **101** as the sole product after 24 hours in the presence of ionic liquid 1-butylpyridinium tetrafluoroborate [bupy]BF₄ and catalyst Dy(OTf)₃. In the proposed mechanism, the indole-imine adduct **123** undergoes elimination to yield the benzylidene-indole intermediate **98**, which then reacted with a second molecule of indole to produce **101** (Scheme 71).^[147]

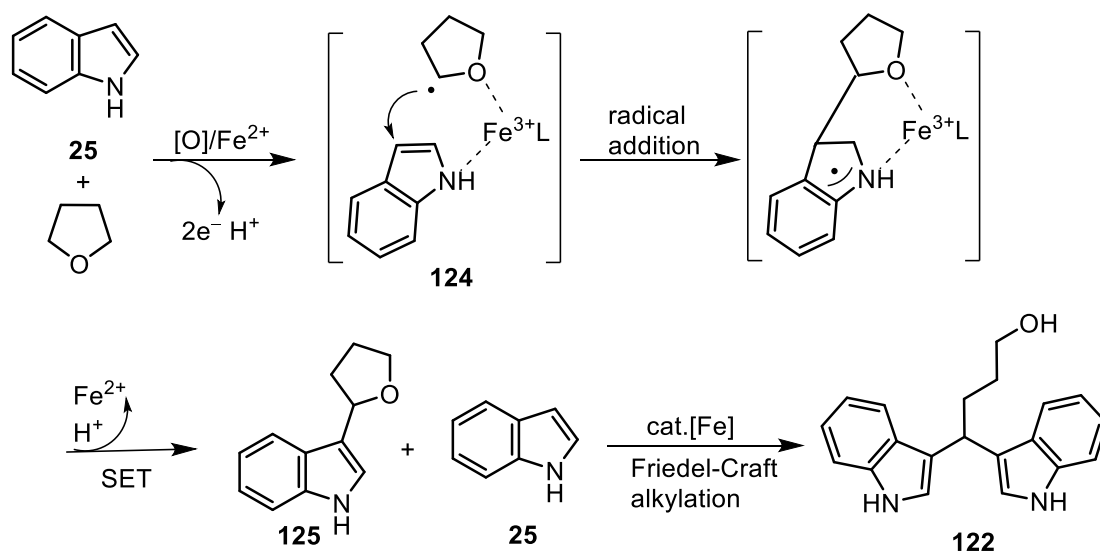


Scheme 71. Dy(OTf)₃ catalyzed reactions of indole with imines in [bupy]BF₄.

2.2.1.4 Synthesis from indoles bearing other functional groups

An efficient protocol to synthesize symmetrical bisindolmethanes by iron-catalyzed C-H bond oxidation and C-O bond cleavage between indole and THF was proposed by Li et al.^[148]. The plausible mechanism for this reaction would involve the H-abstraction from THF to generate a radical intermediate, which forms a complex **124** with indole **25** and iron(II). The product **125** can be isolated after radical addition and oxidative coupling of two organic ligands, the corresponding bisindolmethanes **122** are formed via Friedel-Crafts alkylation (Scheme 72). Notably, the addition of a different indole to product **125** resulted in unsymmetrical

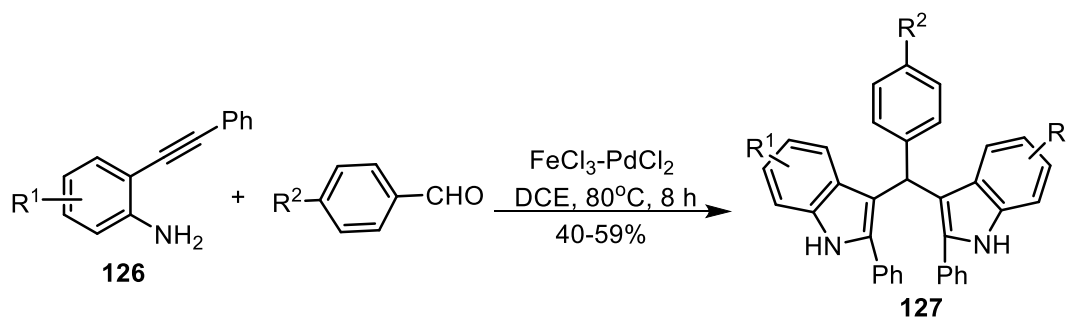
bisindolylmethane derivatives.



Scheme 72. Mechanism for the formation of bisindolylmethanes.

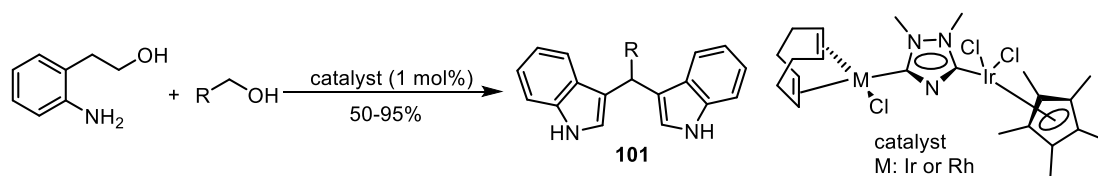
2.2.1.5 Miscellaneous methods for the synthesis of symmetrical bisindolylmethanes

Campagne et al.^[149] reported the selective synthesis of N-H indoles from the parent aniline **126** using a novel $FeCl_3$ - $PdCl_2$ catalytic combination in dichloroethane (DCE) (Scheme 73). Low loadings of transition metal complexes have been shown to be effective in annulation reactions. A one-pot annulation/Friedel-Crafts alkylation and annulation/1,4-Michael addition sequences were successfully developed, providing a route to bisindolylmethanes **127**.



Scheme 73. Synthesis of bisindolylmethanes from aniline.

In 2008, Peris et al.^[150] reported a one-pot synthesis of **101** via the oxidative cyclization of 2-aminophenyl ethyl alcohol to indole, followed by the alkylation of the resulting indole by aldehydes that were obtained from the in situ oxidation of alcohols. The reaction is catalyzed by dinuclear complexes of 1,2,4-trimethyltriazolium and iridium-rhodium. Alkylated indole **101** is the product of these reactions (Scheme 74).



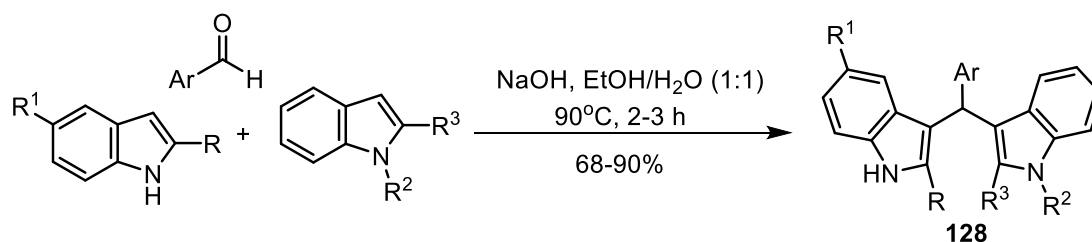
Scheme 74. Conversion of amino alcohol to bisindolymethanes.

2.2.2 Synthesis of unsymmetrical bisindolymethanes

Compared to symmetrical bisindolymethanes, unsymmetrical bisindolymethanes contain non-identical units of the indole ring. Under the conventional synthetic conditions for symmetrical bisindolymethanes, the introduction of two different structural indoles leads to a mixture of different cross-coupled products. Therefore, a viable alternative should be presented. Indolymethanols, indolymethanamine derivatives, 3-vinylindoles, indolymethanthio derivatives and other materials can successfully synthesize unsymmetrical bisindolymethanes.

2.2.2.1 Direct three-component coupling

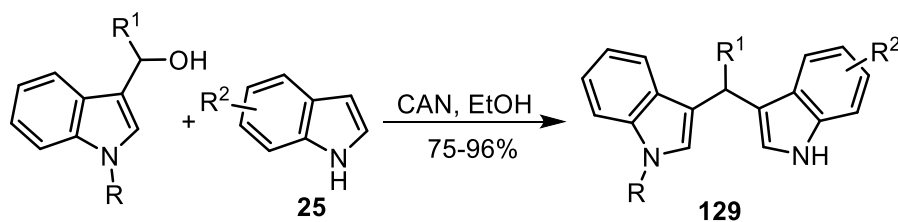
Baruah et al.^[151] proposed a 3-component cascade approach for the synthesis of unsymmetrical bisindolymethanes **128**. The reaction was promoted by sodium hydroxide in mixed solvent (EtOH:H₂O/ 1:1) at 90°C and finally produced the target in excellent yield (Scheme 75). However, electron-rich aldehydes gave few amount of symmetrical bisindolymethane, which limited the application of this method.



Scheme 75. Synthesis of unsymmetrical bisindolymethanes.

2.2.2.2 Synthesis from indolymethanols

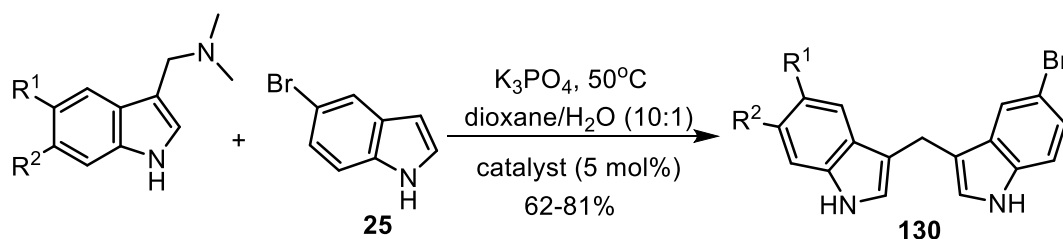
Nucleophilic substitution of alcohols with indoles typically results in alkylation of the indoles. Ji and co-workers^[152] performed the reaction between indoles **25** and (1H-indol-3-yl)(alkyl) methanols to afford the unsymmetrical bisindolymethanes **129** in good to excellent yields (Scheme 76). The reaction was efficiently catalyzed by ceric ammonium nitrate (CAN) under ultrasonic irradiation at room temperature.



Scheme 76. CAN-catalyzed unsymmetrical bisindolymethanes.

2.2.2.3 Synthesis from indolylmethanamine derivatives

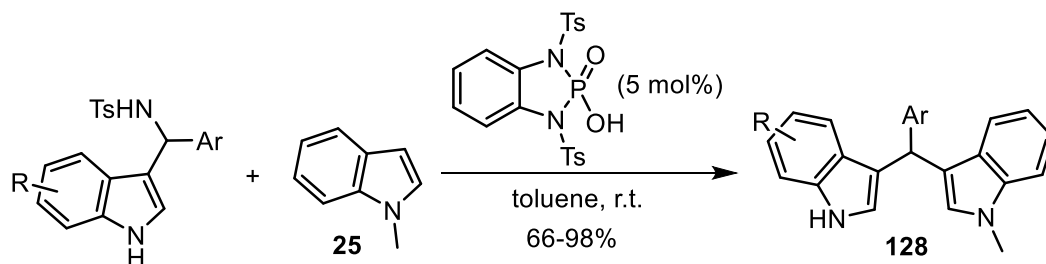
Starting from gramines and 5-bromoindole **25** in the presence of Ir(I) or Rh(I) as catalysts, a new family of unsymmetric bisindolymethanes **130** was generated (Scheme 77).^[153] This reaction is attractive to synthetic chemists because gramines are readily prepared by the Mannich reaction, and other materials are readily available. The reaction is also popular because it can be carried out in aqueous media, which helps to design efficient manufacturing processes.



catalyst, [(cod)RhCl]₂; [(cod)Rh]BF₄; [(cod)IrCl]₂;

Scheme 77. Gramines in the preparation of unsymmetrical bisindolymethanes.

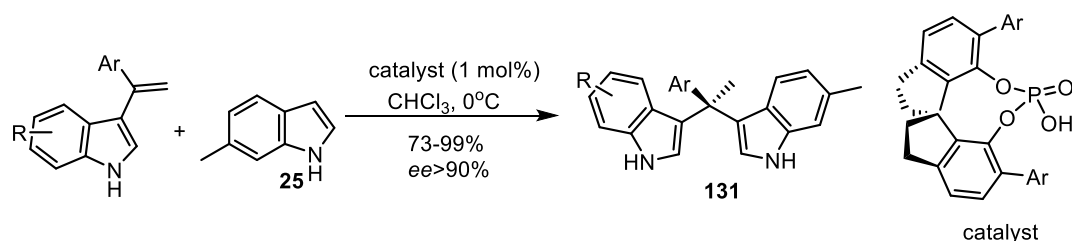
The conversion of amino to amido derivatives can increase the leaving group aptitude. Therefore, the reaction between *N*-tosyl-3-indolylmethanamines and indole derivatives **25** can generate unsymmetrical bisindolymethanes **128** with excellent yields under the conditions of using phosphoric acid in toluene at room temperature (Scheme 78).^[154]



Scheme 78. Synthesis of unsymmetrical bisindolymethanes.

2.2.2.4 Synthesis from 3-vinylindoles

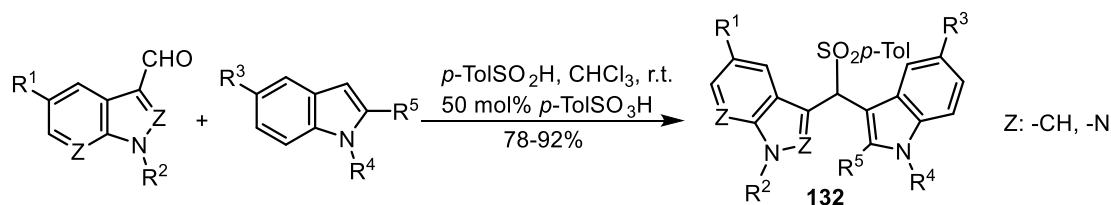
The protonation of 3-vinylindoles forms a benzylic-type carbocationic, that can react with indole **25** to afford unsymmetrical bisindolymethanes **131** in the presence of chiral phosphoric acid (Scheme 79).^[155] The yields of the target are 73-99% and the ees are higher than 90%, excellent yields and enantioselectivities show that the reaction can be performed in an atom-economical manner.



Scheme 79. Synthesis of unsymmetrical bisindolymethanes from 3-vinylindoles.

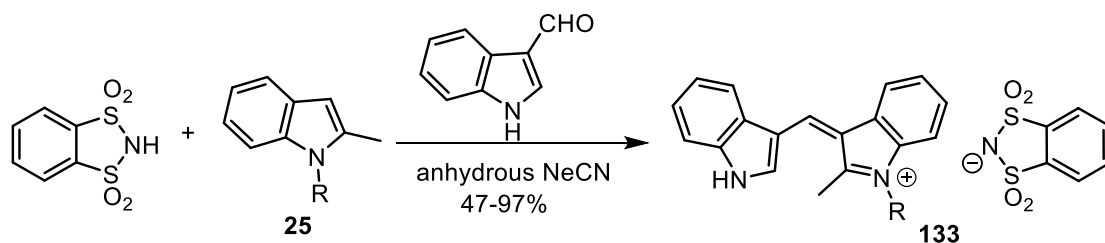
2.2.2.5 Synthesis from indolymethanthio derivatives

As the three-component coupling route for sulfonyl indoles, 3-formylindoles can be used as the carbonyl derivative to synthesize unsymmetrical bisindolymethanes **132** in good yield (Scheme 80).^[156] In addition, this simple, feasible and efficient method can also be applied to 3-formylindazoles and 3-formyl-7-azaindole derivatives.



Scheme 80. Synthesis of (arylsulfonyl)bisindolymethanes from three-component coupling.

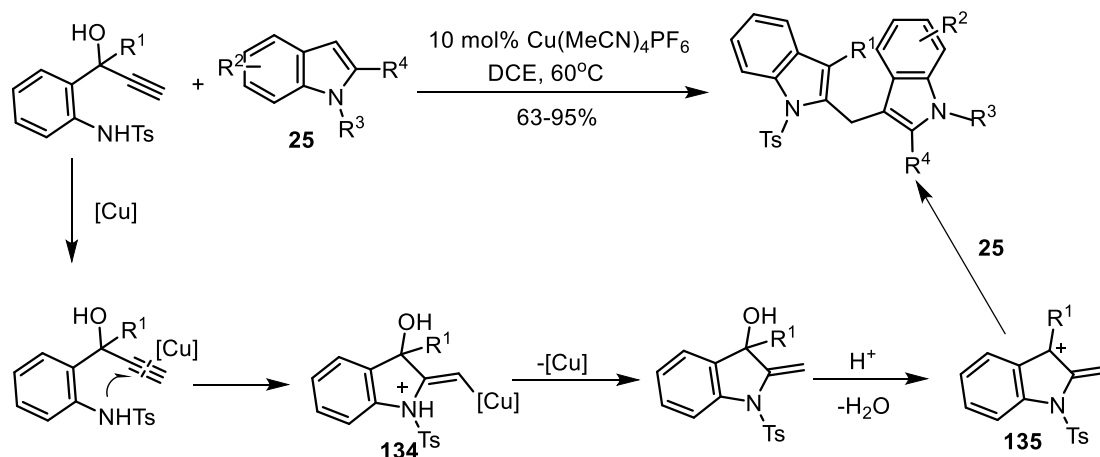
Indole derivatives **25** can react with aromatic aldehyde and *o*-benzenedisulfonimide to form unsymmetrical bisindolymethane salts **133** in good yield after half an hour (Scheme 81).^[157]



Scheme 81. Synthesis of *o*-benzenedisulfonimide salts.

2.2.2.6 Synthesis by ring closure of alkyne derivatives

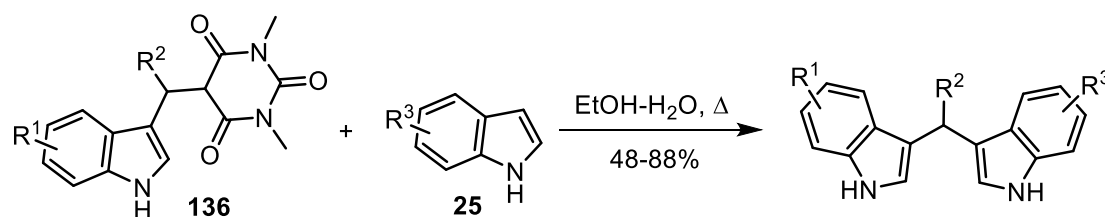
The copper-promoted reaction between 1-arylpropargyl alcohols and indoles **25** can efficiently afford 2,3'-bisindolylmethanes. The proposed mechanism is that the copper interaction with triple bond leads to the formation of hydroxyindoline **134** through promoting the 5-*exo-dig* ring closure; then the corresponding cationic **135** can be obtained after metal protonolysis and dehydration; finally, the Friedel-Crafts reaction between **135** and **25** affords the targets in high yield (Scheme 82).^[158]



Scheme 82. Synthesis of 2,3'-bisindolylmethanes from 1-arylpropargyl alcohols.

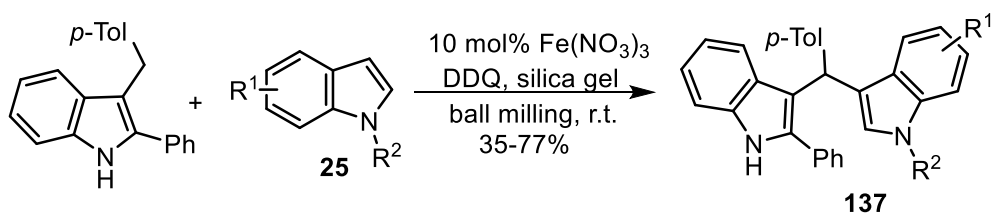
2.2.2.7 Miscellaneous methods for the synthesis of unsymmetrical bisindolylmethanes

Recently, it was reported that a three-component reaction of indole, aldehyde and *N,N'*-dimethylbarbituric acid leads to 3-alkylated indoles **136**. Equimolar amounts of **136** and indole were refluxed in ethanol-water for 30 min and subjected to an elimination-addition reaction to afford unsymmetrical bisindolylmethanes in excellent yield after workup (Scheme 83).^[159]



Scheme 83. Synthesis of unsymmetrical diindolylmethanes.

In addition, Su et al.^[160] proposed a cross dehydrogenative coupling between aryl(indolyl)methane and nucleophilic behavior indoles **25**. The reaction afforded unsymmetrical bisindolylmethanes **137** in moderate to good yield under conditions of Fe(III) as catalyst, DDQ as oxidant and ball milling at room temperature (Scheme 84).



Scheme 84. Cross dehydrogenative coupling reactions of 3-benzylic indoles with indoles.

2.3 The combination of organic synthesis and biological testing

2.3.1 Necessity of combining organic synthesis and biological testing

The main purpose of organic synthesis is to discover a more convenient way to obtain known compounds or new unknown compounds. Considering that it is difficult to perform clinical trials for every product that comes from synthesis and the risk of direct use without any testing. Therefore, it's really important to biologically test properties after synthesizing compounds with potential anti-cancer, anti-inflammatory, antioxidant and anti-cardiovascular activity. Moreover, other unexpected effects may be found through biological tests. The best known success story of finding other effects is sildenafil, which is a compound developed by Pfizer for the treatment of angina pectoris. After a series of biological tests, another effect in the treatment of pulmonary arterial hypertension was found, and marketed as RevatioH.^[161] The reason is that the concentration of phosphodiesterase 5 (PDE-5) is high when a person has the symptom of pulmonary hypertension lungs, and sildenafil can inhibit PDE-5 protein.

Besides organic synthesis, biological tests are able to determine the existence or not of a putative biological activity. Although a large number of anti-diabetic drugs are already available, sulfonylureas can be used as common drugs for diabetic patients who are not overweight or have metformin contraindications or inadequate glycemic control.^[162] Dom ínguez and co-workers^[163] considered sulfonylureas as potential antimalarial compounds due to the presence of some pharmacophoric groups with antimalarial properties. Based on this assumption, they did some antimalarial tests, including the inhibition of *in vitro* development of chloroquine-resistant strains of *Plasmodium falciparum*, *in vitro* hemoglobin hydrolysis, heme formation, and development of *Plasmodium berghei* in murine malaria. The results indicated that sulfonylureas have relatively higher antimalarial activity, and they can be regarded as good antimalarial drugs in practice.

2.3.2 Commonly used biological testing methods

The general way of testing biological activity includes multiple spectroscopic techniques like fluorescence, UV-vis absorption, dynamic light scattering (DLS), circular dichroism (CD), infrared, and isothermal titration calorimetry, molecular docking. Human serum albumin was chosen as an example to list the role of different testing methods.

2.3.2.1 Fluorescence Spectroscopy

Owing to the high sensitivity, selectivity, reproducibility, easy operation and rich theoretical basis, fluorescence spectroscopy has become the most popular method for measuring biological activity. The traditional fluorescence tools are steady-state fluorescence, synchronous fluorescence, and three-dimensional fluorescence. The examination always needs to set excitation wavelength. Taking human serum albumin as an example, when the excitation wavelength is selected as 280 nm, the fluorescence intensity of proteins comes from tryptophan, tyrosine and phenylalanine. However, the fluorescence is contributed only by tryptophan if the excitation wavelength was fixed at 295 nm. The reason is the very low quantum yield of phenylalanine and the almost disappearance of the fluorescence intensity of tyrosine after ionization.^[164] Fluorescence intensity, red or blue shift, energy transfer and configuration changes can be acquired from a series of fluorescence experiments. In addition, thermodynamic parameters like quenching constant, binding constant, the number of binding sites, enthalpy change, entropy change, and Gibbs free energy can be obtained after data analysis.

Time-resolved fluorescence (TRF) is a special tool that is particularly sensitive to the microenvironment and helps determine the type of quenching. In contrast to the relative of steady-state fluorescence, TRF is absolute.

To understand the pharmacokinetic properties of 2,4-diacetylphloroglucinol (DAPG) which is known for its antimicrobial, antiviral, anti-helminthic and anticancer properties, Natarajan and co-workers^[165] reported the molecular interaction between DAPG and human serum albumin. The fluorescence spectroscopy results indicated that the intrinsic fluorescence of HSA was strongly quenched by the dynamic quenching mechanism due to the interaction with DAPG. The quenching mechanism can also be sure by TRF. The binding of DAPG to human serum albumin

is an exothermic and spontaneous process, and the main force in this process is hydrophobic force.

2.3.2.2 UV-vis absorption spectroscopy

UV-Vis absorption spectroscopy is a simple and effective method to measure the structural changes, determine the mechanisms, and test the contents of certain functional groups. In general, human serum albumin has two absorption peaks, one at 200–230 nm represents the backbone of the polypeptide, and the other one at 260–300 nm represents aromatic amino acids (tryptophan, tyrosine and phenylalanine). The difference between the graphs before and after binding (absorbance or wavelength) illustrates the changes of secondary structure changes. Moreover, it can also determine the binding mechanism, the binding constant and the number of binding sites, or the contents of functional groups. Wu et al.^[166] used UV-vis absorption spectroscopy to measure the interaction between 5-fluorouracil and human serum albumin. Through the red shift and the increasing of absorbance after binding, it was concluded that a complex was formed between 5-fluorouracil and protein, and the alteration in the microenvironment of protein (Figure 3).

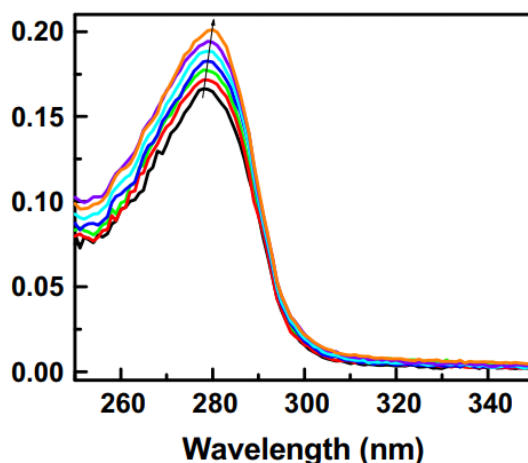


Figure 3. UV-Vis absorption spectra of human serum albumin after interaction with 5-fluorouracil.

2.3.2.3 Dynamic light scattering

DLS is an advantageous technique for reflecting the structural information of biological macromolecules in solution. It can provide the binding information by comparing the dimensional changes before and after binding to find out whether the protein tends to expand or not. Liu et al.^[167] measured the size changes of human serum albumin and water-soluble luminescent colloidal quantum dots after binding,

found that the conformation of protein changed slightly, and each quantum dot bound six human serum albumin.

2.3.2.4 Circular dichroism spectroscopy

CD spectroscopy is largely used to evaluate the secondary structure of proteins in biochemistry and structural biology. The far-UV wavelength of 200–250 nm represents the conformation of the polypeptide backbone in the protein. The secondary structure includes α -helix, β -sheet, β -turn and random coils. Serum albumin has two negative bands at 208 and 220 nm, which are caused by $\pi \rightarrow \pi^*$ and $n \rightarrow \pi^*$. Keswani and Kishore^[168] used CD spectroscopy to examine the secondary structure and tertiary structure changes of anticancer drug mitoxantrone and human serum albumin, concluding that the conformation of human serum albumin was almost unchanged before and after binding.

2.3.2.5 Isothermal titration calorimetry

Isothermal titration calorimetry is a simple and direct method to measure intermolecular interactions. Not only the binding constant and the number of binding sites, but also the enthalpy change and entropy change can be obtained from a single experiment. According to the selected site binding model, a series of thermodynamic parameters such as binding constant, number of binding sites, enthalpy change, and entropy change were obtained to determine the type of force and the mechanism of action. Li and Yang^[169] performed the interaction between oridonin and human serum albumin by using isothermal titration calorimetry combined with UV-Vis absorption spectroscopy and fluorescence spectroscopy. Compared with fluorescence calculates the enthalpy and entropy change through altering temperatures, isothermal titration calorimetry shows that the binding of oridonin to human serum albumin is an enthalpy-driven process, and the main forces are hydrogen bonds and van der Waals forces via a single experiment (Figure 4).

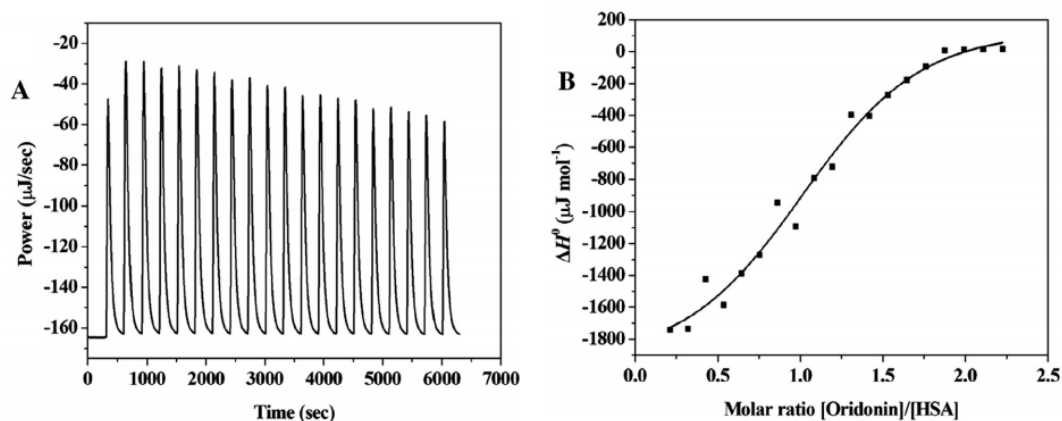


Figure 4. (A) Raw data for the titration of oridonin with human serum albumin; (B) Integrated heat profile of the calorimetric titration shown in panel A.

2.3.2.6 Molecular docking

Molecular docking can determine the location of the binding and the energy changes during the binding process by simulating the binding of proteins to drugs. In addition, it can provide more evidence for experimental data as well as provide a basis for preparation before experiments. Chakrabarti et al.^[170] simulated the binding of virstatin to human serum albumin, and finally determined that the drug was bound to the IIA site of the protein (Figure 5), which provided evidence for the conclusion of the spectroscopic method.

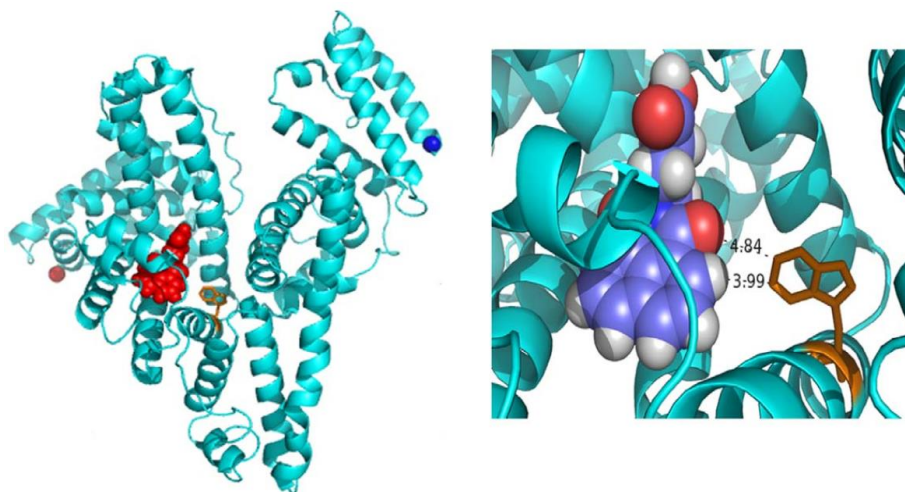


Figure 5. Cartoon representation of human serum albumin with the bound virstatin (red).

2.4 Synthesis of unsymmetrical bisindolymethanes by reaction of indolymagnesium bromides with sulfonyl indoles and their anti-cancer activity test

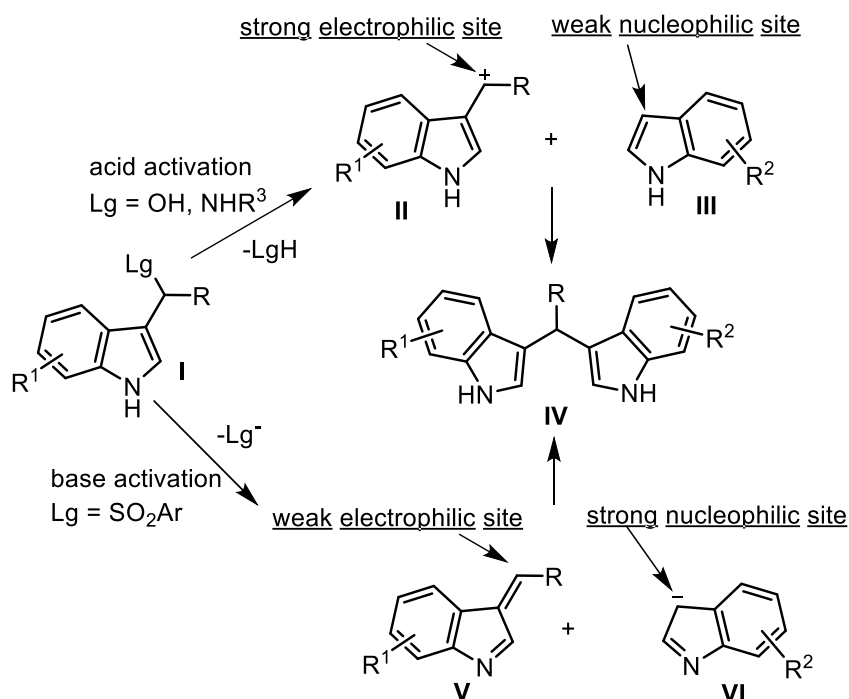
2.4.1 State of the art

Bisindolymethanes, an indole derivative, have always been present in the genus Brassica such as broccoli, Brussels sprouts, cabbage, and kale.^[171] In addition, their abilities to regulate plant growth and prevent cancer have attracted people's attention.

In general, the symmetrical bisindolymethanes can be easily prepared by the Friedel-Crafts reaction of a carbonyl derivative with an excess of the indole reactant under acid-catalyzed conditions.^[172] However, the synthesis of unsymmetrical bisindolymethanes is still rare and challenging. In most existing methods, researchers have continued the Friedel-Crafts reaction with a leaving group strategy. The indole substrate **I** with a good leaving group (-OH, -NHR₃) at the benzylic position can generate stabilized carbocation **II** under acidic conditions.^[173] Because of its strong electrophilic characteristic, it can react with weak nucleophiles **III** (a neutral indole) to form the unsymmetrical bisindolymethane **IV** (Scheme 85).^[157] Although this strategy is useful, it also has some limitations: the use of harmful Lewis acid or Brønsted acid catalysts, the formation of large amounts of waste or by-products, the high catalyst loadings, and the limited substrate scope.^[174] Considering that sulfonyl indoles **I** (Lg=SO₂Ar) can effectively convert to both cationic intermediates **III** and alkylideneindolenines **V** effectively, and indoles can easily deprotonate (N-H bond, pK_a=16.2),^[175] a new synthetic route for unsymmetrical bisindolymethanes was envisaged. Base can promote the elimination of sulfonyl indoles **I** to generate a weakly electrophilic alkylideneindolenine **V**, a fairly strong and stabilized nucleophilic indole **VI** can also be obtained from indole. Alkylideneindolenine **V** and indole reagent **VI** can be regarded as vinylogous imine and stabilized azaenolate anion, respectively.^[176] They can produce the target product by being involved in a Michael-type process.

Basic systems for the conversion of alkylideneindolenine **V** and indole reagent **VI** include metal hydrides, organolithiums, and Grignard reagents. However, alkali metal cations always react with the nitrogen atom to form a strongly ionic *N*-metal bond, which can promote reaction with electrophiles. It is widely used in various

reactions aimed at *N*-protection of indoles.^[177] To obtain C-3 substituted derivatives, the less electropositive metals can be used to form a covalent bond with the nitrogen atom, which can increase the nucleophilic character of the indole ring. Grignard reagents can be considered as a good choice.



Scheme 85. Synthetic approaches to unsymmetrical bisindolylmethanes.

The bioactivity assay after synthesis is also essential. Queiroz et al.^[178] and Contractor et al.^[179] concluded that unsymmetrical bisindolylmethanes are known for their AChE inhibitory effect and anticancer activity, respectively. In this section, a simple and effective synthesis of unsymmetrical bisindolylmethanes was justified by reacting sulfonyl indoles with 1-indolylmagnesium bromides under mild reaction conditions was founded. Moreover, the anti-cancer activity of five samples was tested and compared with cisplatin.

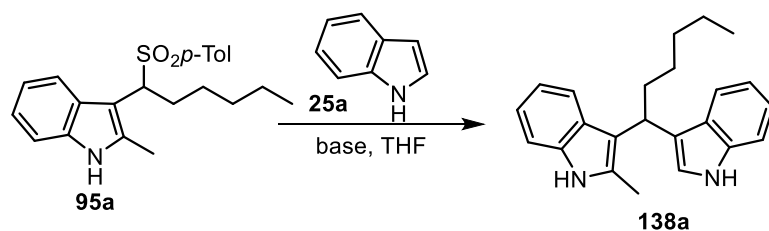
2.4.2 Results and discussion

2.4.2.1 Synthesis and characterization of unsymmetrical bisindolylmethanes

Alkylideneindolenines **V** have never reacted with metalated aromatic and heteroaromatic compounds. Therefore, a suitable base should be found to generate the corresponding nucleophiles. Sulfonyl indole **95a** and indole **25a** were selected for initial exploration. As shown in Table 8, the common basic systems containing alkali

metal counterions did not give satisfactory results (entries 1, 2).^[180] However, indolylmagnesium bromide prepared by indole **25a** and MeMgBr gave significant result at low temperature (entry 3). And the yield increased dramatically with increasing temperature (entries 4, 5). The changes from 2 to 1.5 equivalents (**25a:95a**) showed no improvement (entry 6). Bergman and VenemaIm^[181] reported that ZnCl₂ can transmetallate Grignard reagents to increase the yield, and Ishihara et al.^[182] use ZnCl₂ as a catalyst to facilitate the reaction between aldimines and Grignard reagents. Therefore, tried to use both an excess or a catalytic amount of ZnCl₂. Unfortunately, the yield is only slightly increased compared to indolylmagnesium bromide (entry 7). Considering that Lewis acid can promote the elimination of the arylsulfinyl group from sulfonyl indoles,^[183] magnesium salts can help to generate the alkylideneindolenine intermediate **V**.

Table 8. Optimization of the reaction conditions.^[a]



Entry	Base	T ^o C	Yield ^[b] (%)
1	NaH	20	5
2	<i>n</i> -BuLi	0	23
3	MeMgBr	-20	60
4	MeMgBr	0	75
5	MeMgBr	20	76
6 ^[c]	MeMgBr	20	41
7 ^[d]	MeMgBr, ZnCl ₂	20	77

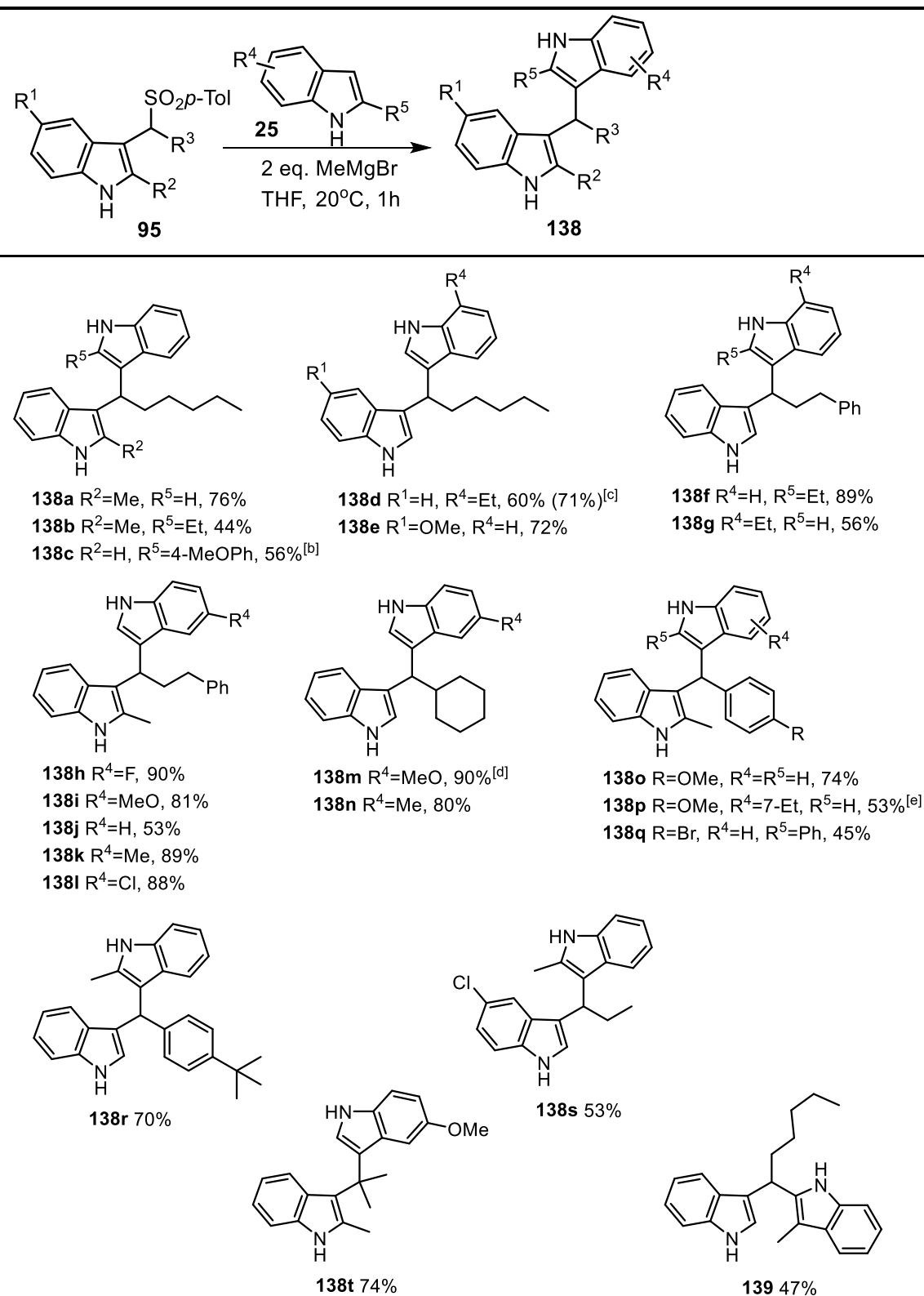
[a] Conditions: indole **25a** (0.6 mmol), base (0.6 mmol) then after 30 min sulfonyl indole **95a** (0.3 mmol), THF (2.0 mL), 1 h.

[b] Isolated yield after chromatography on silica gel.

[c] 1.5 eq. of **25a** and 1.5 eq of MeMgBr were used.

[d] 2 eq. of dry ZnCl₂ were added after deprotonation of **25a** with 2 eq. of MeMgBr.

Table 9. Scope of the reaction between sulfonyl indoles **95** and indoles **25**.^[a]



[a] Reaction conditions: Indole **25** (2 mmol), MeMgBr (2 mmol) at r.t., after 30 min sulfonyl indole **95** (1 mmol).

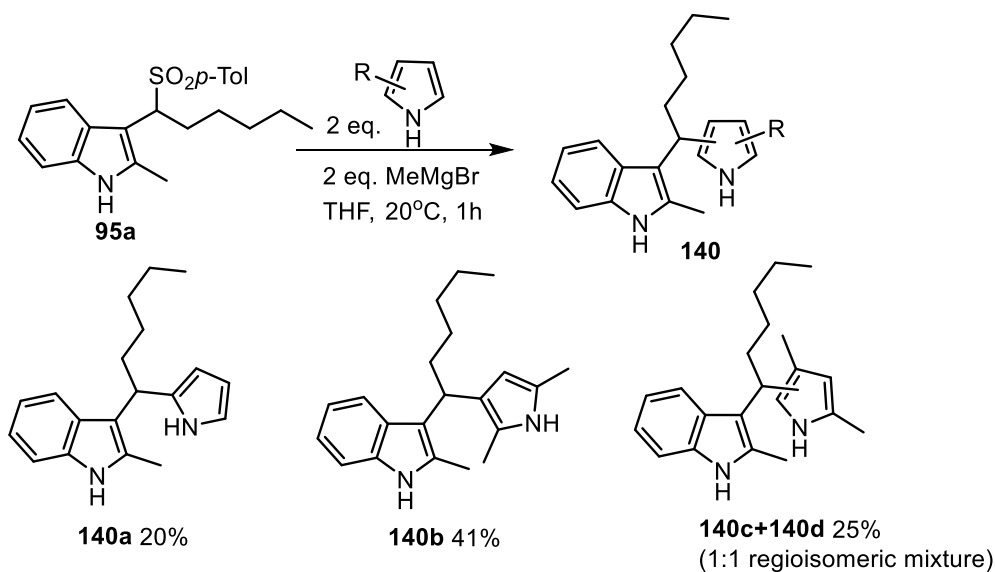
[b] Purified by crystallization (EtOAc/hexane).

[c] Yield in parenthesis refers to the reaction of indole with 7-ethyl-3-(1-tosylhexyl)-1*H*-indole.

[d] Reaction time 1.5 h. [e] Reaction time 3.5 h.

These optimized conditions can be extended to sulfonyl indoles **95** and indoles **25** with different substituents, and the corresponding results are shown in Table 9. Sulfonyl indoles **95** having aliphatic or aromatic side chains can react well with indolylmagnesium bromide and obtain satisfactory results. The effective conversion of **138f** and **138r** showed that 2-substituted indoles **25** are also beneficial for the reaction. However, the presence of 2-methyl substituted sulfonyl indoles **95** attenuates their advantages. Regardless of the electronic aptitude, indoles **25** with different substituents in the benzene portion are always favorable to the reaction. The optimized condition can also be applied to 2-methyl-3-(2-tosylpropan-2yl)-1H indole in which the sulfonyl moiety linked to a tertiary carbon atom, and the product **138t** is obtained in good yield (74%). The generation of the 3,2'-bisindolylmethane compound **139** in moderate yield (47%) from 3-methylindolylmagnesium bromide also demonstrated the versatility of this procedure. Unfortunately, no relevant products were obtained from other benzazole derivatives such as indazole and 6-azaindole.

The reaction of the *N*-metalated pyrroles with sulfonyl indoles was also attempted to verify the boundaries of this synthetic approach. Since it is known that the C-alkylation of pyrroles proceeds via the corresponding pyrrolylmagnesium halide,^[184] one would expect the same behavior. The reaction between sulfonyl indole **95a** and pyrrole or a couple of bismethylated pyrrole derivatives was also tested under the same conditions, and the results are shown in Scheme 86. The successful synthesis of **140a** proved that the prominent reactivity of pyrrole at position 2, 2,5-dimethylpyrrole with two equivalent positions 3 and 4 also afforded compound **140b** due to the only addition position. Moreover, an equimolar mixture of regioisomers **140c, d** from 2,4-dimethylpyrrole was obtained. These results imply that both free positions in the pyrrole ring can be activated by the electron donating effect of the methyl groups.



Scheme 86. Reaction of pyrrolylmagnesium bromides with sulfonyl indoles.

2.4.2.2 Anti-cancer activity test of selected compounds

The *in vitro* cytotoxicity of unsymmetrical bisindolylmethane on HeLa cells was carried out using the 3-(4,5-dimethylthiazol-2-yl)-2,5-diphenyltetrazolium bromide (MTT) assay, and the half-maximal inhibitory concentration (IC_{50}) values for the corresponding compounds were listed in Figure 6. As one of the most active anticancer agents currently in use, cisplatin has the apparent inhibitory effect on HeLa cells ($IC_{50}=1.07 \mu\text{M}$). The value differs from the study of Minagawa, which showed that the IC_{50} value of cisplatin was $2.2 \mu\text{M}$.^[185] This may be due to the difference in the amount of cells and concentrations of cisplatin. However, parallel testing can resolve this concern.

Effective inhibition of HeLa cells by five selected compounds indicates that unsymmetrical bisindolylmethanes have anticancer activity, although some of them are weaker than cisplatin. The better inhibitory effect of **138i** compared to cisplatin proves that unsymmetrical bisindolylmethanes can be considered as good anti-cancer reagents. Compounds with substituents such as -fluoro, -chloro, and -methyl can enhance their anti-cancer activity. However, -methoxy has the opposite effect. Although the trend of ability has nothing to do with electronic aptitude, the possession of anti-cancer activity is an uplifting result.

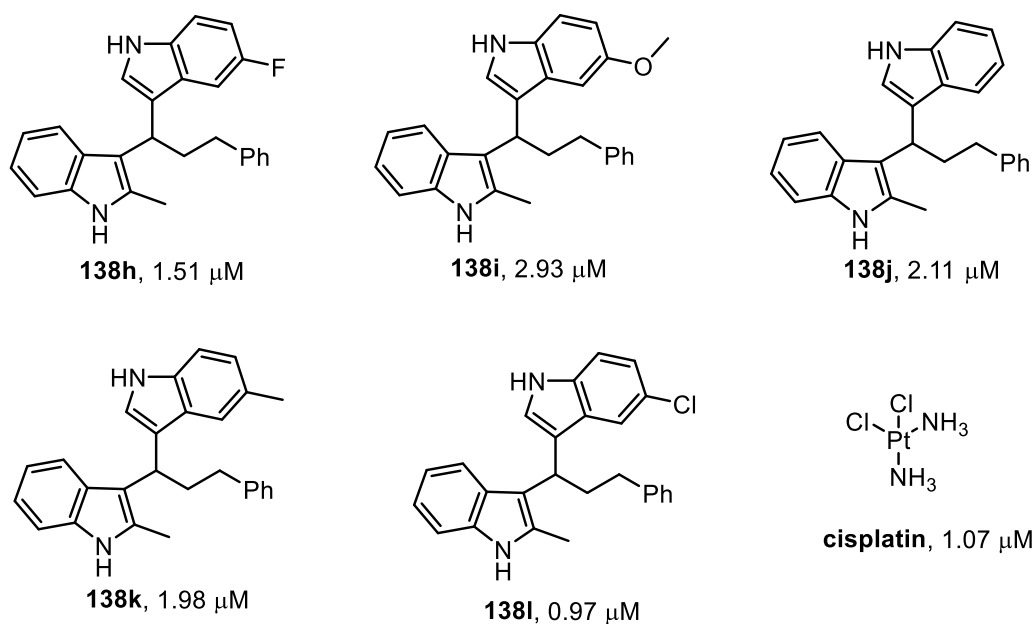


Figure 6. IC_{50} values for unsymmetrical bisindolylmethanes as determined by the MTT assay.

2.4.3 Conclusion

A new simple and efficient approach to unsymmetrical bisindolylmethanes was realized by using sulfonyl indoles with an excess of indolylmagnesium bromides. The first equivalent of the metalated indole reactant can play the role of basic system promoting the elimination of the arylsulfinate anion to form an alkylideneindolenine intermediate. Then the excess of indolylmagnesium bromide reacts with the intermediate leading to the final product with a complete 1,4-regioselectivity. Using this method a series of bisindolylmethane compounds under mild reaction conditions and in moderate to good yields can be obtained. Under these conditions, pyrrolylmagnesium bromides react with sulfonyl indoles giving rather modest yields of adducts. Some of the tested compounds show anti-cancer activity against Hela cells, especially that bearing a chloro substituent.

2.4.4 Experimental section

Unsymmetrical bisindolylmethanes (**138**): CH_3MgBr (0.67 mL, 3 M solution in diethyl ether, 2 mmol) was added dropwise into a stirred solution of indole **25** (2 mmol) with THF (15 mL) under nitrogen at 20 °C. After stirring for 30 minutes, the sulfonyl indole **95** (1 mmol) dissolved in THF (10 mL) was added dropwise. The resulting reaction mixture was stirred for 1 h and then treated with a saturated aqueous solution of NH_4Cl (6 mL) and the aqueous layer extracted with CH_2Cl_2 (3×15 mL).

The crude product **138** obtained after filtration and removal of the solvent at reduced pressure, was purified by column chromatography (hexane/EtOAc, 8:2).

2.4.4.1 Cell culture of selected unsymmetrical bisindolylmethanes

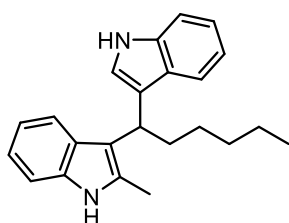
The anti-cancer activity of selected samples was determined by measuring the growth inhibition of human cervical cancer HeLa cells using the MTT assay. The cells were cultured in serum-containing medium under the conditions of 37 °C and humidified atmosphere environment containing 5% CO₂. After the third generation, the cells were plated in 96-well plates at a density of 3×10³ cells per well and maintained 24 h. Then the medium was replaced with different concentrations of samples (0.1, 0.5, 1, 2, 5, 10 μM) for 48 h. Afterward, 20 μL of MTT (5 mg/mL in PBS) was added to each well, and the plates were further incubated for 4 h in the dark. After removing the solution, 150 μL of DMSO was added to each well. Finally, the absorbance was detected at 570 nm by using a microplate reader (Elx 808; Bio tek, USA). The cytotoxicity can be calculated as follows:^[186]

$$\text{Cytotoxicity} = (A-B)/A \times 100\% \quad (1)$$

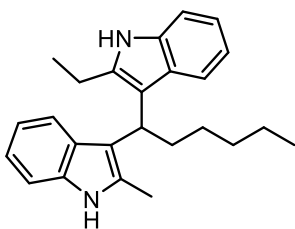
where *A* and *B* are the absorbance of the cells incubated with the normal culture medium and unsymmetrical bisindolylmethanes, respectively. All experiments were performed in triplicate.

The anti-cancer activity of compounds can be represented by IC₅₀, which can be obtained from Compusyn software.

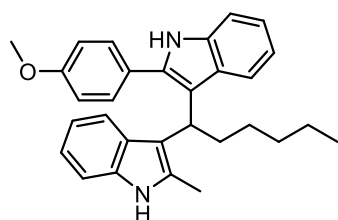
2.4.4.2 Spectroscopic data for compounds **138**, **139** and **140**:



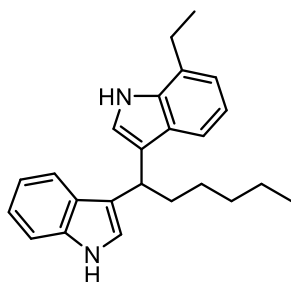
138a. Yield 0.251 g (76%). White solid, mp: 50-53°C. IR (neat) ν : 423, 498, 742, 1009, 1460, 3388 cm⁻¹. ¹H-NMR (DMSO-d₆, 400MHz) δ : 0.79 (t, 3H, *J* = 6.4 Hz), 1.09-1.41 (m, 6H), 2.08-2.28 (m, 2H), 2.39 (s, 3H), 4.28 (t, 1H, *J* = 7.3 Hz), 6.71-7.00 (m, 4H), 7.15 (d, 1H, *J* = 8.1 Hz), 7.19-7.31 (m, 3H), 7.42 (d, 1H, *J* = 8.1 Hz), 10.59 (br s, 1H), 10.70 (br s, 1H). ¹³C-NMR (DMSO-d₆, 100MHz) δ : 12.6, 14.7, 22.9, 28.1, 32.1, 33.3, 34.6, 111.0, 111.8, 113.7, 118.3, 118.5, 119.3, 119.8, 120.1, 121.3, 122.0, 127.8, 128.1, 131.6, 136.0, 137.0. GC-MS (70 eV): *m/z*: 330 ([M⁺], 14), 259 (100), 217 (4), 129 (9). Anal. Calcd. For C₂₃H₂₆N₂ (330.47): C: 83.59; H: 7.93; N: 8.48. Found: C: 83.71; H: 7.82; N: 8.57



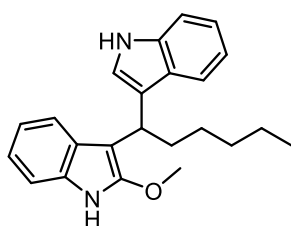
138b. Yield 0.158 g (44%). Yellow solid, mp: 135-137°C. IR (neat) v: 435, 484, 738, 1304, 1460, 3397 cm^{-1} . $^1\text{H-NMR}$ (DMSO- d_6 , 400MHz) δ : 0.79 (t, 3H, $J = 6.4$ Hz), 1.10 (t, 3H, $J = 8.1$ Hz), 1.15-1.37 (m, 6H), 2.23-2.36 (m, 2H), 2.29 (s, 3H), 2.62-2.77 (m, 2H), 4.33 (t, 1H, $J = 7.7$ Hz), 6.73-6.82 (m, 2H), 6.84-6.93 (m, 2H), 7.12-7.21 (m, 2H), 7.43-7.54 (m, 2H), 10.60 (br s, 2H). $^{13}\text{C-NMR}$ (DMSO- d_6 , 100MHz) δ : 13.0, 14.6, 14.7, 20.0, 22.9, 28.7, 32.1, 34.8, 35.3, 111.0, 111.2, 113.7, 114.6, 118.5, 119.3, 119.6, 120.0, 120.1, 128.1, 128.5, 131.6, 135.7, 136.0, 137.6. GC-MS (70 eV): m/z : 358 ($[\text{M}^+]$, 15), 287 (100), 257 (10), 130 (10). Anal. Calcd. for $\text{C}_{25}\text{H}_{30}\text{N}_2$ (358.53): C: 83.75; H: 8.43; N: 7.81. Found: C: 83.91; H: 8.49; N: 7.77.



138c. Yield 0.236 g (56%). The crude product was purified by crystallization using EtOAc/hexane. White solid, mp: 174-177°C. IR (neat): 741, 831, 1246, 1454, 1502, 1611, 3371, 3402 cm^{-1} . $^1\text{H-NMR}$ (DMSO- d_6 , 400 MHz) δ : 0.72 (t, 3H, $J = 6.4$ Hz), 1.11-1.25 (m, 6H), 2.20-2.32 (m, 2H), 3.80 (s, 3H), 4.44-4.56 (m, 1H), 6.74 (t, 1H, $J = 7.3$ Hz), 6.82 (t, 1H, $J = 7.3$ Hz), 6.90-7.00 (m, 2H), 7.03-7.10 (m, 3H), 7.17 (s, 1H), 7.23-7.30 (m, 2H), 7.50 (d, 2H, $J = 8.5$ Hz), 7.55 (d, 1H, $J = 8.1$ Hz), 10.72 (s, 1H), 10.99 (s, 1H). $^{13}\text{C-NMR}$ (DMSO- d_6 , 100 MHz) δ : 14.6, 22.8, 28.2, 32.0, 33.7, 35.0, 55.9, 111.8, 112.0, 114.4, 114.8, 118.6, 118.7, 119.3, 119.6, 120.9, 121.2, 121.3, 122.4, 126.5, 127.6, 127.9, 130.5, 135.3, 136.9, 137.0, 159.4. GC-MS (70 eV): m/z : 422 ($[\text{M}^+]$, 13), 351 (100), 281 (13), 207 (21), 175 (11), 73 (7). Anal. Calcd. for $\text{C}_{29}\text{H}_{30}\text{N}_2\text{O}$ (422.57): C: 82.43; H: 7.16; N: 6.63. Found: C: 82.29; H: 7.21; N: 6.75.

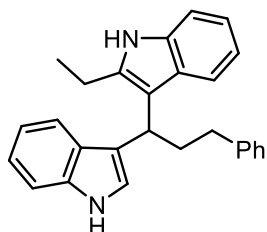


138d. Yield 0.207 g (60%). Purple oil. IR (neat): 441, 487, 739, 1301, 1465, 3401 cm^{-1} . $^1\text{H-NMR}$ (DMSO- d_6 , 400 MHz) δ : 0.80 (t, 3H, $J = 7.3$ Hz), 1.15-1.35 (m, 6H), 1.21 (t, 3H, $J = 7.3$ Hz), 2.09-2.20 (m, 2H), 2.78 (q, 2H, $J = 7.3$ Hz), 4.32 (q, 1H, $J = 7.3$ Hz), 6.76-6.87 (m, 3H), 6.96 (t, 1H, $J = 7.7$ Hz), 7.14 (d, 1H, $J = 2.3$ Hz), 7.18 (d, 1H, $J = 2.3$ Hz), 7.26 (dd, 1H, $J = 0.9, 8.1$ Hz), 7.32 (dd, 1H, $J = 2.3, 6.6$ Hz), 7.48 (d, 1H, $J = 7.7$ Hz), 10.66 (s, 1H), 10.69 (s, 1H). $^{13}\text{C-NMR}$ (DMSO- d_6 , 100 MHz) δ : 14.7, 15.0, 22.9, 24.3, 28.3, 32.1, 34.2, 35.7, 112.0, 117.4, 118.5, 118.8, 119.6, 119.7, 119.9, 120.0, 121.2, 122.2, 122.5, 127.2, 127.3, 127.4, 135.8, 137.1. GC-MS (70 eV): m/z : 344($[\text{M}^+]$, 28), 273(100), 257(9), 243(18), 129(9). Anal. Calcd. for $\text{C}_{24}\text{H}_{28}\text{N}_2$ (344.50): C: 83.68; H: 8.19; N: 8.13. Found: C: 83.54; H: 8.25; N: 8.04.

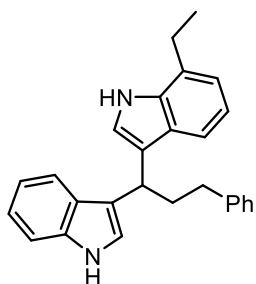


138e. Yield 0.249 g (72%). Pink oil. IR (neat) v: 740, 1208, 1454, 1622, 3411 cm^{-1} . $^1\text{H-NMR}$ (DMSO- d_6 , 400MHz) δ : 0.80 (t, 3H, $J = 7.3$ Hz), 1.16-1.36 (m, 6H), 2.07-2.21 (m, 2H), 3.64 (s, 3H), 4.30 (t, 1H, $J = 7.3$ Hz), 6.63 (dd, 1H, $J = 2.1, 8.5$ Hz), 6.84 (t, 1H, $J = 7.7$

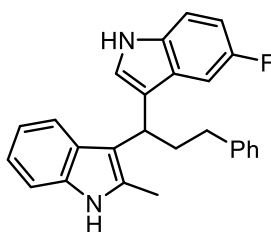
Hz), 6.92-6.99 (m, 2H), 7.12-7.18 (m, 2H), 7.21 (d, 1H, $J = 2.1$ Hz), 7.27 (d, 1H, $J = 8.1$ Hz), 7.48 (d, 1H, $J = 7.7$ Hz), 10.54 (s, 1H), 10.71 (s, 1H). $^{13}\text{C-NMR}$ (DMSO- d_6 , 100MHz) δ : 14.7, 22.9, 28.2, 32.0, 34.0, 35.6, 55.9, 101.9, 110.9, 112.0, 112.5, 118.5, 119.3, 119.5, 119.7, 121.2, 122.6, 123.3, 127.4, 127.7, 132.3, 137.2, 153.1. GC-MS (70 eV): m/z : 346 ($[\text{M}^+]$, 13), 275 (100), 243 (5), 130 (9). Anal. Calcd. for $\text{C}_{23}\text{H}_{26}\text{N}_2\text{O}$ (346.47): C: 79.73; H: 7.56; N: 8.09. Found: C: 79.91; H: 7.49; N: 7.96.



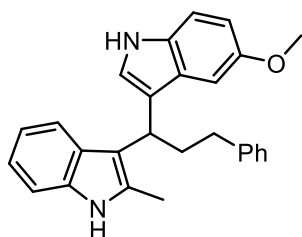
138f. Yield 0.337 g (89%). White solid, mp: 61-64°C. IR (neat) ν : 427, 503, 698, 744, 1262, 1456, 3395 cm^{-1} . $^1\text{H-NMR}$ (DMSO- d_6 , 400MHz) δ : 1.19 (t, 3H, $J = 7.7$ Hz), 2.38-2.67 (m, 4H), 2.76 (q, 2H, $J = 7.7$ Hz), 4.36 (dd, 1H, $J = 5.1, 9.4$ Hz), 6.75-6.83 (m, 2H), 6.87-6.97 (m, 2H), 7.08-7.32 (m, 9H), 7.49 (d, 1H, $J = 7.7$ Hz), 10.65 (s, 1H), 10.72 (s, 1H). $^{13}\text{C-NMR}$ (DMSO- d_6 , 100MHz) δ : 15.1, 19.8, 33.1, 34.7, 36.8, 111.2, 111.9, 112.5, 118.4, 118.5, 119.2, 119.5, 119.6, 120.3, 121.3, 122.2, 126.3, 127.7, 127.8, 128.9, 136.3, 137.0, 137.8, 143.1. GC-MS (70 eV): m/z : 378 ($[\text{M}^+]$, 17), 273 (100), 257 (12), 233 (5). Anal. Calcd. for $\text{C}_{27}\text{H}_{26}\text{N}_2$ (378.52): C: 85.68; H: 6.92; N: 7.40. Found: C: 85.75; H: 6.98; N: 7.49



138g. Yield 0.212 g (56%). Pink solid, mp: 56-59°C. IR (neat) ν : 423, 465, 699, 740, 1455, 3413 cm^{-1} . $^1\text{H-NMR}$ (DMSO- d_6 , 400MHz) δ : 1.22 (t, 3H, $J = 7.3$ Hz), 2.44-2.48 (m, 2H), 2.56-2.63 (m, 2H), 2.76-2.83 (m, 2H), 4.37 (t, 1H, $J = 7.3$ Hz), 6.77-6.88 (m, 3H), 6.98 (t, 1H, $J = 6.8$ Hz), 7.11-7.33 (m, 9H), 7.47 (d, 1H, $J = 8.5$ Hz), 10.71 (s, 1H), 10.75 (s, 1H). $^{13}\text{C-NMR}$ (DMSO- d_6 , 100MHz) δ : 15.0, 24.3, 33.9, 34.8, 37.6, 112.0, 117.3, 118.6, 118.9, 119.2, 119.6, 119.6, 120.0, 121.3, 122.4, 122.7, 126.3, 127.1, 127.3, 127.4, 128.9, 129.0, 135.9, 137.2, 143.1. GC-MS (70 eV): m/z : 378($[\text{M}^+]$, 14), 273(100), 243(10), 217(4). Anal. Calcd. for $\text{C}_{27}\text{H}_{26}\text{N}_2$ (378.52): C: 85.68; H: 6.92; N: 7.40. Found: C: 85.55; H: 6.84; N: 7.37.

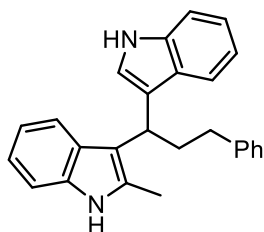


138h. Yield 0.344 g (90%). White solid, mp: 55-58°C. IR (neat) ν : 426, 700, 738, 1454, 1482, 3409 cm^{-1} . $^1\text{H-NMR}$ (DMSO- d_6 , 400MHz) δ : 2.36 (s, 3H), 2.48-2.65 (m, 4H), 4.23-4.25 (m, 1H), 6.74-6.84 (m, 3H), 6.90 (t, 1H, $J = 7.7$ Hz), 7.09-7.30 (m, 7H), 7.39-7.47 (m, 2H), 10.69 (s, 1H), 10.86 (s, 1H). $^{13}\text{C-NMR}$ (DMSO- d_6 , 100MHz) δ : 12.5, 33.0, 34.5, 36.3, 103.6, 103.8, 109.3, 109.5, 111.1, 112.7, 112.8, 112.9, 118.5, 119.2, 119.6, 119.7, 120.3, 124.4, 126.3, 127.7, 127.8, 127.9, 128.9, 129.0, 132.0, 133.7, 136.1, 143.0, 155.7, 158.0. GC-MS (70 eV): m/z : 328 ($[\text{M}^+]$, 16), 277 (100), 251 (16), 207 (30), 130 (12). Anal. Calcd. for $\text{C}_{26}\text{H}_{23}\text{FN}_2$ (382.48): C: 81.65; H: 6.06; N: 7.32. Found: C: 81.60; H: 6.13; N: 7.25.



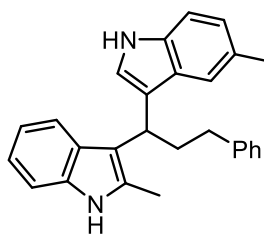
138i. Yield 0.320 g (81%). Yellow solid, mp: 172-175°C. IR (neat) ν : 499, 701, 745, 1214, 1482, 3383, 3409 cm^{-1} . $^1\text{H-NMR}$ (DMSO- d_6 , 400MHz) δ : 2.38 (s, 3H), 2.45-2.66 (m, 4H), 3.58 (s, 3H), 4.21-4.33 (m, 1H), 6.58-6.68 (m, 2H), 6.81 (t, 1H, $J = 7.7$ Hz), 6.91 (t, 1H, $J =$

7.7 Hz), 7.09-7.33 (m, 8H), 7.51 (d, 1H, $J = 7.7$ Hz), 10.56 (s, 1H), 10.67 (s, 1H). $^{13}\text{C-NMR}$ (DMSO- d_6 , 100MHz) δ : 12.6, 33.0, 34.5, 36.2, 55.7, 101.3, 111.1, 112.5, 113.1, 118.4, 119.2, 119.4, 120.2, 122.9, 126.3, 127.9, 128.0, 128.9, 129.0, 131.9, 132.2, 136.2, 143.0, 153.1. GC-MS (70 eV): m/z : 394 ($[\text{M}^+]$, 19), 289 (100), 271 (23), 207 (40), 130 (18). Anal. Calcd. for $\text{C}_{27}\text{H}_{26}\text{N}_2\text{O}$ (394.52): C: 82.20; H: 6.64; N: 7.10. Found: C: 82.31; H: 6.67; N: 7.19.



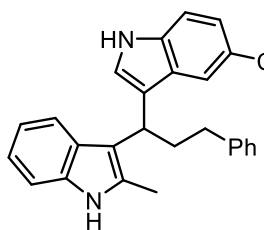
138j. Yield 0.193 g (53%). Brown solid, mp: 187-190°C. IR (neat) ν : 424, 503, 743, 1009, 1458, 3396 cm^{-1} . $^1\text{H-NMR}$ (DMSO- d_6 , 400MHz) δ : 2.36 (s, 3H), 2.51-2.65 (m, 4H), 4.26-4.37 (m, 1H), 6.79 (t, 2H, $J = 7.3$ Hz), 6.90 (t, 1H, $J = 7.7$ Hz), 6.95 (t, 1H, $J = 7.7$ Hz), 7.11-7.32 (m, 9H), 7.48 (d, 1H, $J = 8.1$ Hz), 10.66 (br s, 1H), 10.74 (br s, 1H).

$^{13}\text{C-NMR}$ (DMSO- d_6 , 100MHz) δ : 12.6, 33.0, 34.6, 36.4, 111.1, 111.9, 113.3, 118.4, 118.6, 119.2, 119.3, 119.4, 120.2, 121.3, 122.2, 126.3, 127.7, 128.0, 128.9, 129.0, 131.9, 136.1, 137.0, 143.0. GC-MS (70 eV): m/z : 364 ($[\text{M}^+]$, 16), 259 (100), 233 (10), 130 (11). Anal. Calcd. For $\text{C}_{26}\text{H}_{24}\text{N}_2$ (364.49): C: 85.68; H: 6.64; N: 7.69. Found: C: 85.80; H: 6.71; N: 7.61.



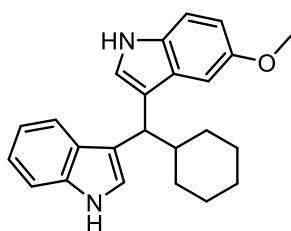
138k. Yield 0.337 g (89%). Brown solid, mp: 73-76°C. IR (neat) ν : 423, 699, 738, 1459, 3401 cm^{-1} . $^1\text{H-NMR}$ (DMSO- d_6 , 400MHz) δ : 2.26 (s, 3H), 2.39 (s, 3H), 2.52-2.62 (m, 4H), 4.27-4.33 (m, 1H), 6.78-6.85 (m, 2H), 6.92 (t, 1H, $J = 7.5$ Hz), 7.01 (s, 1H), 7.13-7.30 (m, 8H), 7.50 (d, 1H, $J = 7.7$ Hz), 10.60 (br s, 1H), 10.67 (br s, 1H). $^{13}\text{C-NMR}$

(DMSO- d_6 , 100MHz) δ : 12.6, 22.1, 33.0, 34.6, 36.5, 111.1, 111.6, 113.3, 118.3, 118.8, 118.9, 119.5, 120.2, 122.3, 122.9, 126.3, 126.7, 127.8, 127.9, 128.9, 129.0, 131.8, 135.3, 136.1, 143.0. GC-MS (70 eV): m/z : 378 ($[\text{M}^+]$, 14), 273 (100), 257 (7), 130 (4). Anal. Calcd. For $\text{C}_{27}\text{H}_{26}\text{N}_2$ (378.52): C: 85.68; H: 6.92; N: 7.40. Found: C: 85.78; H: 6.75; N: 7.47.



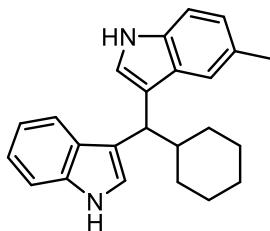
138l. Yield 0.351 g (88%). Pink solid, mp: 60-63°C. IR (neat) ν : 420, 699, 740, 1459, 3407 cm^{-1} . $^1\text{H-NMR}$ (DMSO- d_6 , 400MHz) δ : 2.38 (s, 3H), 2.51-2.67 (m, 4H), 4.29-4.36 (m, 1H), 6.82 (t, 1H, $J = 7.6$ Hz), 6.91-6.99 (m, 2H), 7.12-7.32 (m, 8H), 7.43-7.48 (m, 2H), 10.72 (br s, 1H), 10.99 (br s, 1H). $^{13}\text{C-NMR}$ (DMSO- d_6 , 100MHz) δ : 12.6, 32.9,

34.4, 36.3, 111.1, 112.9, 113.5, 118.4, 118.5, 119.2, 119.3, 120.3, 121.2, 123.1, 124.1, 126.3, 127.8, 128.8, 128.9, 129.0, 132.0, 135.5, 136.1, 142.9. GC-MS (70 eV): m/z : 398 ($[\text{M}^+]$, 17), 293 (100), 256 (10), 207 (9), 130 (6). Anal. Calcd. For $\text{C}_{26}\text{H}_{23}\text{N}_2\text{Cl}$ (398.93): C: 78.28; H: 5.81; N: 7.02; Cl: 8.89. Found: C: 78.12; H: 5.74; N: 7.16; Cl: 8.98.



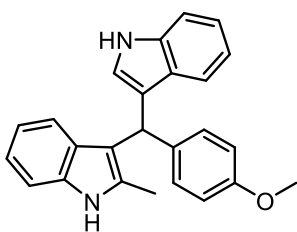
138m. Yield 0.323 g (90%). Brown solid, mp: 64-67°C. IR (neat) ν : 424, 739, 1212, 1454, 2920, 3409 cm^{-1} . $^1\text{H-NMR}$ (DMSO- d_6 , 400MHz) δ : 0.86-1.27 (m, 6H), 1.52-1.79 (m, 4H), 2.19-2.30 (m, 1H), 3.71 (d, 3H, $J = 11.1$ Hz), 4.10 (d, 1H, $J = 9.4$ Hz), 6.63 (d, 1H, $J = 8.1$ Hz), 6.87 (t, 1H, $J = 7.3$ Hz), 6.96 (t, 1H, $J = 7.3$ Hz), 7.04 (s,

1H), 7.14 (d, 1H, $J = 8.5$ Hz), 7.20-7.30 (m, 3H), 7.59 (d, 1H, $J = 8.1$ Hz), 10.54 (s, 1H), 10.70 (s, 1H). ^{13}C -NMR (DMSO- d_6 , 100MHz) δ : 26.7, 27.0, 32.5, 32.6, 42.2, 56.1, 101.9, 110.9, 111.9, 112.4, 118.3, 118.5, 119.7, 121.1, 122.8, 123.5, 127.9, 128.3, 132.0, 136.8, 153.2. GC-MS (70 eV): m/z : 358($[\text{M}^+$], 8), 275(100), 243(5), 207(4), 130(4). Anal. Calcd. for $\text{C}_{24}\text{H}_{26}\text{N}_2\text{O}$ (358.49): C: 80.41; H: 7.31; N: 7.81. Found: C: 80.49; H: 7.19; N: 7.85.



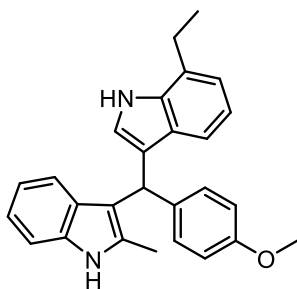
138n. Yield 0.274 g (80%). Purple solid, mp: 75-78°C. IR (neat) ν : 422, 740, 1094, 1455, 2849, 3407 cm^{-1} . ^1H -NMR (DMSO- d_6 , 400MHz) δ : 0.83-1.00 (m, 2H), 1.02-1.27 (m, 4H), 1.49-1.65 (m, 2H), 1.67-1.77 (m, 2H), 2.13-2.28 (m, 1H), 2.32 (s, 3H), 4.11 (d, 1H, $J = 9.4$ Hz), 6.79 (dd, 1H, $J = 1.3, 8.3$ Hz), 6.87 (dt, 1H, $J = 1.1, 7.3$ Hz), 6.97 (dt, 1H, $J = 1.1, 7.3$ Hz), 7.14 (d, 1H, $J = 8.3$ Hz), 7.20 (d, 1H, $J = 2.3$ Hz), 7.23-7.28 (m,

2H), 7.37 (s, 1H), 7.58 (d, 1H, $J = 7.7$ Hz), 10.57 (s, 1H), 10.70 (s, 1H). ^{13}C -NMR (DMSO- d_6 , 100MHz) δ : 22.1, 26.7, 27.0, 32.6, 32.7, 42.5, 111.6, 111.9, 118.1, 118.5, 118.7, 119.1, 119.7, 121.1, 122.8, 122.9, 126.8, 128.0, 128.2, 135.2, 136.8. GC-MS (70 eV): m/z : 342 ($[\text{M}^+$], 8), 259 (100), 243 (8), 217 (5), 130 (3). Anal. Calcd. for $\text{C}_{24}\text{H}_{26}\text{N}_2$ (342.49): C: 84.17; H: 7.65; N: 8.18. Found: C: 84.33; H: 7.71; N: 8.14



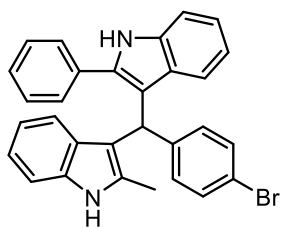
138o. Yield 0.271 g (74%). Orange solid, mp: 97-99°C. IR (neat) ν : 425, 739, 1242, 1507, 3400 cm^{-1} . ^1H -NMR (DMSO- d_6 , 400MHz) δ : 2.23 (s, 3H), 3.67 (s, 3H), 5.75 (s, 1H), 6.59-6.92 (m, 6H), 6.99 (t, 1H, $J = 7.4$ Hz), 7.04-7.25 (m, 5H), 7.32 (d, 1H, $J = 8.1$ Hz), 10.74 (br s, 2H). ^{13}C -NMR (DMSO- d_6 , 100MHz) δ : 12.5, 38.7, 55.6,

111.0, 112.1, 113.7, 114.0, 118.5, 118.6, 118.8, 119.4, 119.7, 120.2, 121.5, 124.3, 127.7, 128.5, 129.9, 132.2, 135.9, 137.2, 137.3, 157.9. GCMS (70 eV): m/z : 366 ($[\text{M}^+$], 100), 351 (62), 259 (37), 207 (29). Anal. Calcd. for $\text{C}_{25}\text{H}_{22}\text{N}_2\text{O}$ (366.46): C: 81.94; H: 6.05; N: 7.64. Found: C: 82.07; H: 5.98; N: 7.77.

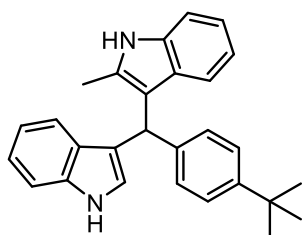


138p. Yield 0.209 g (53%). Brown solid, mp: 101-104°C. IR (neat) ν : 431, 741, 1242, 1458, 1507, 3402 cm^{-1} . ^1H -NMR (DMSO- d_6 , 400MHz) δ : 1.23 (t, 3H, $J = 7.3$ Hz), 2.23 (s, 3H), 2.80 (q, 2H, $J = 7.4$ Hz), 3.67 (s, 3H), 5.72 (s, 1H), 6.59 (s, 1H), 6.68-6.94 (m, 7H), 7.09-7.20 (m, 4H), 10.70 (s, 1H), 10.72 (s, 1H). ^{13}C -NMR (DMSO- d_6 , 100MHz) δ : 12.5, 15.1, 24.3, 38.8, 55.6, 111.0, 113.7,

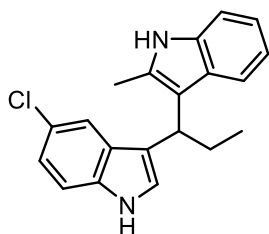
113.9, 117.5, 118.5, 118.9, 119.1, 119.4, 120.2, 124.0, 127.3, 127.5, 128.5, 129.9, 132.2, 135.8, 135.9, 137.3, 157.8. GC-MS (70 eV): m/z : 394 ($[\text{M}^+$], 100), 379 (55), 287 (34), 248 (18). Anal. Calcd. for $\text{C}_{27}\text{H}_{26}\text{N}_2\text{O}$ (394.52): C: 82.20; H: 6.64; N: 7.10. Found: C: 82.07; H: 6.67; N: 7.01.



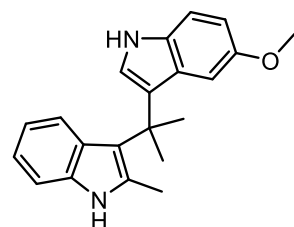
138q. Yield 0.197 g (45%). Brown solid, mp: 194-196°C. IR (neat) ν : 701, 746, 1245, 3390 cm^{-1} . $^1\text{H-NMR}$ (DMSO- d_6 , 400MHz) δ : 1.75 (s, 3H), 6.34 (d, 1H, $J = 8.1$ Hz), 6.61 (s, 1H), 6.68-6.80 (m, 2H), 6.84-7.01 (m, 4H), 7.11 (d, 2H, $J = 8.1$ Hz), 7.18 (d, 1H, $J = 8.1$ Hz), 7.28-7.34 (m, 2H), 7.36-7.48 (m, 3H), 7.53 (d, 1H, $J = 8.1$ Hz), 7.60 (d, 1H, $J = 8.1$ Hz), 11.0 (br s, 2H). $^{13}\text{C-NMR}$ (DMSO- d_6 , 100MHz) δ : 12.6, 57.1, 103.3, 108.2, 111.5, 113.1, 118.5, 119.6, 120.2, 120.8, 121.1, 121.9, 128.3, 129.0, 129.1, 129.4, 129.6, 129.9, 132.4, 133.4, 135.5, 135.7, 137.2, 141.0, 142.7. GC-MS (70 eV): m/z : 193 (100), 165 (20), 96 (7). Anal. Calcd. for $\text{C}_{30}\text{H}_{23}\text{BrN}_2$ (491.43): C: 73.32; H: 4.72; N: 5.70. Found: C: 73.44; H: 4.78; N: 5.73.



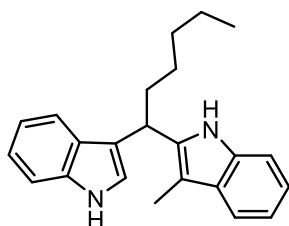
138r. Yield 0.275 g (70%). Pink solid, mp: 80-83°C. IR (neat) ν : 424, 473, 739, 1456, 3401 cm^{-1} . $^1\text{H-NMR}$ (DMSO- d_6 , 400MHz) δ : 1.25 (s, 9H), 2.27 (s, 3H), 5.76 (s, 1H), 6.70 (s, 1H), 6.72 (t, 1H, $J = 7.7$ Hz), 6.81 (t, 1H, $J = 7.7$ Hz), 6.91 (t, 1H, $J = 7.3$ Hz), 7.02 (t, 1H, $J = 7.7$ Hz), 7.10 (d, 1H, $J = 8.1$ Hz), 7.17-7.30 (m, 6H), 7.35 (d, 1H, $J = 8.1$ Hz), 10.73 (s, 2H). $^{13}\text{C-NMR}$ (DMSO- d_6 , 100MHz) δ : 12.3, 31.7, 34.5, 38.9, 110.8, 111.8, 113.3, 118.2, 118.4, 118.6, 119.2, 119.5, 120.0, 121.3, 124.1, 125.1, 127.5, 128.3, 128.4, 132.0, 135.7, 137.0, 142.1, 148.2. GC-MS (70 eV): m/z : 392 ($[\text{M}^+]$, 100), 377 (65), 335 (16), 259 (49), 218 (26). Anal. Calcd. for $\text{C}_{28}\text{H}_{28}\text{N}_2$ (392.55): C: 85.67; H: 7.19; N: 7.14. Found: C: 85.86; H: 7.30; N: 7.23.



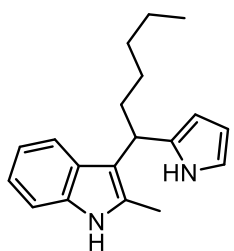
138s. Yield 0.171 g (53%). Pink solid, mp: 56-59°C. IR (neat) ν : 420, 584, 741, 794, 1459, 3403 cm^{-1} . $^1\text{H-NMR}$ (DMSO- d_6 , 400MHz) δ : 0.84 (t, 3H, $J = 6.8$ Hz), 2.03-2.35 (m, 2H), 2.39 (s, 3H), 4.11-4.19 (m, 1H), 6.75 (t, 1H, $J = 7.3$ Hz), 6.84-6.97 (m, 2H), 7.13 (s, 1H), 7.17 (d, 1H, $J = 8.1$ Hz), 7.28 (d, 1H, $J = 8.1$ Hz), 2.32-3.29 (m, 2H), 10.65 (s, 1H), 10.95 (s, 1H). $^{13}\text{C-NMR}$ (DMSO- d_6 , 100MHz) δ : 12.5, 13.4, 27.4, 35.1, 111.1, 113.0, 113.4, 118.4, 118.5, 119.2, 119.6, 120.2, 121.2, 123.1, 124.0, 128.0, 128.9, 132.0, 135.5, 136.0. GC-MS (70 eV): m/z : 322 ($[\text{M}^+]$, 21), 293 (100), 257 (8), 129 (10). Anal. Calcd. For $\text{C}_{20}\text{H}_{19}\text{ClN}_2$ (322.84): C: 74.41; H: 5.93; N: 8.68. Found: C: 74.35; H: 5.84; N: 8.73.



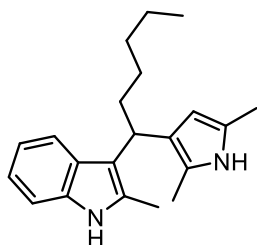
138t. Yield 0.236 g (74%). Yellow solid, mp: 101-104°C. IR (neat) ν : 430, 740, 1211, 1455, 3401 cm^{-1} . $^1\text{H-NMR}$ (DMSO- d_6 , 400MHz) δ : 1.83 (s, 6H), 2.29 (s, 3H), 3.40 (s, 3H), 6.41 (d, 1H, $J = 2.5$ Hz), 6.55 (dd, 1H, $J = 2.5, 8.7$ Hz), 6.62-6.69 (m, 1H), 6.79-6.85 (m, 1H), 7.13 (d, 2H, $J = 8.7$ Hz), 7.20 (d, 1H, $J = 2.5$ Hz), 7.30 (d, 1H, $J = 8.1$ Hz), 10.51 (br s, 2H). $^{13}\text{C-NMR}$ (DMSO- d_6 , 100MHz) δ : 14.9, 31.5, 36.2, 55.4, 103.0, 110.3, 110.8, 112.3, 117.2, 118.1, 119.8, 120.7, 121.3, 126.0, 127.1, 128.6, 130.9, 132.9, 135.7, 152.5. GC-MS (70 eV): m/z : 318 ($[\text{M}^+]$, 31), 303 (100). Anal. Calcd. for $\text{C}_{21}\text{H}_{22}\text{N}_2\text{O}$ (318.42): C: 79.21; H: 6.96; N: 8.80. Found: C: 79.33; H: 6.90; N: 8.89.



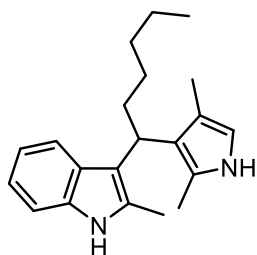
139. Yield 0.155 g (47%). Pale yellow oil. IR (neat) ν : 423, 735, 1457, 3406 cm^{-1} . $^1\text{H-NMR}$ (DMSO- d_6 , 400MHz) δ : 0.80 (t, 3H, $J = 7.3$ Hz), 1.05-1.39 (m, 6H), 2.20 (s, 3H), 2.28-2.39 (m, 2H), 5.80 (t, 1H, $J = 7.7$ Hz), 6.84 (t, 1H, $J = 7.7$ Hz), 6.97 (t, 1H, $J = 7.7$ Hz), 7.01 (t, 1H, $J = 7.7$ Hz), 7.10 (t, 1H, $J = 7.7$ Hz), 7.19 (s, 1H), 7.25 (d, 1H, $J = 8.1$ Hz), 7.33 (d, 1H, $J = 8.1$ Hz), 7.44 (d, 1H, $J = 7.7$ Hz), 7.53 (d, 1H, $J = 2.1$ Hz), 7.66 (d, 1H, $J = 8.3$ Hz), 11.04 (br s, 1H). $^{13}\text{C-NMR}$ (DMSO- d_6 , 100MHz) δ : 10.1, 14.3, 22.5, 26.4, 31.4, 34.8, 52.1, 109.3, 110.3, 111.9, 116.0, 118.4, 118.9, 119.0, 119.1, 121.3, 121.6, 123.5, 124.1, 126.6, 128.6, 136.6, 136.8. GC-MS (70 eV): m/z : 330 ($[\text{M}^+]$, 23), 207 (27), 200 (77), 156 (20), 130 (100). Anal. Calcd. for $\text{C}_{23}\text{H}_{26}\text{N}_2$ (330.48): C: 83.59; H: 7.93; N: 8.48. Found: C: 83.41; H: 8.01; N: 8.58.



140a. Yield 0.056 g (20%). Yellow oil. IR (neat) ν : 737, 1462, 3393 cm^{-1} . $^1\text{H-NMR}$ (DMSO- d_6 , 400MHz) δ : 0.77 (t, 3H, $J = 7.3$ Hz), 1.03-1.30 (m, 6H), 1.93-2.07 (m, 2H), 2.29 (s, 3H), 3.93 (t, 1H, $J = 7.7$ Hz), 5.80-5.86 (m, 1H), 6.42-6.45 (m, 1H), 6.51-6.54 (m, 1H), 6.77 (t, 1H, $J = 7.3$ Hz), 6.88 (t, 1H, $J = 7.3$ Hz), 7.16 (d, 1H, $J = 8.1$ Hz), 7.34 (d, 1H, $J = 7.7$ Hz), 10.30 (br s, 1H), 10.54 (s, 1H). $^{13}\text{C-NMR}$ (DMSO- d_6 , 100MHz) δ : 12.5, 14.7, 22.9, 28.2, 32.1, 34.8, 35.5, 107.8, 110.9, 114.7, 114.9, 117.5, 118.2, 119.7, 120.0, 128.0, 128.2, 131.5, 136.0. GCMS (70 eV): m/z : 280 ($[\text{M}^+]$, 22), 209 (100), 167 (10), 104 (10). Anal. Calcd. for $\text{C}_{19}\text{H}_{24}\text{N}_2$ (280.41): C: 81.38; H: 8.63; N: 9.99. Found: C: 81.35; H: 8.73; N: 9.89.

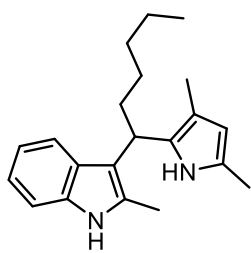


140b. Yield 0.126 g (41%). Yellow solid, mp: 44-47°C. IR (neat) ν : 740, 1460, 2924, 3400 cm^{-1} . $^1\text{H-NMR}$ (DMSO- d_6 , 400MHz) δ : 0.81 (t, 3H, $J = 7.7$ Hz), 1.07-1.32 (m, 6H), 1.89-2.08 (m, 2H), 1.96 (s, 3H), 2.06 (s, 3H), 2.33 (s, 3H), 3.83 (t, 1H, $J = 7.7$ Hz), 5.71 (d, 1H, $J = 2.1$ Hz), 6.82 (t, 1H, $J = 7.7$ Hz), 6.90 (t, 1H, $J = 7.7$ Hz), 7.17 (d, 1H, $J = 8.1$ Hz); 7.52 (d, 1H, $J = 8.1$ Hz), 9.81 (s, 1H), 10.5 (s, 1H). $^{13}\text{C-NMR}$ (DMSO- d_6 , 100MHz) δ : 11.4, 12.3, 13.4, 14.4, 22.6, 28.1, 31.8, 33.5, 35.6, 105.2, 110.6, 115.3, 118.0, 119.5, 119.7, 120.5, 122.8, 123.3, 127.9, 130.5, 135.7. GC-MS (70 eV): m/z : 308 ($[\text{M}^+]$, 17), 280 (10), 237 (100), 207 (27). Anal. Calcd. For $\text{C}_{21}\text{H}_{28}\text{N}_2$ (308.47): C: 81.77; H: 9.15; N: 9.08. Found: C: 81.65; H: 9.10; N: 9.12.



140c. Yield 0.037 g (12%). Yellow solid, mp: 44-47°C. IR (neat) ν : 740, 1460, 2924, 3400 cm^{-1} . $^1\text{H-NMR}$ (DMSO- d_6 , 400MHz) δ : 0.83 (t, 3H, $J = 7.7$ Hz), 1.17-1.33 (m, 6H), 1.81 (s, 3H), 1.97-2.16 (m, 2H), 2.13 (s, 3H), 2.27 (s, 3H), 3.98 (t, 1H, $J = 7.7$ Hz), 6.19 (d, 1H, $J = 1.3$ Hz), 6.81 (t, 1H, $J = 7.7$ Hz), 6.89 (t, 1H, $J = 7.7$ Hz), 7.17 (d, 1H, $J = 8.1$ Hz), 7.36 (d, 1H, $J = 8.1$ Hz), 9.79 (s, 1H), 10.53 (s, 1H). $^{13}\text{C-NMR}$ (DMSO- d_6 , 100MHz) δ : 12.2, 12.7, 13.1, 14.4, 22.7, 28.3, 32.0, 34.6, 34.9, 110.6, 113.3, 114.2, 116.6, 118.1, 119.1, 119.6, 120.5, 122.8, 128.5, 131.2, 135.4. GC-MS (70 eV): m/z : 308 ($[\text{M}^+]$, 11), 237 (100), 221 (5), 111 (5). Anal. Calcd. for $\text{C}_{21}\text{H}_{28}\text{N}_2$ (308.47): C: 81.77; H: 9.15; N: 9.08. Found:

C: 81.81; H: 9.13; N: 9.01.



140d. Yield 0.040 g (13%). Clear oil. IR (neat) ν : 738, 1455, 3388 cm^{-1} . $^1\text{H-NMR}$ (DMSO- d_6 , 400MHz) δ : 0.81 (t, 3H, $J = 7.7$ Hz), 1.08-1.37 (m, 6H), 1.76 (s, 3H), 1.97-2.15 (m, 2H), 2.11 (s, 3H), 2.32 (s, 3H), 4.04 (dd, 1H, $J = 7.1, 8.7$ Hz), 5.35 (d, 1H, $J = 2.1$ Hz), 6.82 (t, 1H, $J = 7.7$ Hz), 6.91 (t, 1H, $J = 7.7$ Hz), 7.17 (d, 1H, $J = 8.1$ Hz), 7.52 (d, 1H, $J = 8.1$ Hz), 9.88 (s, 1H), 10.55 (s, 1H). $^{13}\text{C-NMR}$ (DMSO- d_6 , 100MHz) δ : 11.8, 12.3, 13.4, 14.4, 22.6, 27.9, 31.7, 33.3, 33.7, 107.6, 110.6, 112.0, 113.5, 118.1, 119.1, 119.9, 123.7, 127.7, 129.3, 131.1, 135.6. GC-MS (70 eV): m/z : 308 ($[\text{M}^+]$, 15), 237 (100), 170 (13). Anal. Calcd. for $\text{C}_{21}\text{H}_{28}\text{N}_2$ (308.47): C: 81.77; H: 9.15; N: 9.08. Found: C: 81.69; H: 9.14; N: 9.16.

CHAPTER THREE

**Effect of the Binding of Piceatannol and Oxyresveratrol to
Soybean Protein Isolate on the Structural and Functional
Properties**

3.1 Synthesis of stilbene representatives and their functions

Stilbenes, a class of plant polyphenols, have attracted great interest due to their conjugated structures and diverse biological activities. These compounds and their derivatives are important for drug research and development because of their potential in therapeutic or preventive applications, especially resveratrol (**141**, Figure 7).^[187]

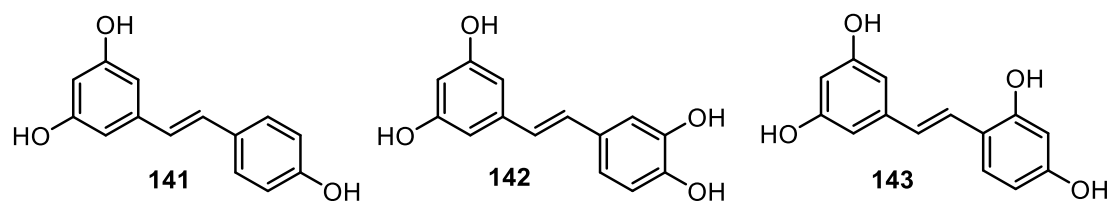


Figure 7. Structures of resveratrol, piceatannol and oxyresveratrol.

Resveratrol is known for its promising and selective activity *in vitro* and *in vivo* against a range of disease states, including inflammation, heart disease, aging and cancer. Actually, it can be found in relatively high concentration in red wines but almost none in white varieties and grape juice.^[188] Piceatannol (**142**, PIC, Figure 7) and oxyresveratrol (**143**, OXY, Figure 7) are two hydroxylated analogs of resveratrol with an additional hydroxyl group. Since they contain a common stilbene backbone and differ only in the absence and presence or position of hydroxyl groups on the ring, they consistently have similar biological activities such as anti-inflammatory, antioxidant, anti-cardiovascular and anti-cancer activity.^[189] In addition, they are useful as phytoalexins and tyrosinase inhibitors. They are now attracting widespread attention as potential pharmaceutical and nutritional molecules. Therefore, their synthesis and application are vital to human-life.

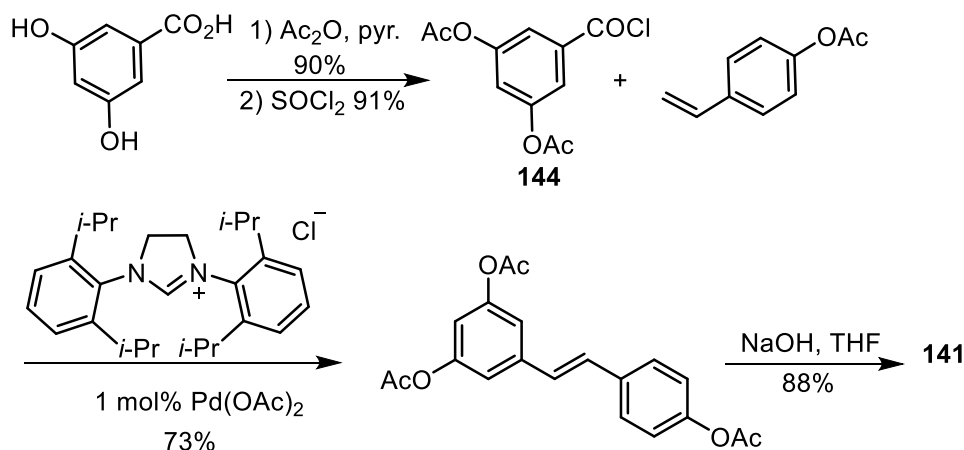
3.1.1 Synthesis of resveratrol

The synthesis of resveratrol can be efficiently performed by Heck, Wittig and Sonogashira reaction with the use of various starting materials.

3.1.1.1 Synthesis of resveratrol by Heck reaction

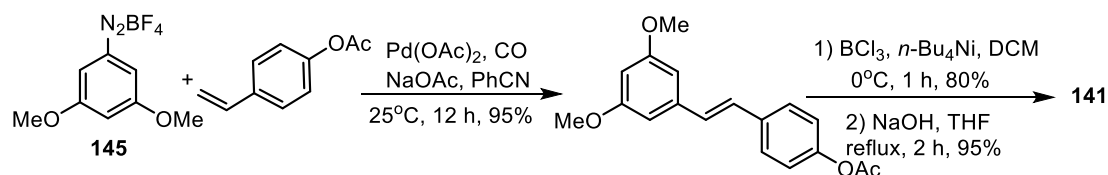
The Heck reaction is the most common followed strategy for preparing resveratrol. Andrus and co-workers^[190] reported an efficient and direct route to resveratrol starting from inexpensive resorcylic acid using a palladium-catalyzed decarbonylative Heck coupling reaction. First, resorcylic acid was protected by acetic

anhydride in pyridine, then the protected acid was converted to acid chloride **144** using thionyl chloride. After that, **144** was coupled with a styrene derivative in the presence of palladium(II) acetate and *N,N*-bis-(2,6-diisopropyl) dihydroimidazolium chloride which was used as carbene type ligand to promote the reaction. Therefore, resveratrol triacetate was obtained in good yield, and easily converted into resveratrol **141** through basic hydrolysis (Scheme 87). The total yield is 53%, and only four steps from resorcylic acid.



Scheme 87. Synthesis of resveratrol from resorcylic acid with styrene.

Arenediazonium salt **145** and 4-acetoxystyrene can also form a resveratrol precursor smoothly in 95% yield after 12 h. After demethylation with BCl_3 in the presence of $n\text{-Bu}_4\text{NI}$ and deacetylation with aqueous sodium hydroxide, resveratrol **141** was obtained with excellent yield (Scheme 88).^[191] This route is particularly appealing since it is short, straightforward and featured by a good yield.

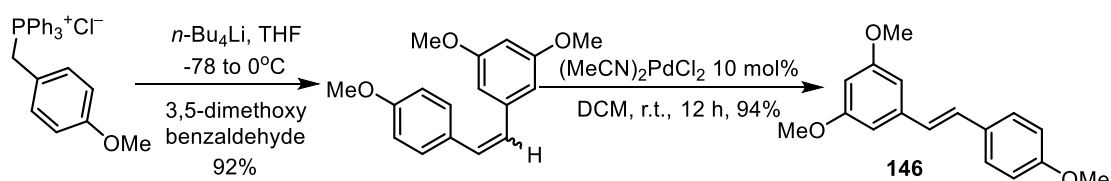


Scheme 88. Synthesis of resveratrol from arenediazonium salt.

3.1.1.2 Synthesis of resveratrol from the Wittig reaction

The Wittig reaction between benzylphosphonium salt and benzaldehyde can give arylalkenes. Thus a facile method for the preparation of trimethoxyresveratrol **146** via palladium(II)-catalyzed isomerization of *cis*-arylalkenes was proposed by Spencer et al.^[192] Despite the rather high catalyst loading (10 mol%), the synthetic potential of this method was demonstrated in the high yield preparation of **146** (Scheme 89).

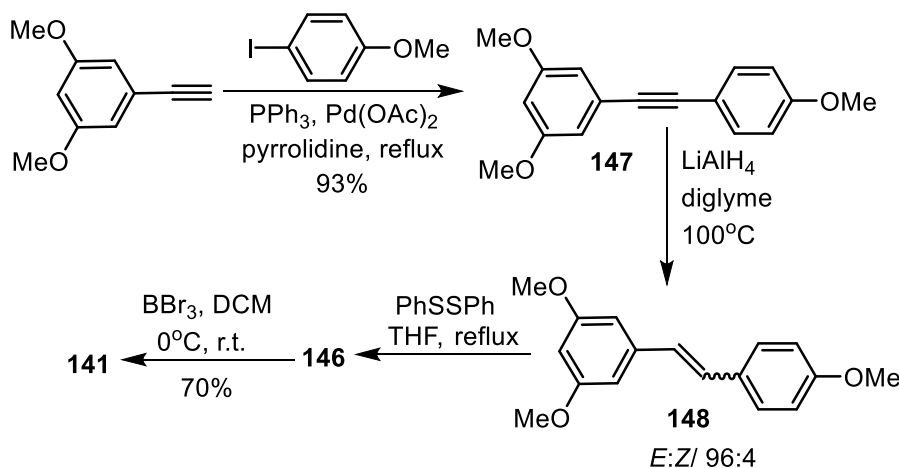
Resveratrol **141** can be obtained after simple demethylation of the latter derivative.



Scheme 89. Synthesis of resveratrol by Wittig reaction.

3.1.1.3 Synthesis of resveratrol by Sonogashira coupling reaction

As displayed in Scheme 90, Lara-Ochoa and co-workers^[193] proposed a new way to synthesize resveratrol with the following steps: (i) Sonogashira coupling of 3,5-dimethoxy-1-ethynylbenzene with 4-iodoanisole to give precursor **147** in 93% isolated yield under the condition of Pd(OAc)₂, triphenylphosphine, pyrrolidine as solvent and refluxing; (ii) *trans* addition of the hydride to the triple bond by the reduction of LiAlH₄ gives a reductive mixture **148** with a ratio of 96:4 (*E/Z*) in quantitative yield; (iii) diphenyl disulfide in refluxing THF converts **148** to **146** by double bond isomerization; (iv) deprotection from BBr₃ provides the final product resveratrol **141**. In summary, this easy-handle, and high-efficient four-step protocol affords pure resveratrol with 62% yield, in short reaction time.



Scheme 90. Synthesis of resveratrol from 3,5-dimethoxy-1-ethynylbenzene.

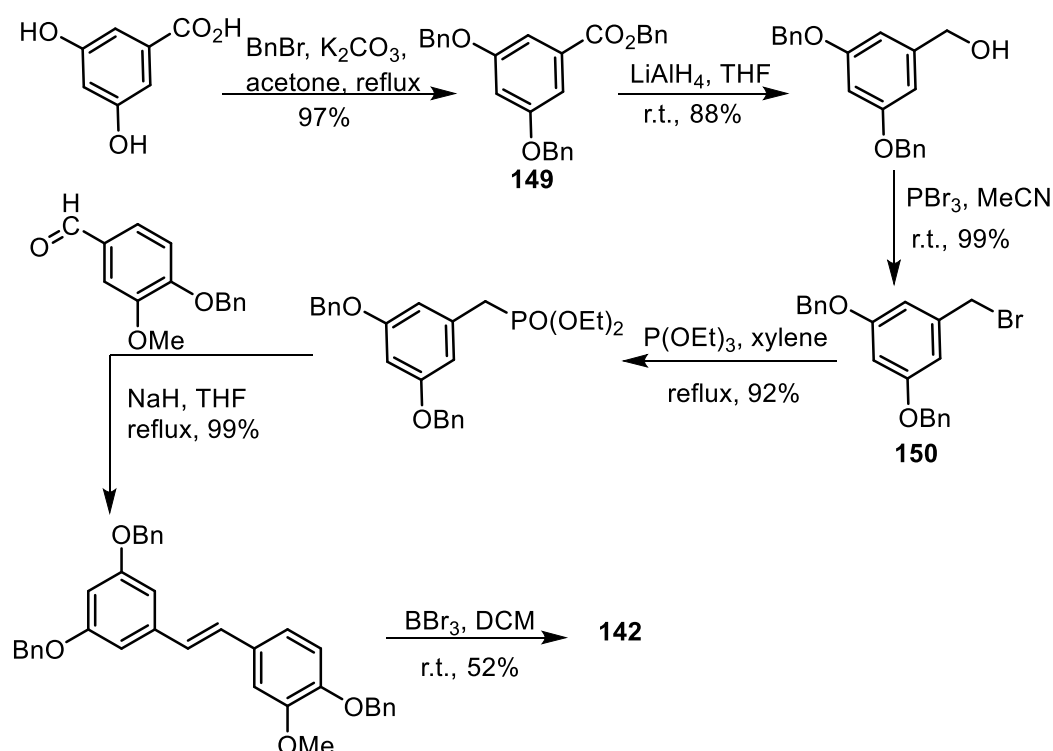
3.1.2 Synthesis of piceatannol and oxyresveratrol

The only difference between PIC and OXY is the position of extra hydroxyl from resveratrol. Therefore, the routes for synthesizing them have close similarities.

3.1.2.1 Synthesis from Horner-Emmons-Wadsworth reaction

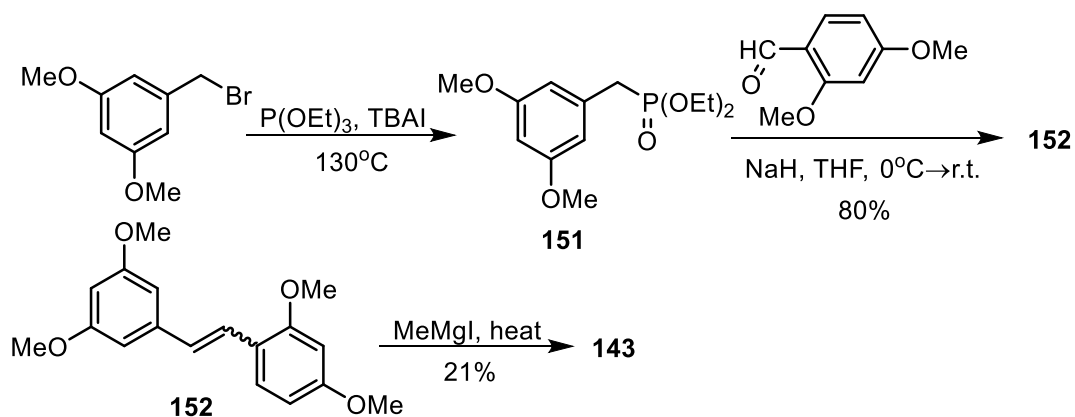
Reaction of 3,5-dihydroxybenzoic acid in acetone with benzyl bromide and

potassium carbonate at reflux gave the benzylated ester **149** in 97% yield. Benzyl alcohol was obtained in 88% yield by reducing **149** in the presence of LiAlH_4 . Bromination of alcohol with PBr_3 gave benzyl bromide **150** in 99% yield at room temperature. Phosphonylation of **150** with triethyl phosphite in xylene at reflux provided diethyl phosphonate in 92% yield, and the following Wittig-Horner reaction with benzylated vanillin using NaH in THF afforded the desired (*E*)-stilbene with 99% yield. After final dealkylation, PIC **142** can be obtained with moderate yield (Scheme 91).^[194] The synthetic process includes benzylation, metal hydride reduction, bromination, phosphonation, Wittig-Horner reaction and dealkylation. Despite of the several steps, this route is more efficient compared to other procedures.



Scheme 91. Synthesis of piceatannol through Horner-Emmons-Wadsworth reaction.

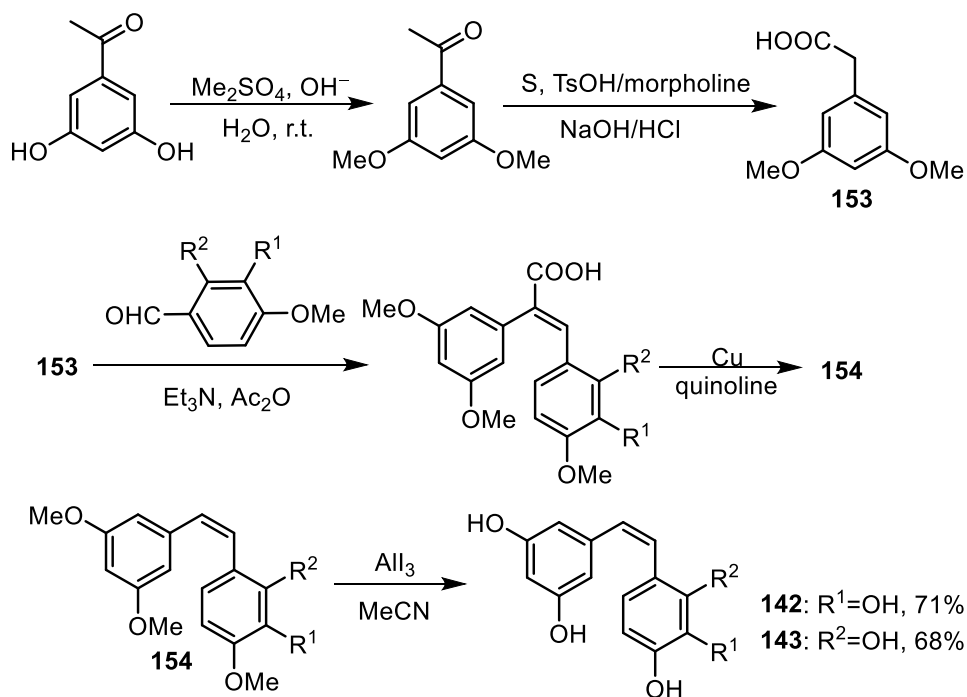
OXY was also prepared by standard synthetic procedures. Starting from commercially available 3,5-dimethoxybenzyl bromide upon reaction with triethyl phosphite by Michael-Arbuzov process, phosphonate **151** was obtained. The subsequent Horner-Emmons-Wadsworth reaction of **151** with 2,4-dimethoxybenzaldehyde gave a diastereomeric mixture of stilbenes **152** in 80% yield. Finally, **152** was demethoxylated by thermal treatment with methylmagnesium iodide to provide OXY **143** in 21% yield (Scheme 92).^[195]



Scheme 92. Synthesis of oxyresveratrol through Horner-Emmons-Wadsworth reaction.

3.1.2.2 Synthesis by Perkin-type reactions

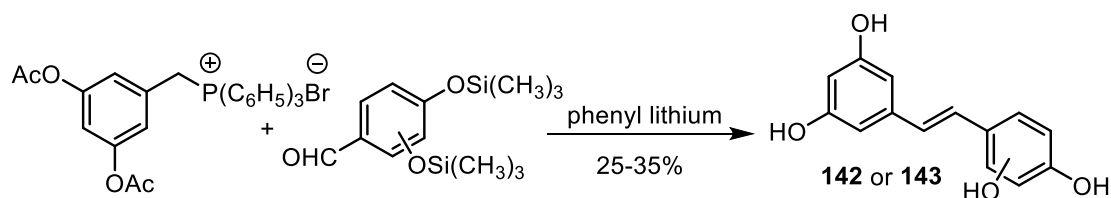
The synthesis of PIC and OXY started from the inexpensive and commercially available 3,5-dihydroxyacetophenone. A common intermediate, 3,5-dimethoxyphenylacetic acid **153**, was synthesized via methylation and Willgerodt-Kindler reaction. The Perkin condensation of **153** with methoxybenzaldehyde afforded *E*-2,3-diarylacrylic acids, which gave *Z*-stilbenes intermediate **154** through decarboxylation in quinoline with copper powder. Finally, the targets were obtained after a simultaneous demethylation/isomerization process in the presence of AlI_3 (Scheme 93).^[196] The route is viable, practical and provides PIC and OXY in high overall yields.



Scheme 93. The synthetic route of piceatannol and oxyresveratrol.

3.1.2.3 Synthesis by Wittig reaction

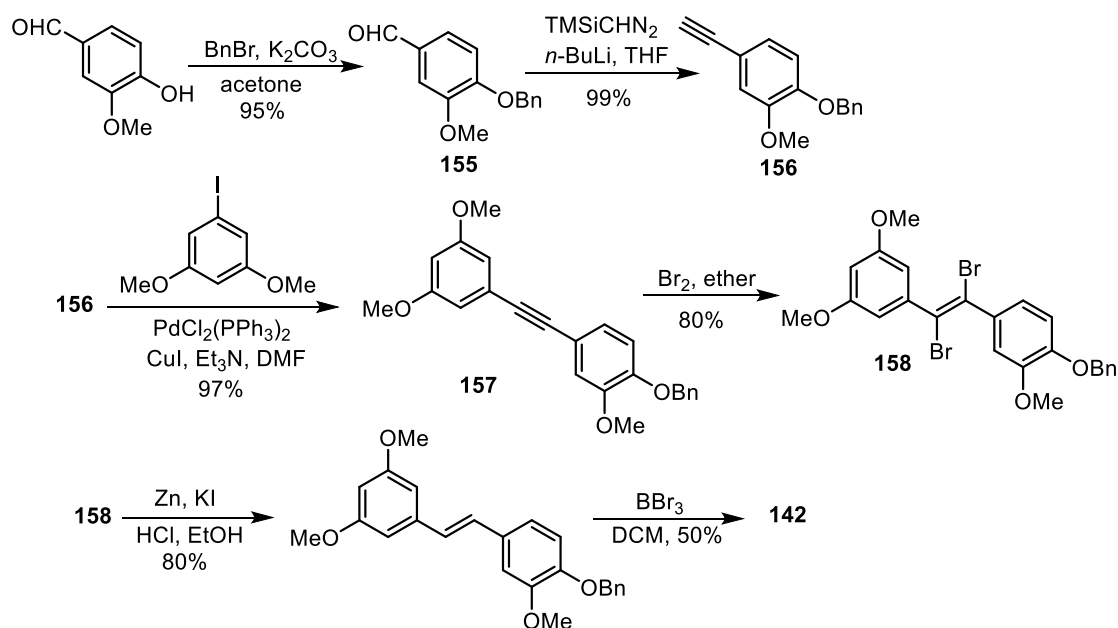
Reimann^[197] proposed a synthetic protocol involving the Wittig reaction between triphenyl-[3,5-dihydroxybenzyl]-phosphonium bromide and silylated 2,4(or 3,4)-dihydroxybenzaldehyde in the presence of an excess of phenyl lithium. This approach can provide PIC **142** and OXY **143** with modest yields (Scheme 94).



Scheme 94. Synthesis of piceatannol and oxyresveratrol by Wittig reaction.

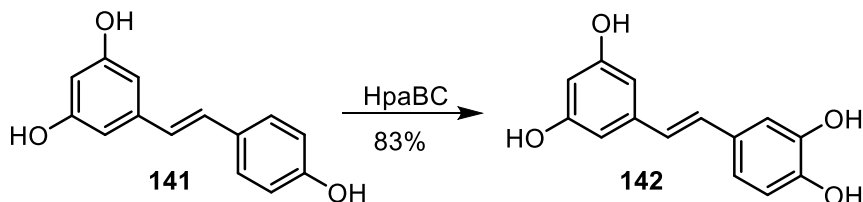
3.1.2.4 Other synthetic routes for piceatannol and oxyresveratrol

In addition to the above methods, other protocols involving Sonogashira coupling, Heck reaction and biosynthesis can also be used for the synthesis of PIC and OXY. Jun et al.^[198] chose vanillin as starting material to prepare PIC through the following steps: (i) vanillin reacts with benzyl bromide in the presence of potassium carbonate to generate benzylated vanillin **155** in 95% yield; (ii) Colvin rearrangement between **155** and trimethylsilyl diazomethane under the condition of *n*-butyllithium in THF at -78°C afforded ethynylbenzene **156** in 99% yield; (iii) **157** in 97% yield were provided by the Sonogashira coupling between **156** and 1-iodo-3,5-dimethoxybenzene by using $\text{PdCl}_2(\text{PPh}_3)_2/\text{CuI}/\text{Et}_3\text{N}$ in DMF; (iv) **157** reacted with bromine at -78°C to give (*E*)-dibromostilbene **158** in 80% yield; (v) the reductive debromination of **158** by $\text{Zn}/\text{KI}/\text{HCl}$ gave 80% yield of (*E*)-stilbene; (vi) BBr_3 in methylene chloride dealkylate (*E*)-stilbene to form PIC **142** at 50% yield (Scheme 95). The first five steps are very productive, even though the conditions required are rather severe. The sixth step limits the final yield and applications of this route.



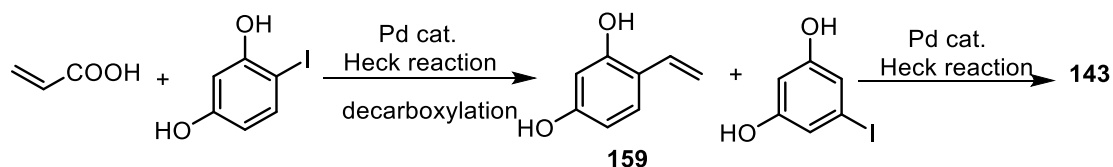
Scheme 95. Synthesis of piceatannol by Sonogashira coupling reaction.

In addition, PIC can be prepared by biosynthesis, such as the regioselective hydroxylation of resveratrol **141**. Furuya and Kino^[199] concluded that flavin-dependent monooxygenase HpaBC, from *Pseudomonas aeruginosa*, is useful for the regioselective conversion of **141** into PIC **142** in high-yield (Scheme 96).



Scheme 96. Regioselective hydroxylation of resveratrol to piceatannol by HpaBC.

Recently, a simple two-step synthesis of OXY was reported.^[200] Acrylic acid reacts with 2,4-dihydroxyiodobenzene under Heck reaction conditions to give an intermediate **159**, which generates OXY **143** after decarboxylation and coupling with 3,5-dihydroxyiodobenzene (Scheme 97).



Scheme 97. Synthesis of oxyresveratrol by Heck reaction.

3.2 Effect of the binding of piceatannol and oxyresveratrol to soybean protein isolate on the structural and functional properties

3.2.1 State of the art

Soy protein isolate (SPI), derived from soybeans, has always been used for food processing because it is inexpensive, renewable, of high nutritional value, and similar to animal proteins.^[201] After ultracentrifugation, SPI can be divided into four parts: 2S, 7S, 11S, and 15S globulins. 7S and 11S can account for about 30% and 40% of the total weight, respectively.^[202] Yang et al.^[203] found that the combination of SPI and resveratrol can increase the solubility and antioxidant activity of resveratrol. You et al.^[204] investigated the interaction between SPI and (-)-epigallocatechin-3-gallate to test their foaming, emulsifying, and antioxidant properties. Zhang et al.^[205] concluded that the presence of SPI can improve the stability of chlorophyll to achieve favorable food appearance. Considering that plant foods have a great impact on human health and well-being,^[206] SPI can be used as a carrier protein for encapsulating active ingredients. It is meaningful to test the interaction between SPI and biological reagents. However, to date, there has been no report on the study of the binding between PIC/OXY and SPI. At present, there are many synthetic pathways for PIC/OXY, which are often divided into multiple steps and accompanied with moderate yields. However, considering the price of PIC/OXY and the significance of biological activity tests, this part avoids synthetic work and directly performs biological assays.

In this section, the interaction between PIC/OXY and SPI under physiological conditions was investigated using multiple spectroscopic techniques and molecular docking simulations. By CD spectroscopy, DLS, and fluorescence spectroscopy, the changes of various functional properties and structures of SPI caused by the binding of PIC/OXY can also be obtained. The effects of SPI–PIC/OXY interaction on the foaming and emulsifying properties of SPI as well as the antioxidant activity and *in vitro* digestion of PIC/OXY were also investigated.

3.2.2 Results and discussion

3.2.2.1 Fluorescence spectroscopic analysis

As shown in Figure 8, the maximal fluorescence intensity of SPI was observed at 342 nm, it is almost consistent with Miao's study.^[207] And there is a significant red-shift after binding to PIC (16 nm) or OXY (18 nm), this means the environment surrounded with Trp and Tyr residues in SPI molecules were more hydrophilic.^[208] The decreasing fluorescence intensities of SPI in Figure 8 mean that the SPI molecule was quenched by PIC/OXY. And the quenching extents were 62.6% and 54.2% for PIC and OXY (20 μM), respectively. It demonstrated that the binding between PIC and SPI was stronger than that between OXY and SPI.^[209] In addition, isobestic points also occurred in the spectra which indicate the equilibrium between free and bound form of PIC/OXY.^[210]

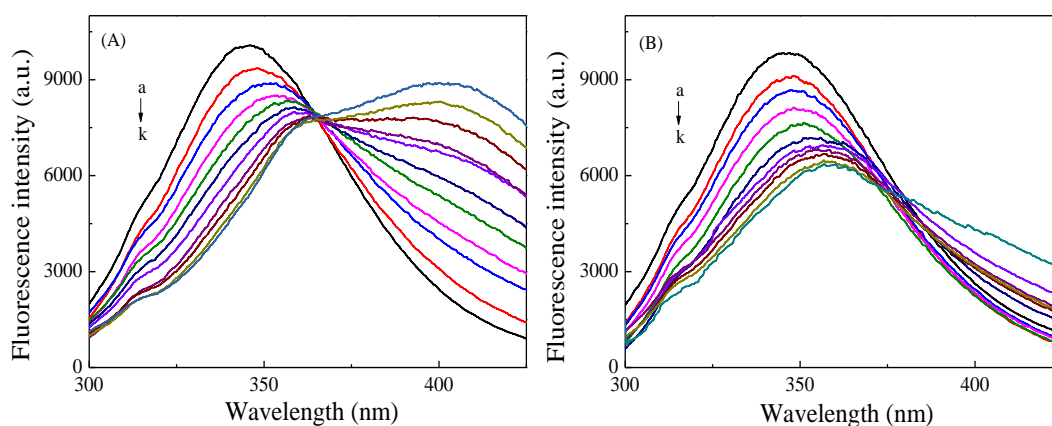


Figure 8. Fluorescence quenching spectra of SPI (a) in the presence of various concentrations of (A) PIC and (B) OXY at 298.2 K (a→k: 0-20 μM).

Quenching mechanism of SPI–PIC/OXY

After performing a linear fitting according to Eq. 3, the fitted curves of PIC–SPI and OXY–SPI at 298.2 K were shown in Figure 9A, and the corresponding k_q were listed in Table 10. As shown in Figure 9A, the fitted curves were straight lines and the values of R^2 were larger than 0.99. This meant that only one quenching mechanism existed in the binding. The value of k_q was larger than $2.0 \times 10^{10} \text{ L mol}^{-1} \text{ s}^{-1}$ showed the existence of static quenching.^[211] However, the temperature has a slight beneficial effect on k_q , which is opposite to normal static quenching. This phenomenon also

occurred in the system of PIC–bovine serum albumin which binds through static quenching mechanism.^[212] For further confirmation of the mechanism, Förster resonance energy transfer (FRET) and TRF analyses were also performed.

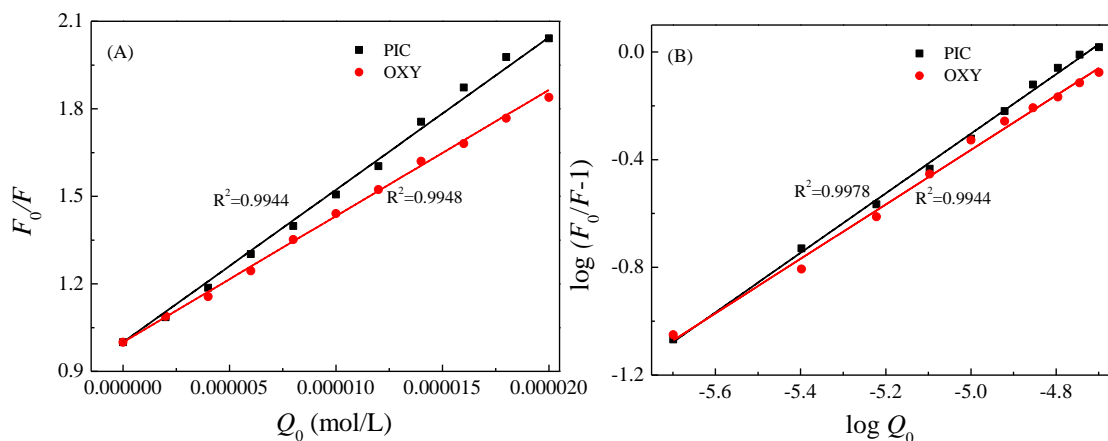


Figure 9. Stern-Volmer (A) and double-logarithm (B) plots for the fluorescence quenching of SPI by PIC (black) and OXY (red) at 298.2 K.

Table 10. Thermodynamic parameters for the interaction of PIC/OXY with SPI at different temperatures.

	T (K)	k_q ($\times 10^{12}$ $L \cdot mol^{-1} \cdot s^{-1}$)	K_a ($\times 10^4$ M^{-1})	n	ΔG° ($kJ \cdot mol^{-1}$)	ΔH° ($kJ \cdot mol^{-1}$)	ΔS° ($J \cdot mol^{-1} \cdot K^{-1}$)
PIC	298.2	5.22±0.07	16.80±0.32	1.11±0.02	-29.83±0.05		
	302.2	5.39±0.08	11.44±0.20	1.07±0.03	-29.26±0.04	-87.42±0.09	-192.92±2.94
	306.2	6.04±0.04	6.65±0.14	1.01±0.02	-28.27±0.05		
	310.2	6.15±0.05	4.42±0.11	0.97±0.02	-27.59±0.06		
OXY	298.2	4.32±0.05	4.94±0.11	1.01±0.03	-26.79±0.05		
	302.2	4.78±0.04	3.02±0.07	0.96±0.01	-25.92±0.06	-78.26±0.11	-172.81±1.71
	306.2	5.41±0.08	2.13±0.06	0.92±0.02	-25.37±0.07		
	310.2	6.02±0.06	1.43±0.02	0.87±0.01	-24.68±0.04		

The overlap in Figure 10 demonstrated that there is a binding between SPI and PIC/OXY. After calculation, the values of r in the two systems were listed in Table 11. The values of r were within the range of 2–8 nm and had the tendency of $0.5 R_0 < r < 1.5 R_0$. It means that the energy can be transferred from SPI to PIC or OXY, and there is a static quenching process in the binding.^[213]

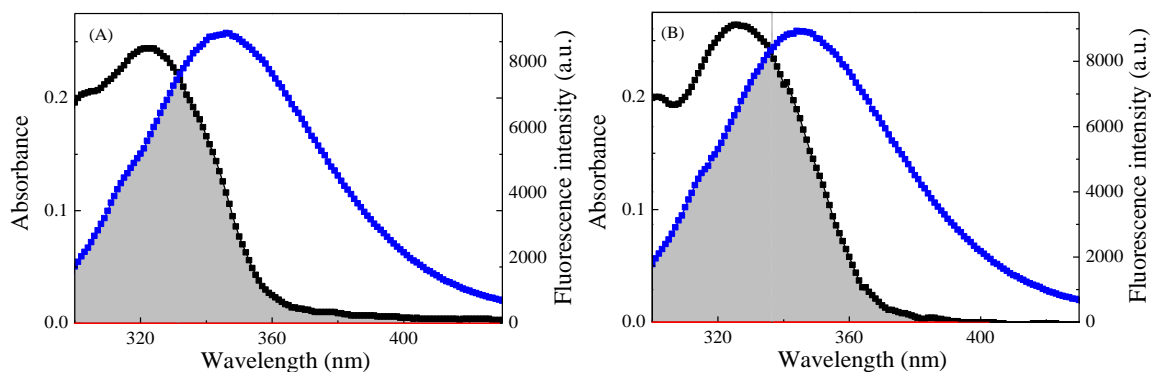


Figure 10. Overlap of the fluorescence emission spectrum of SPI (blue) with the absorption spectrum for (A) PIC and (B) OXY (black).

Table 11. Energy transfer efficiency and distance between SPI and PIC/OXY.

	$J (\times 10^{-14} \text{ cm}^3 \cdot \text{L} \cdot \text{mol}^{-1})$	R_0 (nm)	r (nm)	E
PIC	2.57	2.87	2.99	0.44
OXY	3.31	2.99	3.00	0.50

The data for TRF measurements are shown in Table 12. The value of χ^2 is less than 1.3, which can indicate the best fit to the data.^[214] Moreover, the value of life-time is almost constant with various concentrations of PIC and OXY. It represents the existence of static quenching.^[215]

Table 12. Fluorescence lifetime of SPI in the absence and presence of PIC/OXY.

	C (μM)	τ_1 (ns)	α_1 (%)	τ_2 (ns)	α_2 (%)	τ (ns)	χ^2
	0	2.4039	48.53	4.2577	51.47	3.36	1.118
PIC	10	2.6841	86.21	7.1436	13.79	3.30	1.097
	30	2.8825	93.57	9.2356	6.43	3.29	1.045
	50	2.7897	93.39	9.4432	6.61	3.23	1.215
OXY	10	2.6741	68.34	4.7968	31.66	3.35	1.043
	30	2.3842	55.27	4.3517	44.73	3.26	1.086
	50	2.7234	73.81	4.7849	26.19	3.26	1.148

Binding information about SPI–PIC and SPI–OXY

The liner-fitting of Eq. 4 was shown in Figure 9B, and the values of the binding constant (K_a) and the number of binding sites (n) were listed in Table 10. The linearity of the plot ($R^2 > 0.99$) and the value of number of binding sites is close to 1. It

suggested that only one binding site existed for the binding of PIC/OXY to SPI. The stronger binding between PIC and SPI was proved by the higher binding constant. And this is consistent with the greater degree of SPI being quenched by PIC. This may be caused by the stronger activity of hydroxyls at ortho position than those at meta position.^[216] The same binding order also appears in lysozyme,^[217] but it's the exact opposite of human serum albumin^[218] and trypsin.^[217] This may be due to the different structures and characteristics of the various proteins. Furthermore, temperature has an adverse effect on the binding, i.e. the binding process was exothermic. It means that moderate heating will shorten the storage of PIC or OXY and release them to achieve a better nutritional level for food application.^[219]

Generally, four binding forces occurred in the binding: hydrogen bonds, van der Waals attractions, electrostatic interactions, and hydrophobic interactions.^[220] And they can be determined by enthalpy change (ΔH°) and entropy change (ΔS°). The negative of ΔH° and ΔS° directed that the binding process was exothermic, and the major interaction forces were van der Waals forces and hydrogen bonding. The same driving forces may be due to the similar structure of PIC and OXY. Furthermore, the stronger binding caused the more negative values of ΔH° and ΔS° in the PIC–SPI system. The negative value of ΔG° represented the spontaneous of the binding between SPI and PIC/OXY.

Synchronous fluorescence spectroscopy analysis

The $\Delta\lambda$ values of 15 nm and 60 nm can indicate the characteristic information of tyrosine and tryptophan residues, respectively.^[221] As shown in Figure 11, all intensities decreased with the increasing concentrations of PIC/OXY. PIC can make the maximum emission wavelengths of tyrosine and tryptophan blue-shift (1.8 nm) and red-shift (1.2 nm), respectively. At the same time, the blue-shifted (0.8 nm) and red-shifted (2.0 nm) of the maximum wavelengths of tyrosine and tryptophan were also observed in SPI–OXY. It indicated that the environments around tyrosine and tryptophan had a subtle change, and the shifting direction of tryptophan was the same as that in the steady-state emission fluorescence studies. In addition, the ratio of synchronous fluorescence quenching (RSFQ, which equals to $1-F/F_0$) can represent the residues participating in the interaction.^[222] It can be seen in Figure 12 that the values of RSFQ were larger in the SPI–PIC system, indicating that the binding

strength of PIC was stronger than that of OXY. The result was consistent with the higher values of K_a in the PIC–SPI system. Moreover, the values of RSFQ for tryptophan were higher than those for tyrosine. It demonstrated that tryptophan played an important role in the binding between SPI and PIC or OXY.

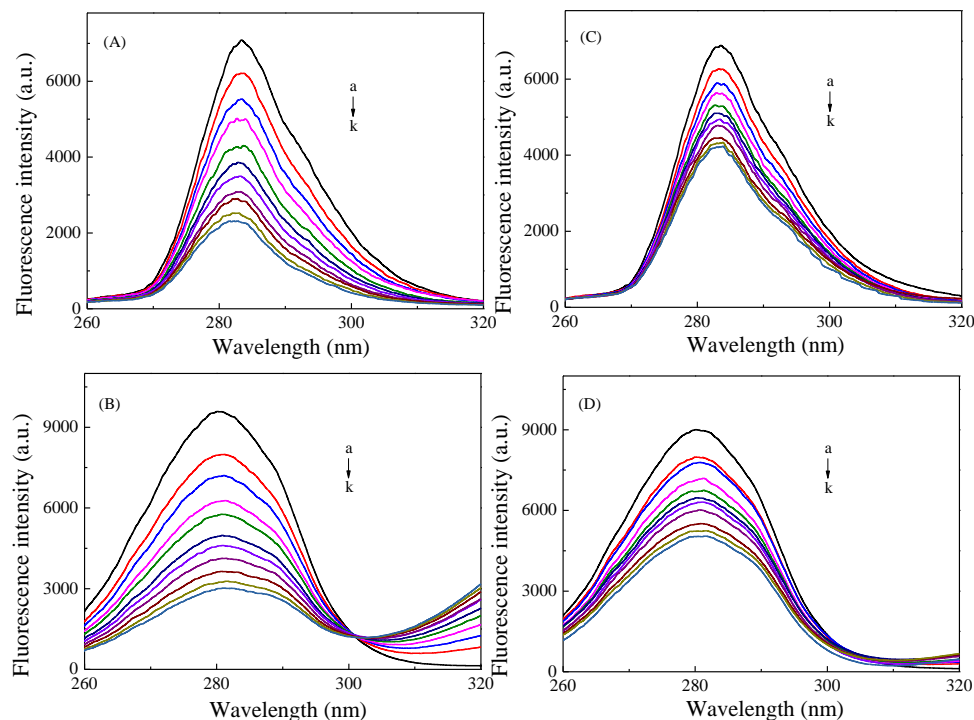


Figure 11. Synchronous fluorescence spectra of (A) PIC and (C) OXY with $\Delta\lambda=15$ nm, (B) PIC and (D) OXY with $\Delta\lambda=60$ nm at 298.2 K (a→k: 0-20 μM).

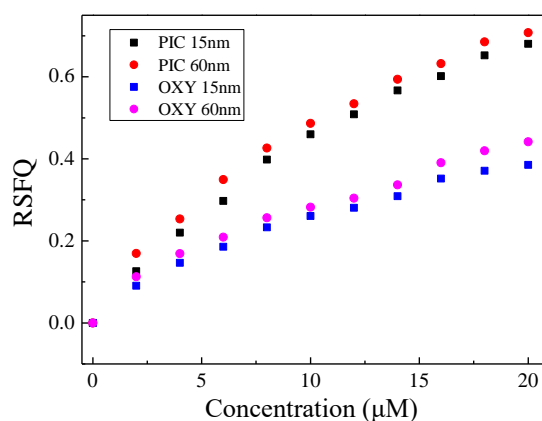


Figure 12. RSFQ values of SPI in the presence of different concentrations of PIC or OXY at 298.2 K.

3.2.2.2 Surface hydrophobicity

The surface hydrophobicity (H_0) represents the quantity of hydrophobic groups on the surface of protein. After the liner-plot, the values of H_0 were shown in Table 13.

The H_0 decreased from 3812 to 3020 and 2670 after adding PIC or OXY, it demonstrated that the surface polarity of SPI increased due to the binding.^[223] The changes can be explained as: (i) introduction of the hydrophilic hydroxyl groups of PIC/OXY; (ii) blocking of hydrophobic residues; (iii) exposure of some previously buried hydrophilic regions.^[224] In addition, the change in the SPI–OXY system was larger than that in the SPI–PIC system. It means that the surface polarity of SPI in the SPI–OXY system was stronger than that in the SPI–PIC system, this may be due to the more hydrogen bonds between OXY and SPI (details in 3.2.2.5).^[225]

Table 13. The surface hydrophobicity (H_0), sulfhydryl group contents (SH), particle size, and ζ -potential of SPI in the absence and presence of PIC/OXY.

	C (μM)	H_0	SH ($\mu\text{M/g}$)	Size (nm)	ζ -potential (mV)
	0	3812 \pm 49	3.20 \pm 0.02	32.33 \pm 0.21	-10.1 \pm 0.11
PIC	10	3020 \pm 27	3.82 \pm 0.04	46.13 \pm 0.27	-3.62 \pm 0.04
	30		6.88 \pm 0.05	52.09 \pm 0.31	-2.11 \pm 0.03
	50		8.82 \pm 0.07	59.88 \pm 0.25	-1.59 \pm 0.01
OXY	10	2670 \pm 33	3.46 \pm 0.02	35.44 \pm 0.17	-5.09 \pm 0.04
	30		3.93 \pm 0.05	38.56 \pm 0.42	-4.29 \pm 0.02
	50		4.04 \pm 0.04	42.10 \pm 0.35	-2.30 \pm 0.03

3.2.2.3 SH contents calculation

-SH is an important group in stabilizing the tertiary structures of proteins, and it can also affect the functional properties of the protein. After calculating by Eq. 10, the contents of -SH were listed in Table 13. The -SH contents of SPI increased with the increasing concentration of PIC/OXY, it may be due to the exposure of SH and the unfolding of protein.^[226] Moreover, the increase was more obvious in the SPI–PIC system. This means that the more exposure of SH and the more unfolded structure of SPI during the stronger binding between PIC and SPI.

3.2.2.4 Structural and conformational changes

Particle size and ζ -potential measurements

DLS is a powerful technique for displaying the structural information of proteins. As shown in Table 13, the size of native SPI was 32.33 nm, which was consistent

with the previous research.^[227] In addition, the sizes of SPI were increased to 59.88 and 42.10 nm after adding PIC and OXY (50 μ M). It means that SPI turns to a looser structure due to the binding.^[228] Moreover, the changes in the SPI–PIC system were more obvious than that in the SPI–OXY system. It demonstrates that SPI was more unfolded, which may be due to the higher binding strength of PIC. This conclusion is consistent with the result of the -SH content calculation.

The ζ -potential of SPI was -10.1 mV, there is no significant difference from the previous study.^[229] With the increasing concentration of PIC and OXY, the less negative ζ -potential can be seen in Table 13. It means that the electronic distribution of SPI changed after the binding.^[227] In addition, the degree of changes was more obvious in the PIC–SPI system. This may be due to the stronger binding between PIC and SPI.

CD spectroscopy measurement

CD spectroscopy is one of the powerful techniques for evaluating the conformational changes of proteins. After the analysis by software, the contents of α -helix, β -sheet, β -turns, and random coils were listed in Table 14. The content of α -helix decreased with the gradually addition of PIC and OXY, however, β -sheet has the opposite tendency. It means that the secondary structure of SPI was altered after the binding.

Table 14. Contents of α -helix, β -sheet, β -turn, and random coils of SPI with and without PIC/OXY.

	<i>C</i> (μ M)	α -Helix (%)	β -Sheet (%)	β -Turn (%)	random coils (%)
	0	5.8 \pm 0.2	33.7 \pm 0.2	18.5 \pm 0.3	41.9 \pm 0.5
PIC	10	4.2 \pm 0.1	37.2 \pm 0.4	18.5 \pm 0.2	40.1 \pm 0.5
	30	3.6 \pm 0.0	38.2 \pm 0.2	18.2 \pm 0.3	40.0 \pm 0.4
	50	3.3 \pm 0.1	38.7 \pm 0.2	17.9 \pm 0.1	40.2 \pm 0.3
OXY	10	4.5 \pm 0.1	36.8 \pm 0.4	18.7 \pm 0.3	40.0 \pm 0.4
	30	3.9 \pm 0.2	37.5 \pm 0.2	18.5 \pm 0.3	40.1 \pm 0.2
	50	3.5 \pm 0.0	38.4 \pm 0.4	18.0 \pm 0.2	40.1 \pm 0.3

Moreover, the changes in SPI–PIC system were more obvious compared to SPI–OXY system. It means that the structure of SPI was more unfolded in SPI–PIC

system, and this may be caused by the stronger binding between SPI and PIC. The result is consistent with the conclusions of -SH contents and size measurements.

3.2.2.5 Molecular docking experiments

Molecular docking can be a powerful tool to predict the binding sites or energies for the interaction between ligands and macromolecules. According to the lowest binding energy, the docking information between PIC/OXY and 11S or 7S was shown in Figure 13. As shown in Figure 13, PIC and OXY can bind to 7S or 11S at the same position due to their similar structures. Compared to the binding energies in SPI–PIC and SPI–OXY system, PIC can bind with SPI with higher binding affinity. In addition, the binding energies for PIC–7S (-9.15 kcal/mol) and OXY–7S (-8.71 kcal/mol) were lower than those obtained from steady-state fluorescence experiments (Table 10). However, the predicated energies for PIC–11S (-6.84 kcal/mol) and OXY–11S (-6.03 kcal/mol) were higher than those obtained from thermodynamic calculation. It may be due to the differences between X-ray crystals and the solvent system structure of SPI, or the insufficient desolution energy under vacuum simulation.^[205, 230]

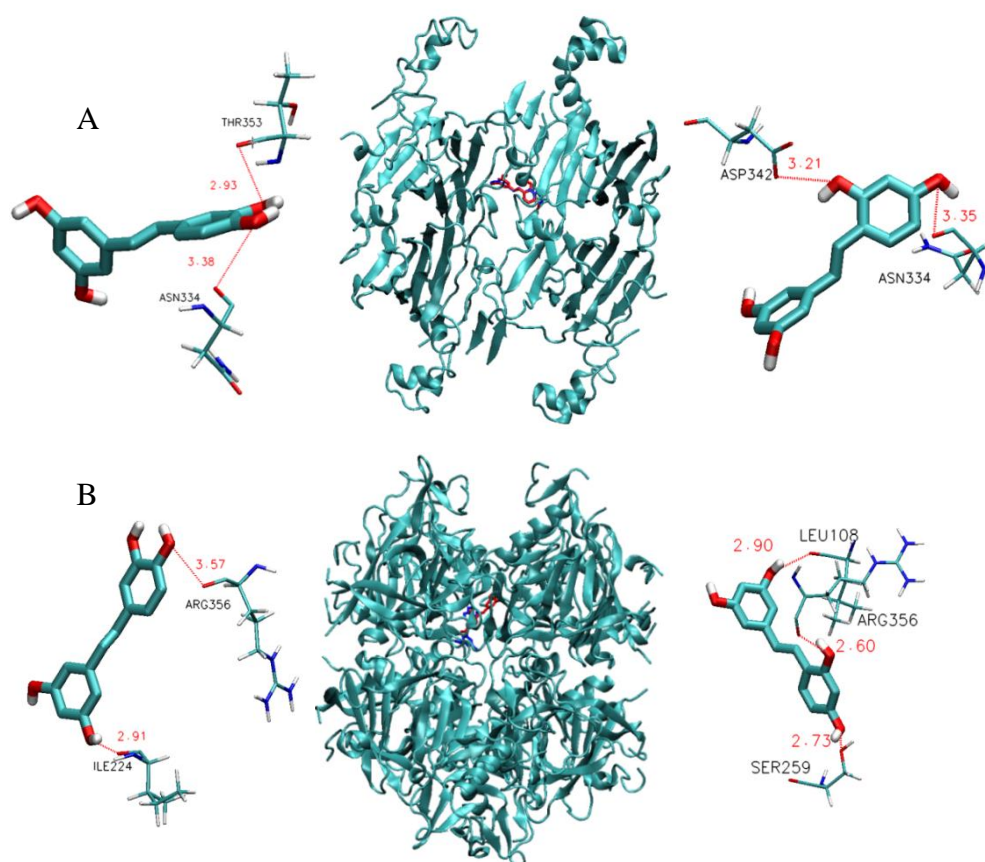


Figure 13. Molecular docking between 11S (A) or 7S (B) and PIC (blue, left) or OXY (red, right).

The hydrogen bonds during the binding can also be observed after docking. PIC can bind with ILE 224, ASN 334, THR 353, and ARG 356 through hydrogen bonds with distances of 2.91, 3.38, 2.93, and 3.57 Å. For OXY, it can bind with LEU 108, SER 259, ASN 334, ASP 342, and ARG 356 with distances of 2.90, 2.73, 3.35, 3.21, and 2.60 Å. The more hydrogen bonds can lead to a pronounced red-shift and reduction in surface hydrophobicity in the OXY–SPI system.

3.2.2.6 Foaming and emulsifying properties

The foaming and emulsifying properties of protein are vital characteristics in food processing. Foaming properties include foam expansion (FE) and foam stability (FS). Emulsifying properties include emulsifying ability index (EAI) and emulsion stability index (ESI). As shown in Figure 14A, the values of FE increased with the increasing PIC/OXY. It means that PIC/OXY can improve the foaming ability of SPI. Except for PIC 50, the foaming stability of SPI–PIC/OXY was better than native SPI, even the stability declined with the addition of PIC/OXY. Considering the rapid diffusion of proteins with unfolded structure can generate the foam, the enhanced properties may be due to the moderately unfolded structure of SPI.^[231]

As shown in Figure 14B, PIC and OXY had similar behavior on the emulsifying properties. With the increasing PIC/OXY, the emulsifying ability increased, and the stability decreased. However, the stability was much better than the native SPI. The improving ability of foaming or emulsifying may be due to the lower surface tension that comes from the increasing concentration of PIC/OXY.^[204] (–)-Epigallocatechin-3-gallate^[204] and anthocyanins^[232] can also enhance the foaming and emulsifying abilities. However, curcumin couldn't alter the foaming and emulsifying abilities obviously.^[233] The phenomenon showed that PIC/OXY can enhance the functional properties of SPI to obtain a plant-food with good performance. Since the changes of half-life time can interfere with the characteristic of foam and emulsion, the decrease of their stability after the binding may be caused by the reduction of half-time. This phenomenon also occurred in the interaction between 11S and stevioside, where the stability of complexes at higher concentrations is lower than 11S itself.^[234]

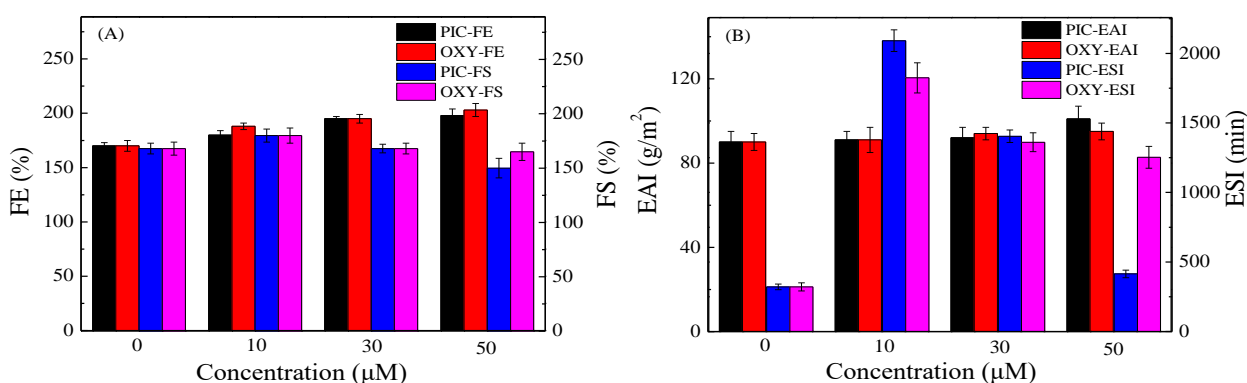


Figure 14. Comparisons of the functional properties of SPI at different PIC/OXY concentrations.

3.2.2.7 ABTS⁺ scavenging activity

Since antioxidants can reduce the absorbance of ABTS⁺ by scavenging radical, their antioxidant ability can be obtained by ABTS⁺ test. The antioxidant activity can be determined by experimental scavenging capacity (ESC), theoretical scavenging capacity (TSC) and synergistic effect (SE). The native SPI can only scavenge 3.89% ABTS⁺ with weaker force (data not shown), and the other corresponding data was listed in Table 15. Choosing 3 μM as an example for analysis, PIC and OXY can scavenge 47.43% and 37.41% ABTS⁺, respectively. Moreover, they can scavenge 53.27% and 42.70% ABTS⁺ after binding with SPI. The values were larger than the sum of absolute PIC/OXY and SPI. Therefore, synergistic effect existed in the PIC–SPI and OXY–SPI systems. SE>1 can also be regarded as evidence. The same phenomenon also occurred in the binding between whey protein and chlorogenic acid.^[235] The results indicated that the PIC/OXY–SPI complexes can be used as good nutritional materials with perfect antioxidant ability. In spite of the presence or absence of SPI, the scavenge ability of PIC was higher than OXY. This may be caused by the slight difference in their structures and binding strength with SPI.

Table 15. The ESC, TSC, and SE values of PIC/OXY in the absence and presence of SPI.

C (μM)	ESC (%)				SE	
	PIC	OXY	PIC–SPI	OXY–SPI	PIC–SPI	OXY–SPI
1	7.93±0.08	4.17±0.05	13.49±0.15	9.74±0.12	1.17±0.01	1.23±0.02
2	28.51±0.31	14.19±0.09	33.66±0.23	19.05±0.20	1.08±0.02	1.09±0.01
3	47.43±0.42	37.41±0.42	53.27±0.26	42.70±0.33	1.08±0.02	1.07±0.00
4	63.84±0.35	54.24±0.45	69.40±0.43	59.25±0.52	1.06±0.00	1.06±0.01
5	77.61±0.38	63.98±0.37	83.31±0.50	69.40±0.44	1.06±0.01	1.06±0.01

3.2.2.8 *In vitro* digestion

After calculating by Eq. 18, the recovery percentage of PIC or OXY in the absence and presence of SPI was shown in Figure 15. As shown in the figure, PIC and OXY were more digestible in the stomach compared to the intestine. Since PIC can induce changes in gene expression in human gastric cancer cells^[236] and OXY can cure gastric ulcer,^[237] their more consumption in the stomach is beneficial to human beings. Furthermore, the consumption of PIC or OXY is reduced in the presence of SPI. It may be caused by the encapsulation effect of SPI on PIC and OXY, which can reduce their release to achieve a sustained release goal. In summary, PIC or OXY can bind with SPI to show their excellent nutritional with good stomach protective values. The binding is beneficial for exerting nutritional and pharmacological values in food and clinical medicine.

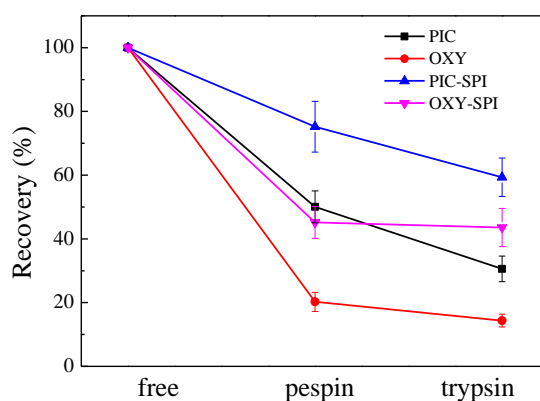


Figure 15. Recovery of PIC and OXY in the absence and presence of SPI during different stages of digestion.

3.2.3 Conclusion

In this part, multiple spectroscopic methods and molecular docking were used to test the binding information between PIC/OXY and SPI. Steady-state fluorescence, FRET, and TRF studies can determine the static quenching. The binding process was spontaneous and exothermic, van der Waals forces and hydrogen bonding were major driving forces. The binding strength of PIC to SPI was stronger than that of OXY, and tryptophan played an important role in the binding. DLS and CD studies showed that the structure of SPI turns unfolded due to the binding of PIC and OXY. The stronger binding of PIC resulted in a more unfolded structure of SPI. The emulsifying and foaming properties of SPI were improved after the binding. Synergistic antioxidant effects between PIC/OXY and SPI can be observed using the ABTS⁺ assay. The more

digestibility of PIC and OXY in the stomach could facilitate the healing of gastric cancer and ulcer. The results also show that the PIC–SPI and OXY–SPI complexes can be considered as good nutritional molecules with stomach-protective effects. The research will provide theoretical guidance for the application of PIC and OXY as food ingredients with excellent performance.

3.2.4 Experimental section

The fluorescence and absorbance spectra were measured using F-7000 spectrofluorometer (Hitachi, Japan) with a 1 cm path length cell and UV–vis spectrophotometer (U-3900H, Hitachi, Japan), respectively. Time-resolved fluorescence measurements were performed using an FLS-1000 spectrometer (Edinburgh, England). The particle size and ζ -potential were measured using a Zetasizer Nano ZS (Malvern Instruments, Worcestershire, UK). The CD spectroscopy was performed using a Jasco J-810 Spectropolarimeter (Tokyo, Japan) in the range of 185–280 nm at room temperature with a quartz cuvette of 0.1 cm optical length. The content of PIC or OXY *in vitro* digestion can be obtained by high performance liquid chromatography with an Agilent ZORBAX Eclipse XDB-C18 column (4.6×250 mm, 5-Micron).

All the chemicals used are commercial.

3.2.4.1 Measurement of fluorescence spectra

Steady-state fluorescence spectra

The concentration of SPI was kept constant at 0.5 mg/mL, and the concentrations of PIC/OXY were 0, 2, 4, 6, 8, 10, 12, 14, 16, 18, 20 μ M. After 30 min incubation at four different temperatures (298.2, 302.2, 306.2, and 310.2 K), the samples can be tested at λ_{ex} 280 nm and recorded in the range of 300–425 nm. The fluorescence curves were scanned at a voltage of 585 V, and the slits were both set at 5 nm. In order to offset the inner-filter effect, the fluorescence intensities can be corrected with the following equation:^[238]

$$F_{\text{corr}} = F_{\text{obs}} \times e^{(A_{\text{ex}}+A_{\text{em}})/2} \quad (2)$$

where F_{obs} and F_{corr} are the fluorescence intensities before and after correction, respectively. A_{em} and A_{ex} are the absorbance at the emission and excitation

wavelength, respectively.

The quenching mechanism can be determined by the quenching rate constant k_q , which can be calculated by Eq. 3. For static quenching, the binding constant (K_a) and the number of binding sites (n) can be obtained from Eq. 4:^[239]

$$F_0 / F = 1 + k_q \tau_0 [Q]_0 \quad (3)$$

$$\log(F_0 / F - 1) = \log K_a + n \log [Q]_0 \quad (4)$$

where F_0 and F represent the fluorescence intensities of SPI in the absence and presence of PIC/OXY, respectively. $[Q]_0$ is the concentration of PIC/OXY and τ_0 is the lifetime of the SPI (10^{-8} s).

In addition, the forces during binding can be roughly determined by enthalpy change (ΔH°) and entropy change (ΔS°). The values of ΔH° , ΔS° , and Gibbs free energy change (ΔG°) can be obtained by the following equations:^[240]

$$\ln K_a = -\frac{\Delta H^\circ}{RT} + \frac{\Delta S^\circ}{R} \quad (5)$$

$$\Delta G^\circ = \Delta H^\circ - T\Delta S^\circ = -RT \ln K_a \quad (6)$$

where R is the gas constant ($8.314 \text{ J mol}^{-1} \text{ K}^{-1}$).

For synchronous fluorescence spectra, the solution with the same concentration of the above were measured with the wavelength intervals ($\Delta\lambda = \lambda_{em} - \lambda_{ex}$) of 15 and 60 nm, respectively.

Förster resonance energy transfer analyses

FRET analyses can be performed by the fluorescence of SPI (0.5 mg/mL) with or without PIC/OXY (10 μ M) and the absorbance of pure PIC/OXY. The energy transfer efficiency E can be calculated by the following equations:^[241]

$$E = 1 - F / F_0 = R_0^6 / (R_0^6 + r^6) \quad (7)$$

$$R_0^6 = 8.80 \times 10^{-25} \kappa^2 n^{-4} \phi J \quad (8)$$

$$J = \frac{\sum F(\lambda) \varepsilon(\lambda) \lambda^4 \Delta\lambda}{\sum F(\lambda) \Delta\lambda} \quad (9)$$

F_0 and F are the fluorescence intensities of SPI in the absence and presence of PIC/OXY, respectively. R_0 is the critical energy transfer distance when the efficiency is 50%, and r is the binding distance. κ^2 , n , and ϕ are the space factor of orientation,

refractive index, and fluorescence quantum yield of donor. Their values are 2/3, 1.336 and 0.15, respectively. $F(\lambda)$ is the fluorescence intensity of SPI at wavelength (λ), $\epsilon(\lambda)$ is the molar absorption coefficient of PIC/OXY at λ .

Time resolved fluorescence measurements

The concentration of SPI was 1 mg/mL, and the concentrations of PIC/OXY were 0, 10, 30, and 50 μ M. The excitation and emission wavelengths were 280 nm and 342 nm, and their slits were 26 and 13 nm, respectively.

Surface hydrophobicity test

The samples, PIC/OXY (10 μ M) with various concentrations of SPI (0, 0.1, 0.2, 0.3, 0.4, 0.5, 0.6, 0.7, 0.8, 0.9, and 1 mg/mL), were incubated in the dark for 30 min after the addition of 200 μ M ANS. The excitation was set at 390 nm, both excitation and emission slits were set at 10 nm. And the fluorescence intensities were recorded in the range of 400–650 nm. The values of surface hydrophobicity can be obtained from the slope of the linear plot (the relative fluorescence intensity of SPI in the presence of ANS against its concentration).

3.2.4.2 SH contents

Ellman's reagent: 4 mg of DTNB dissolved in 1 mL Tris-glycine solution (0.086 M Tris, 0.09 M glycine, 4 mM Na₂EDTA, pH 8.0). The SPI solutions (2 mg/mL) in the presence of PIC/OXY (0, 10, 30, and 50 μ M) were incubated for 30 min at 298.2 K, then added 50 μ L DTNB and tested the absorbance at 412 nm. The buffer was used as a blank. The SH contents can be calculated by Eq. 10:^[242]

$$SH(\mu\text{mol/g}) = \frac{73.53 \times A_{412}}{C} \quad (10)$$

where A_{412} is the absorbance at 412 nm, and C is the concentration of SPI (mg/mL). The constant 73.53 is obtained from $10^6 / (1.36 \times 10^4)$, and 1.36×10^4 is the molar extinction coefficient of SPI.

3.2.4.3 Structural and conformational changes

CD spectroscopy

The concentration of SPI was 1 mg/mL, and the concentrations of PIC/OXY were 0, 10, 30, and 50 μM . The CD data can be handled by using the CONTIN algorithm at the DichroWeb server (<http://dichroweb.cryst.bbk.ac.uk>).^[243]

Particle size and ζ -potential measurements

The concentration of SPI was kept at 1 mg/mL, and the concentrations of PIC/OXY were 0, 10, 30, and 50 μM . After 30 min incubation at 298.2 K and being filtered through a 0.22 μm filter, the values of particle size and ζ -potential can be obtained.

3.2.4.4 Molecular docking study

7S and 11S were selected as representatives to test the docking between SPI and PIC/OXY. The crystal structures of 7S (PDB ID: 3AUP) and 11S (PDB ID: 1OD5) were obtained from the Protein Data Bank (<https://www.rcsb.org/>). And the structures of PIC and OXY were conducted and optimized by the software of Material Studio. Molecular docking was conducted using the AutoDock 4.0 software with the Lamarckian genetic algorithm. The box size and grid spacing were set at 126 \times 126 \times 126 \AA and 1 \AA , respectively. The binding information can be obtained through VMD software after 100 docking random runs.

3.2.4.5 Functional properties

Evaluation of the foaming properties

The samples of SPI (4 mg/mL, 20 mL) in the presence of PIC/OXY (0, 10, 30, and 50 μM) were homogenized for 1 min, and then recorded the volume immediately. After being placed for another 30 min, the volume was recorded again.

Evaluation of the emulsifying properties

Homogenized the SPI samples (2 mg/mL, 15 mL) in the presence of PIC/OXY (0, 10, 30, and 50 μM) and 5 mL peanut oil for 1 min, and then withdrawn 50 μL of

samples in the bottom to add into 10 mL 0.1% (w/v) SDS. The absorbance at 500 nm was measured after 0 and 30 min.

The values of FE, FS, EAI, and ESI can be calculated by the following equations.^[232]

$$FE(\%) = \frac{V_0}{V} \times 100 \quad (11)$$

$$FS(\%) = \frac{V_{30}}{V} \times 100 \quad (12)$$

$$EAI(m^2/g) = \frac{2 \times 2.303 \times A_0 \times DF}{10000 \times \theta \times L \times C} \quad (13)$$

$$ESI(\text{min}) = \frac{A_0 \times 30}{A_0 - A_{30}} \quad (14)$$

where V , V_0 and V_{30} are the volumes before whipping, 0 and 30 min after whipping. DF , θ , L , and C are the dilution factor (100), oil fraction in the emulsion (0.25), optical path length (1 cm), and concentration of SPI (g/mL), respectively. A_0 and A_{30} are the absorbance at 0 and 30 min, respectively.

3.2.4.6 Determination of antioxidant activity

ABTS⁺ radical solution: mix 5 mM ABTS and 2 mM AIBA, and dilute the absorbance to 0.74 at 734 nm. The concentration of SPI was 0.1 mg/mL, and the concentrations of PIC/OXY were 1, 2, 3, 4, and 5 μ M, respectively. After 30 min incubation at 298.2 K, test the absorbance of ABTS⁺ radical, ABTS⁺-SPI, ABTS⁺-PIC/OXY, ABTS⁺-(SPI-PIC/OXY). The values of ESC, TSC and SE can be calculated using the following equations.^[244]

$$ESC(\%) = (1 - A/A_0) \times 100 \quad (15)$$

$$TSC = ESC_1 + ESC_2 - (ESC_1 \times ESC_2) / 100 \quad (16)$$

$$SE = ESC_{1,2} / TSC \quad (17)$$

3.2.4.7 *In vitro* digestion

At pH 2.0 and 310.2 K, the samples of 200 μ M PIC/OXY with or without 10 mg/mL SPI were incubated for 1 h with shaking in the presence of pepsin (25 mg/mL). After adjusting the pH to 6.5, the samples continued to be digested with trypsin (2 mg/mL) and bile salt (12 mg/mL) for 2 h. The volume ratios of pepsin and the mixed

solution of trypsin and bile salt to the sample were 1:20 and 1:4, respectively. The wavelengths for PIC and OXY were 322 and 327 nm, respectively. The mobile phase consisted of MeCN and water with a volume ratio of 55:45. The pH value was adjusted by 1 mol/L HCl or NaOH, and all samples were filtered by 0.22 μ m membrane (Millipore) before analysis. The contents of PIC and OXY can be represented by the percentage of recovery which can be calculated by Eq. 18.^[245]

$$\text{Recovery \%} = \frac{C_{\text{samples}}}{C_{\text{control}}} \times 100 \quad (18)$$

C_{control} and C_{samples} are the contents of PIC/OXY before and after digestion, respectively.

3.2.4.8 Statistical analysis

All experiments were performed in triplicate. The results were reported as mean \pm standard deviation except for the results of FRET and TRF studies. Graphical representations were made using Origin (Version 8.5). Statistical analysis was performed by one-way analysis of variance (ANOVA) using SPSS software version 19.0. $p < 0.05$ indicates a statistically significant difference.

CHAPTER FOUR

References and ^1H NMR & ^{13}C NMR Spectra

4.1 References

- [1] Z.Y. Wu, M. Hu, J.X. Li, W.Q. Wu, H.F. Jiang, *Organic & Biomolecular Chemistry* 19 (2021) 3036-3054.
- [2] Njardarson Group, “Top 200 Small Molecule Pharmaceuticals by Retail Sales in 2019”, can be found under <https://njardarson.lab.arizona.edu>.
- [3] S.S. Gholap, *European Journal of Medicinal Chemistry* 110 (2016) 13-31.
- [4] R. Ballini, L. Barboni, F. Fringuelli, A. Palmieri, F. Pizzo, L. Vaccaro, *Green Chemistry* 9 (2007) 823-838.
- [5] C. Bellec, D. Bertin, R. Colau, S. Deswarte, P. Maitte, C. Viel, *Journal of Heterocyclic Chemistry* 16 (1979) 1657-1659.
- [6] E.J. Corey, H. Estreicher, *Tetrahedron Letters* 22 (1981) 603-606.
- [7] R. Schneider, P. Gerardin, B. Loubinoux, *Tetrahedron* 49 (1993) 3117-3124.
- [8] G. Minetto, L.F. Raveglia, A. Sega, M. Taddei, *European Journal of Organic Chemistry* 2005 (2005) 5277-5288.
- [9] R. Ballini, A. Rinaldi, *Tetrahedron Letters* 35 (1994) 9247-9250.
- [10] A. Palmieri, S. Gabrielli, S. Sampaolesi, R. Ballini, *Synlett* 26 (2015) 1207-1212.
- [11] R.A. Kunetsky, A.D. Dilman, K.P. Tsvaygboym, S.L. Ioffe, Y.A. Strelenko, V.A. Tartakovsky, *Synthesis* 2003 (2003) 1339-1346.
- [12] S. Gabrielli, E. Chiurchiù, S. Sampaolesi, R. Ballini, A. Palmieri, *Synthesis* 49 (2017) 2980-2984.
- [13] M. Dell'Aera, F.M. Perna, P. Vitale, A. Altomare, A. Palmieri, L.C.H. Maddock, L.J. Bole, A.R. Kennedy, E. Hevia, V. Capriati, *Chemistry—A European Journal* 26 (2020) 8742-8748.
- [14] B.H. Lipshutz, *Chemical Reviews* 86 (1986) 795-819.
- [15] E. Chiurchiù, S. Gabrielli, R. Ballini, A. Palmieri, *Molecules* 24 (2019) 4575.
- [16] S.C. Valdez, J.L. Leighton, *Journal of the American Chemical Society* 131 (2009) 14638-14639.
- [17] E.M. Fleming, T. McCabe, S.J. Connon, *Tetrahedron Letters* 47 (2006) 7037-7042.
- [18] T. Arai, A. Awata, M. Wasai, N. Yokoyama, H. Masu, *The Journal of Organic Chemistry* 76 (2011) 5450-5456.
- [19] M. Büschleb, S. Dorich, S. Hanessian, D. Tao, K.B. Schenthal, L.E. Overman, *Angewandte Chemie International Edition* 55 (2016) 4156-4186.
- [20] A.R. Choudhury, M.S. Manna, S. Mukherjee, *Chemical Science* 8 (2017) 6686-6690.
- [21] E. Chiurchiù, S. Xhafa, R. Ballini, G. Maestri, S. Protti, A. Palmieri, *Advanced Synthesis & Catalysis* 362 (2020) 4680-4686.
- [22] C. Raviola, C. Carrera, M. Serra, A. Palmieri, G. Lupidi, G. Maestri, S. Protti, *ChemPhotoChem* 5 (2021) 871-875.
- [23] R. Ballini, S. Gabrielli, A. Palmieri, *Current Organic Chemistry* 14 (2010) 65-83.
- [24] K. Jayakanthan, K.P. Madhusudanan, Y.D. Vankar, *Tetrahedron* 60 (2004) 397-403.

- [25] R. Ballini, D. Fiorini, A. Palmieri, *Tetrahedron Letters* 45 (2004) 7027-7029.
- [26] A. Palmieri, S. Gabrielli, R. Ballini, *Green Chemistry* 15 (2013) 2344-2348.
- [27] E. Lewandowska, *Tetrahedron* 62 (2006) 4879-4883.
- [28] P.A. Coghlan, C.J. Easton, *Tetrahedron Letters* 40 (1999) 4745-4748.
- [29] T.A. Alston, D.J.T. Porter, H.J. Bright, *Accounts of Chemical Research* 16 (1983) 418-424.
- [30] R. Ballini, N.A. Bazán, G. Bosica, A. Palmieri, *Tetrahedron Letters* 49 (2008) 3865-3867.
- [31] S. Benetti, R. Romagnoli, C. De Risi, G. Spalluto, V. Zanirato, *Chemical Reviews* 95 (1995) 1065-1114.
- [32] M. Ma, C. Li, L. Peng, F. Xie, X. Zhang, J. Wang, *Tetrahedron Letters* 46 (2005) 3927-3929.
- [33] A. Palmieri, S.V. Ley, A. Polyzos, M. Ladlow, I.R. Baxendale, *Beilstein Journal of Organic Chemistry* 5 (2009) 23.
- [34] A. Palmieri, S. Gabrielli, R. Ballini, *Advanced Synthesis & Catalysis* 352 (2010) 1485-1492.
- [35] R. Ballini, S. Gabrielli, A. Palmieri, *Synlett* 2009 (2009) 965-967.
- [36] O. Afzal, S. Kumar, M.R. Haider, M.R. Ali, R. Kumar, M. Jaggi, S. Bawa, *European Journal of Medicinal Chemistry* 97 (2015) 871-910.
- [37] S. Manfredini, S. Vertuani, B. Pavan, F. Vitali, M. Scaglianti, F. Bortolotti, C. Biondi, A. Scatturin, P. Prasad, A. Dalpiaz, *Bioorganic & Medicinal Chemistry* 12 (2004) 5453-5463.
- [38] H. Saburi, S. Tanaka, M. Kitamura, *Angewandte Chemie International Edition* 44 (2005) 1730-1732.
- [39] S. Gabrielli, A. Giardinieri, S. Sampaolesi, R. Ballini, A. Palmieri, *Molecules* 21 (2016) 776.
- [40] J. Mao, Q. Hua, G. Xie, J. Guo, Z. Yao, D. Shi, S. Ji, *Advanced Synthesis & Catalysis* 351 (2009) 635-641.
- [41] A. Palmieri, S. Gabrielli, C. Cimarelli, R. Ballini, *Green Chemistry* 13 (2011) 3333-3336.
- [42] A. Palmieri, S. Gabrielli, M. Parlapiano, R. Ballini, *RSC Advances* 5 (2015) 4210-4213.
- [43] S. Gabrielli, L. Ciabattoni, S. Sampaolesi, R. Ballini, A. Palmieri, *RSC Advances* 6 (2016) 44341-44344.
- [44] A. Palmieri, S. Gabrielli, D. Lanari, L. Vaccaro, R. Ballini, *Advanced Synthesis & Catalysis* 353 (2011) 1425-1428.
- [45] K. Alfonsi, J. Colberg, P.J. Dunn, T. Fevig, S. Jennings, T.A. Johnson, H.P. Kleine, C. Knight, M.A. Nagy, D.A. Perry, M. Stefaniak, *Green Chemistry* 10 (2008) 31-36.
- [46] X.L. Hou, H.Y. Cheung, T.Y. Hon, P.L. Kwan, T.H. Lo, S.Y. Tong, H.N.C. Wong, *Tetrahedron* 54 (1998) 1955-2020.
- [47] R. Ballini, S. Gabrielli, A. Palmieri, *Synlett* 2010 (2010) 2468-2470.
- [48] Y. Tohda, N. Yamawaki, H. Matsui, T. Kawashima, M. Ariga, Y. Mori, *Bulletin of the Chemical Society of Japan* 61 (1988) 461-465.
- [49] R. Ballini, G. Bosica, S. Gabrielli, A. Palmieri, *Tetrahedron* 65 (2009) 2916-2920.
- [50] R. Ballini, A. Palmieri, M.A. Talaq, S. Gabrielli, *Advanced Synthesis & Catalysis* 351 (2009) 2611-2614.

- [51] I. Yavari, S. Souri, M. Sirouspour, H. Djahaniani, *Synthesis* 2006 (2006) 3243-3249.
- [52] H. Huang, E.N. Jacobsen, *Journal of the American Chemical Society* 128 (2006) 7170-7171.
- [53] D.K. Nair, S.M. Mobin, I.N.N. Namboothiri, *Organic Letters* 14 (2012) 4580-4583.
- [54] D.A. Evans, S. Mito, D. Seidel, *Journal of the American Chemical Society* 129 (2007) 11583-11592.
- [55] T.A. Alston, D.J.T. Porter, H.J. Bright, *Bioorganic Chemistry* 13 (1985) 375-403.
- [56] M.L. Leroux, T. Le Gall, C. Mioskowski, *Tetrahedron: Asymmetry* 12 (2001) 1817-1823.
- [57] J.M. Rodríguez, M. Dolors Pujol, *Tetrahedron Letters* 52 (2011) 2629-2632.
- [58] R. Ballini, R. Castagnani, M. Petrini, *The Journal of Organic Chemistry* 57 (1992) 2160-2162.
- [59] D. Amantini, F. Fringuelli, O. Piermatti, F. Pizzo, L. Vaccaro, *Green Chemistry* 3 (2001) 229-232.
- [60] S. Fioravanti, L. Pellacani, P.A. Tardella, M.C. Vergari, *Organic Letters* 10 (2008) 1449-1451.
- [61] M. Fujii, *Chemistry Letters* 21 (1992) 933-934.
- [62] A.S. Franklin, *Synlett* 2000 (2000) 1154-1156.
- [63] C. Jubert, P. Knochel, *The Journal of Organic Chemistry* 57 (1992) 5425-5431.
- [64] T. Sakakibara, I. Takai, E. Ohara, R. Sudoh, *Chemical Communications* (1981) 261-262.
- [65] S.E. Denmark, L.R. Marcin, *The Journal of Organic Chemistry* 58 (1993) 3850-3856.
- [66] M.Y. Chang, C.H. Lin, H.Y. Tai, *Tetrahedron Letters* 54 (2013) 3194-3198.
- [67] S. Maity, S. Manna, S. Rana, T. Naveen, A. Mallick, D. Maiti, *Journal of the American Chemical Society* 135 (2013) 3355-3358.
- [68] G.D. Buckley, J.L. Charlsh, *Journal of the Chemical Society (Resumed)* (1947) 1472-1474.
- [69] A. Barco, S. Benetti, G.P. Pollini, G. Spalluto, V. Zanirato, *Tetrahedron Letters* 32 (1991) 2517-2520.
- [70] J.E. Bäckvall, U. Karlsson, R. Chinchilla, *Tetrahedron Letters* 32 (1991) 5607-5610.
- [71] P. Jakubec, A. Hawkins, W. Felzmann, D.J. Dixon, *Journal of the American Chemical Society* 134 (2012) 17482-17485.
- [72] R. Chowdhury, G.B. Vamisetti, S.K. Ghosh, *Tetrahedron: Asymmetry* 25 (2014) 516-522.
- [73] S. Belot, A. Quintard, N. Krause, A. Alexakis, *Advanced Synthesis & Catalysis* 352 (2010) 667-695.
- [74] X.T. Guo, F. Sha, X.Y. Wu, *Synthesis* 49 (2017) 647-656.
- [75] M. Tsakos, M. Trifonidou, C.G. Kokotos, *Tetrahedron* 68 (2012) 8630-8635.
- [76] A. Barco, S. Benetti, C. De Risi, C.F. Morelli, G.P. Pollini, V. Zanirato, *Tetrahedron* 52 (1996) 9275-9288.
- [77] H.B. Kagan, O. Riant, *Chemical Reviews* 92 (1992) 1007-1019.
- [78] A.B. Xia, D.Q. Xu, C. Wu, L. Zhao, Z.Y. Xu, *Chemistry—A European Journal* 18 (2012) 1055-1059.

- [79] S. Karimi, S. Ma, Y. Liu, K. Ramig, E.M. Greer, K. Kwon, W.F. Berkowitz, G. Subramaniam, *Tetrahedron Letters* 58 (2017) 2223-2227.
- [80] J.A. Marshall, *Chemical Reviews* 96 (1996) 31-48.
- [81] P.V. Ramachandran, D. Pratihar, D. Biswas, *Chemical Communications* (2005) 1988-1989.
- [82] J. Lu, S.J. Ji, Y.C. Teo, T.P. Loh, *Tetrahedron Letters* 46 (2005) 7435-7437.
- [83] V. Nair, S. Ros, C. Jayan, S. Viji, *Synthesis* 2003 (2003) 2542-2546.
- [84] V. Nair, C.N. Jayan, S. Ros, *Tetrahedron* 57 (2001) 9453-9459.
- [85] J. Lu, M.L. Hong, S.J. Ji, Y.C. Teo, T.P. Loh, *Chemical Communications* (2005) 4217-4218.
- [86] Y.C. Teo, J.D. Goh, T.P. Loh, *Organic Letters* 7 (2005) 2743-2745.
- [87] K.M. Waltz, J. Gavenonis, P.J. Walsh, *Angewandte Chemie* 114 (2002) 3849-3852.
- [88] S. Yamasaki, K. Fujii, R. Wada, M. Kanai, M. Shibasaki, *Journal of the American Chemical Society* 124 (2002) 6536-6537.
- [89] R. Wada, K. Oisaki, M. Kanai, M. Shibasaki, *Journal of the American Chemical Society* 126 (2004) 8910-8911.
- [90] K.R. Fandrick, D.R. Fandrick, J.J. Gao, J.T. Reeves, Z. Tan, W. Li, J.J. Song, B. Lu, N.K. Yee, C.H. Senanayake, *Organic Letters* 12 (2010) 3748-3751.
- [91] G.W. Kabalka, C. Narayana, N.K. Reddy, *Tetrahedron Letters* 37 (1996) 2181-2184.
- [92] T.R. Wu, L. Shen, J.M. Chong, *Organic Letters* 6 (2004) 2701-2704.
- [93] J. Yadav, A. Antony, J. George, B.V. Subba Reddy, *European Journal of Organic Chemistry* 2010 (2010) 591-605.
- [94] D. Prajapati, D.D. Laskar, J.S. Sandhu, *Tetrahedron Letters* 41 (2000) 8639-8643.
- [95] J.W.J. Kennedy, D.G. Hall, *Journal of the American Chemical Society* 124 (2002) 11586-11587.
- [96] N. Shinohara, T. Tsuduki, J. Ito, T. Honma, R. Kijima, S. Sugawara, T. Arai, M. Yamasaki, A. Ikezaki, M. Yokoyama, K. Nishiyama, K. Nakagawa, T. Miyazawa, I. Ikeda, *Biochimica et Biophysica Acta (BBA)-Molecular and Cell Biology of Lipids* 1821 (2012) 980-988.
- [97] R. Ballini, L. Barboni, G. Bosica, D. Fiorini, E. Mignini, A. Palmieri, *Tetrahedron* 60 (2004) 4995-4999.
- [98] U. Schneider, S. Kobayashi, *Angewandte Chemie International Edition* 46 (2007) 5909-5912.
- [99] M. Yamaguchi, N. Morita, U. Schneider, S. Kobayashi, *Advanced Synthesis & Catalysis* 352 (2010) 1461-1465.
- [100] R. Weingarten, G.A. Tompsett, W.C. Conner, G.W. Huber, *Journal of Catalysis* 279 (2011) 174-182.
- [101] A.L. de Jesus Lopes Ribeiro, G. Degiacomi, F. Ewann, S. Buroni, M.L. Incandela, L.R. Chiarelli, G. Mori, J. Kim, M. Contreras-Dominguez, Y.S. Park, *PloS ONE* 6 (2011) e26675.
- [102] M.H. Shaikh, D.D. Subhedar, M. Arkile, V.M. Khedkar, N. Jadhav, D. Sarkar, B.B. Shingate, *Bioorganic & Medicinal Chemistry Letters* 26 (2016) 561-569.
- [103] A.S. Fauci, *The Journal of Infectious Diseases* 197 (2008) 1493-1498.

- [104] A.A. Velayati, M.R. Masjedi, P. Farnia, P. Tabarsi, J. Ghanavi, A.H. ZiaZarifi, S.E. Hoffner, *Chest* 136 (2009) 420-425.
- [105] S. Loewenberg, *The Lancet* 379 (2012) 205.
- [106] G. Manina, M. Bellinzoni, M.R. Pasca, J. Neres, A. Milano, A.L. de Jesus Lopes Ribeiro, S. Buroni, H. Škovierová, P. Dianišková, K. Mikušová, *Molecular Microbiology* 77 (2010) 1172-1185.
- [107] K.G. Nazarenko, N.A. Shtil, A.N. Chernega, M.O. Lozinskii, A.A. Tolmachev, *Synthesis* 2004 (2004) 1195-1202.
- [108] D. Todorov, M. Ilarionova, R. Gupta, J. Molnar, N. Motohashi, *Heterocyclic Communications* 1 (1995) 153-156.
- [109] A. Sharifi, M. Ansari, H.R. Darabi, M.S. Abaee, *Tetrahedron Letters* 57 (2016) 529-532.
- [110] V.V. Pelipko, R.I. Baichurin, R.P. Kustin, A.P. Vinogradov, S.V. Makarenko, *Chemistry of Heterocyclic Compounds* 54 (2018) 729-735.
- [111] N.D. Heindel, J.R. Reid, J.E. Willis, *Journal of Medicinal Chemistry* 14 (1971) 453-453.
- [112] E. Chiurchiù, Y. Patehebieke, S. Gabrielli, R. Ballini, A. Palmieri, *Advanced Synthesis & Catalysis* 361 (2019) 2042-2047.
- [113] J. Wegner, S. Ceylan, A. Kirschning, *Advanced Synthesis & Catalysis* 354 (2012) 17-57.
- [114] P. Anastas, N. Eghbali, *Chemical Society Reviews* 39 (2010) 301-312.
- [115] A.J. Kochanowska-Karamyan, M.T. Hamann, *Chemical Reviews* 110 (2010) 4489-4497.
- [116] R. Ballini, A. Palmieri, M. Petrini, E. Torregiani, *Organic Letters* 8 (2006) 4093-4096.
- [117] P. Thirupathi, S.S. Kim, *The Journal of Organic Chemistry* 74 (2009) 7755-7761.
- [118] M. Shiri, M.A. Zolfigol, H.G. Kruger, Z. Tanbakouchian, *Chemical Reviews* 110 (2010) 2250-2293.
- [119] A. Palmieri, M. Petrini, *The Journal of Organic Chemistry* 72 (2007) 1863-1866.
- [120] P. Maity, D.M. Shacklady-McAtee, G.P.A. Yap, E.R. Sirianni, M.P. Watson, *Journal of the American Chemical Society* 135 (2013) 280-285.
- [121] A. Padwa, C.L. Muller, A. Rodriguez, S.H. Watterson, *Tetrahedron* 54 (1998) 9651-9666.
- [122] E. Chiurchiù, A. Palmieri, M. Petrini, *Arkivoc* 2019 (2019) 69-79.
- [123] L.L. Cao, Z.S. Ye, G.F. Jiang, Y.G. Zhou, *Advanced Synthesis & Catalysis* 353 (2011) 3352-3356.
- [124] L.L. Cao, X.N. Li, F.Y. Meng, G.F. Jiang, *Tetrahedron Letters* 53 (2012) 3873-3875.
- [125] A. Fürstner, *Synthesis* 8 (1989) 571-590.
- [126] T. Mecozi, M. Petrini, *Tetrahedron Letters* 41 (2000) 2709-2712.
- [127] F. Maertens, A. Van den Bogaert, F. Compennolle, Georges J. Hoornaert, *European Journal of Organic Chemistry* 2004 (2004) 4648-4656.
- [128] R.R. Shaikh, A. Mazzanti, M. Petrini, G. Bartoli, P. Melchiorre, *Angewandte Chemie* 120 (2008) 8835-8838.
- [129] Y. Li, F.Q. Shi, Q.L. He, S.L. You, *Organic Letters* 11 (2009) 3182-3185.

- [130] L. Marsili, A. Palmieri, M. Petrini, *Organic & Biomolecular Chemistry* 8 (2010) 706-712.
- [131] R. Ballini, A. Palmieri, M. Petrini, R.R. Shaikh, *Advanced Synthesis & Catalysis* 350 (2008) 129-134.
- [132] L. Jing, J. Wei, L. Zhou, Z. Huang, Z. Li, D. Wu, H. Xiang, X. Zhou, *Chemistry–A European Journal* 16 (2010) 10955-10958.
- [133] Z. Zuo, S. Zhang, R. Wang, W. He, S. Wu, X. Xie, D. Qin, L. Jing, *Synthesis* 45 (2013) 2832-2842.
- [134] F.A. Luzzio, *Tetrahedron* 57 (2001) 915-945.
- [135] A. Palmieri, M. Petrini, E. Torregiani, *Tetrahedron Letters* 48 (2007) 5653-5656.
- [136] S. Lancianesi, A. Palmieri, M. Petrini, *Chemical Reviews* 114 (2014) 7108-7149.
- [137] R. Ballini, S. Gabrielli, A. Palmieri, M. Petrini, *Advanced Synthesis & Catalysis* 352 (2010) 2459-2462.
- [138] G. Rosini, R. Ballini, P. Sorrenti, *Tetrahedron* 39 (1983) 4127-4132.
- [139] M. Petrini, R.R. Shaikh, *Tetrahedron Letters* 49 (2008) 5645-5648.
- [140] S. Protti, A. Palmieri, M. Petrini, M. Fagnoni, R. Ballini, A. Albini, *Advanced Synthesis & Catalysis* 355 (2013) 643-646.
- [141] S. Imran, M. Taha, N. Hadiani Ismail, *Current Medicinal Chemistry* 22 (2015) 4412-4433.
- [142] D.K. Sharma, B. Rah, M.R. Lambu, A. Hussain, S.K. Yousuf, A.K. Tripathi, B. Singh, G. Jamwal, Z. Ahmed, N. Chanauria, A. Nargotra, A. Goswami, D. Mukherjee, *MedChemComm* 3 (2012) 1082-1091.
- [143] G.O. Burr, R.A. Gortner, *Journal of the American Chemical Society* 46 (1924) 1224-1246.
- [144] Y.P. Zhu, M.C. Liu, F.C. Jia, J.J. Yuan, Q.H. Gao, M. Lian, A.X. Wu, *Organic Letters* 14 (2012) 3392-3395.
- [145] J. Barluenga, A. Fernández, F. Rodríguez, F.J. Fañanás, *Journal of Organometallic Chemistry* 694 (2009) 546-550.
- [146] J.S. Yadav, B.V.S. Reddy, G. Satheesh, A. Prabhakar, A.C. Kunwar, *Tetrahedron Letters* 44 (2003) 2221-2224.
- [147] X. Mi, S. Luo, J. He, J. P. Cheng, *Tetrahedron Letters* 45 (2004) 4567-4570.
- [148] X. Guo, S. Pan, J. Liu, Z. Li, *The Journal of Organic Chemistry* 74 (2009) 8848-8851.
- [149] V. Terrasson, J. Michaux, A. Gaucher, J. Wehbe, S. Marque, D. Prim, J.M. Campagne, *European Journal of Organic Chemistry* 2007 (2007) 5332-5335.
- [150] A. Zanardi, R. Corberán, J.A. Mata, E. Peris, *Organometallics* 27 (2008) 3570-3576.
- [151] M.L. Deb, B. Deka, P.J. Saikia, P.K. Baruah, *Tetrahedron Letters* 58 (2017) 1999-2003.
- [152] X.F. Zeng, S.J. Ji, S.Y. Wang, *Tetrahedron* 61 (2005) 10235-10241.
- [153] G. de la Herrán, A. Segura, A.G. Csáky, *Organic Letters* 9 (2007) 961-964.
- [154] Q.L. He, F.L. Sun, X.J. Zheng, S.L. You, *Synlett* 07 (2009) 1111-1114.
- [155] Y. Zhang, S.X. Zhang, L.N. Fu, Q.X. Guo, *ChemCatChem* 9 (2017) 3107-3110.

- [156] S. Lancianesi, A. Palmieri, M. Petrini, *Advanced Synthesis & Catalysis* 354 (2012) 3539-3544.
- [157] M. Barbero, S. Cadamuro, F. Cauda, S. Dughera, G. Gervasio, P. Venturello, *The Journal of Organic Chemistry* 77 (2012) 4278-4287.
- [158] H. Li, X.X. Li, H.Y., Wang, G.N. Winston-McPherson, H.M.J. Geng, I.A. Guzei, W.P. Tang, *Chemical Communications* 50 (2014) 12293-12296.
- [159] M.L. Deb, P.J. Bhuyan, *Synthesis* 18 (2008) 2891-2898.
- [160] J.B. Yu, Y. Zhang, Z.J. Jiang, W.K. Su, *The Journal of Organic Chemistry* 81 (2016) 11514-11520.
- [161] L. Tari, N. Vo, S. Liang, J. Patel, C. Baral, J. Cai, *PLoS ONE* 7 (2012) e40946.
- [162] D. Sola, L. Rossi, G.P.C. Schianca, P. Maffioli, M. Bigliocca, R. Mella, F. Corliano, G.P. Fra, E. Bartoli, G. Derosa, *Archives of Medical Science* 11 (2015) 840.
- [163] C. León, J. Rodrigues, N. Gamboa de Dom ínguez, J. Charris, J. Gut, P.J. Rosenthal, J.N. Dom ínguez, *European Journal of Medicinal Chemistry* 42 (2007) 735-742.
- [164] S. Yasmeen, Riyazuddeen, G. Rabbani, *Journal of Thermal Analysis and Calorimetry* 127 (2017) 1445-1455.
- [165] P.L. T, M. Mondal, K. Ramadas, S. Natarajan, *Spectrochimica Acta Part A: Molecular and Biomolecular Spectroscopy* 183 (2017) 90-102.
- [166] X. Xu, Y. Qian, P. Wu, H. Zhang, C. Cai, *Journal of Colloid and Interface Science* 445 (2015) 102-111.
- [167] Q. Xiao, S. Huang, Z.D. Qi, B. Zhou, Z.K. He, Y. Liu, *Biochimica et Biophysica Acta (BBA)-Proteins and Proteomics* 1784 (2008) 1020-1027.
- [168] N. Keswani, N. Kishore, *The Journal of Chemical Thermodynamics* 43 (2011) 1406-1413.
- [169] X. Li, Z. Yang, *Chemico-Biological Interactions* 232 (2015) 77-84.
- [170] T. Chatterjee, A. Pal, S. Dey, B.K. Chatterjee, P. Chakrabarti, *PloS ONE* 7 (2012) e37468.
- [171] C. Hong, G.L. Firestone, L.F. Bjeldanes, *Biochemical Pharmacology* 63 (2002) 1085-1097.
- [172] A. Palmieri, M. Petrini, *Synthesis* 51 (2019) 829-841.
- [173] E. Follet, G. Berionni, P. Mayer, H. Mayr, *The Journal of Organic Chemistry* 80 (2015) 8643-8656.
- [174] H. Wen, L. Wang, L. Xu, Z. Hao, C.L. Shao, C.Y. Wang, J. Xiao, *Advanced Synthesis & Catalysis* 357 (2015) 4023-4030.
- [175] J.A. Joule, K. Mills, *Heterocyclic Chemistry* 5th Ed. (2010).
- [176] A. Palmieri, M. Petrini, R.R. Shaikh, *Organic & Biomolecular Chemistry* 8 (2010) 1259-1270.
- [177] P.G.M. Wuts, *Greene's protective groups in organic synthesis* 5th Ed. (2014) 1120.
- [178] M.M.F. Queiroz, E.F. Queiroz, M.L. Zeraik, S.N. Ebrahimi, L. Marcourt, M. Cuendet, I. Castro-Gamboa, M. Hamburger, J.L. Wolfender, *Journal of Natural Products* 77 (2014) 650-656.

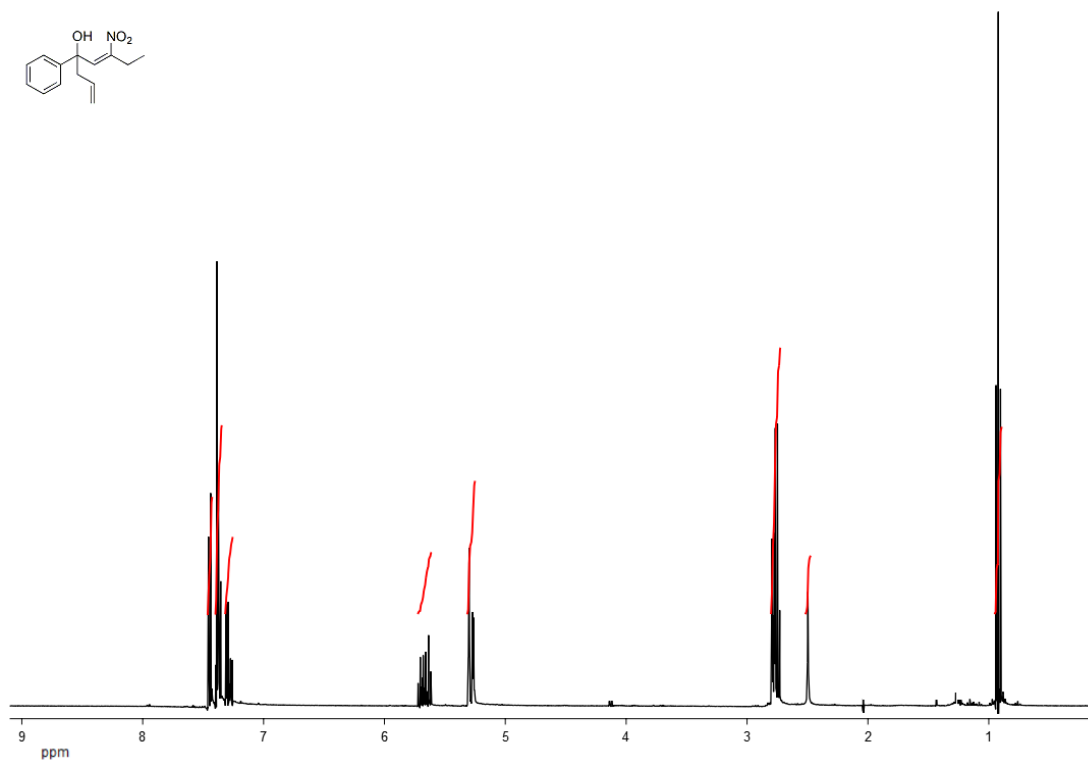
- [179] R. Contractor, I.J. Samudio, Z. Estrov, D. Harris, J.A. McCubrey, S.H. Safe, M. Andreeff, M. Konopleva, *Cancer Research* 65 (2005) 2890-2898.
- [180] M.G. Reinecke, J.F. Sebastian, H.W. Johnson Jr, C. Pyun, *The Journal of Organic Chemistry* 37 (1972) 3066-3068.
- [181] J. Bergman, L. Venemalm, *Tetrahedron* 46 (1990) 6061-6066.
- [182] M. Hatano, S. Suzuki, K. Ishihara, *Journal of the American Chemical Society* 128 (2006) 9998-9999.
- [183] E. Marcantoni, A. Palmieri, M. Petrini, *Organic Chemistry Frontiers* 6 (2019) 2142-2182.
- [184] W. Rush Scaggs, T.D. Scaggs, T.N. Snaddon, *Organic & Biomolecular Chemistry* 17 (2019) 1787-1790.
- [185] Y. Minagawa, J. Kigawa, H. Itamochi, Y. Kanamori, M. Shimada, M. Takahashi, N. Terakawa, *Japanese Journal of Cancer Research* 90 (1999) 1373-1379.
- [186] W.W. Qi, H.Y. Yu, H. Guo, J. Lou, Z.M. Wang, P. Liu, A. Sapin-Minet, P. Maincent, X.C. Hong, X.M. Hu, Y.L. Xiao, *Molecular Pharmaceutics* 12 (2015) 675-683.
- [187] T. Shen, X.N. Wang, H.X. Lou, *Natural Product Reports* 26 (2009) 916-935.
- [188] S.A. Snyder, A.L. Zografos, Y. Lin, *Angewandte Chemie International Edition* 46 (2007) 8186-8191.
- [189] B.C. Akinwumi, K.A.M. Bordun, H.D. Anderson, *International Journal of Molecular Sciences* 19 (2018) 792.
- [190] M.B. Andrus, J. Liu, E.L. Meredith, E. Nartey, *Tetrahedron Letters* 44 (2003) 4819-4822.
- [191] A.V. Moro, F.S.P. Cardoso, C.R.D. Correia, *Tetrahedron Letters* 49 (2008) 5668-5671.
- [192] J. Yu, M.J. Gaunt, J.B. Spencer, *The Journal of Organic Chemistry* 67 (2002) 4627-4629.
- [193] F. Lara-Ochoa, L.C. Sandoval-Minero, G. Espinosa-Pérez, *Tetrahedron Letters* 56 (2015) 5977-5979.
- [194] S. Young Han, H. Suck Lee, D. Hye Choi, J. Woon Hwang, D. Mo Yang, J.G. Jun, *Synthetic Communications* 39 (2009) 1425-1432.
- [195] I. Galindo, B. Hernández, J. Berná J. Fenoll, J.L. Cenis, J.M. Escribano, C. Alonso, *Antiviral Research* 91 (2011) 57-63.
- [196] H.Y. Sun, C.F. Xiao, Y.C. Cai, Y. Chen, W. Wei, X.K. Liu, Z.L. Lv, Y. Zou, *Chemical and Pharmaceutical Bulletin* 58 (2010) 1492-1496.
- [197] E. Reimann, *Tetrahedron Letters* 11 (1970) 4051-4053.
- [198] S.Y. Han, H.B. Bang, H.S. Lee, J.W. Hwang, D.H. Choi, D.M. Yang, J.G. Jun, *Bulletin of the Korean Chemical Society* 29 (2008) 1800-1802.
- [199] T. Furuya, K. Kino, *Tetrahedron Letters* 55 (2014) 2853-2855.
- [200] Z.W. Li, S.Y. Kang, L. Chen, Y. Wang, J.S. Li, *Chinese Journal of Organic Chemistry* 36 (2016) 1143-1147.
- [201] S. Yan, J. Xu, X. Zhang, F. Xie, S. Zhang, L. Jiang, B. Qi, Y. Li, *Process Biochemistry* 101 (2021) 190-198.

- [202] J. Zhang, Z. Tian, L. Liang, M. Subirade, L. Chen, *The Journal of Physical Chemistry B* 117 (2013) 14018-14028.
- [203] Z.L. Wan, J.M. Wang, L.Y. Wang, Y. Yuan, X.Q. Yang, *Food Chemistry* 161 (2014) 324-331.
- [204] Y. You, L. Yang, H. Chen, L. Xiong, F. Yang, *Journal of Agricultural and Food Chemistry* 69 (2021) 2306-2315.
- [205] J. Cao, F. Li, Y. Li, H. Chen, X. Liao, Y. Zhang, *Food Hydrocolloids* 113 (2021) 106465.
- [206] M.A. Grusak, D. DellaPenna, *Annual Review of Plant Biology* 50 (1999) 133-161.
- [207] G. Chen, S. Wang, B. Feng, B. Jiang, M. Miao, *Food Chemistry* 277 (2019) 632-638.
- [208] Y.J. Hu, Y. Liu, X.H. Xiao, *Biomacromolecules* 10 (2009) 517-521.
- [209] L.X. Yuan, M. Liu, G. Liu, D. Li, Z. Wang, B. Wang, J. Han, M. Zhang, *Spectrochimica Acta Part A: Molecular and Biomolecular Spectroscopy* 173 (2017) 584-592.
- [210] S. Balakrishnan, S. Jaldappagari, *Journal of Luminescence* 142 (2013) 17-22.
- [211] S. Zhong, M. Yan, H. Zou, P. Zhao, H. Ye, T. Zhang, C. Zhao, *Food Science & Nutrition* 9 (2021) 1917-1928.
- [212] X. Xu, M. Zhao, Q. Han, H. Wang, H. Zhang, Y. Wang, *Spectrochimica Acta Part A: Molecular and Biomolecular Spectroscopy* 228 (2020) 117706.
- [213] M.S. Ali, H.A. Al-Lohedan, M.Z.A. Rafiquee, A.M. Atta, A.O. Ezzat, *Spectrochimica Acta Part A: Molecular and Biomolecular Spectroscopy* 135 (2015) 147-152.
- [214] J.S. Johansson, *Journal of Biological Chemistry* 272 (1997) 17961-17965.
- [215] M.Y. Li, C.Q. Xiao, Z.Q. Xu, M.M. Yin, Q.Q. Yang, Y.L. Yin, Y. Liu, *Spectrochimica Acta Part A: Molecular and Biomolecular Spectroscopy* 204 (2018) 484-494.
- [216] H. Zhang, *Science in China Series B: Chemistry* 42 (1999) 106-112.
- [217] M. Liu, T. Liu, Y. Shi, Y. Zhao, H. Yan, B. Sun, Q. Wang, Z. Wang, J. Han, *Food & Function* 10 (2019) 8182-8194.
- [218] T. Liu, M. Liu, Q. Guo, Y. Liu, Y. Zhao, Y. Wu, B. Sun, Q. Wang, J. Liu, J. Han, *Journal of Molecular Liquids* 311 (2020) 113364.
- [219] S. Bi, L. Ding, Y. Tian, D. Song, X. Zhou, X. Liu, H. Zhang, *Journal of Molecular Structure* 703 (2004) 37-45.
- [220] T. Hu, Y. Liu, *Journal of Pharmaceutical and Biomedical Analysis* 107 (2015) 325-332.
- [221] S. Tunç, O. Duman, İ. Soylu, B. Kancı Bozoğlan, *Journal of Hazardous Materials* 273 (2014) 36-43.
- [222] T. Liu, M. Liu, H. Liu, Y. Ren, Y. Zhao, H. Yan, Q. Wang, N. Zhang, Z. Ding, Z. Wang, *Food & Function* 12 (2021) 7126-7144.
- [223] J. Jia, X. Gao, M. Hao, L. Tang, *Food Chemistry* 228 (2017) 143-151.
- [224] Z. Wei, W. Yang, R. Fan, F. Yuan, Y. Gao, *Food Hydrocolloids* 45 (2015) 337-350.
- [225] M. Wongon, N. Limpeanchob, *Heliyon* 6 (2020) e03458.
- [226] C. Xi, N. Kang, C. Zhao, H. Song, Y. Liu, T. Zhang, *Journal of Food Science* 85 (2020) 1707-1716.

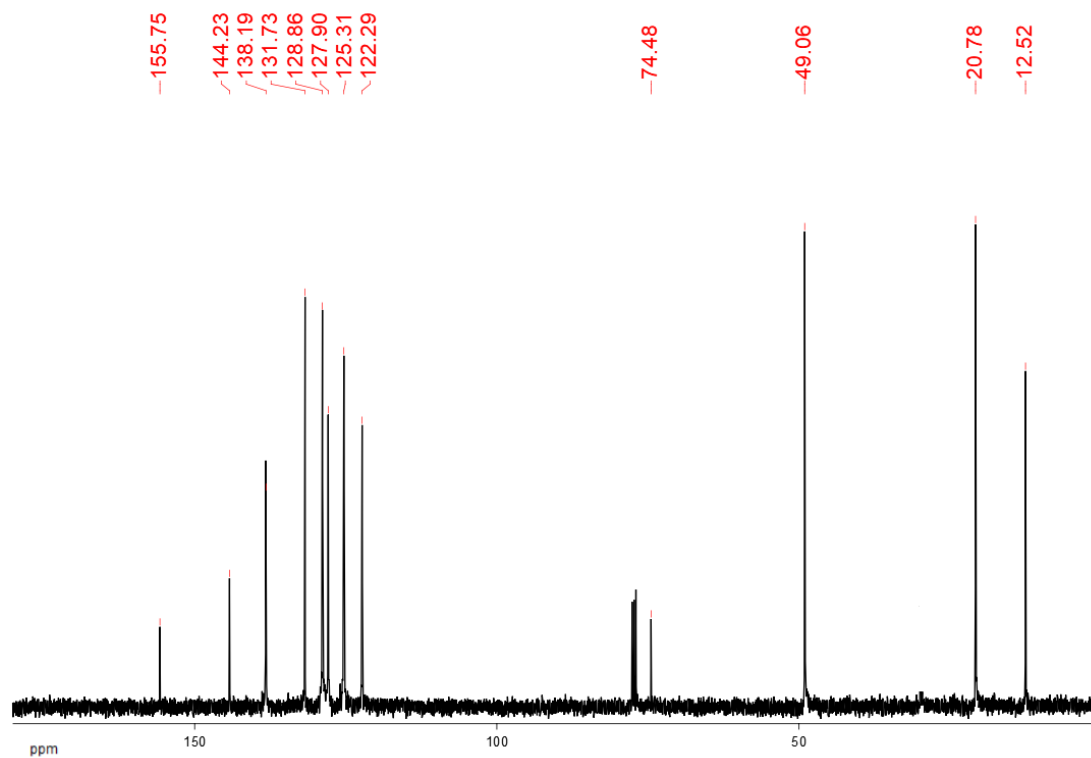
- [227] C. Ren, W. Xiong, D. Peng, Y. He, P. Zhou, J. Li, B. Li, *Food Research International* 112 (2018) 284-290.
- [228] Q. Guo, M. Liu, Y. Zhao, Y. Wu, J. Liu, C. Cai, Y. Shi, J. Han, *Spectrochimica Acta Part A: Molecular and Biomolecular Spectroscopy* 222 (2019) 117213.
- [229] J. Guo, Z. He, S. Wu, M. Zeng, J. Chen, *Food Hydrocolloids* 100 (2020) 105388.
- [230] R. Wang, Y. Liu, X. Hu, J. Pan, D. Gong, G. Zhang, *Food Research International* 120 (2019) 226-234.
- [231] W. Wu, M. Clifford, N.K. Howell, *Journal of the Science of Food and Agriculture* 87 (2007) 1810-1819.
- [232] X. Sui, H. Sun, B. Qi, M. Zhang, Y. Li, L. Jiang, *Food Chemistry* 245 (2018) 871-878.
- [233] A. Tapal, P.K. Tikku, *Food Chemistry* 130 (2012) 960-965.
- [234] Z.L. Wan, L.Y. Wang, J.M. Wang, Y. Yuan, X.Q. Yang, *Journal of Agricultural and Food Chemistry* 62 (2014) 6834-6843.
- [235] Z. He, B. Yuan, M. Zeng, G. Tao, J. Chen, *Food Chemistry* 175 (2015) 457-464.
- [236] D. Jeoung, S.J. Oh, S. Lee, M. Baek, Y.H. Lee, N.I. Baek, H.Y. Kim, *Biotechnology letters* 24 (2002) 463-467.
- [237] R.S. Aziz, A. Siddiqua, M. Shahzad, A. Shabbir, N. Naseem, *Biomedicine & Pharmacotherapy* 110 (2019) 554-560.
- [238] M.S. Ali, J. Muthukumar, M. Jain, T. Santos-Silva, H.A. Al-Lohedan, N.S. Al-Shuail, *Journal of Molecular Liquids* 337 (2021) 116354.
- [239] Y. Liang, T. Zhang, Y. Sun, M. Diao, J. Zhang, L. Ren, *Food Bioscience* 40 (2021) 100913.
- [240] S.K. Pawar, S. Jaldappagari, *Journal of Molecular Recognition* 33 (2020) e2812.
- [241] M.S. Ali, H.A. Al-Lohedan, *ACS Omega* 5 (2020) 9131-9141.
- [242] W.Q. Wang, P.P. Yuan, J.Y. Zhou, Z.H. Gu, *Journal of Food Science* 86 (2021) 1228-1242.
- [243] S. Wilson, C. Martinez-Villaluenga, E. De Mejia, *Journal of Food Science* 73 (2008) T106-T114.
- [244] Â. Lu í, A.P. Duarte, L. Pereira, F. Domingues, *European Food Research and Technology* 244 (2018) 175-185.
- [245] J. Cong, J. Cui, H. Zhang, C.S. Dzah, Y. He, Y. Duan, *Food Research International* 136 (2020) 109530.

4.2 ^1H NMR & ^{13}C NMR Spectra

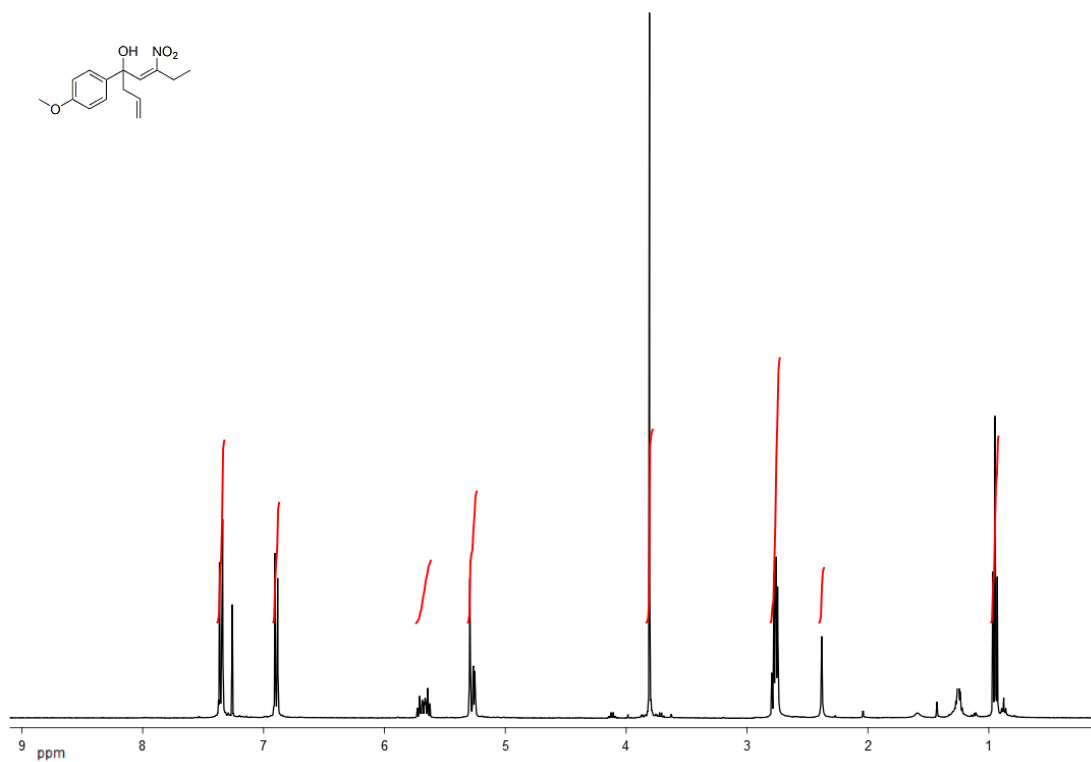
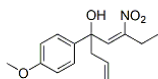
^1H NMR Compound **88a**.



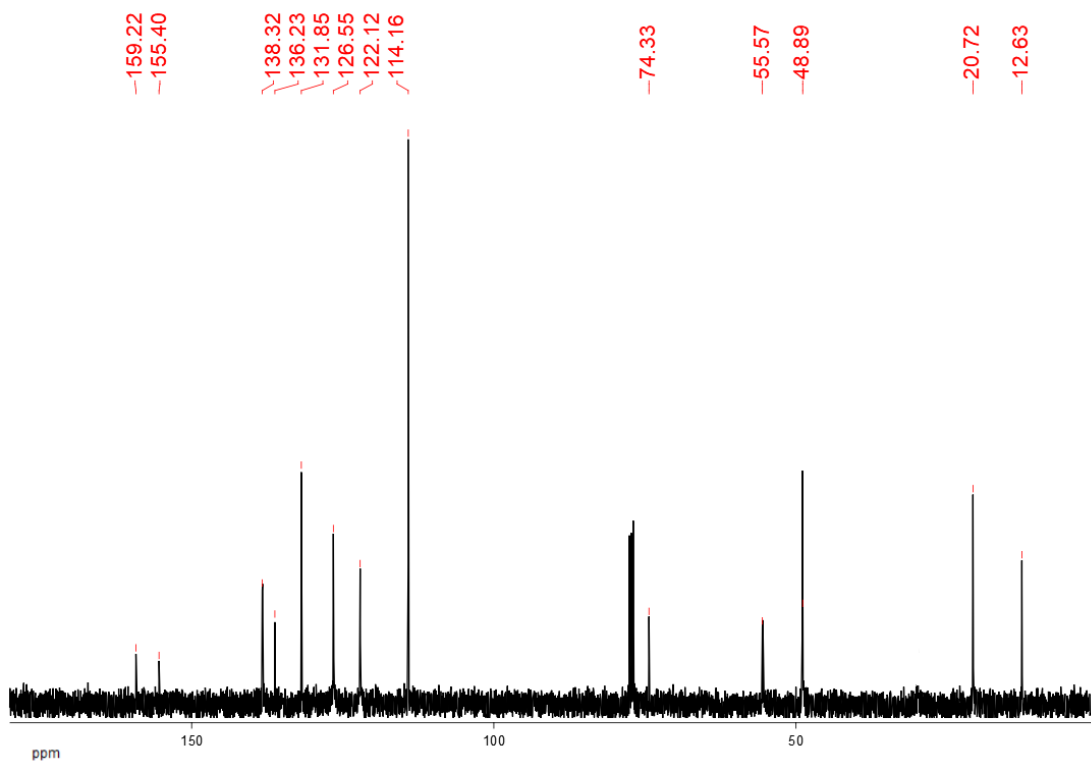
^{13}C NMR Compound **88a**.



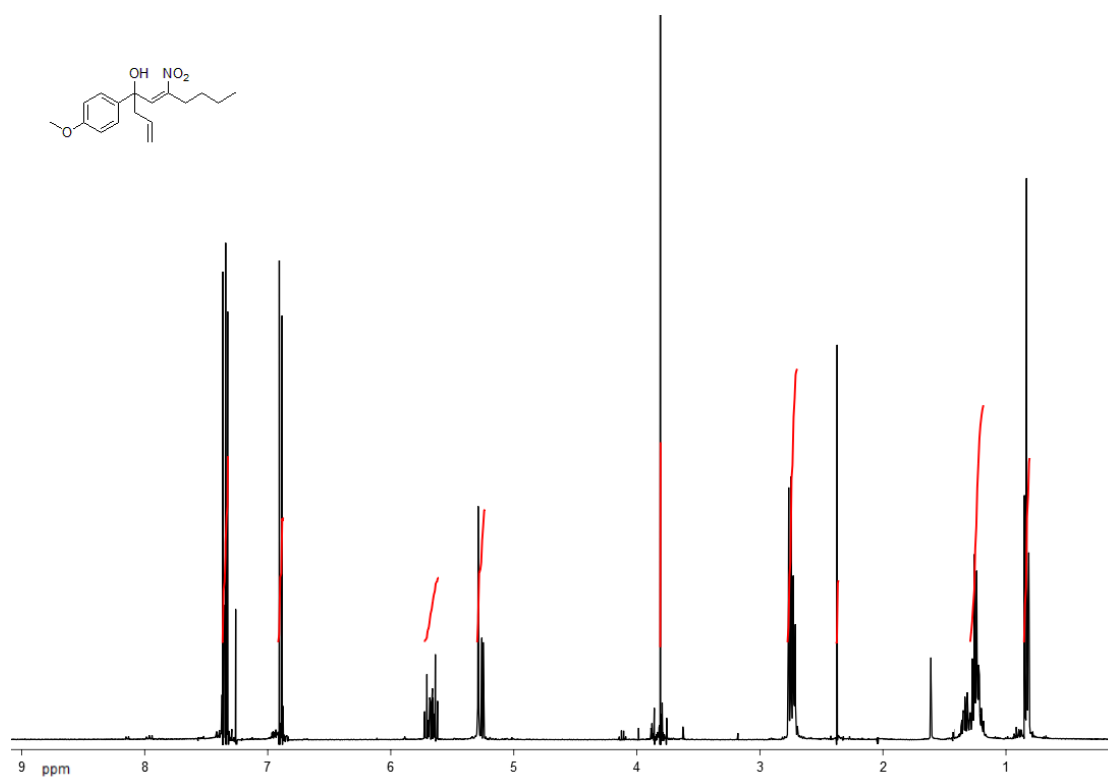
^1H NMR Compound **88b**.



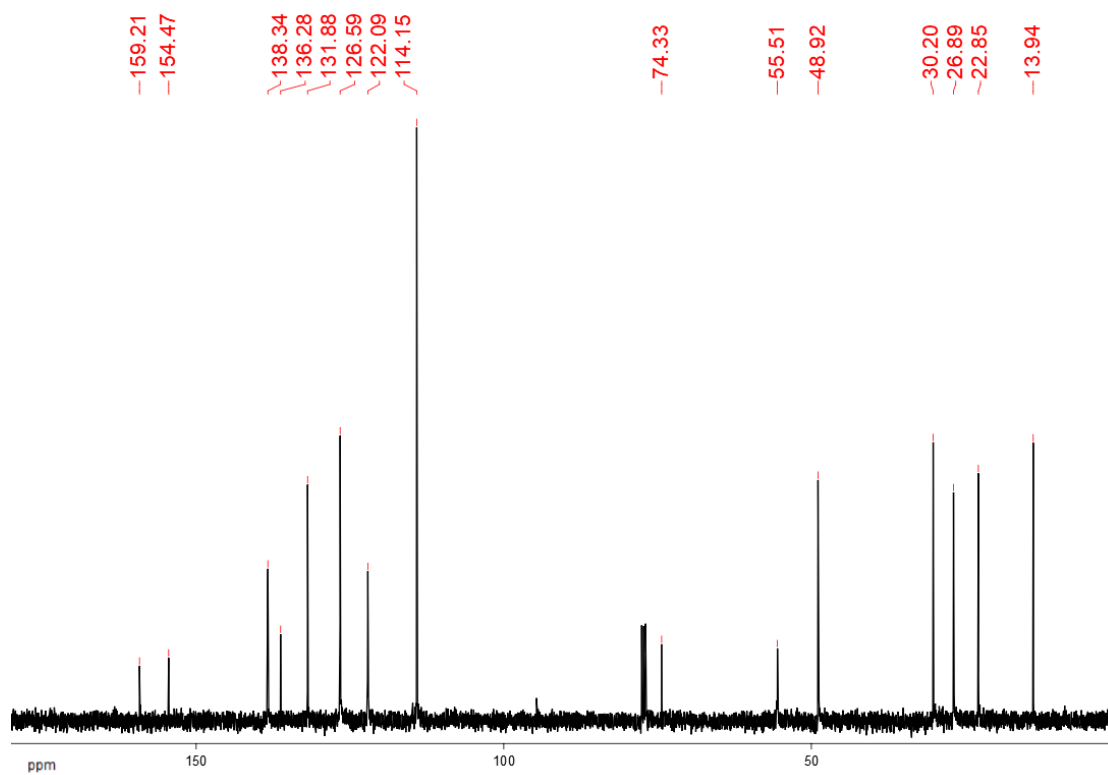
^{13}C NMR Compound **88b**.



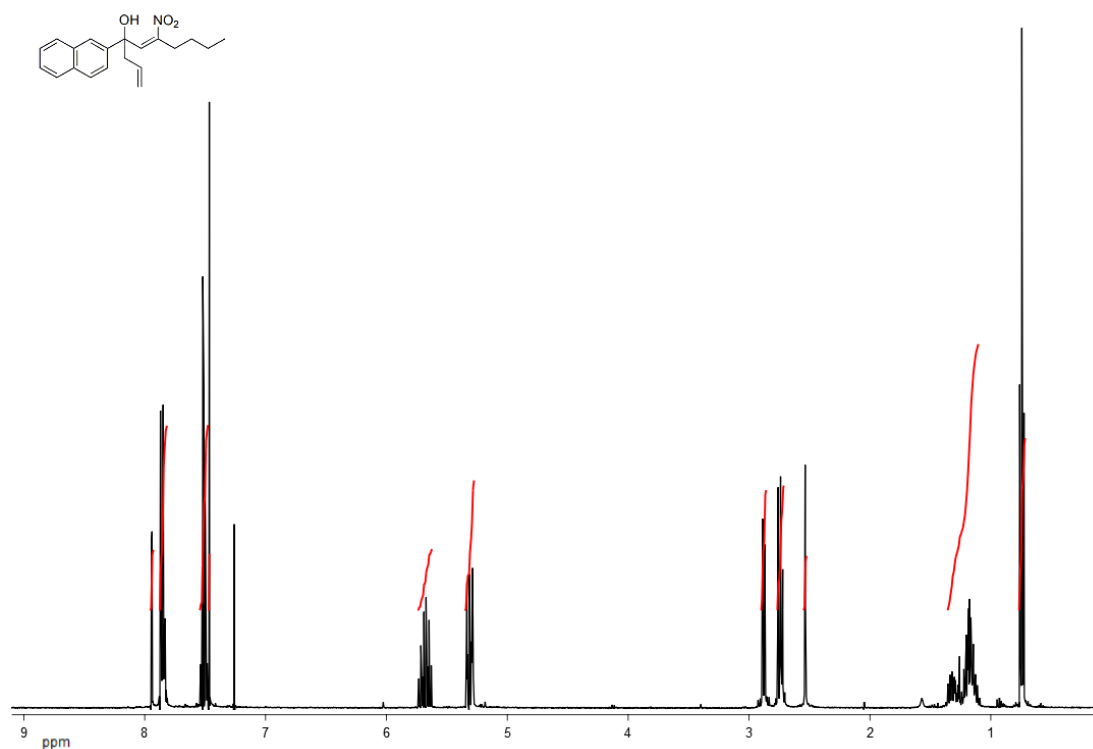
¹H NMR Compound **88c**.



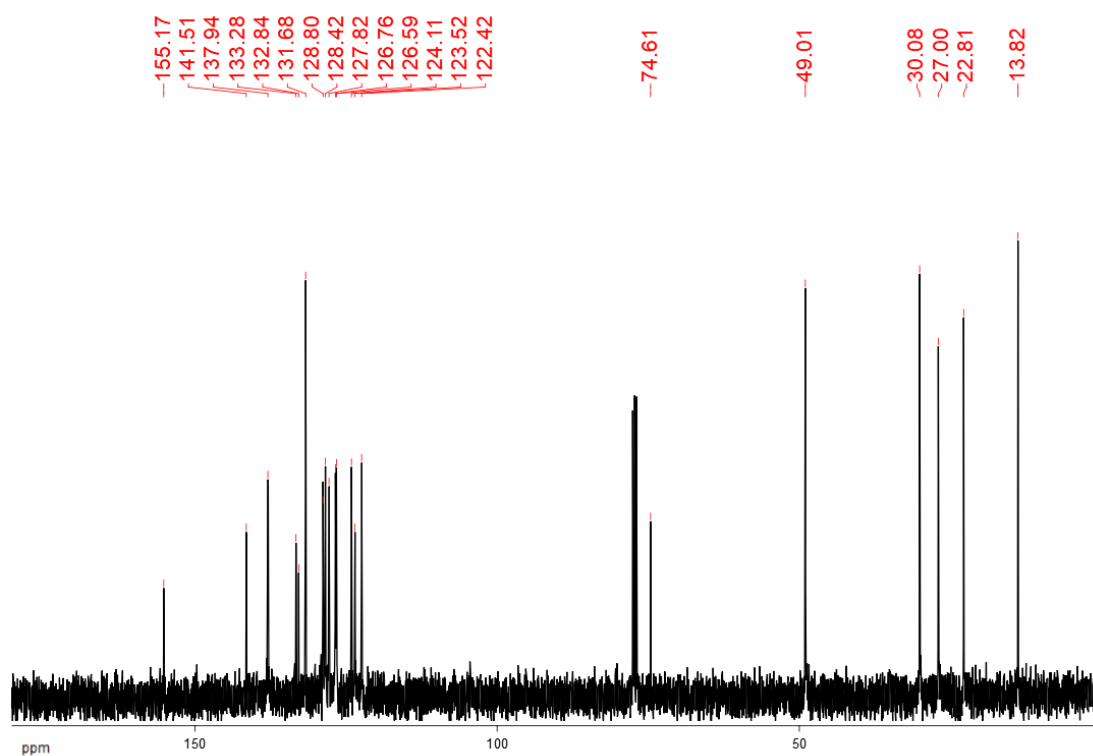
¹³C NMR Compound **88c**.



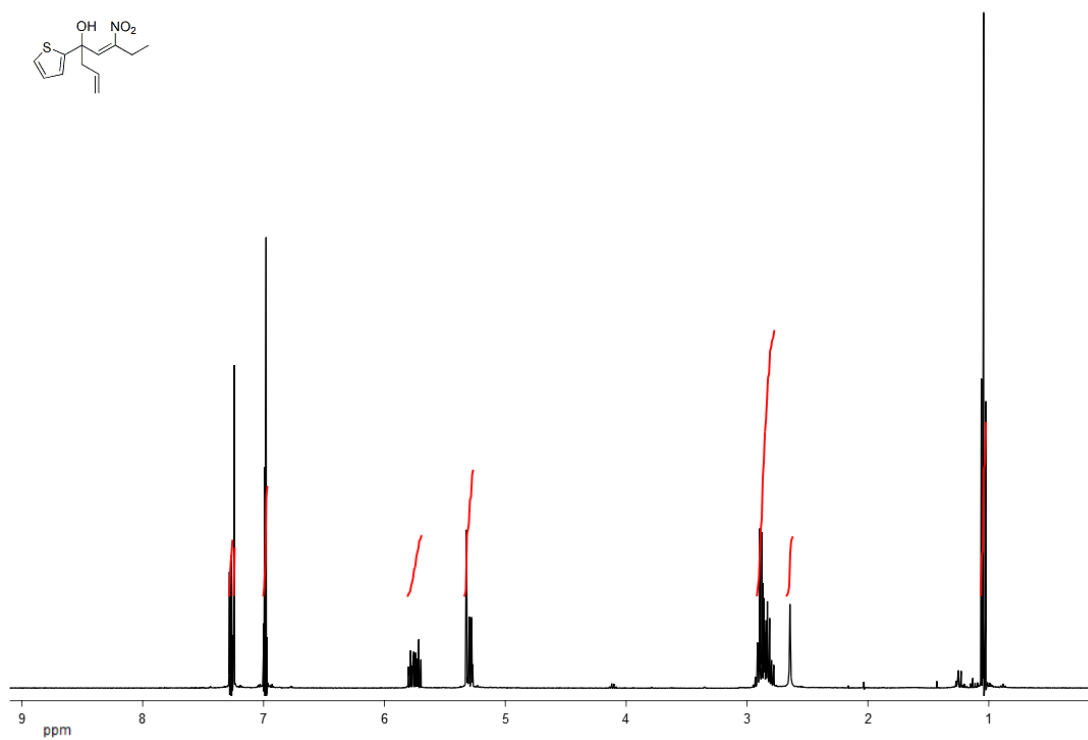
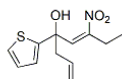
¹H NMR Compound **88d**.



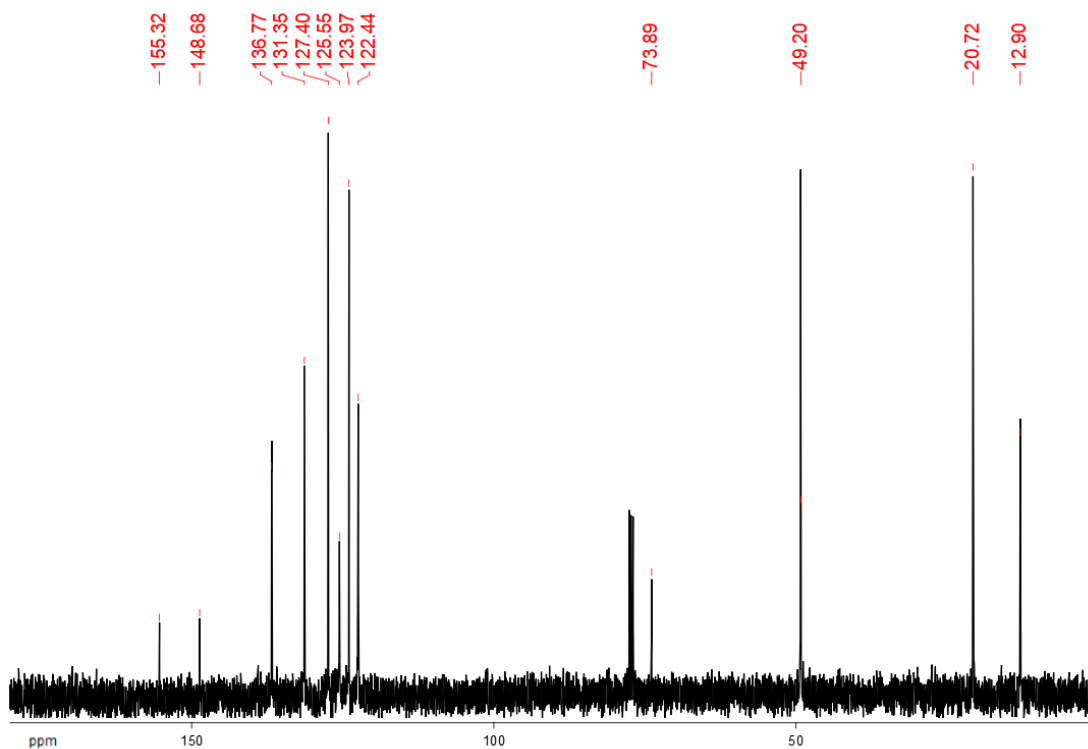
¹³C NMR Compound **88d**.



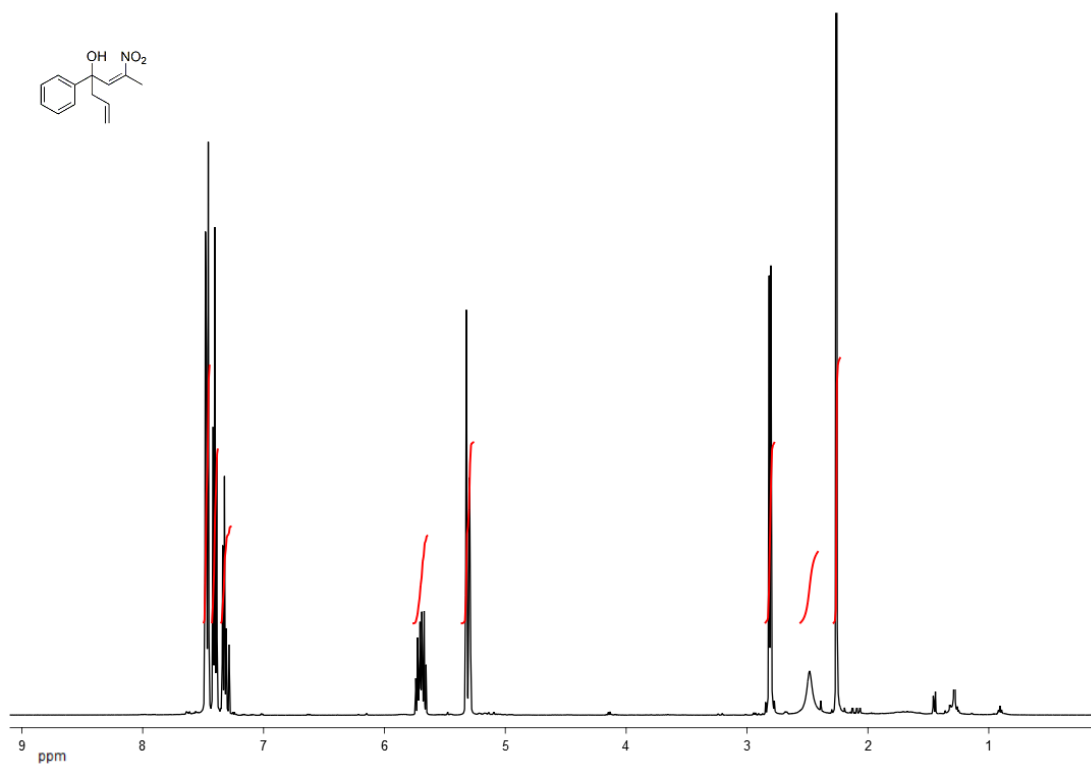
¹H NMR Compound **88e**.



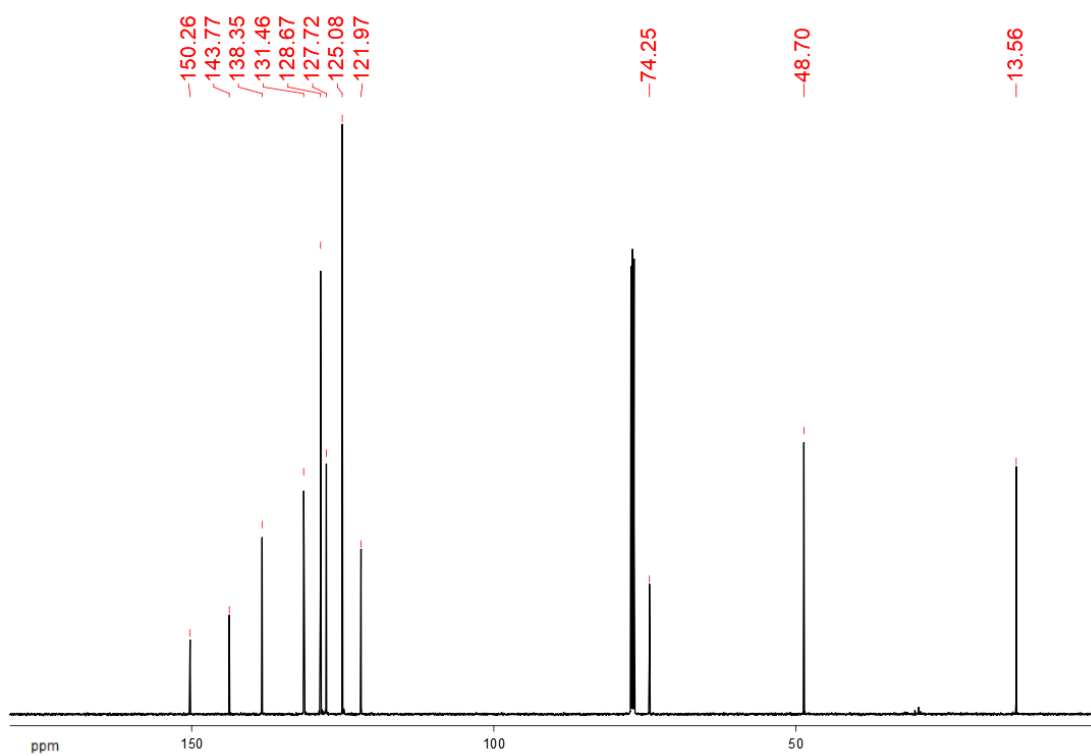
¹³C NMR Compound **88e**.



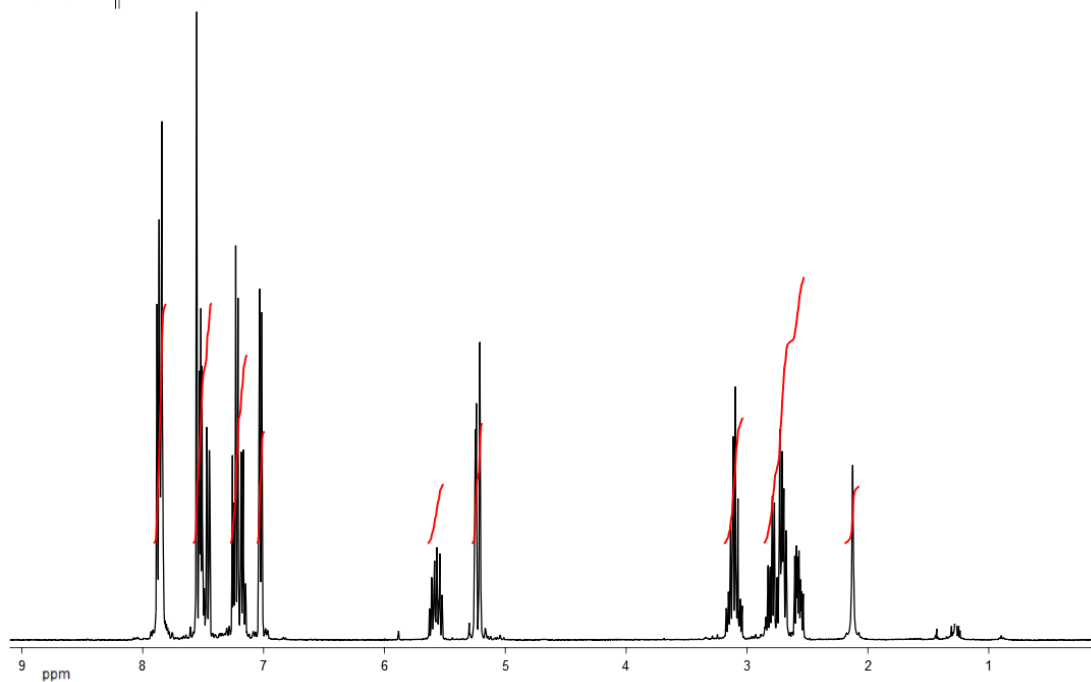
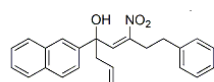
¹H NMR Compound **88f**.



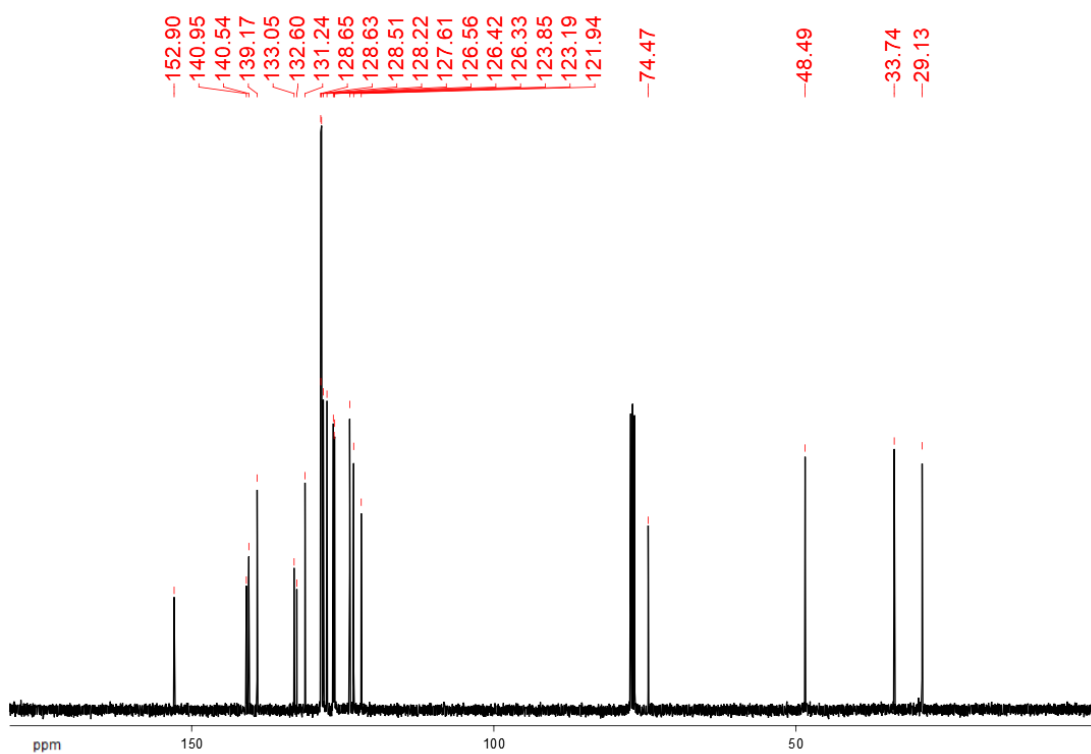
¹³C NMR Compound **88f**.



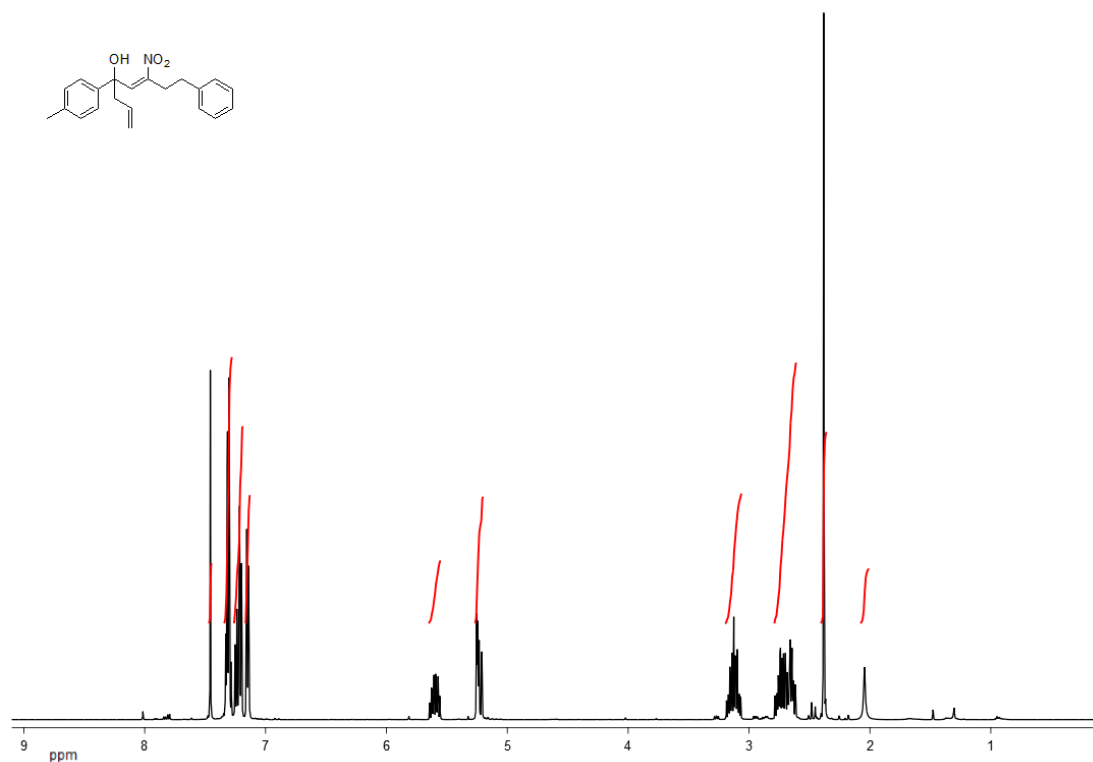
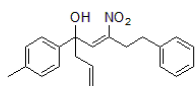
^1H NMR Compound **88g**.



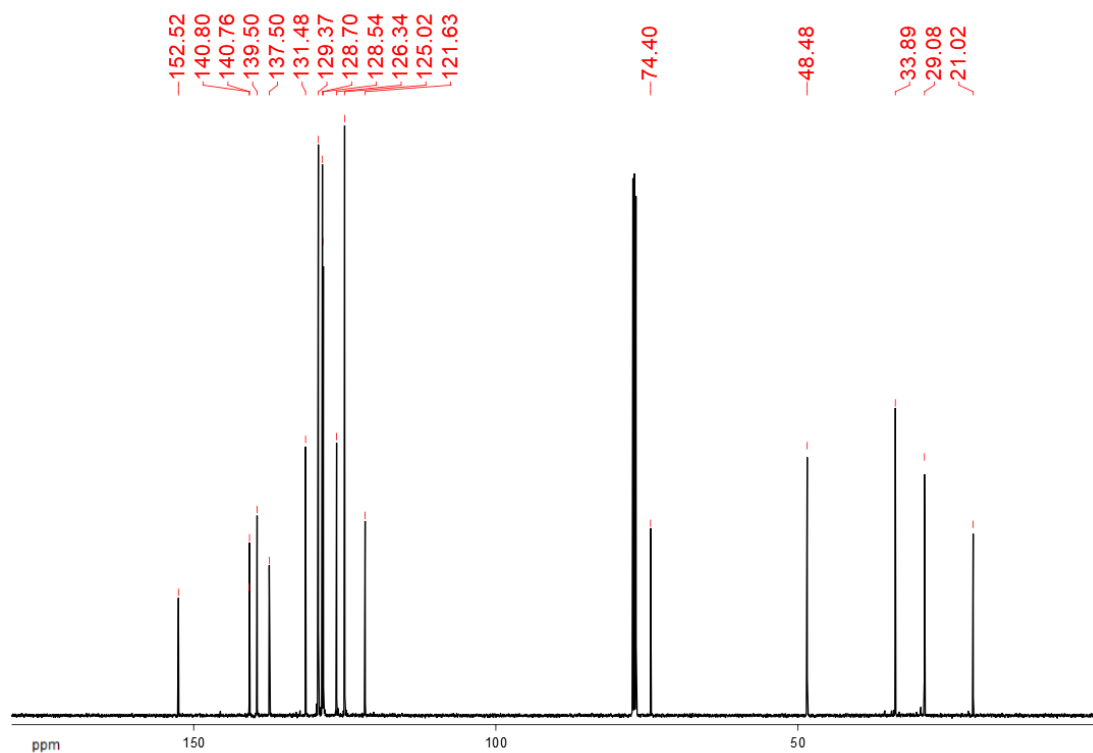
^{13}C NMR Compound **88g**.



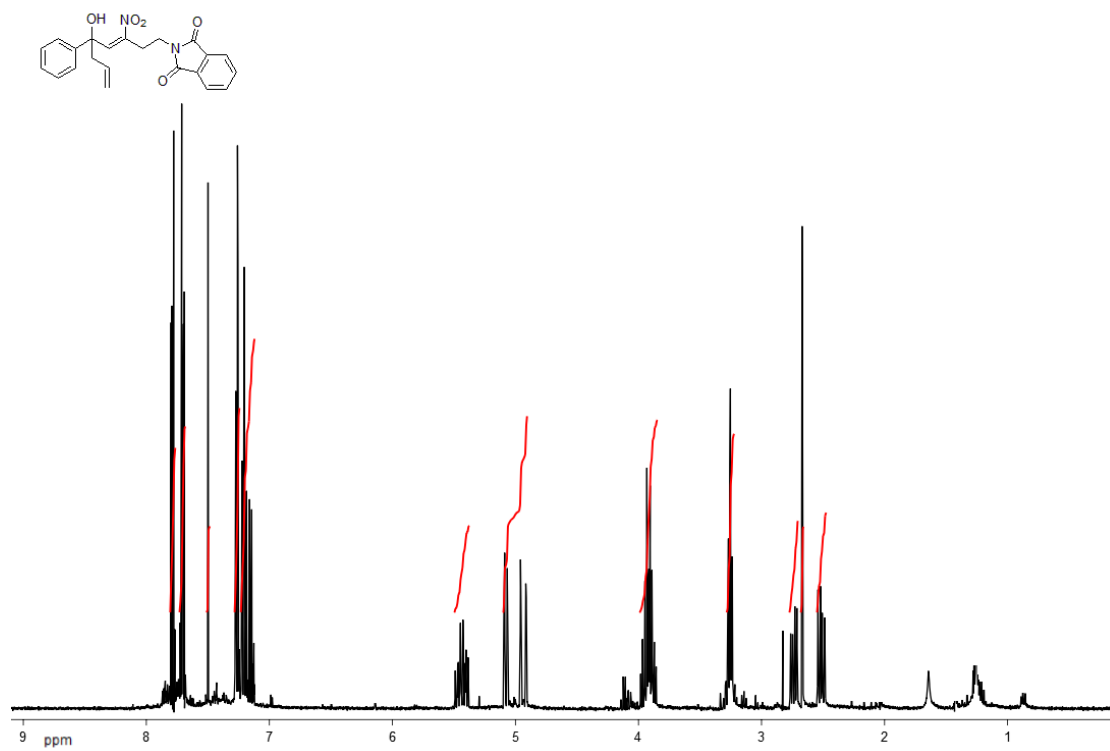
^1H NMR Compound **88h**.



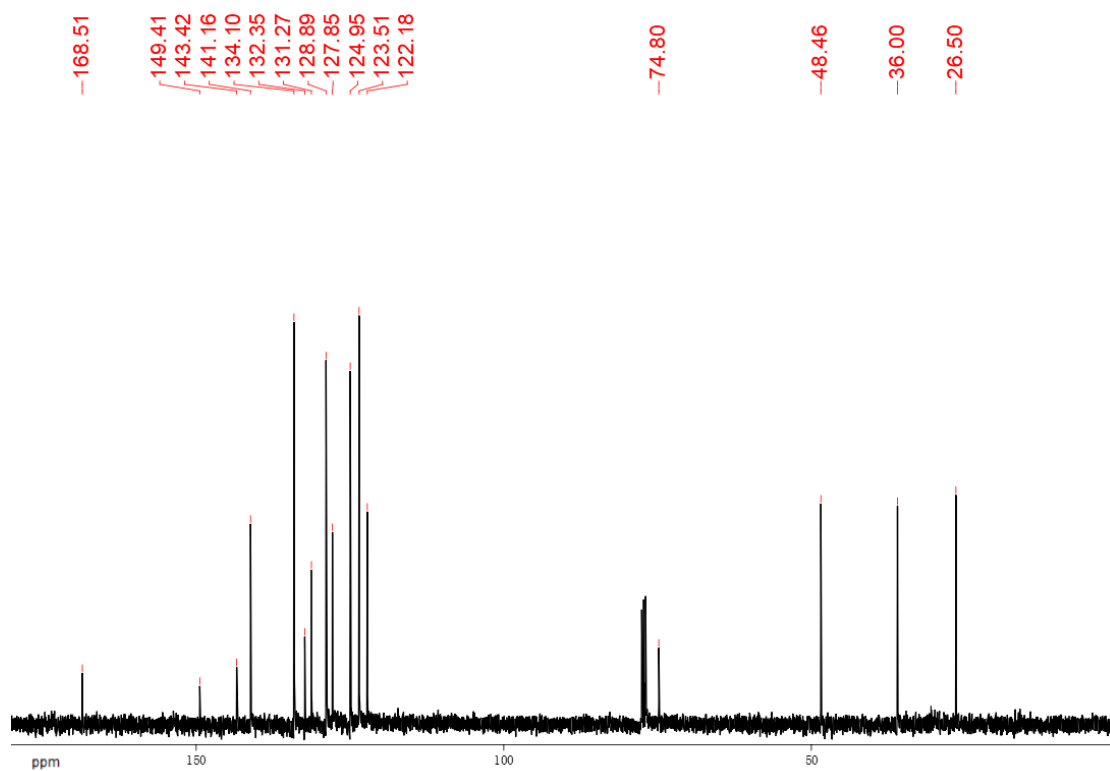
^{13}C NMR Compound **88h**.



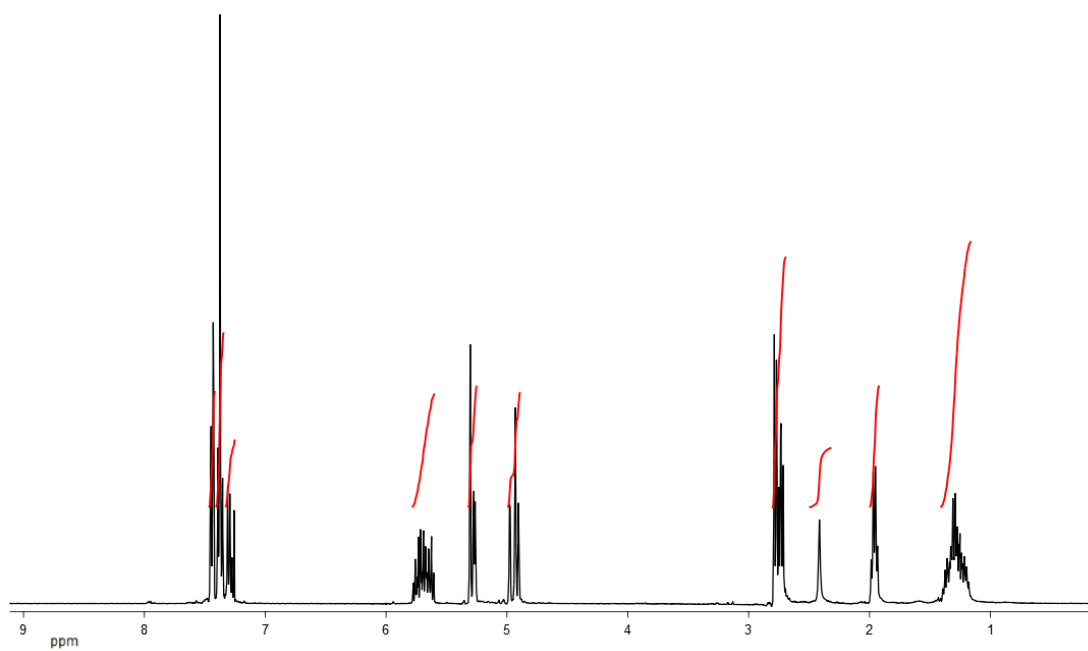
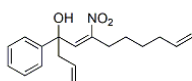
^1H NMR Compound **88i**.



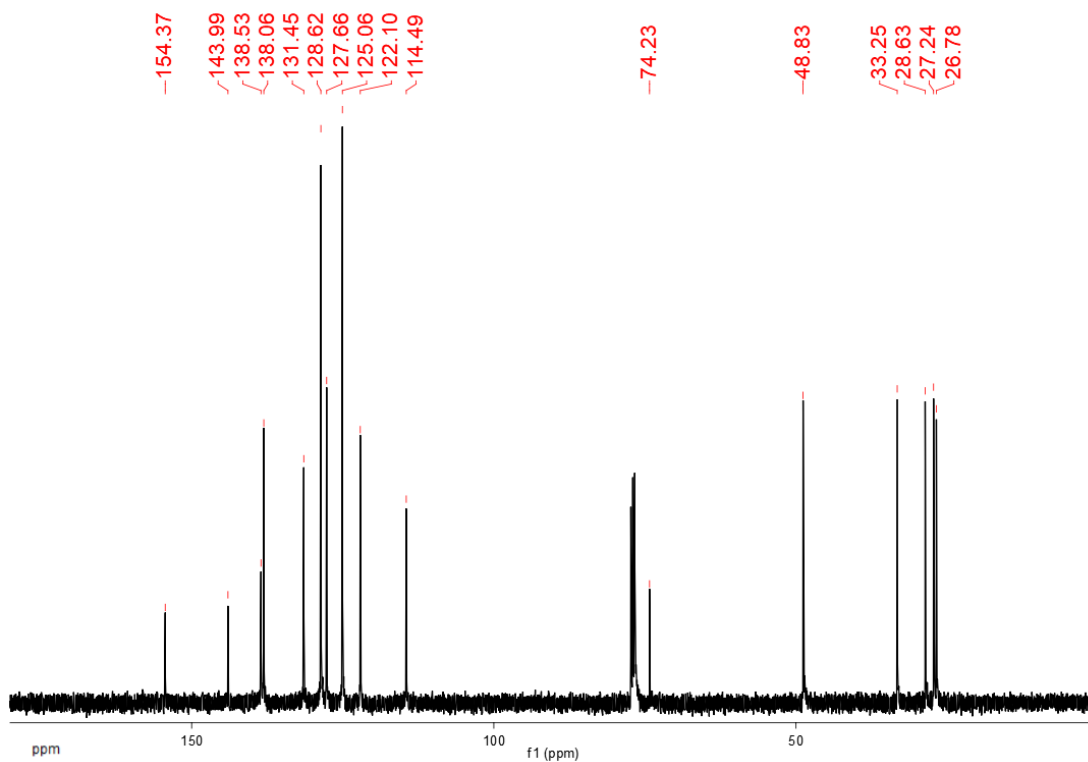
^{13}C NMR Compound **88i**.



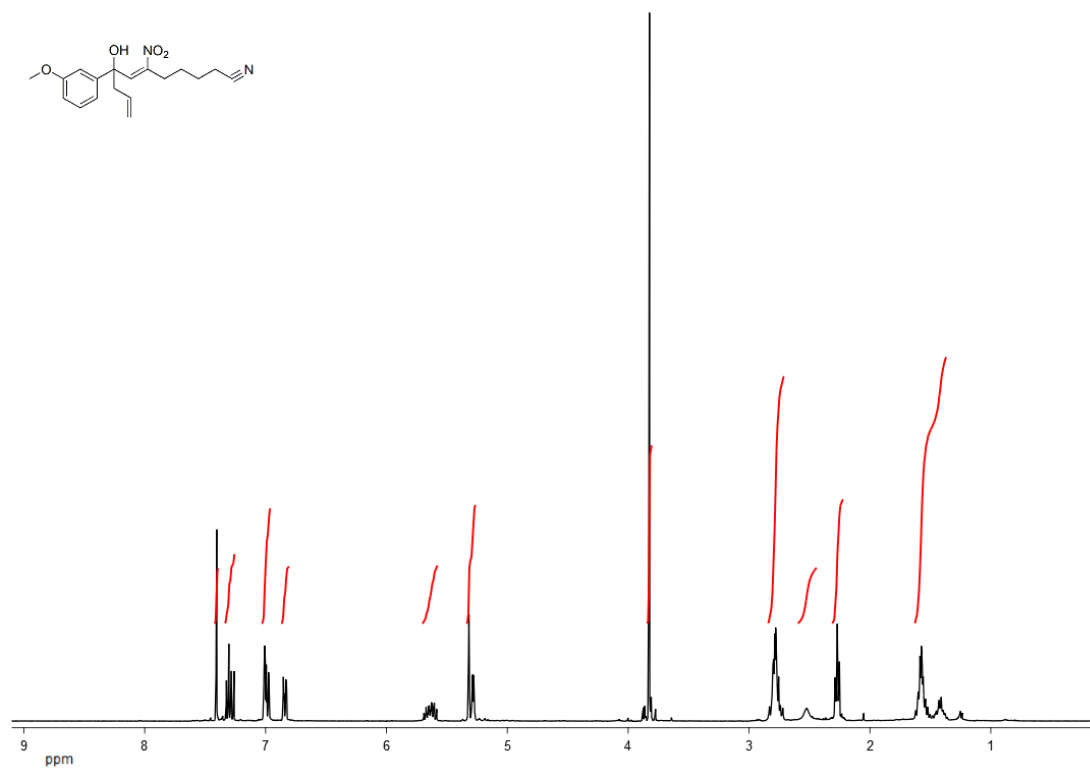
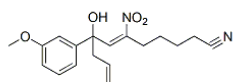
¹H NMR Compound **88j**.



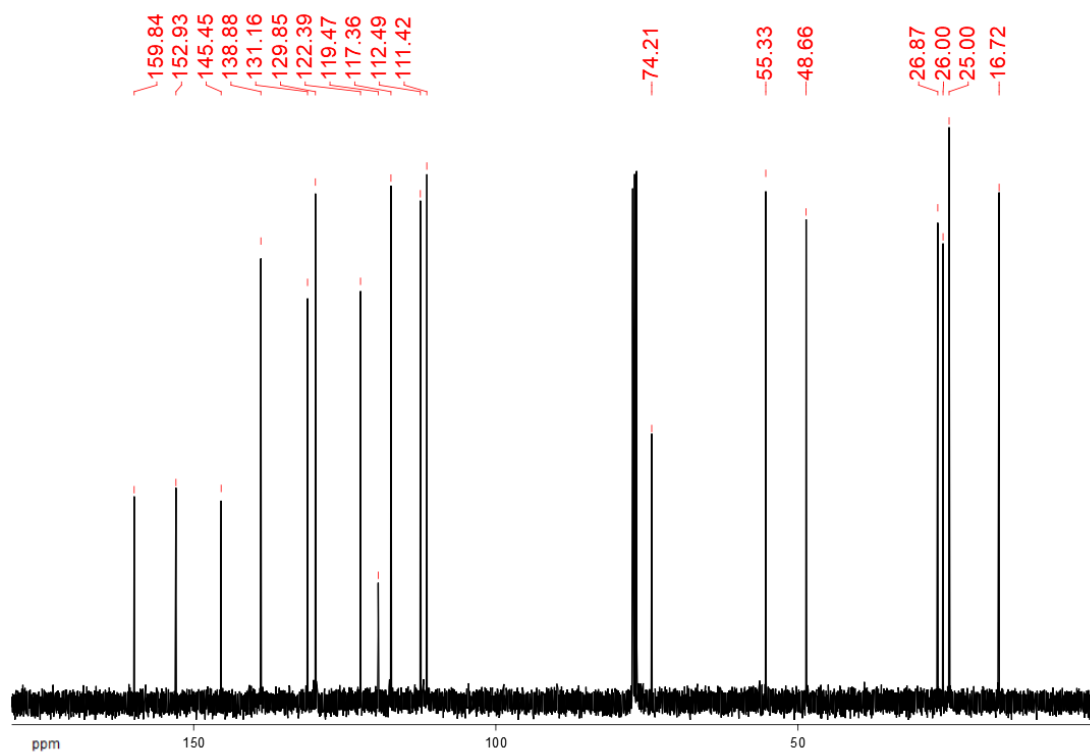
¹³C NMR Compound **88j**.



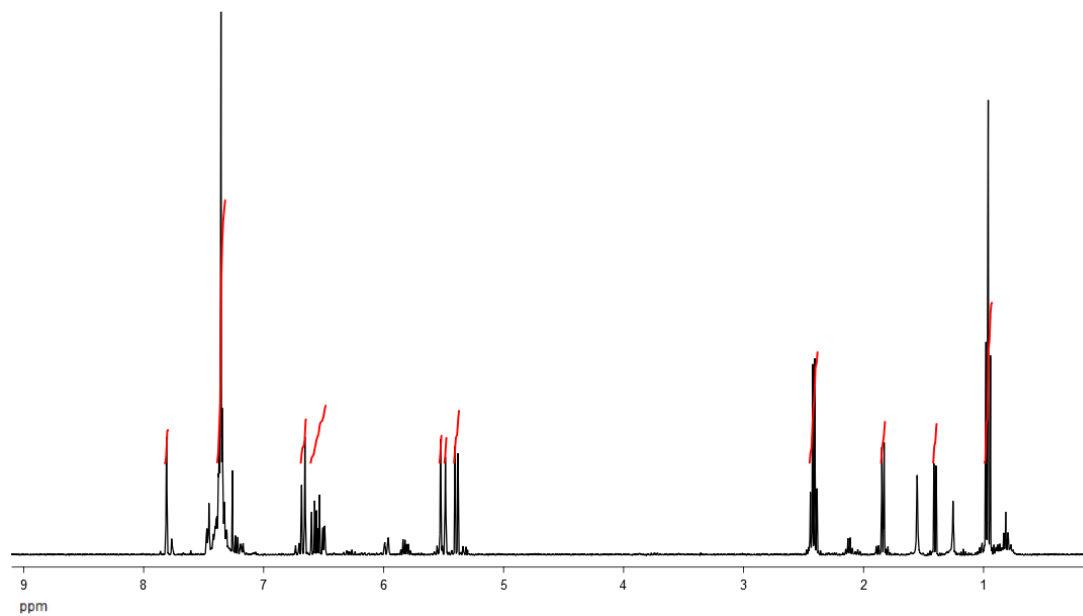
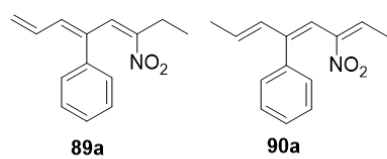
^1H NMR Compound **88k**.



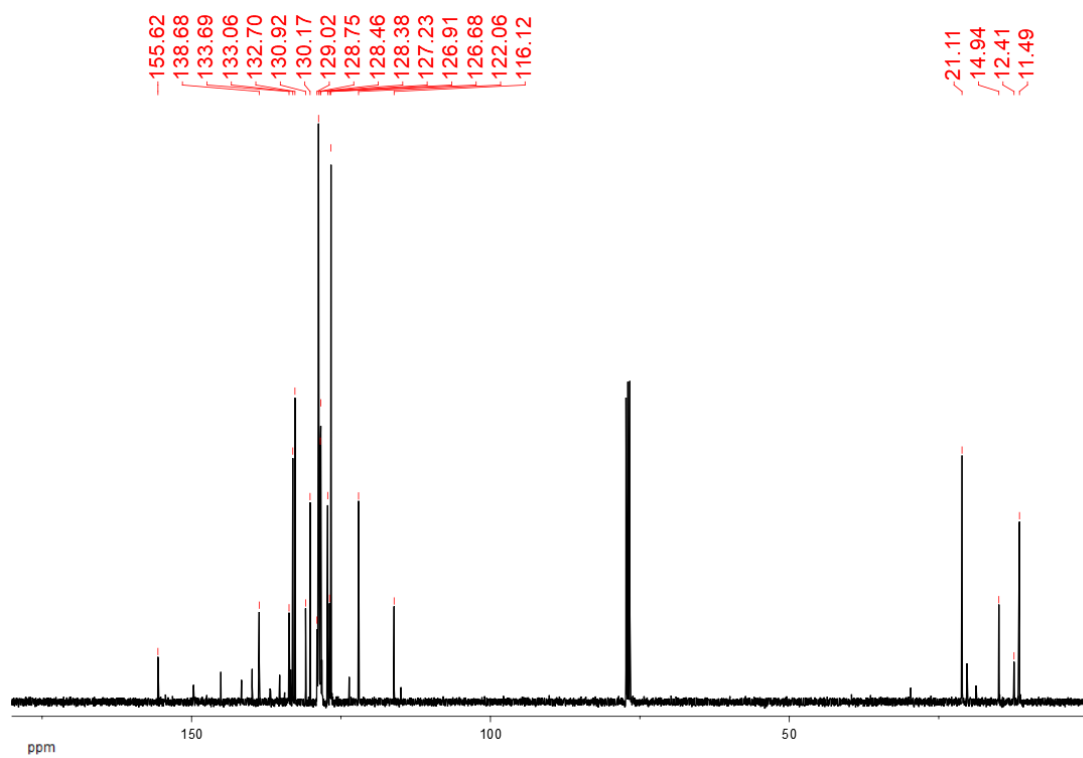
^{13}C NMR Compound **88k**.



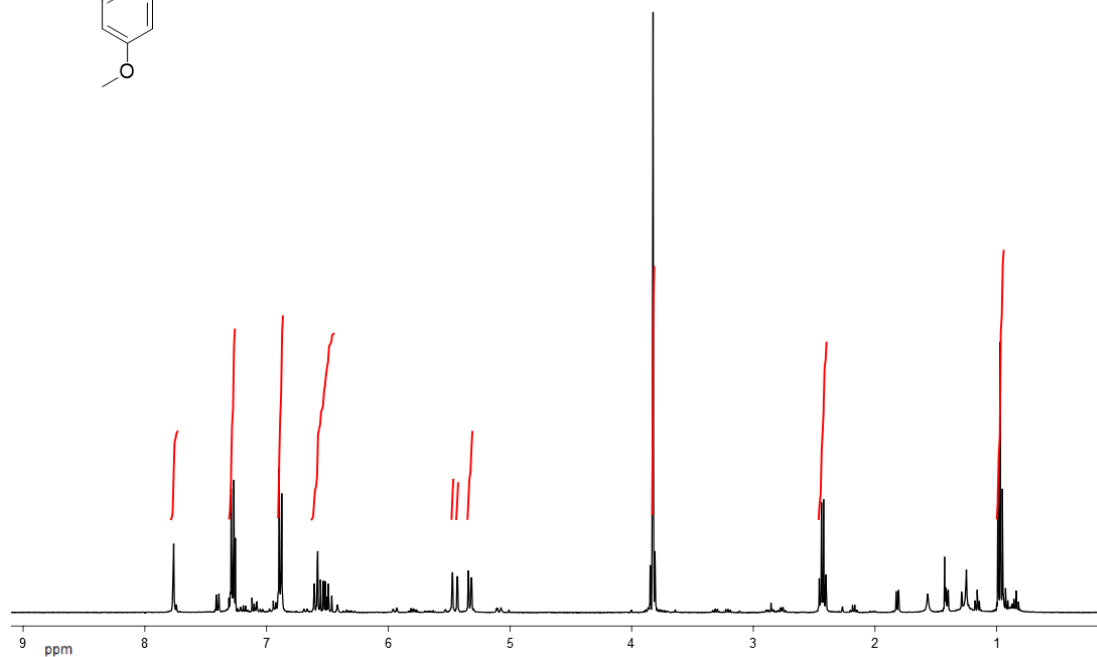
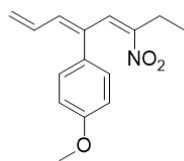
^1H NMR Compounds **89a** and **90a**.



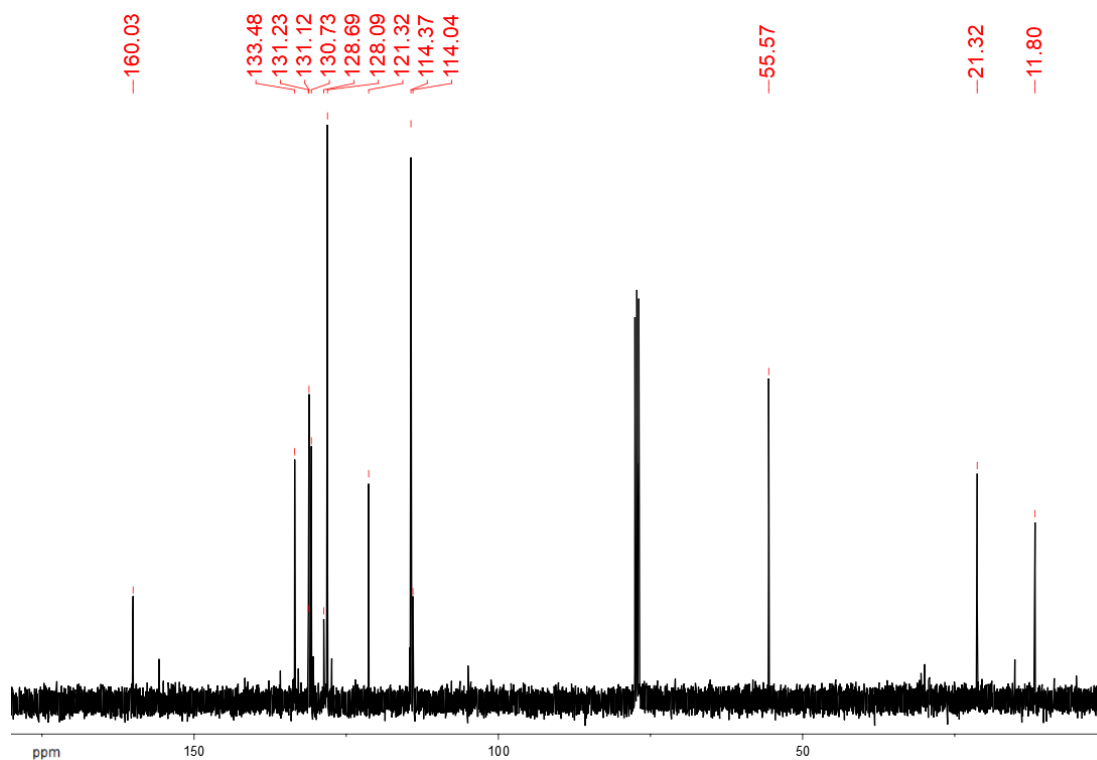
^{13}C NMR Compounds **89a** and **90a**.



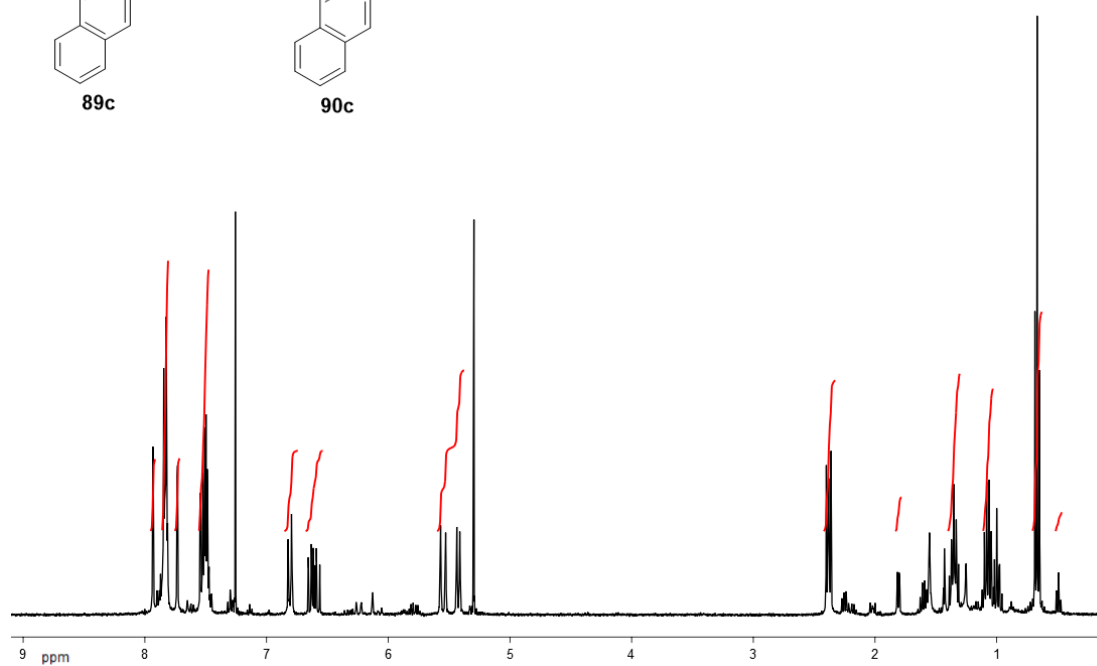
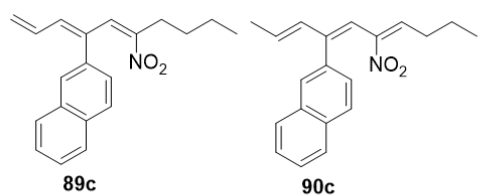
^1H NMR Compound **89b**.



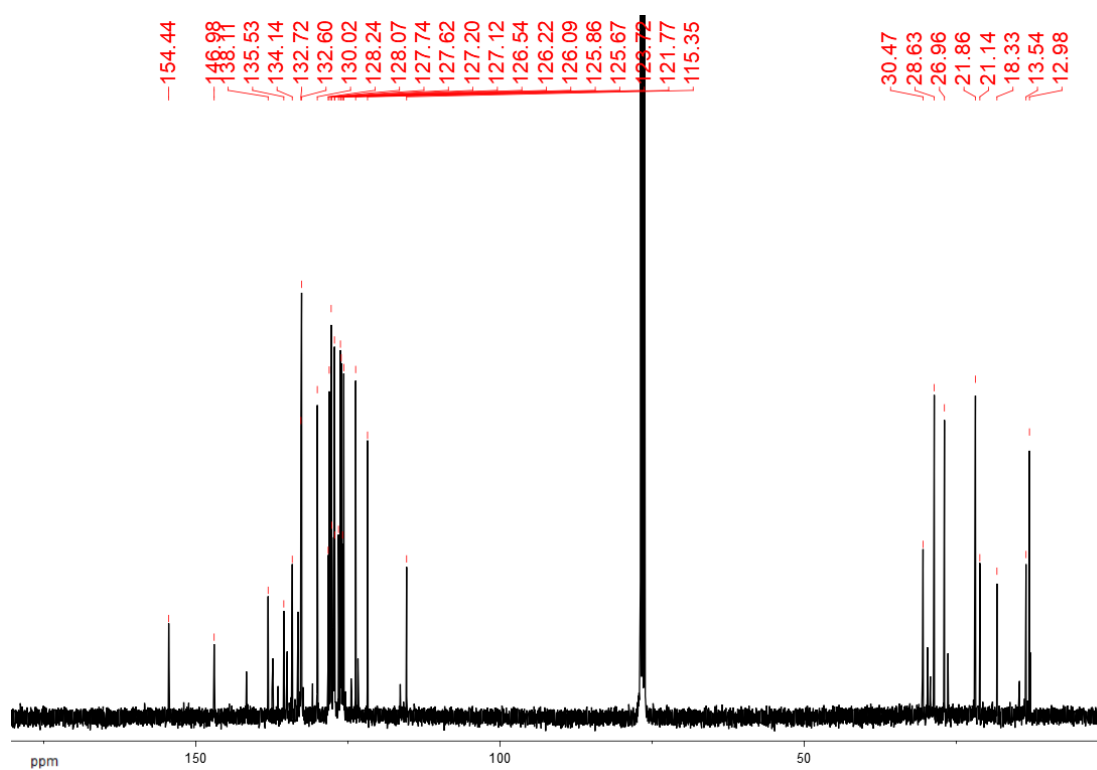
^{13}C NMR Compound **89b**.



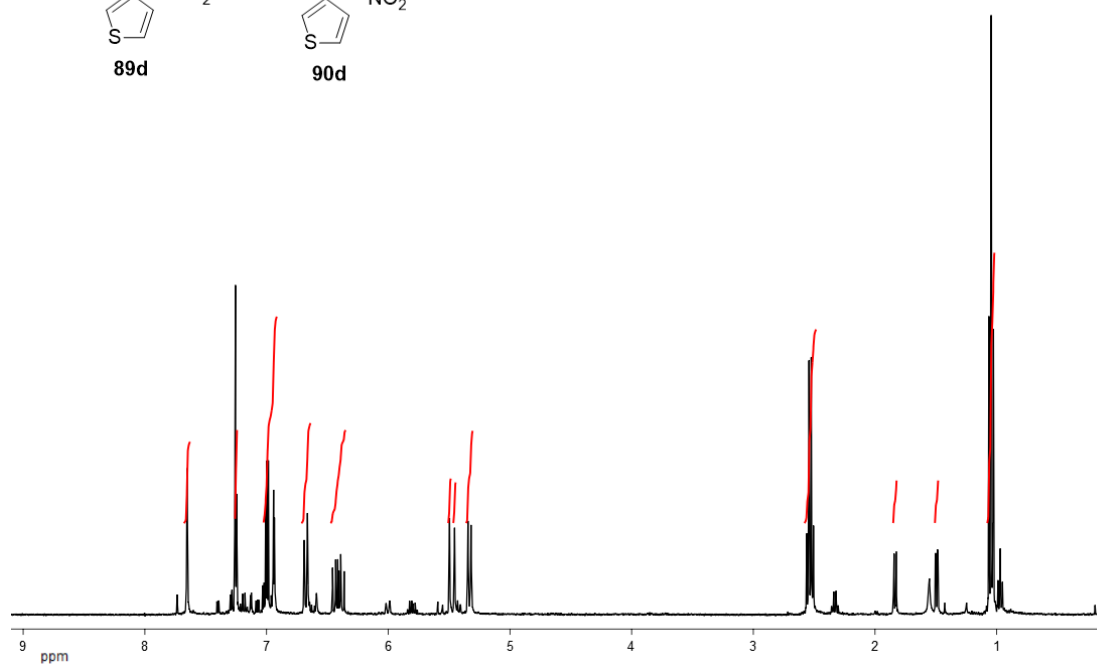
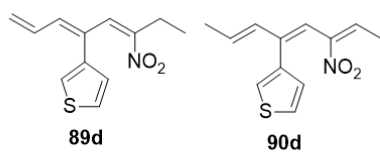
^1H NMR Compounds **89c** and **90c**.



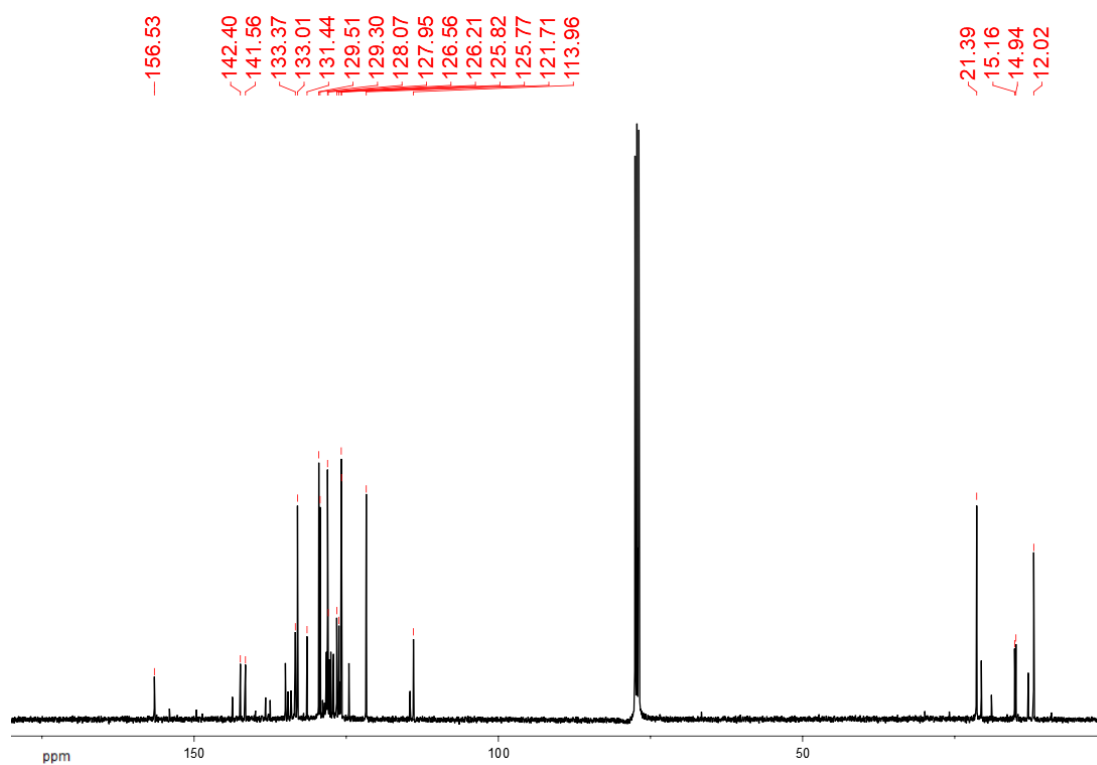
^{13}C NMR Compounds **89c** and **90c**.



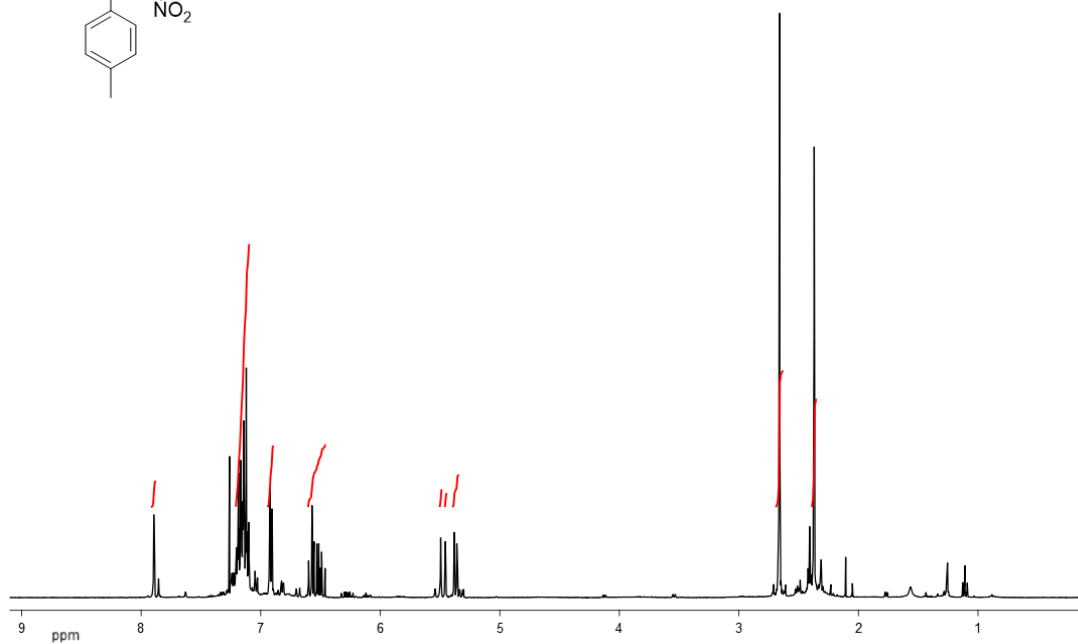
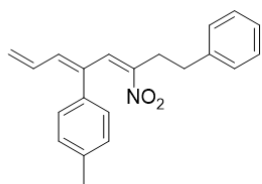
^1H NMR Compounds **89d** and **90d**.



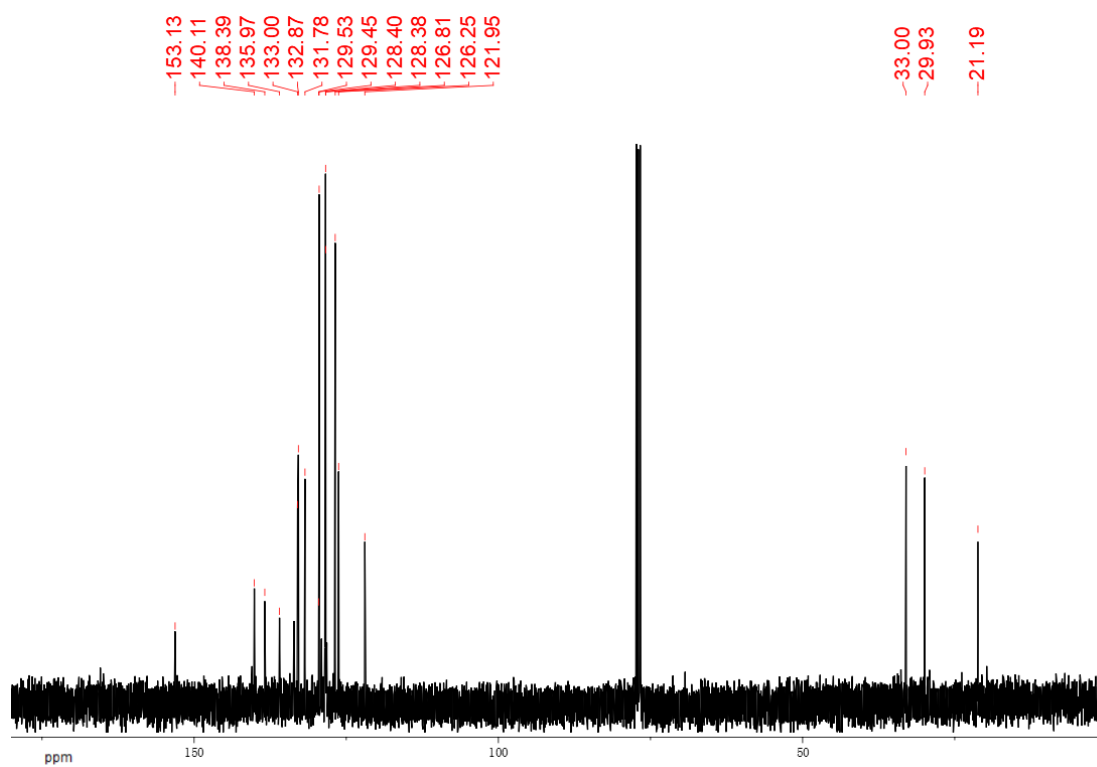
^{13}C NMR Compounds **89d** and **90d**.



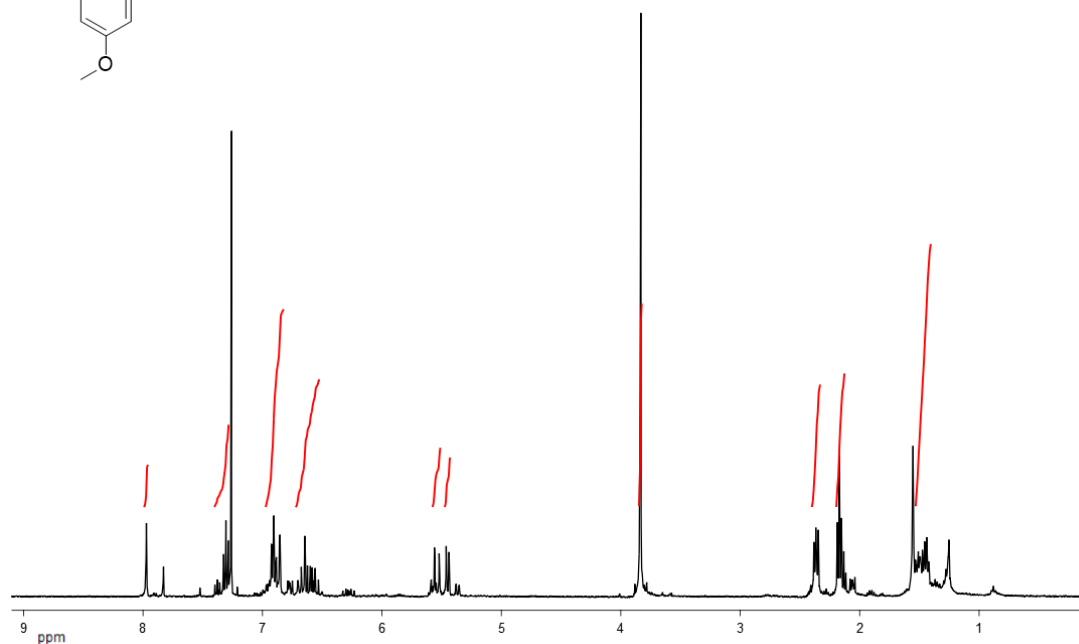
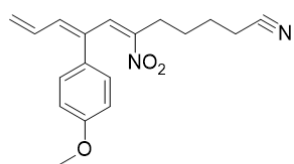
¹H NMR Compound **89e**.



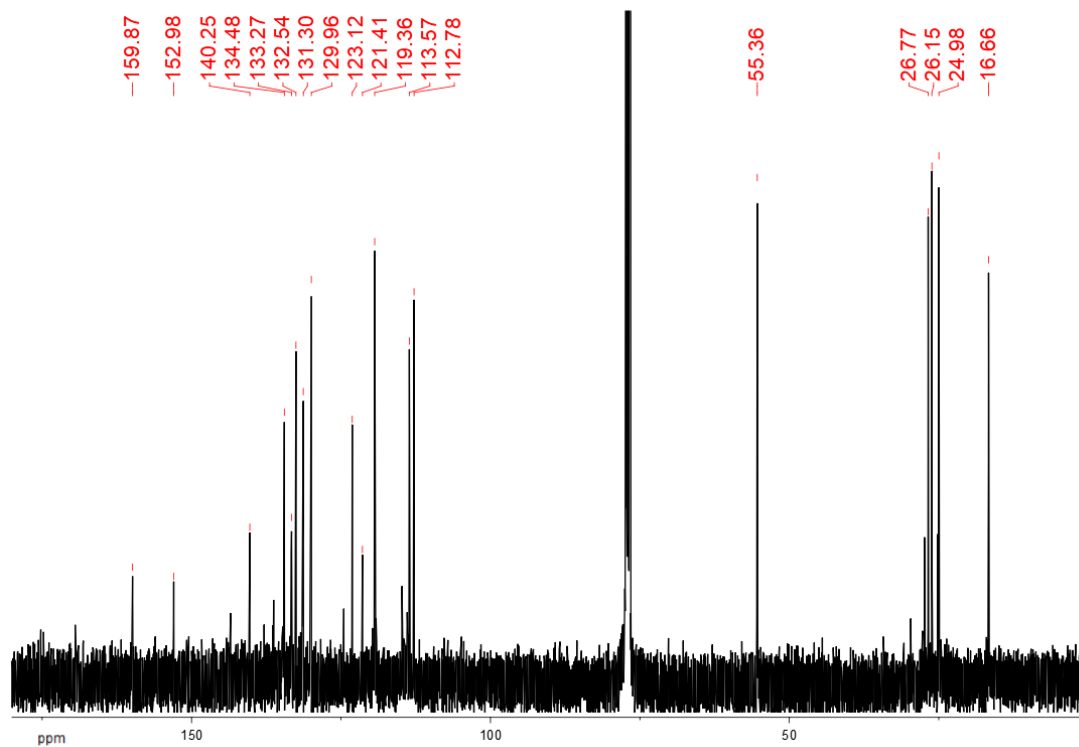
¹³C NMR Compound **89e**.



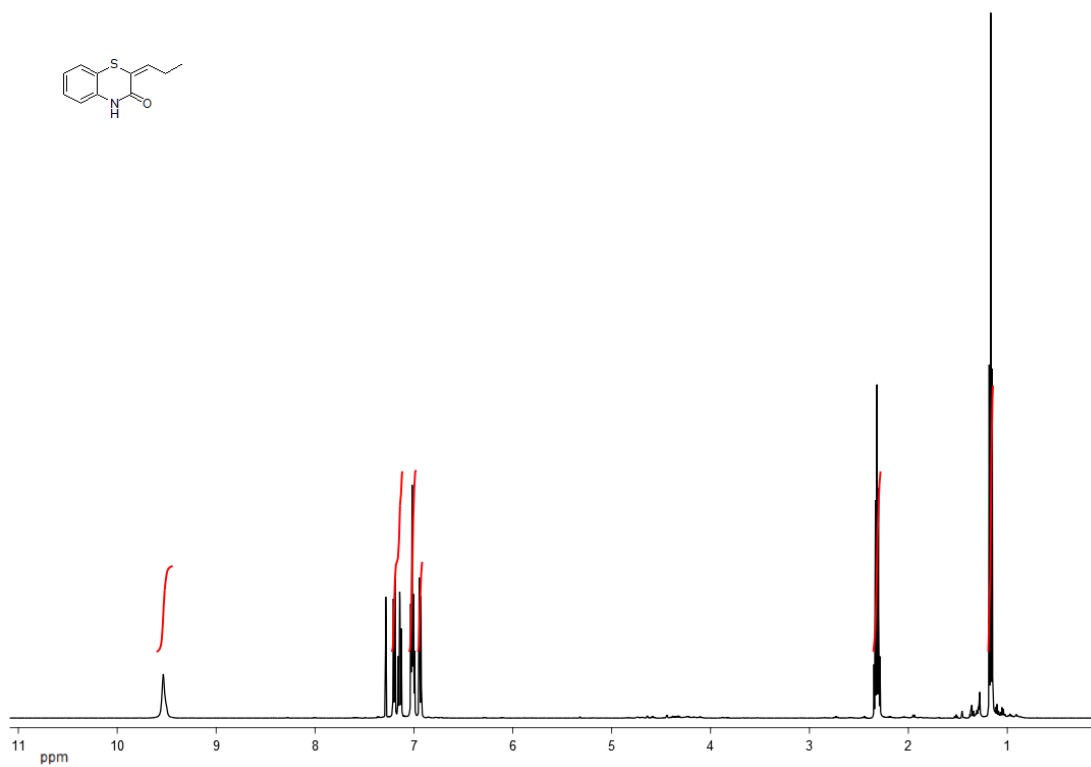
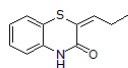
^1H NMR Compound **89f**.



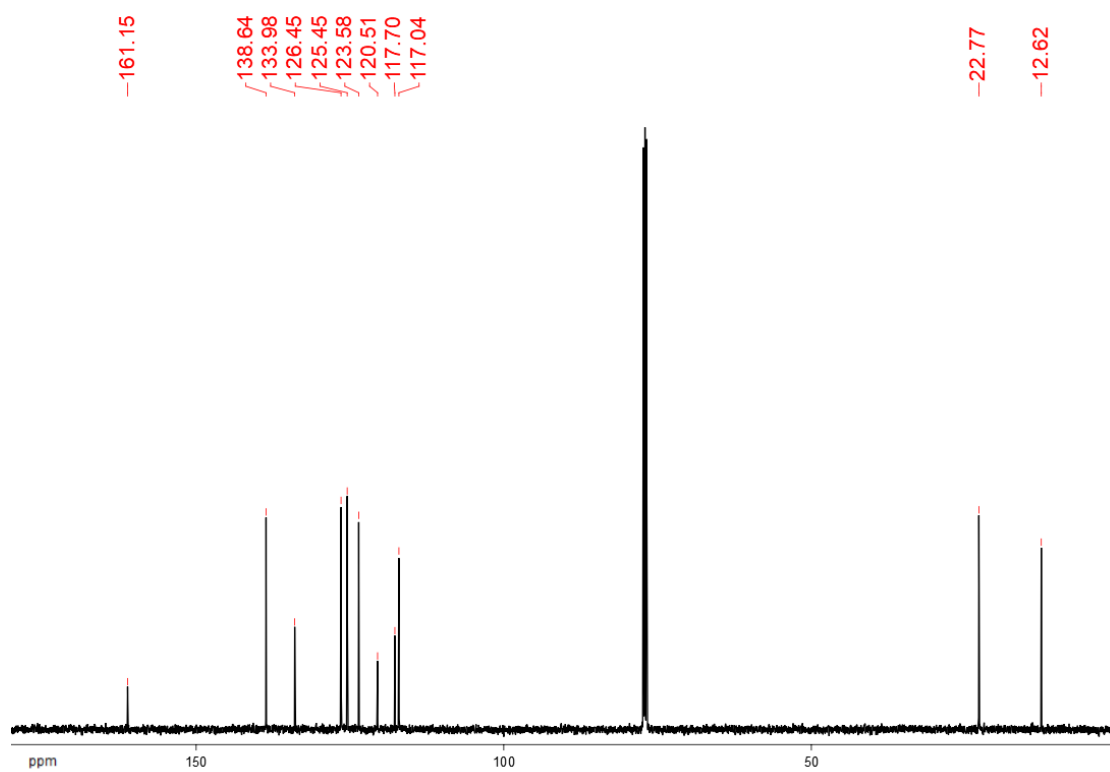
^{13}C NMR Compound **89f**.



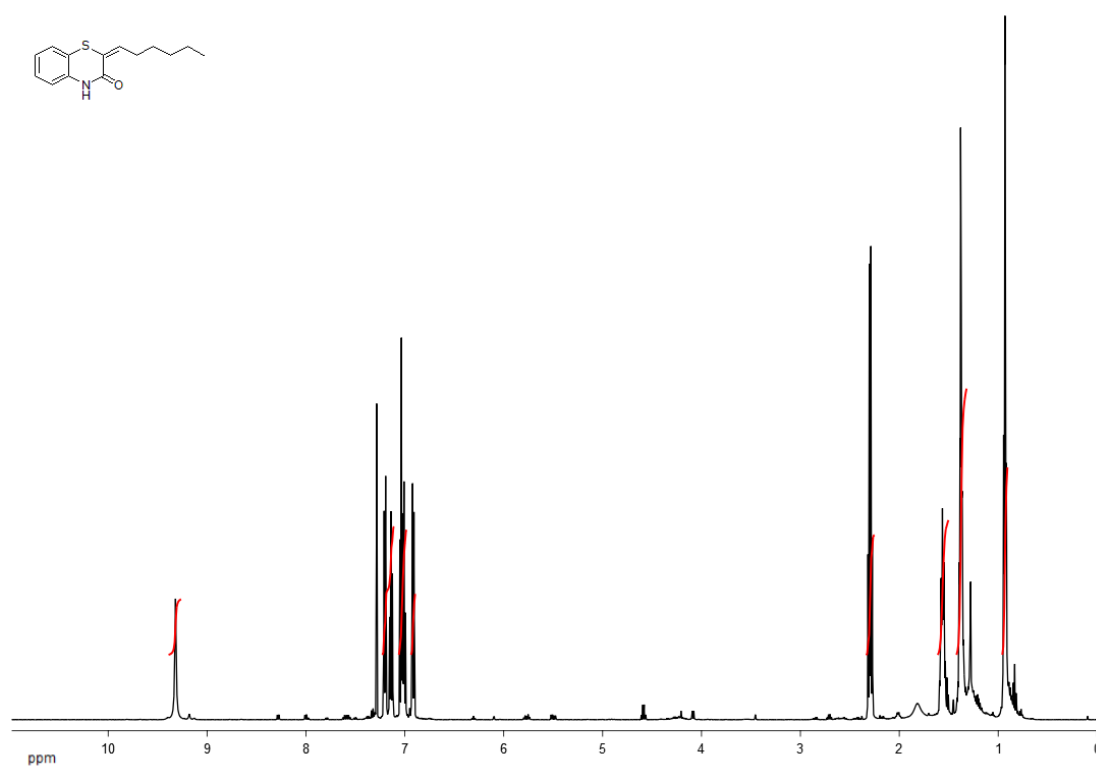
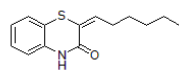
¹H NMR Compound **94a**.



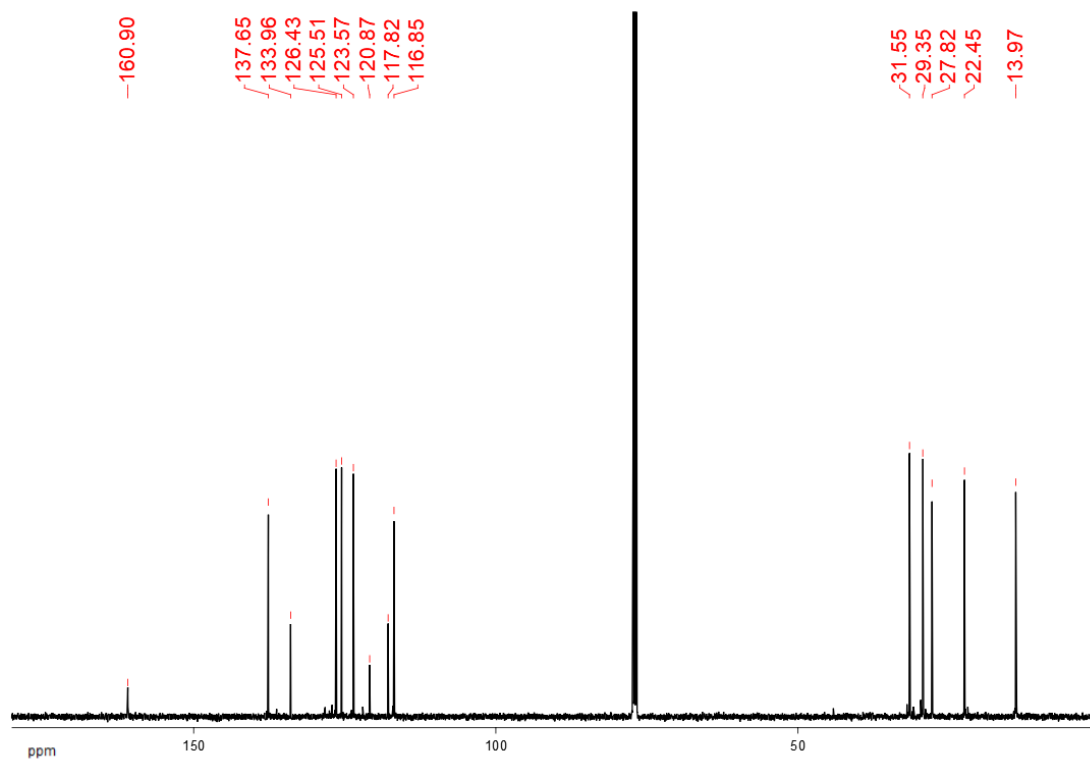
¹³C NMR Compound **94a**.



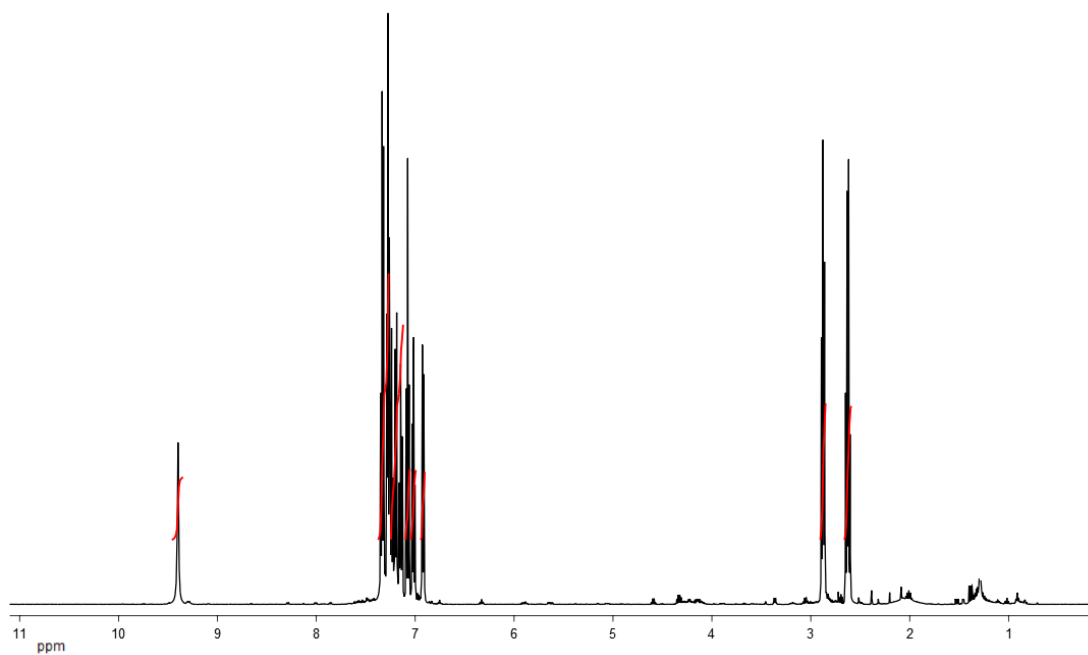
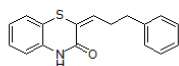
^1H NMR Compound **94b**.



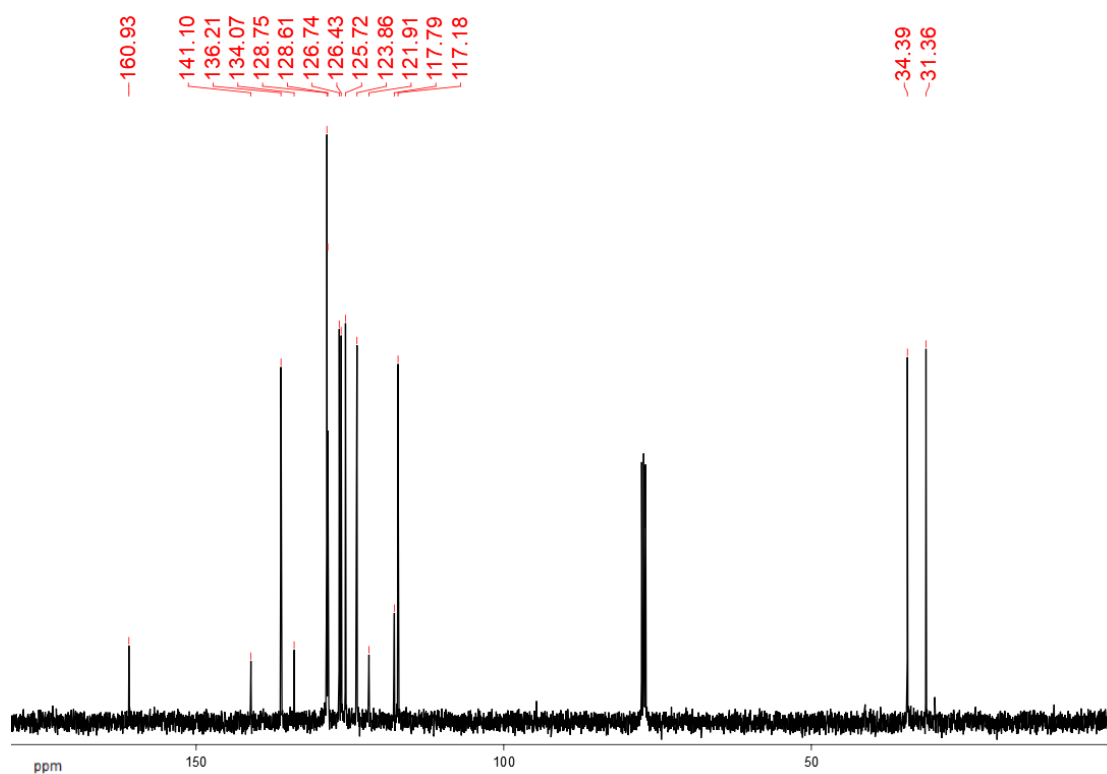
^{13}C NMR Compound **94b**.



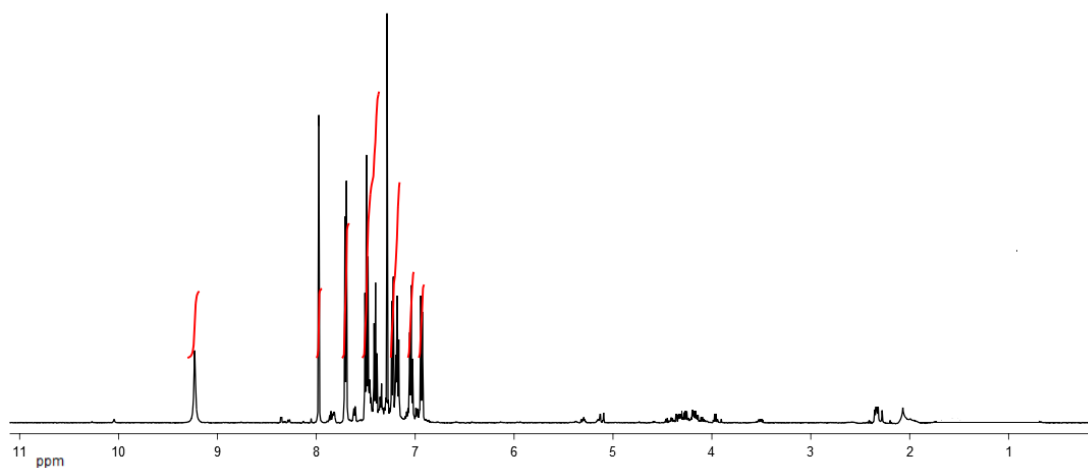
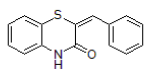
¹H NMR Compound **94c**.



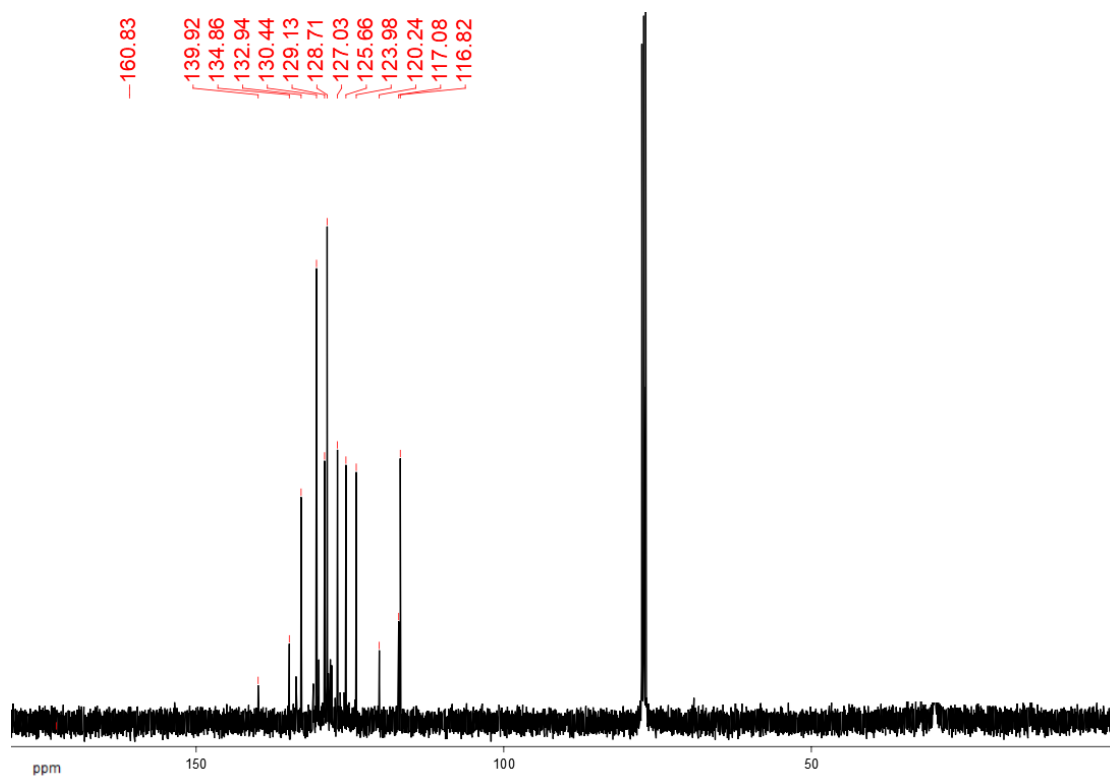
¹³C NMR Compound **94c**.



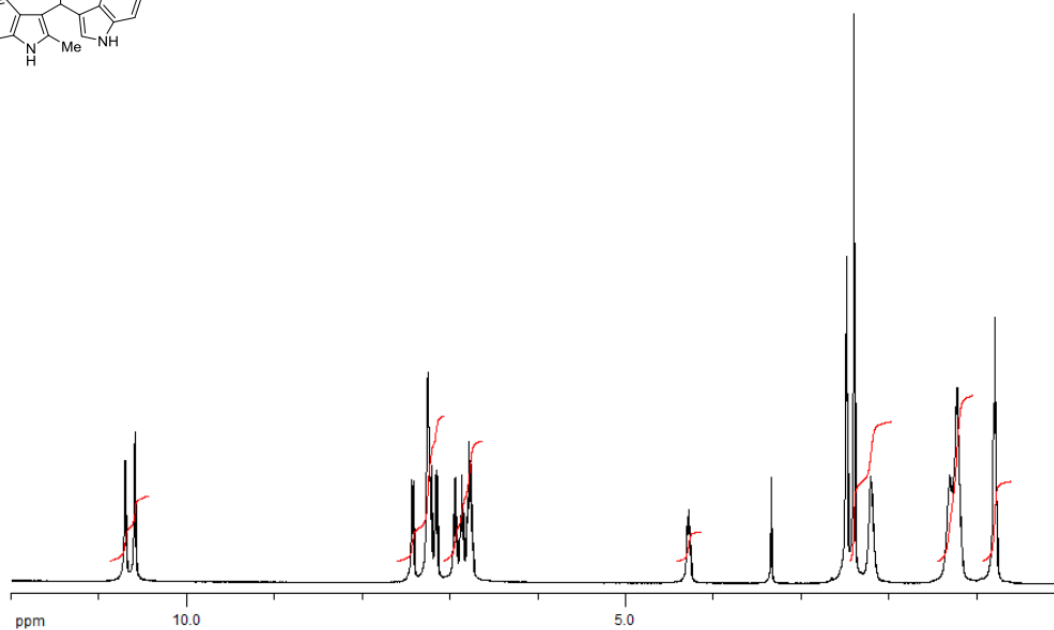
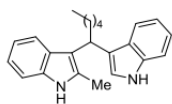
¹H NMR Compound **94d**.



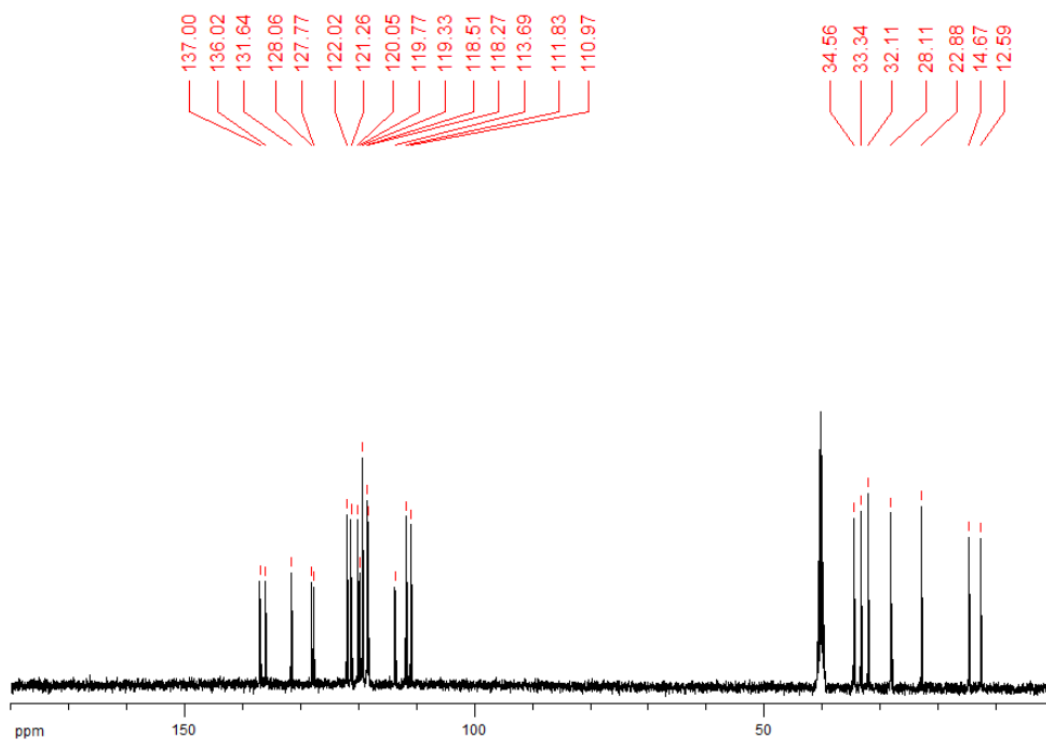
¹³C NMR Compound **94d**



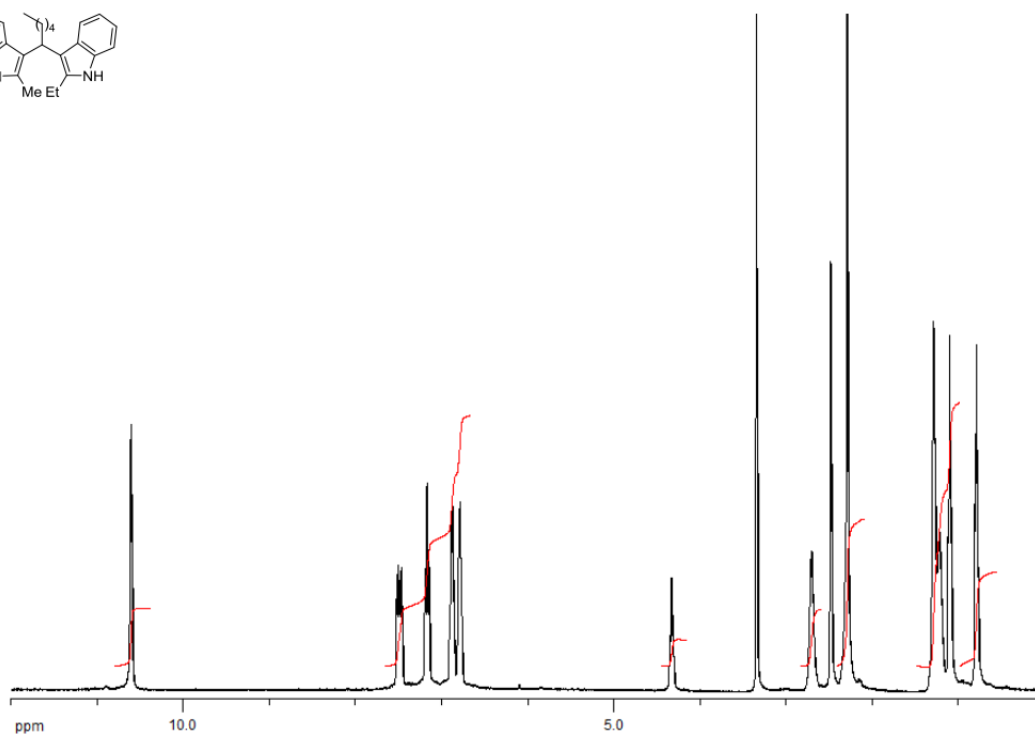
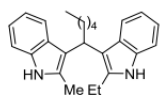
¹H NMR Compound **138a**.



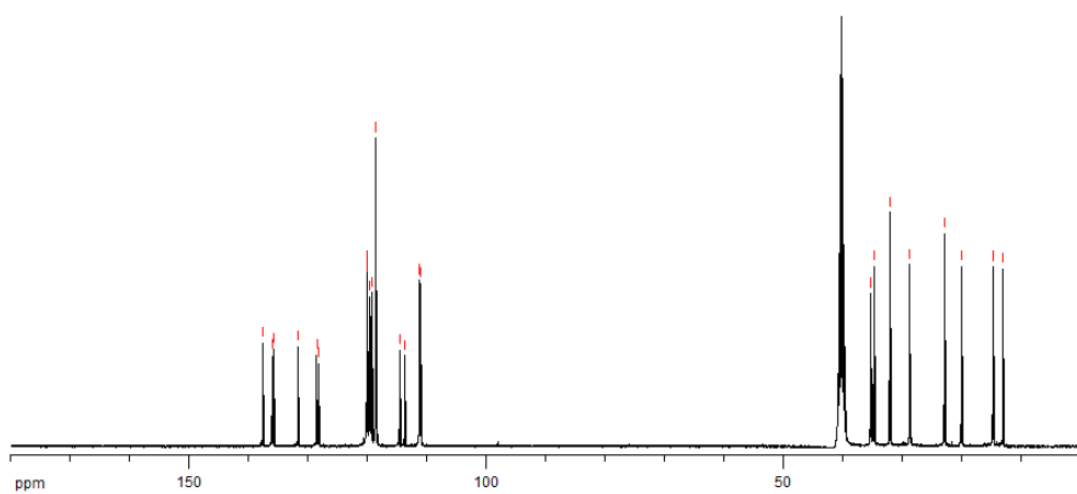
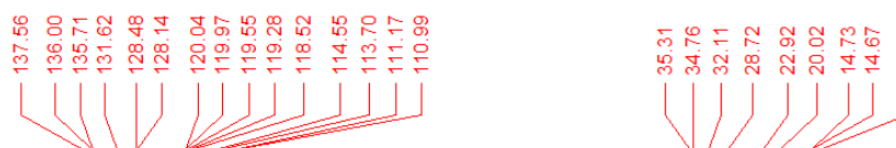
¹³C NMR Compound **138a**.



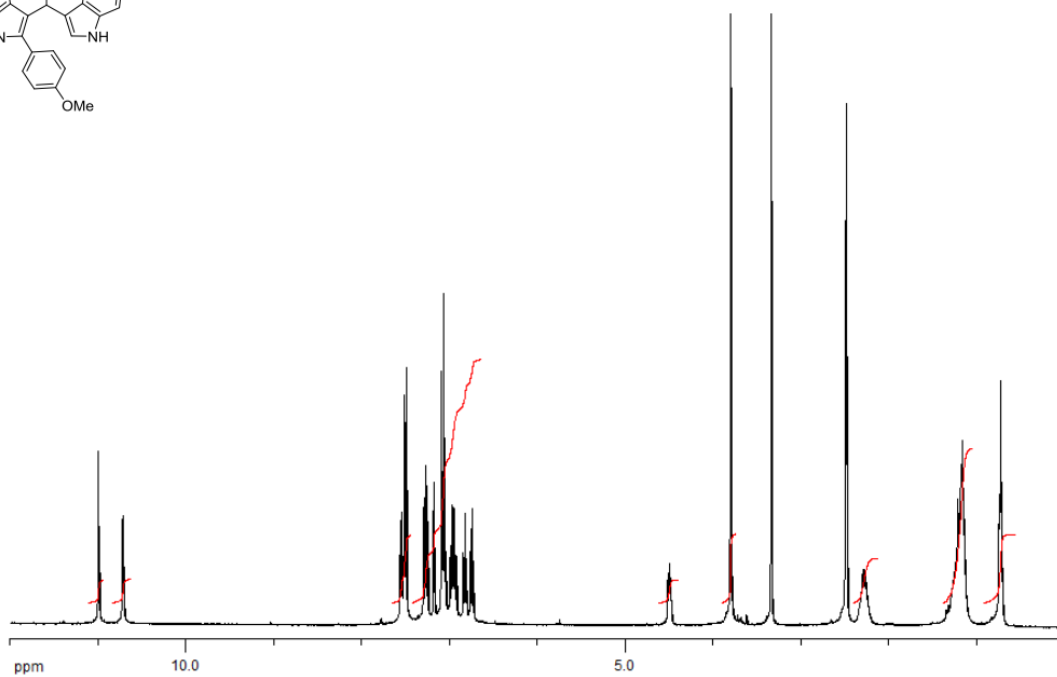
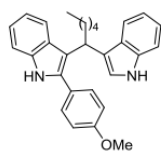
^1H NMR Compound **138b**.



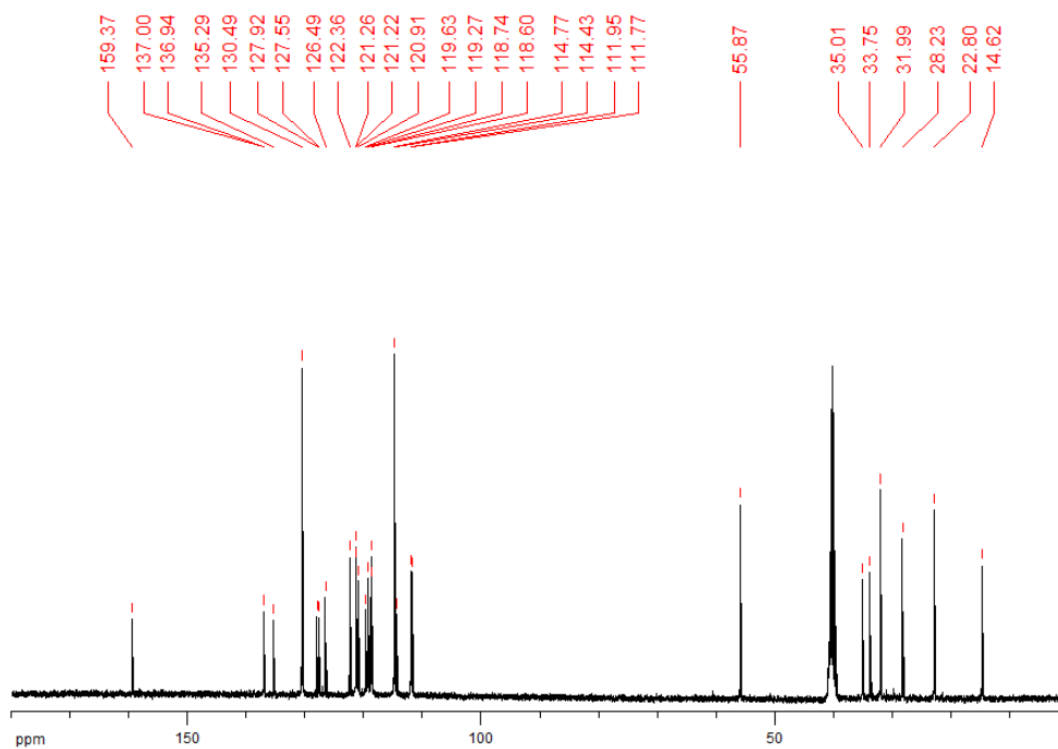
^{13}C NMR Compound **138b**.



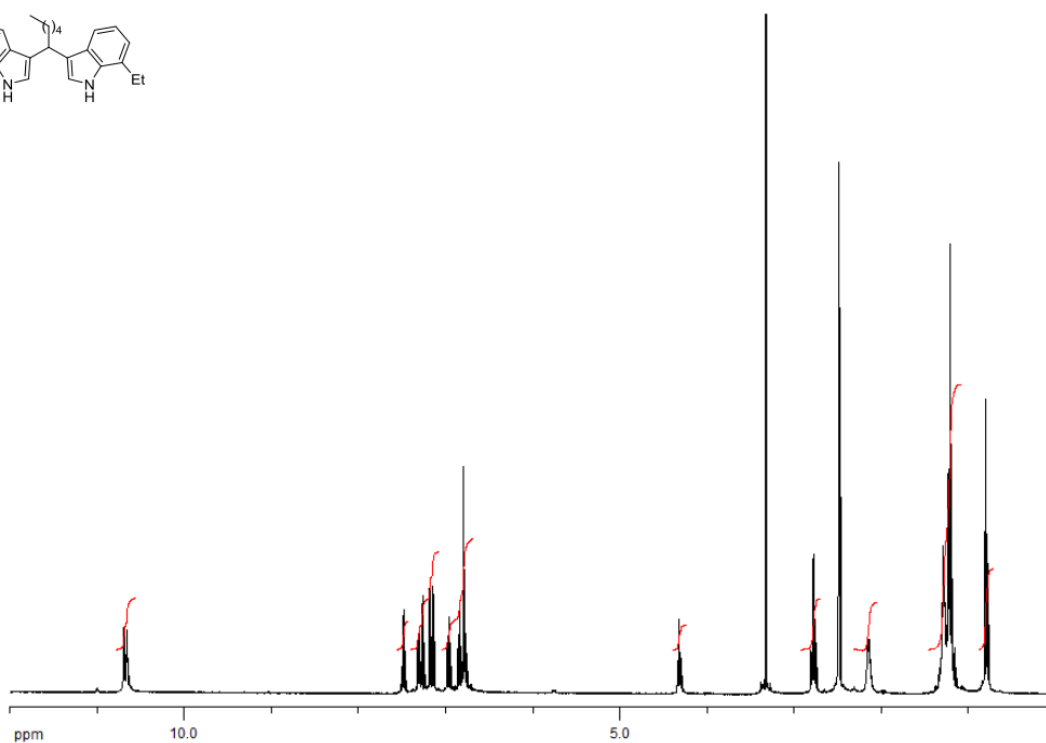
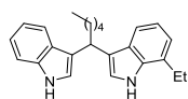
¹H NMR Compound **138c**.



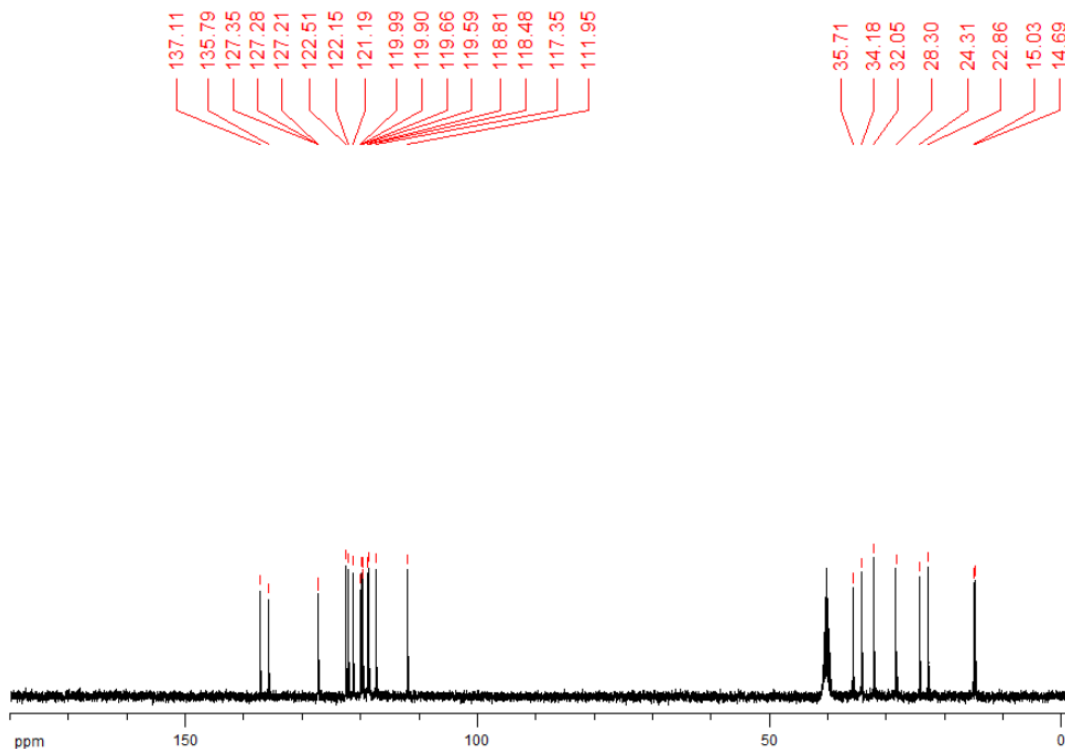
¹³C NMR Compound **138c**.



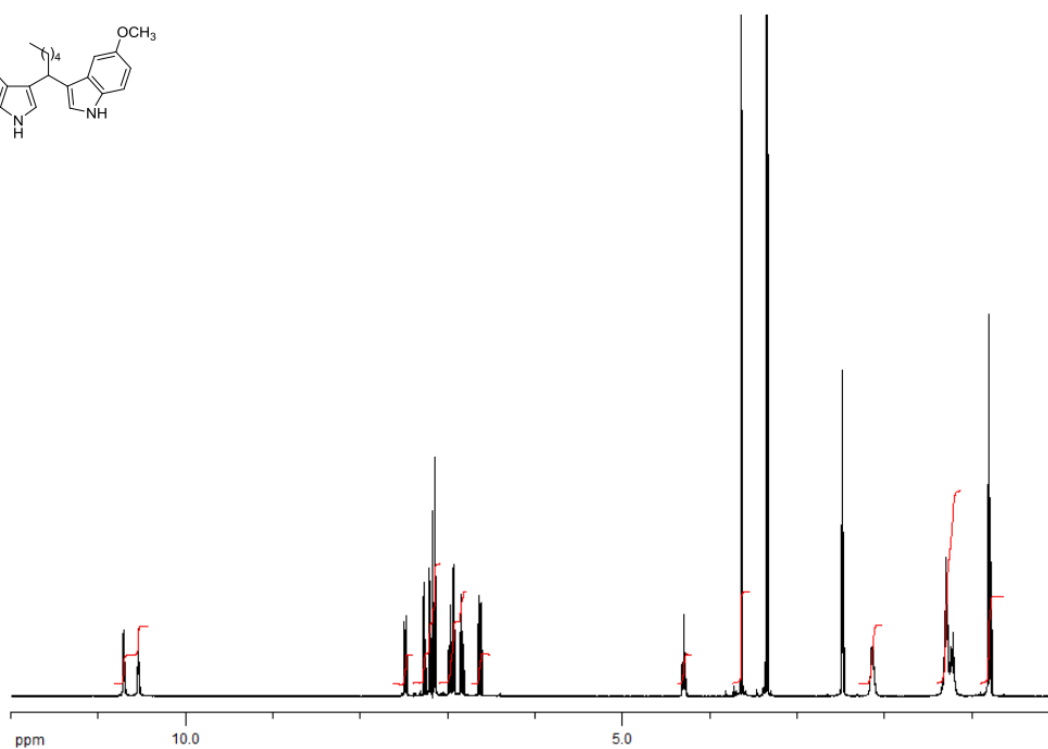
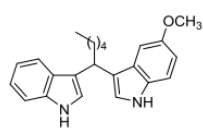
¹H NMR Compound **138d**.



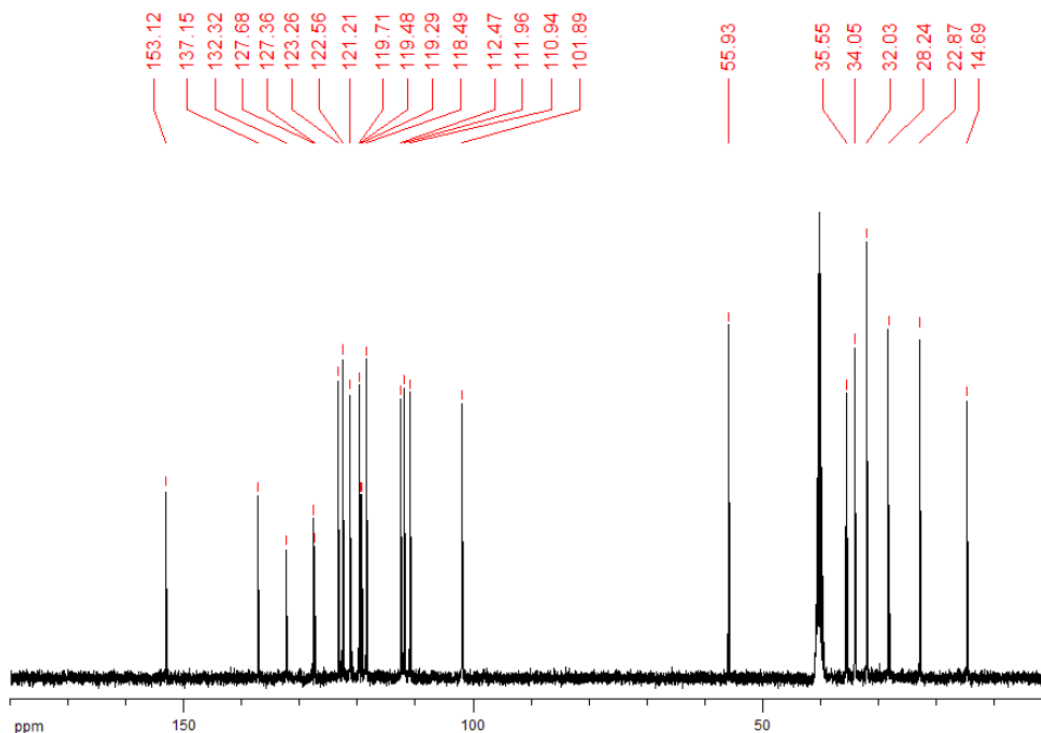
¹³C NMR Compound **138d**.



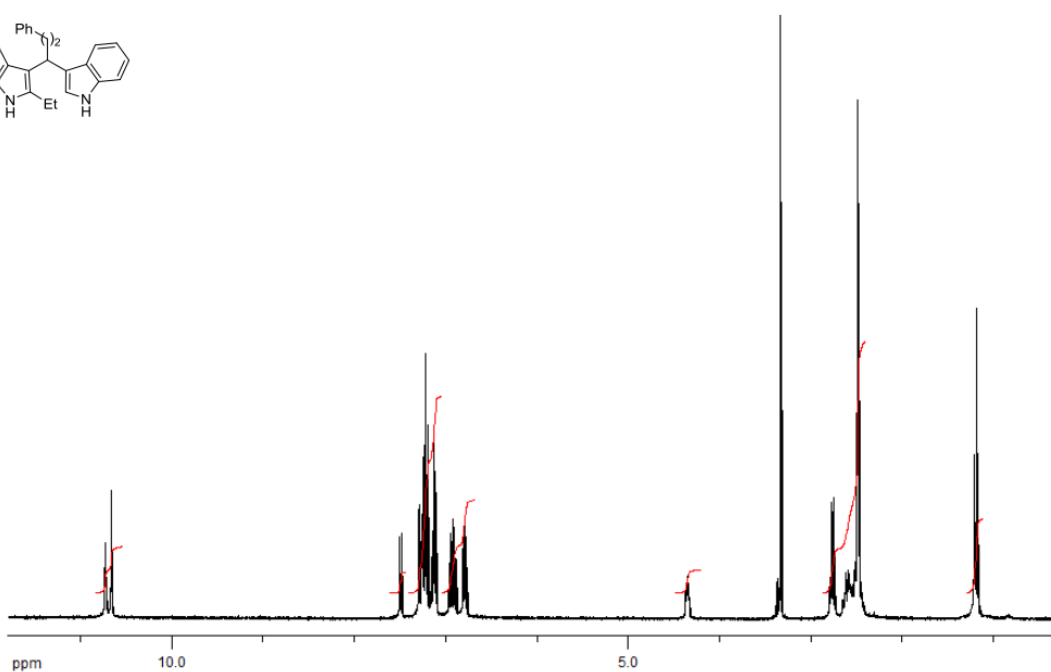
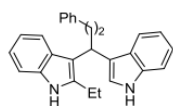
¹H NMR Compound **138e**.



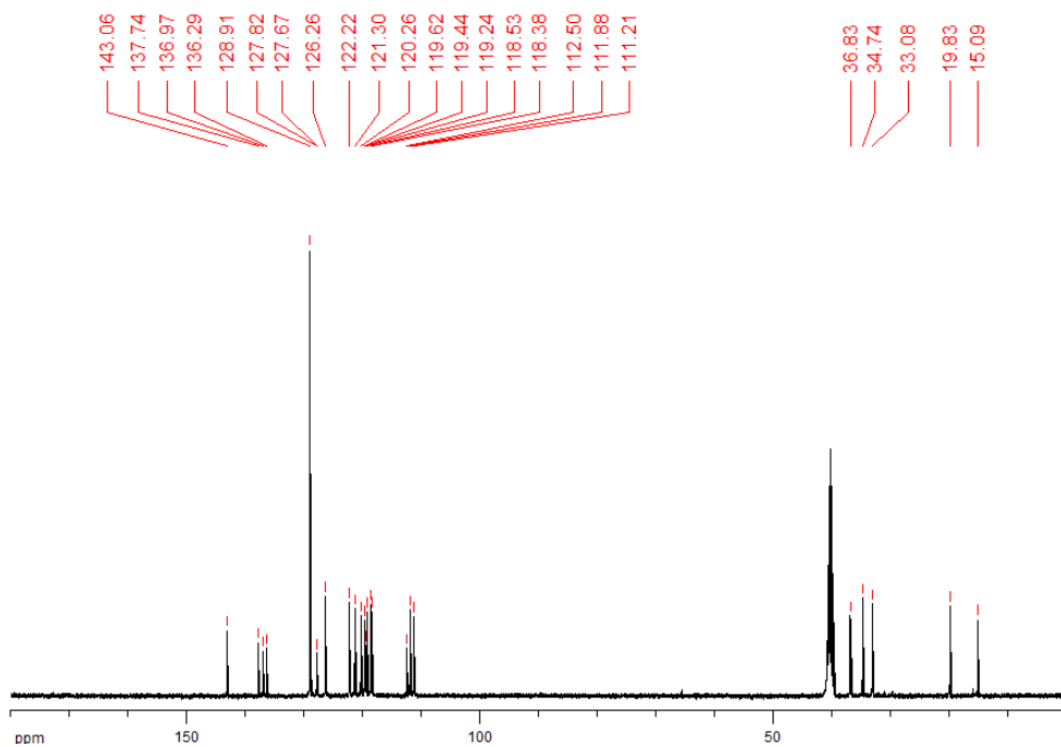
¹³C NMR Compound **138e**.



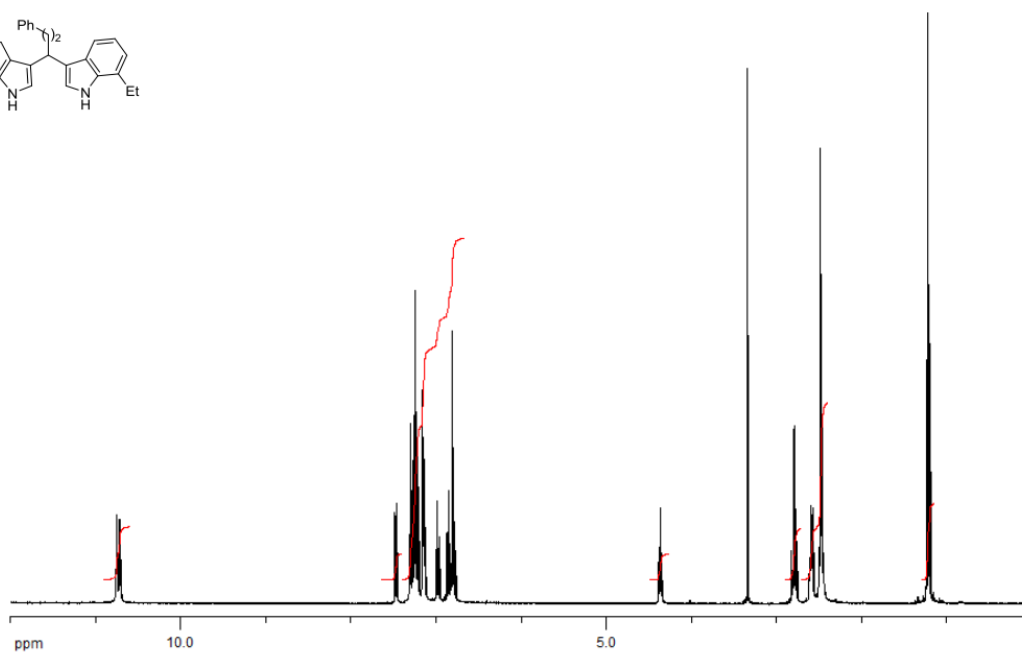
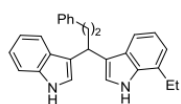
¹H NMR Compound **138f**.



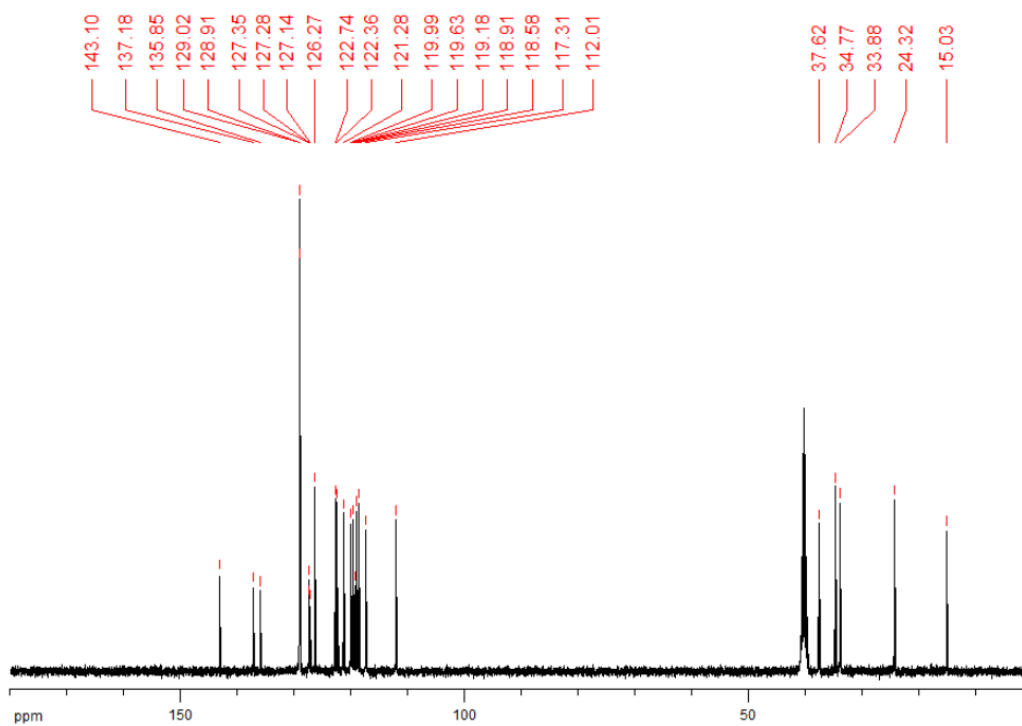
¹³C NMR Compound **138f**.



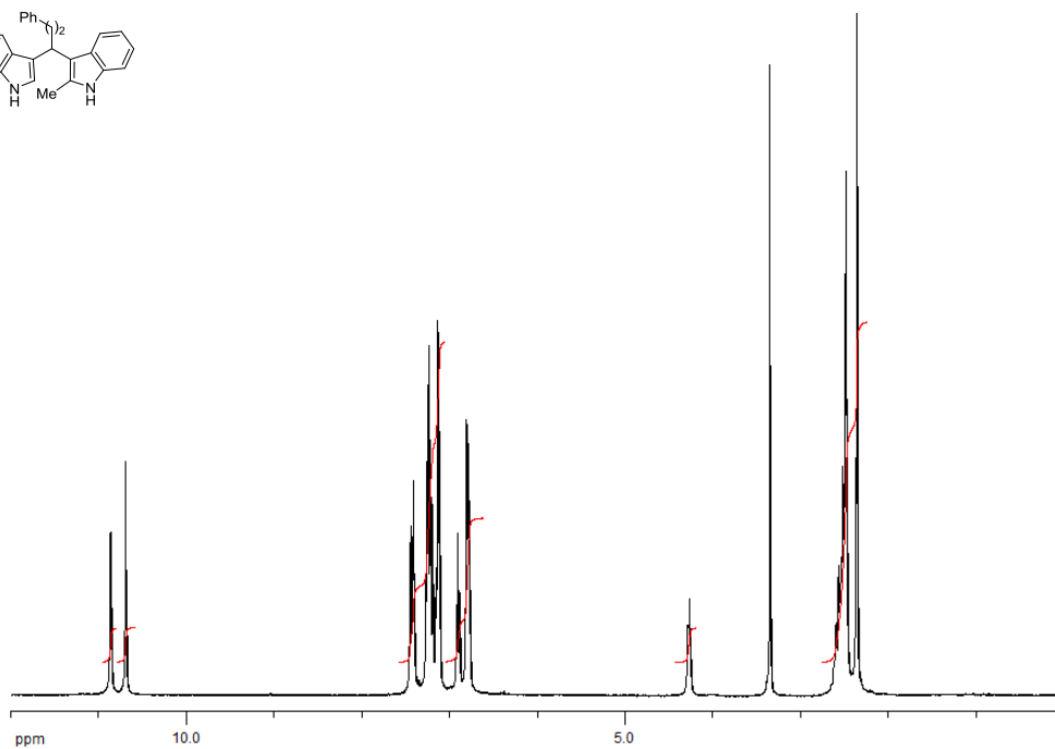
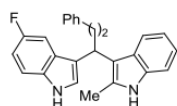
¹H NMR Compound **138g**.



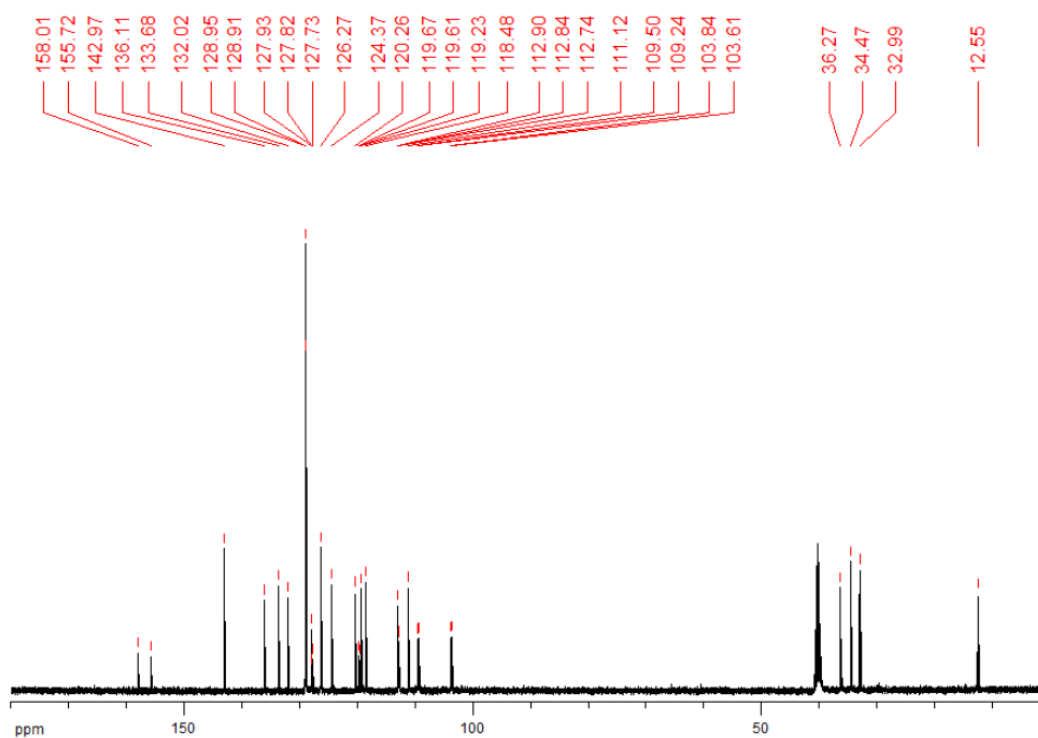
¹³C NMR Compound **138g**.



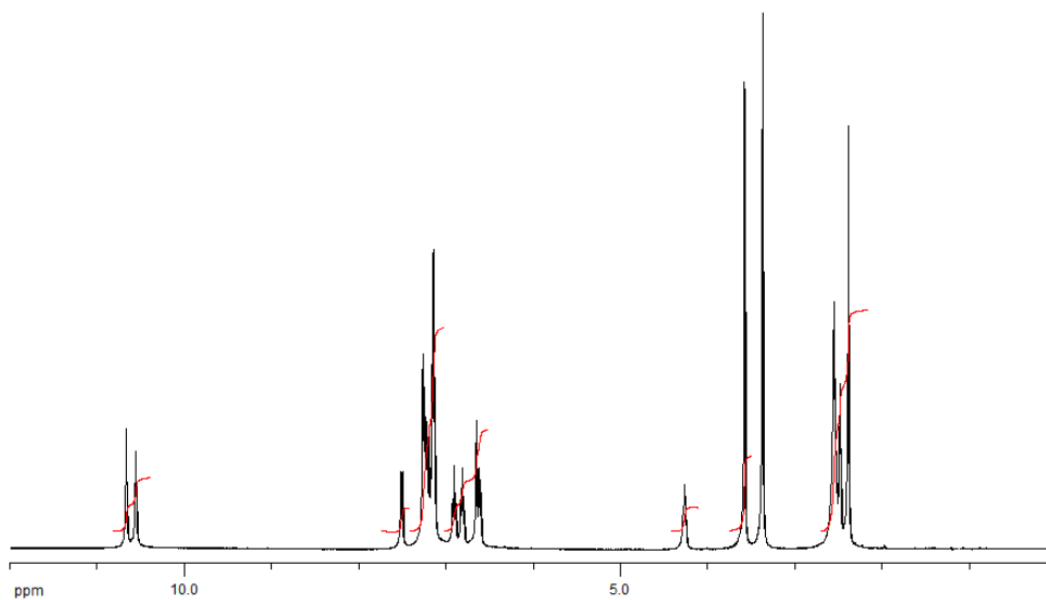
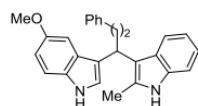
¹H NMR Compound **138h**.



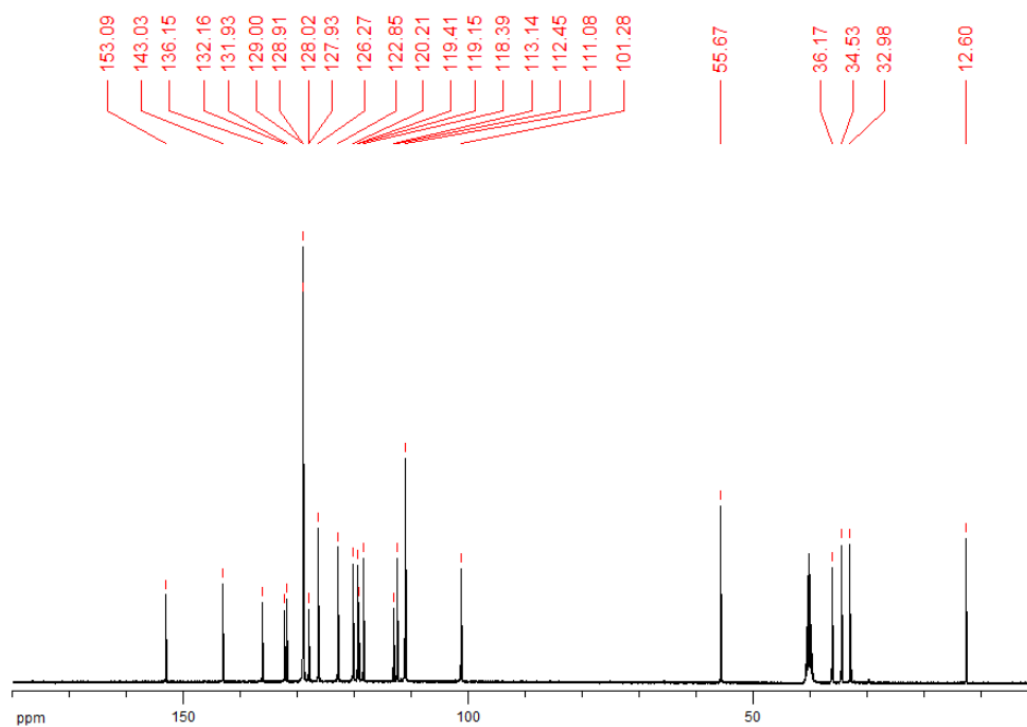
¹³C NMR Compound **138h**.



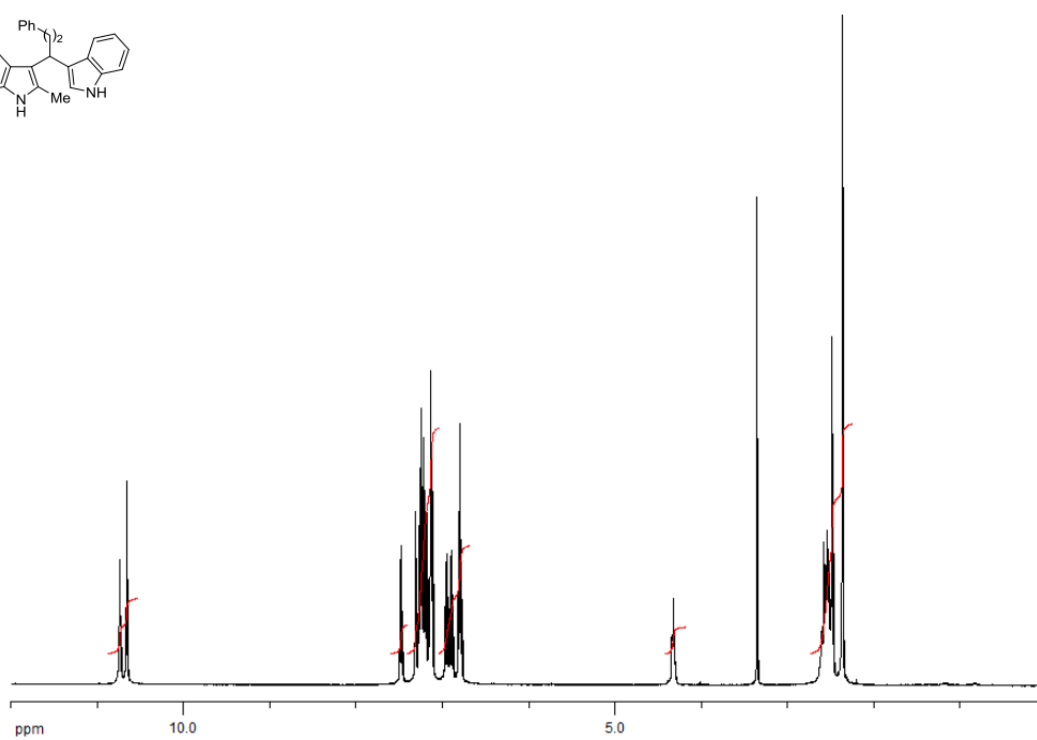
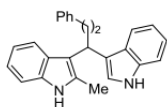
¹H NMR Compound **138i**.



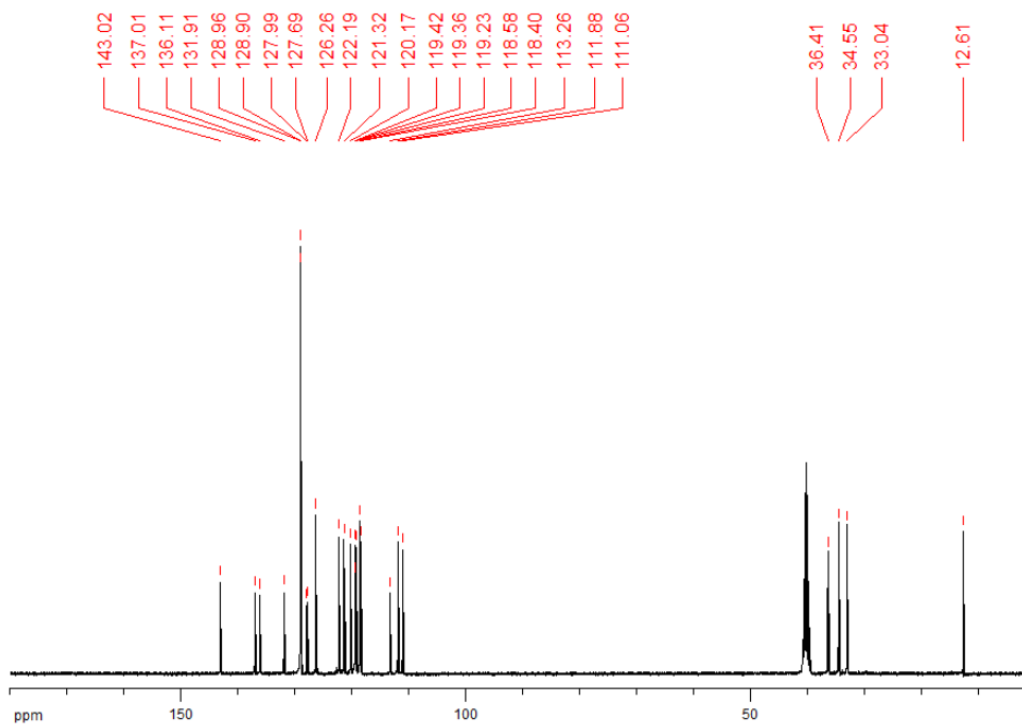
¹³C NMR Compound **138i**.



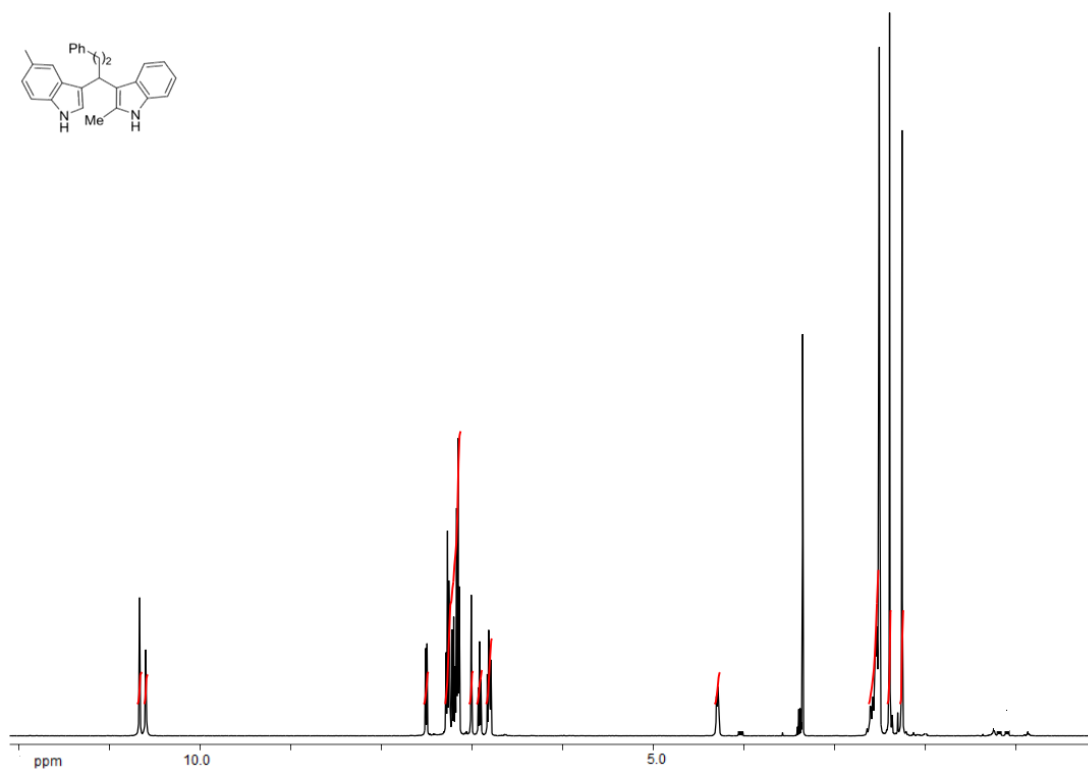
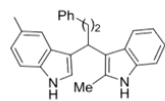
¹H NMR Compound **138j**.



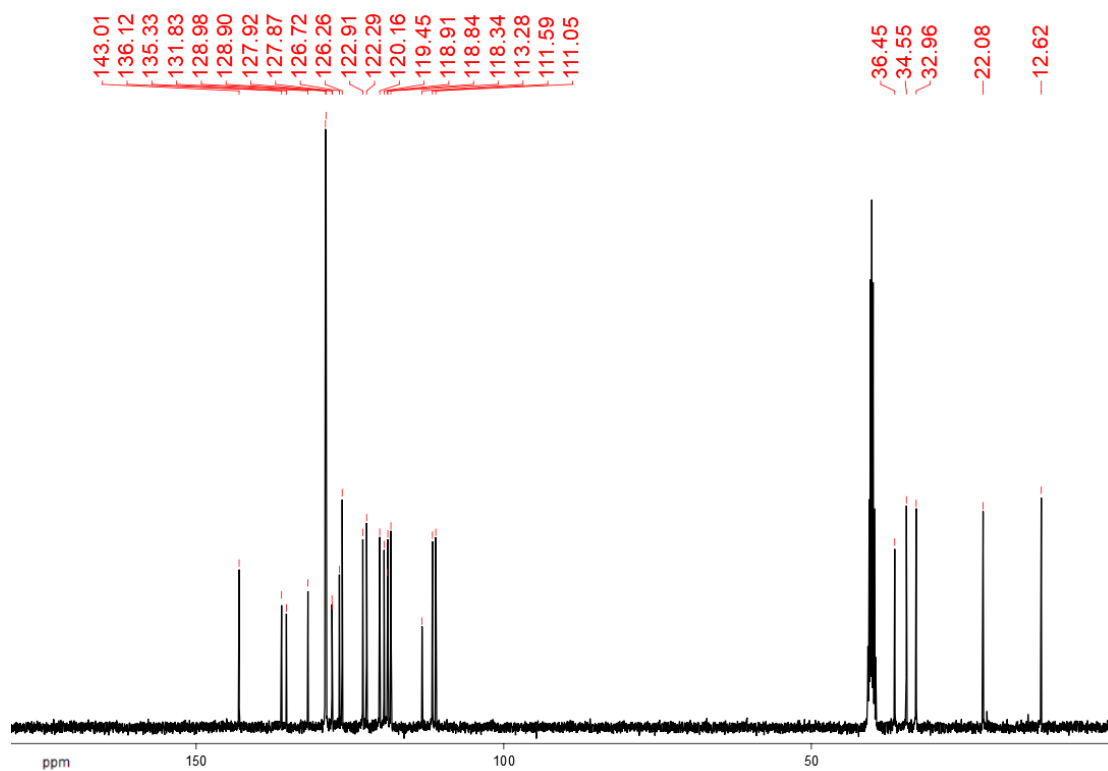
¹³C NMR Compound **138j**.



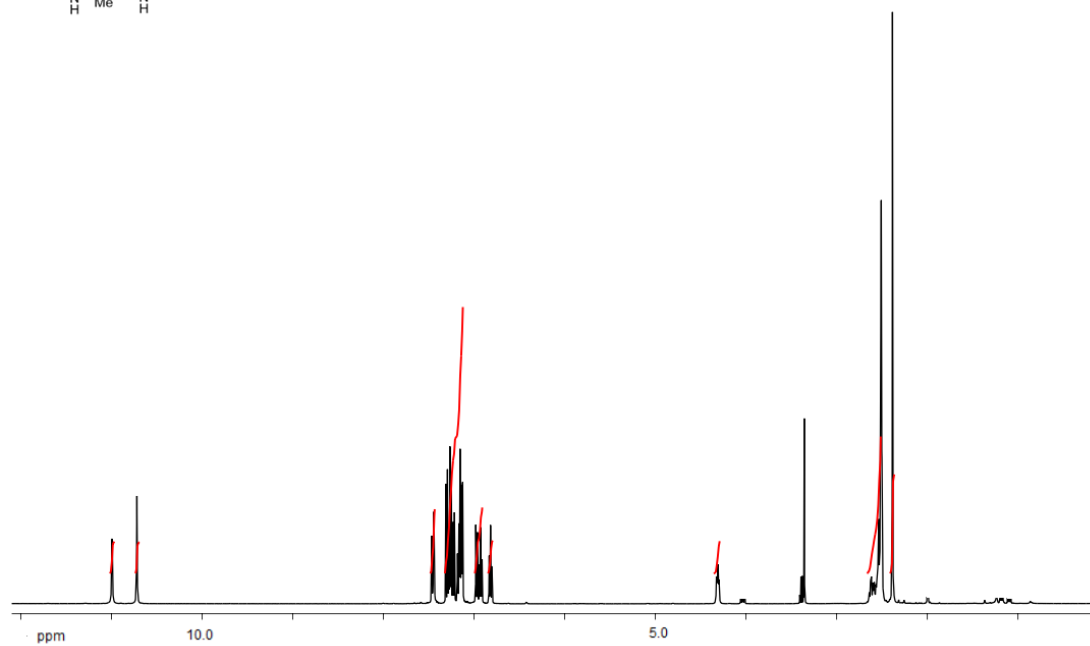
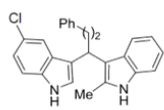
¹H NMR Compound **138k**.



¹³C NMR Compound **138k**.



¹H NMR Compound **138I**.

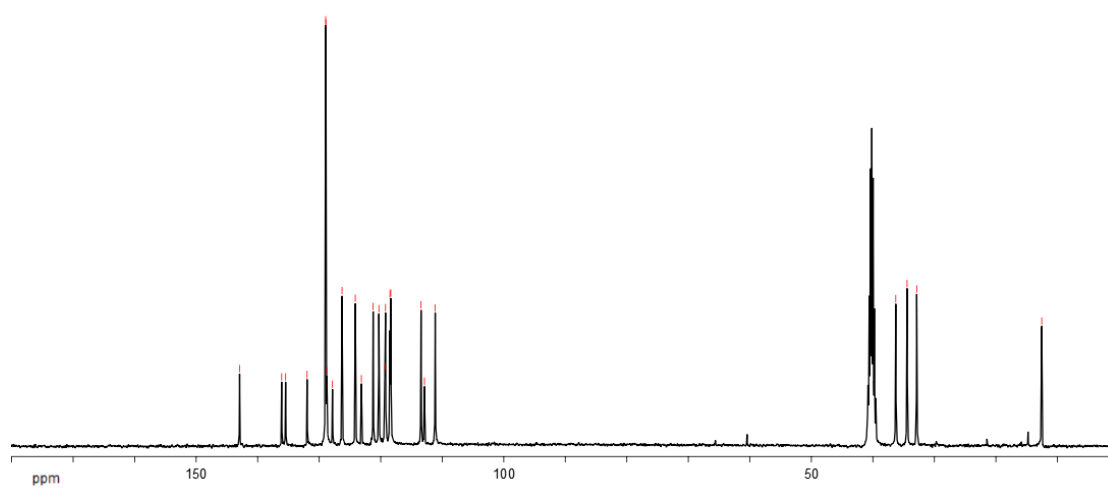


¹³C NMR Compound **138I**.

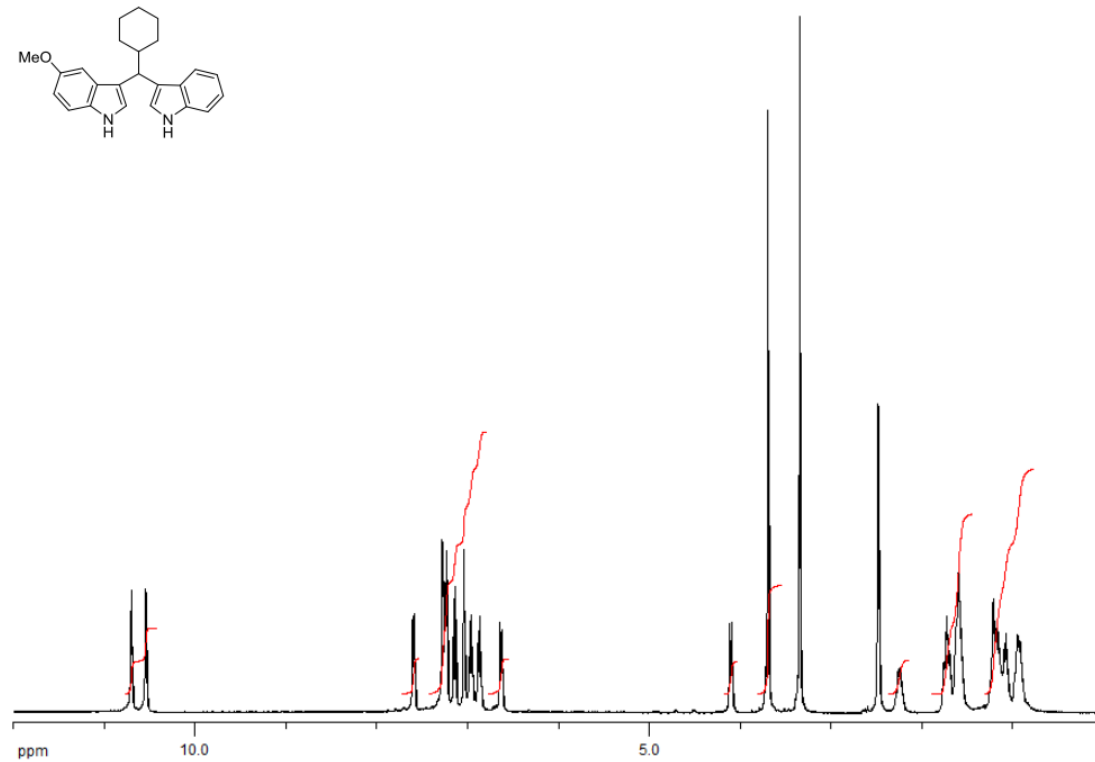
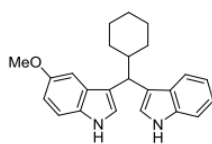
142.94
136.10
135.46
131.97
128.95
128.92
128.75
127.84
126.29
124.13
123.14
121.23
120.30
119.32
119.22
118.49
118.37
113.45
112.89
111.14

36.28
34.44
32.87

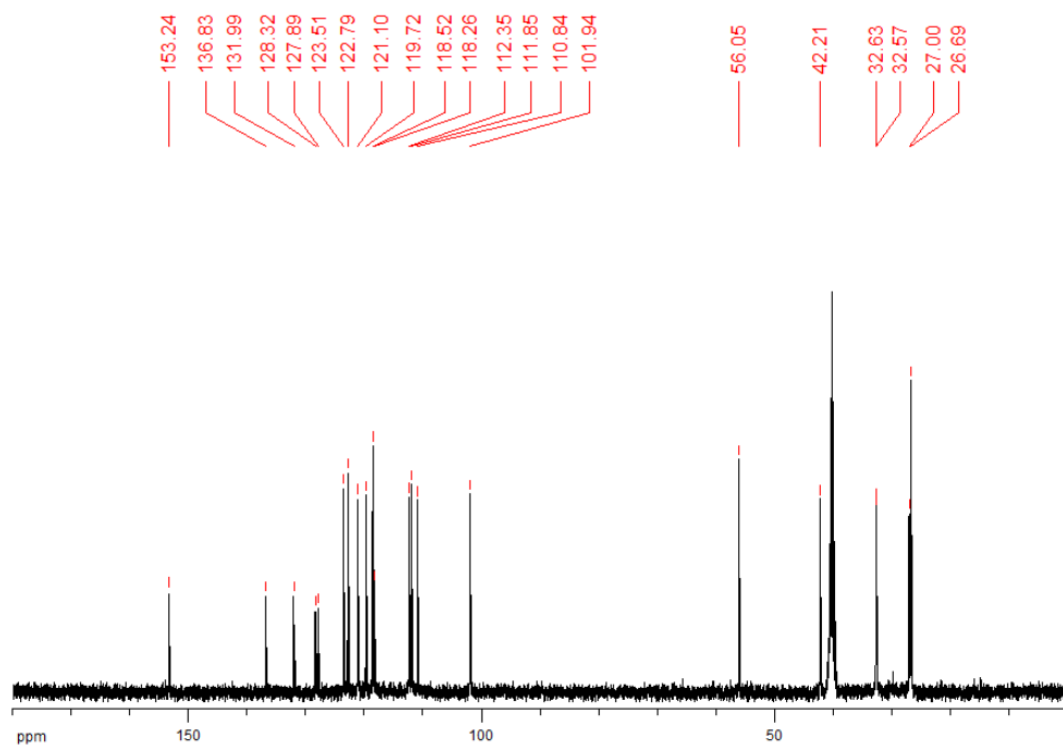
12.55



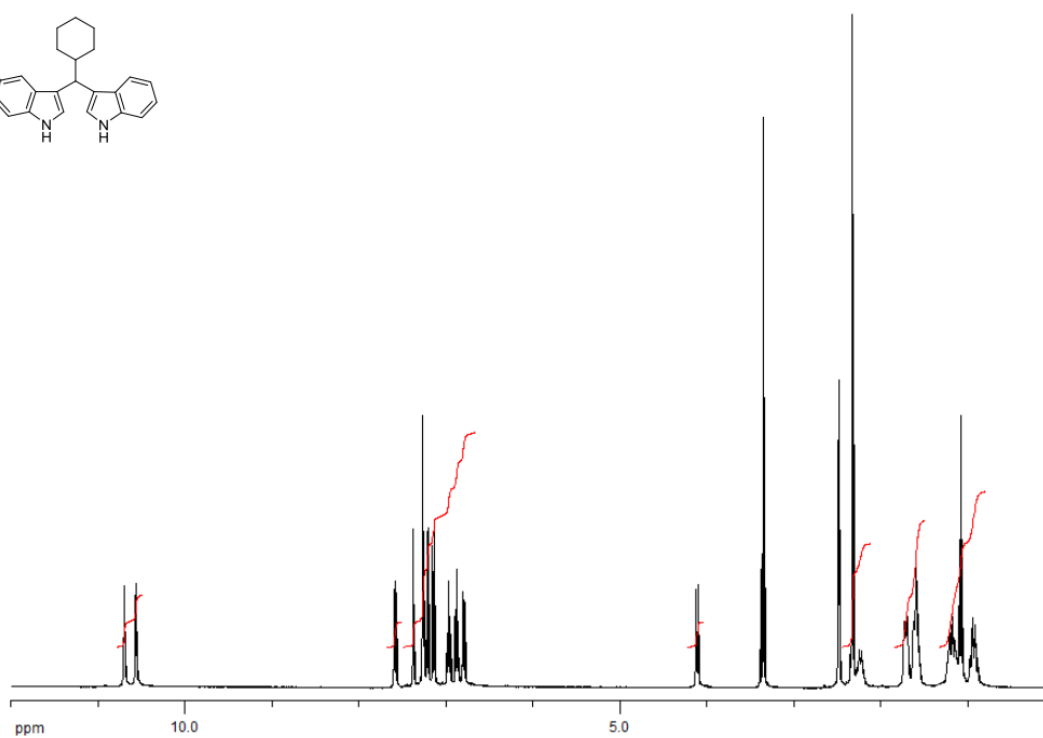
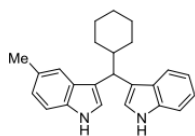
¹H NMR Compound **138m**.



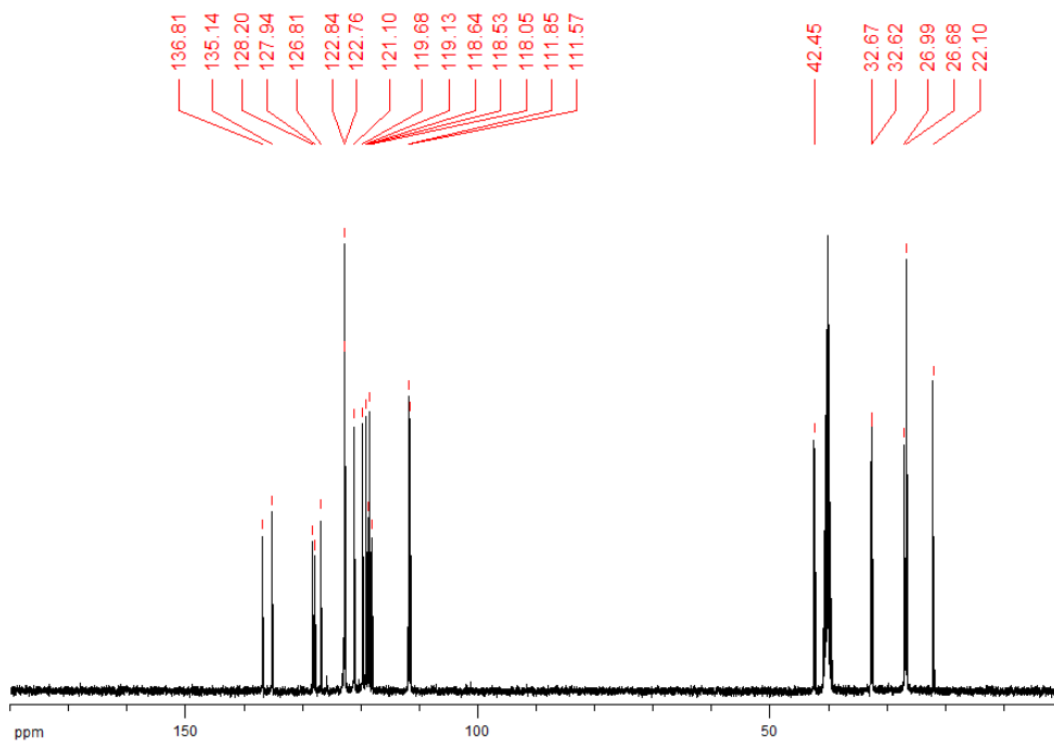
¹³C NMR Compound **138m**.



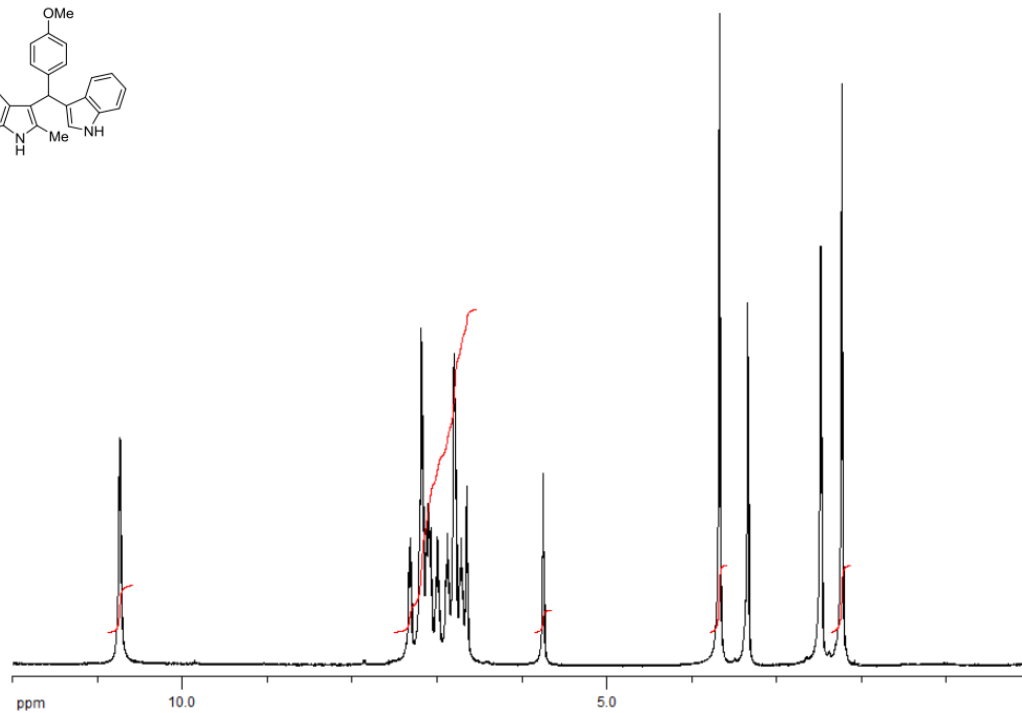
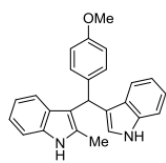
¹H NMR Compound **138n**.



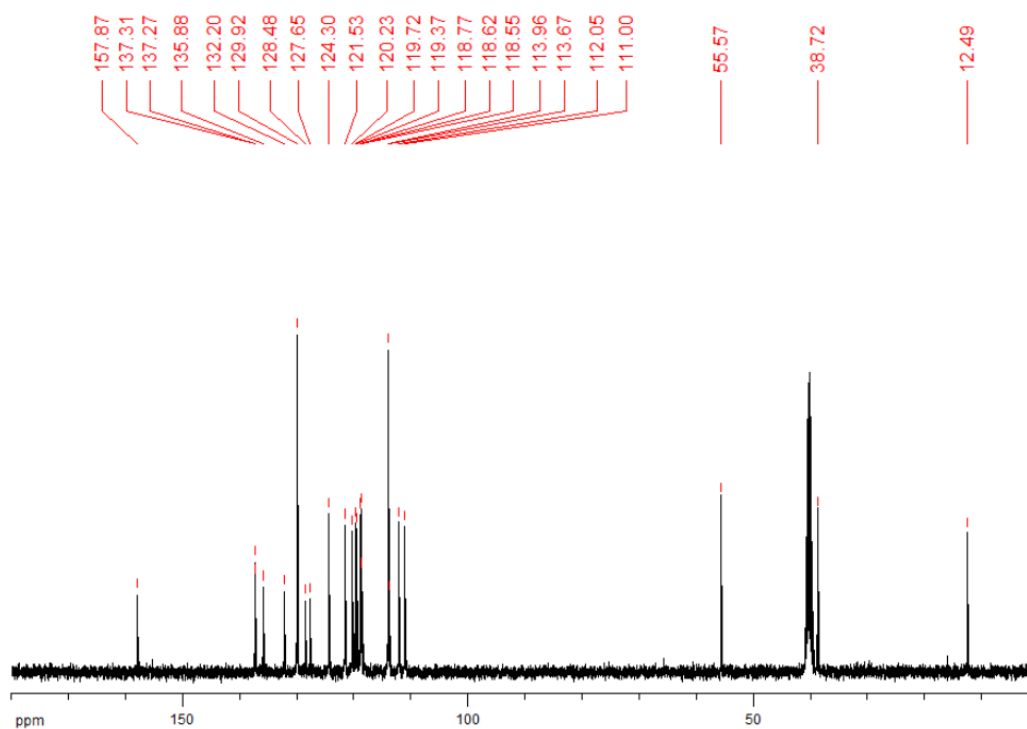
¹³C NMR Compound **138n**.



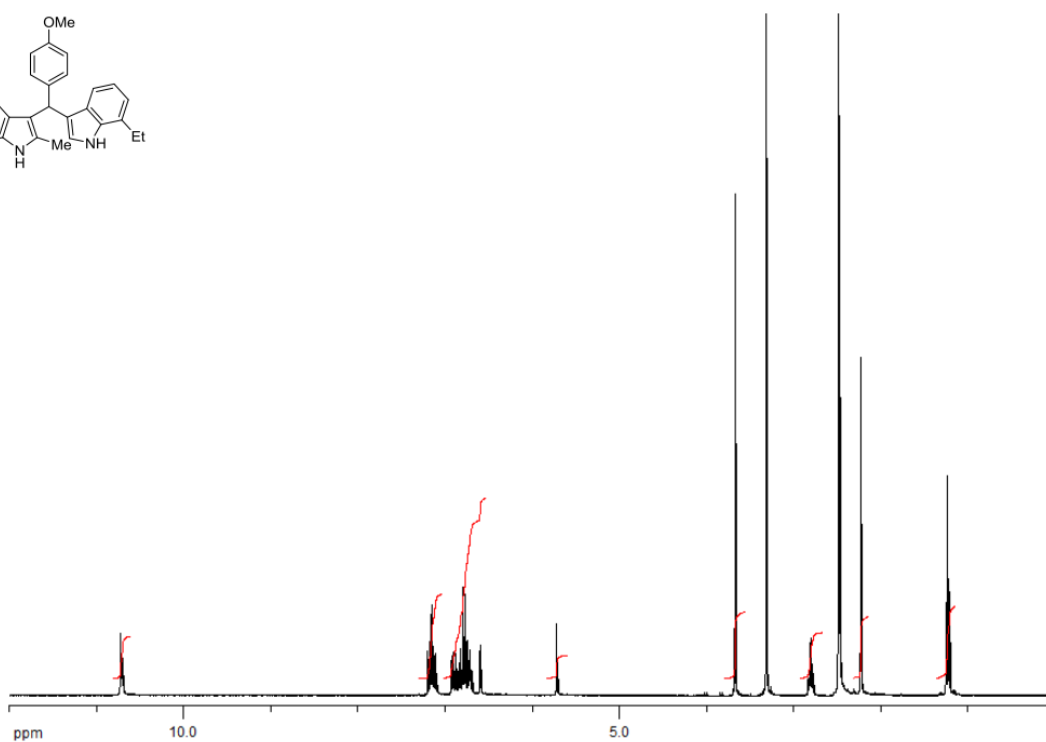
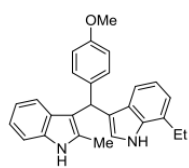
^1H NMR Compound **138o**.



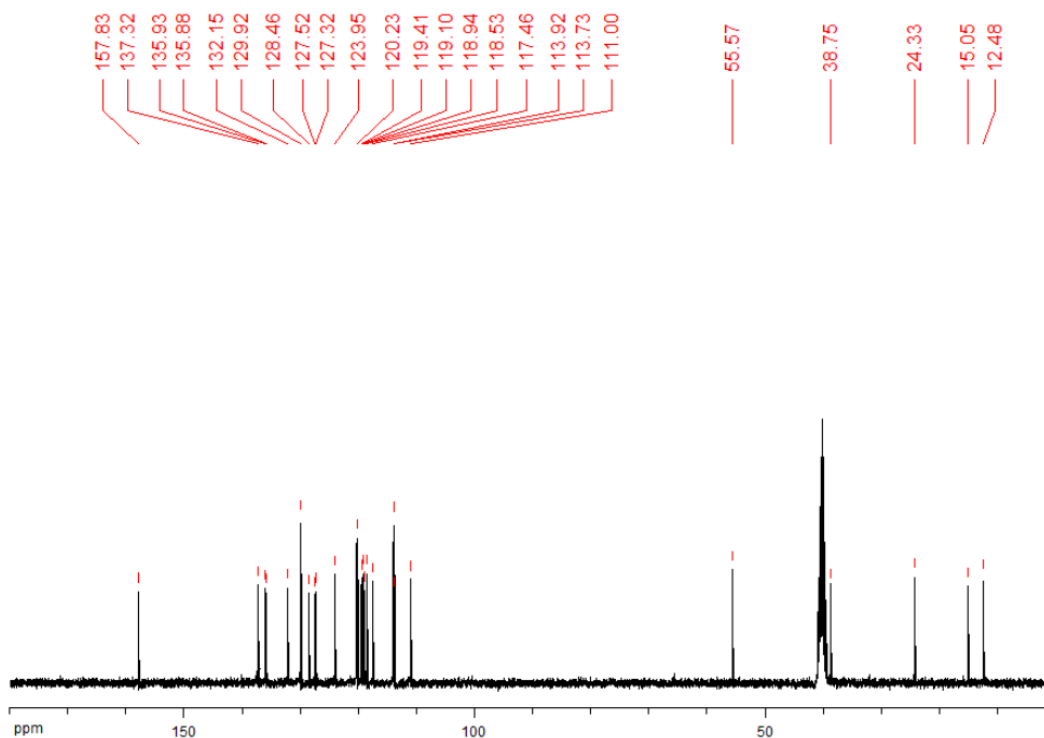
^{13}C NMR Compound **138o**.



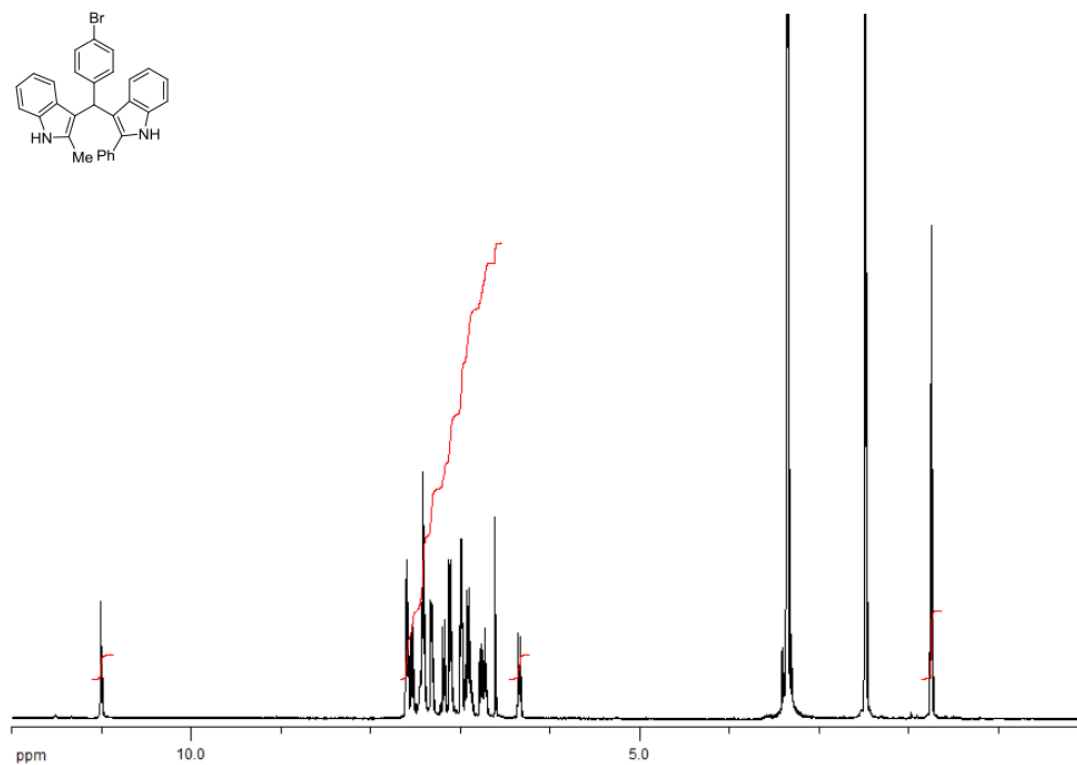
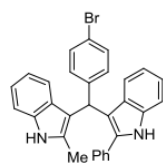
¹H NMR Compound **138p**.



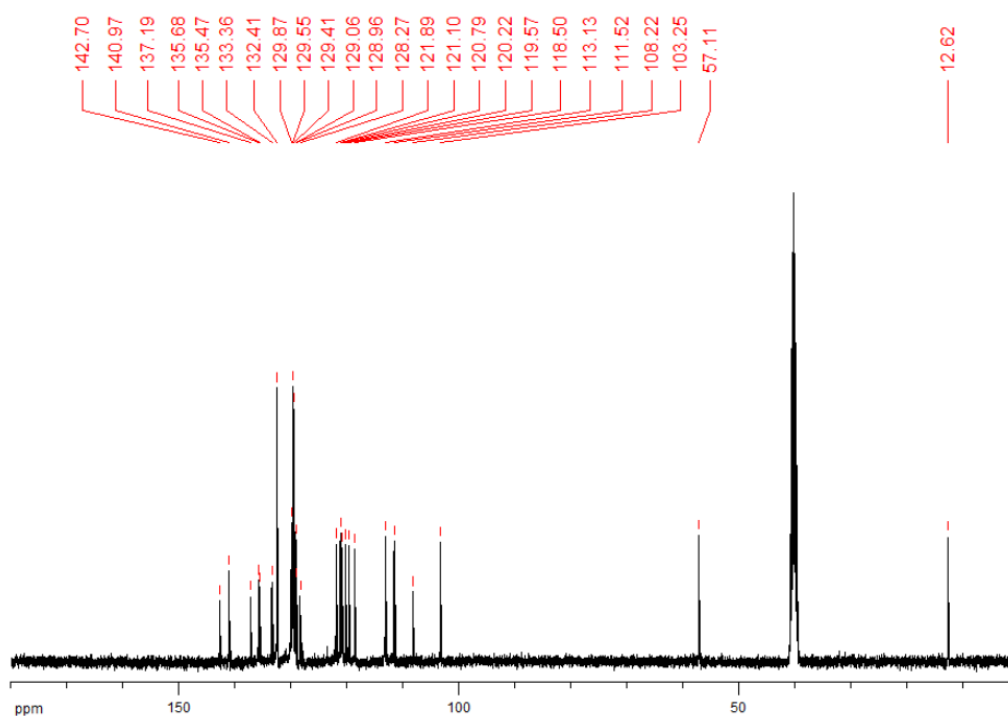
¹³C NMR Compound **138p**.



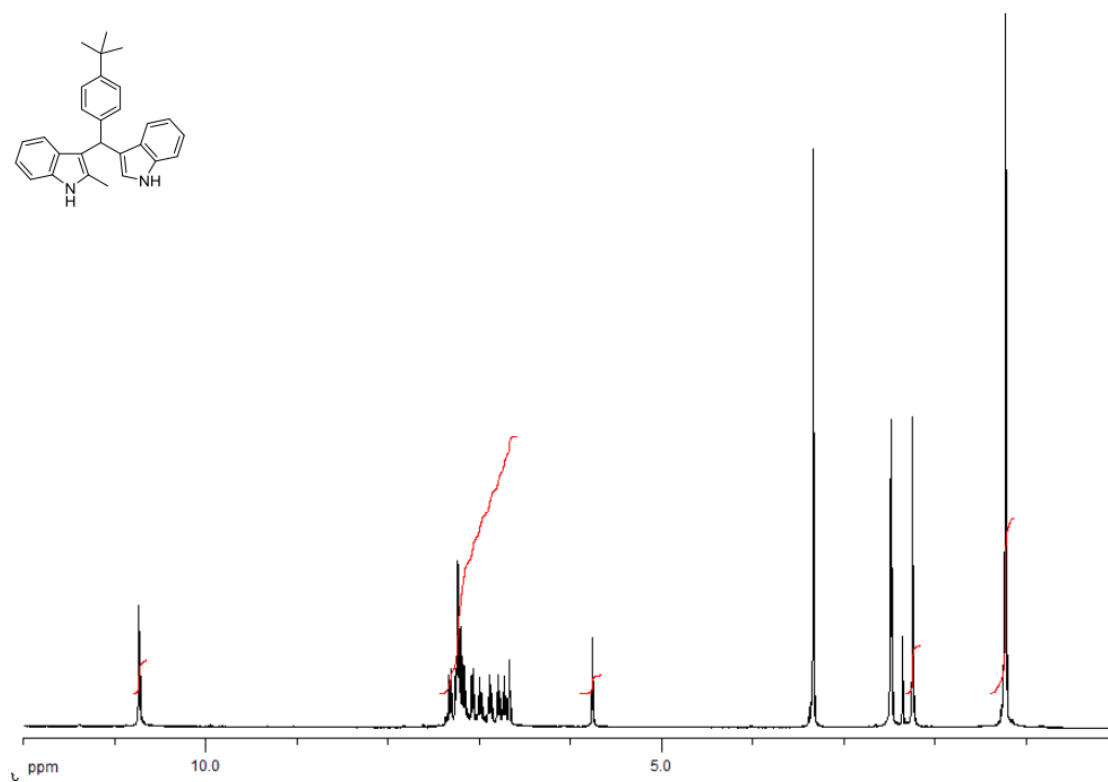
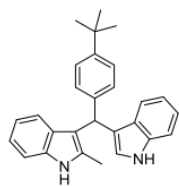
¹H NMR Compound **138q**.



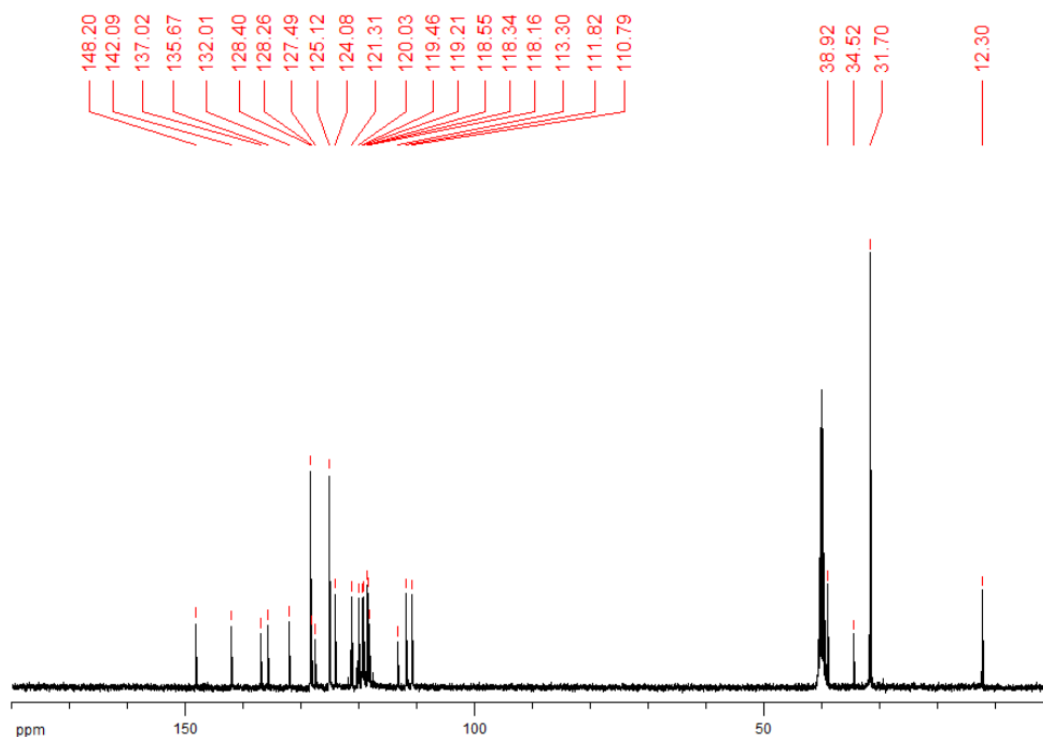
¹³C NMR Compound **138q**.



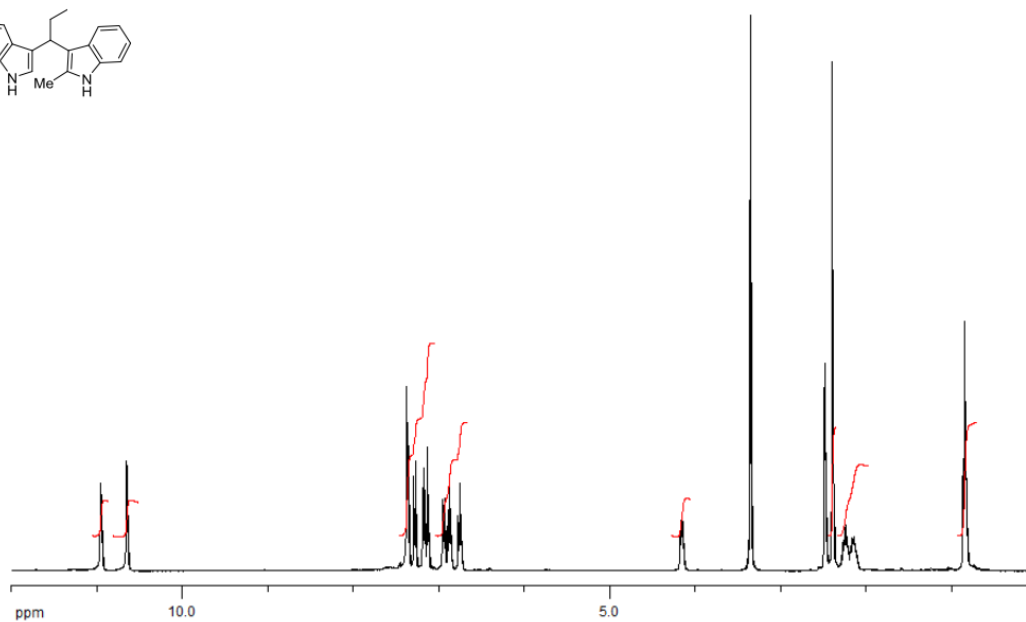
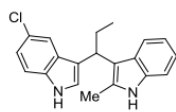
¹H NMR Compound **138r**.



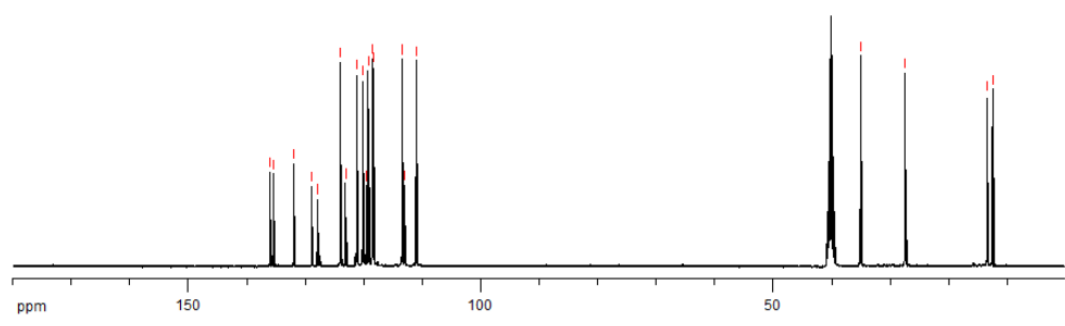
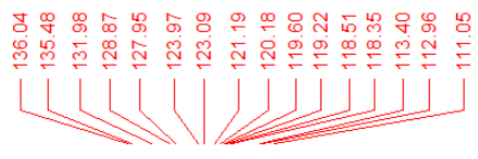
¹³C NMR Compound **138r**.



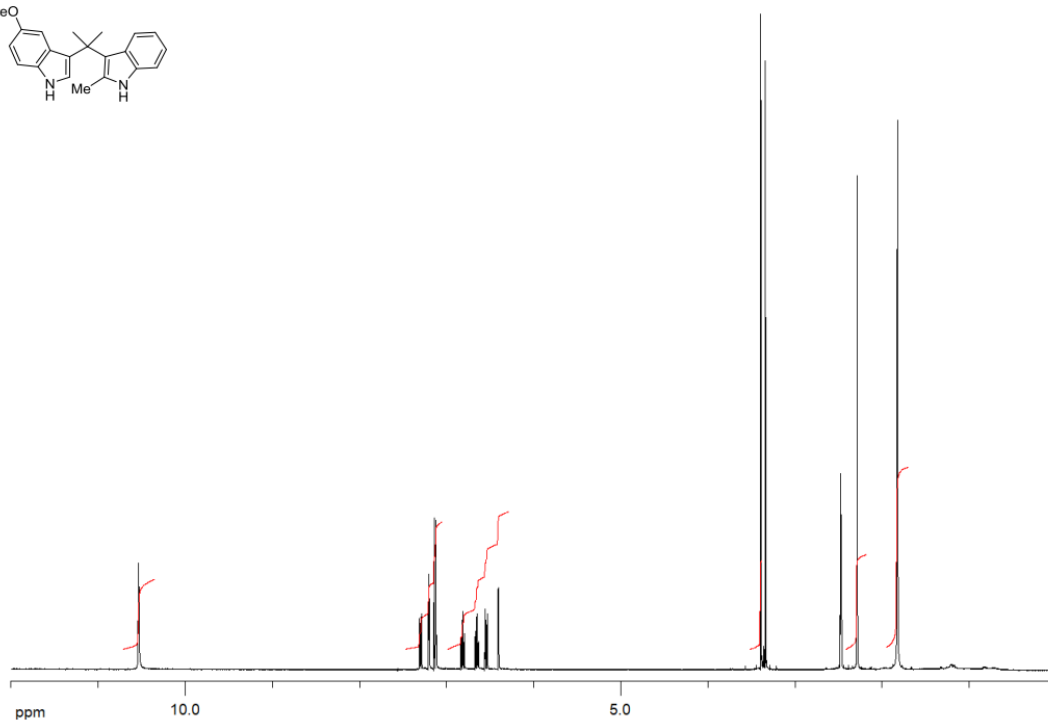
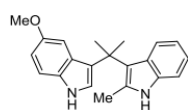
^1H NMR Compound **138s**.



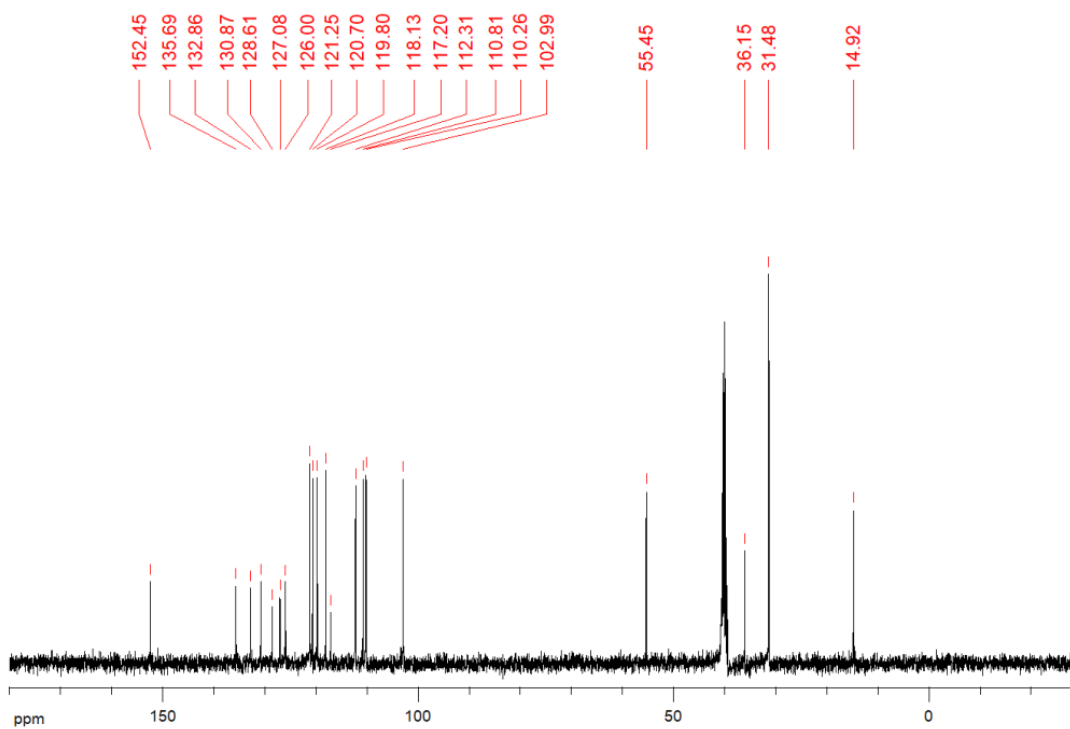
^{13}C NMR Compound **138s**.



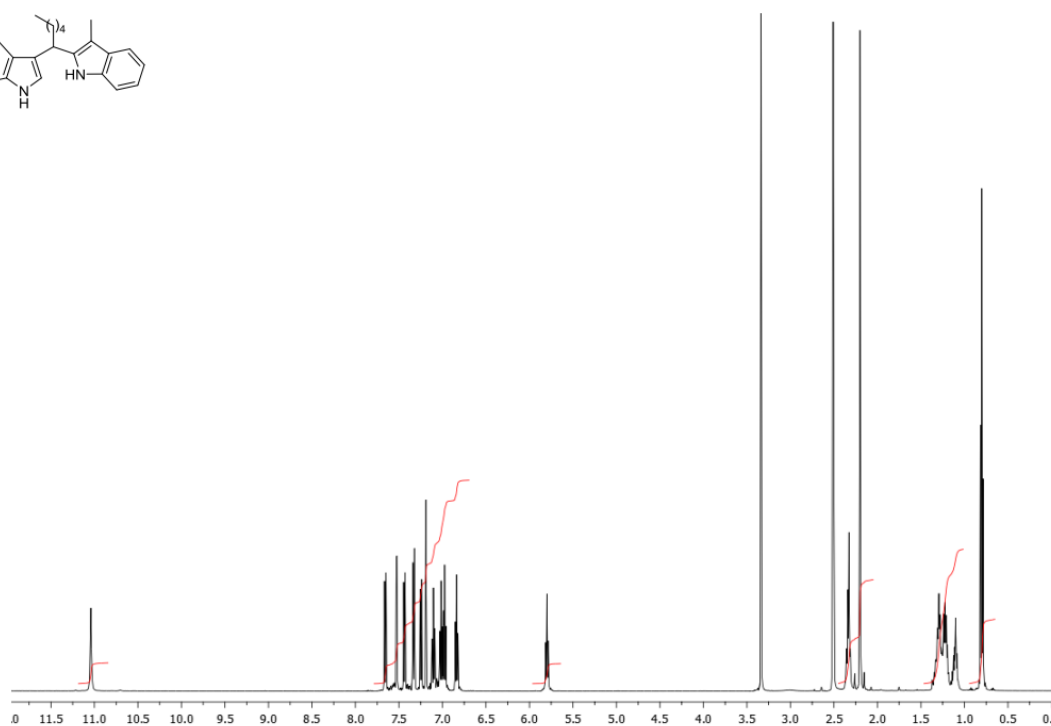
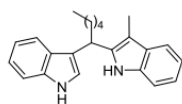
¹H NMR Compound **138t**.



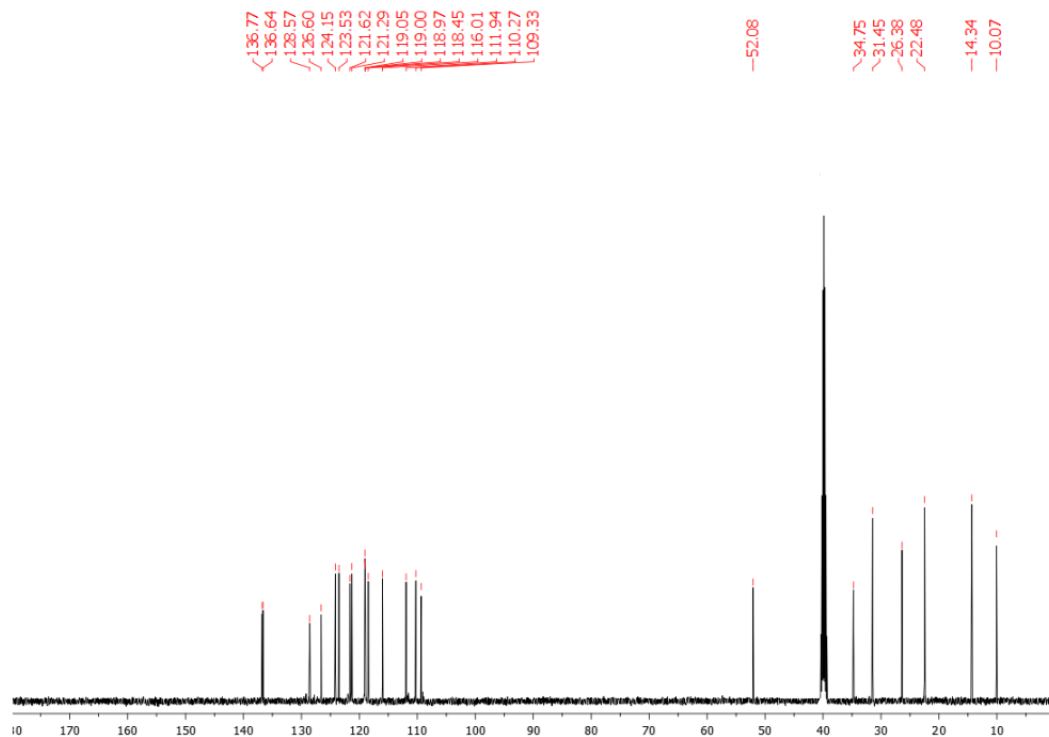
¹³C NMR Compound **138t**.



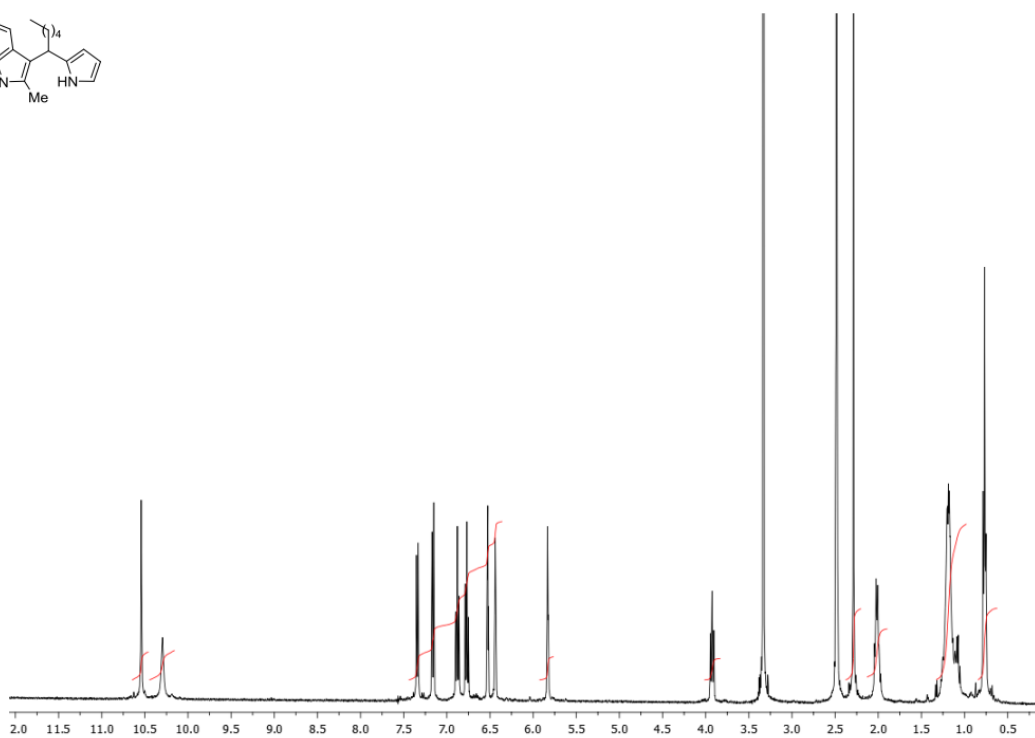
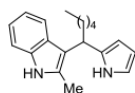
^1H NMR Compound **139**.



^{13}C NMR Compound **139**.



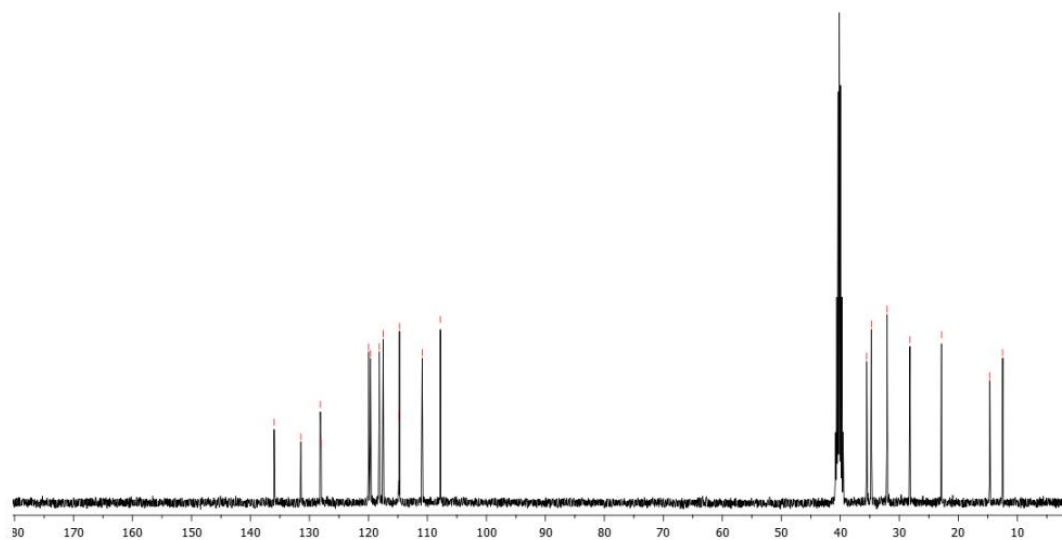
^1H NMR Compound **140a**.



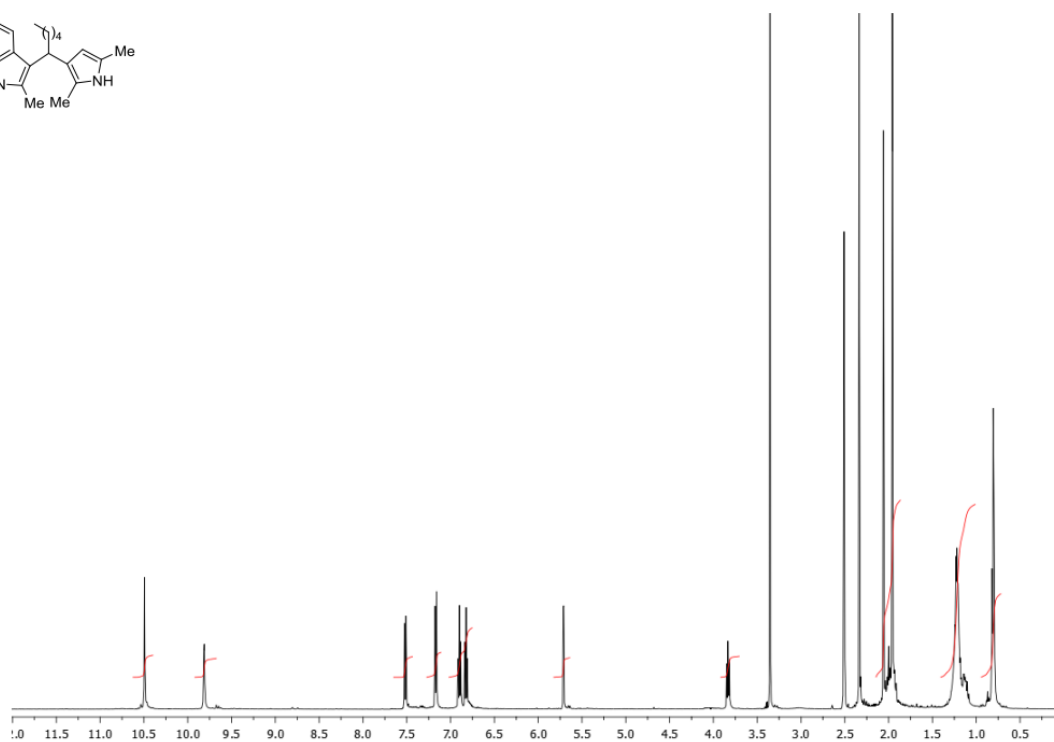
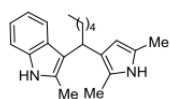
^{13}C NMR Compound **140a**.

135.97
131.45
128.15
128.02
119.97
118.16
117.51
114.85
114.74
110.89
107.80

35.53
34.75
32.08
28.20
22.85
14.67
12.47



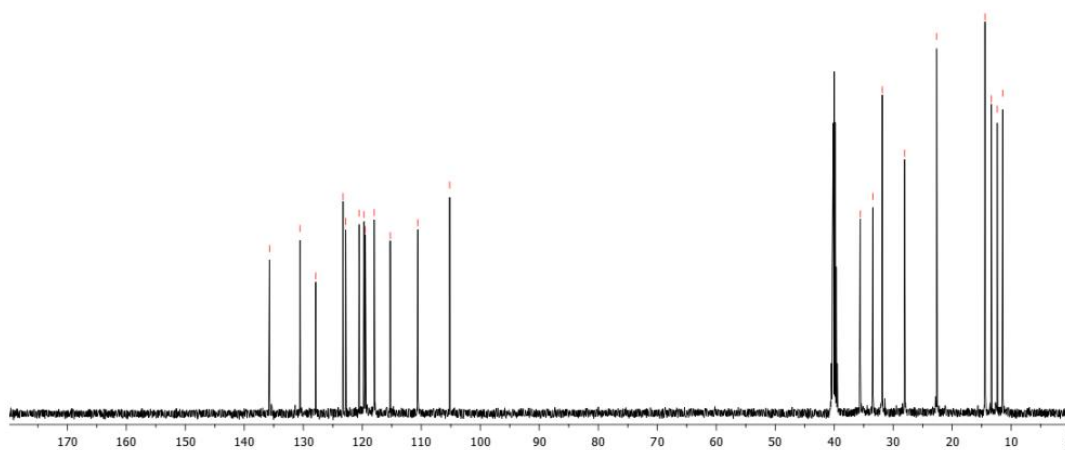
¹H NMR Compound **140b**.



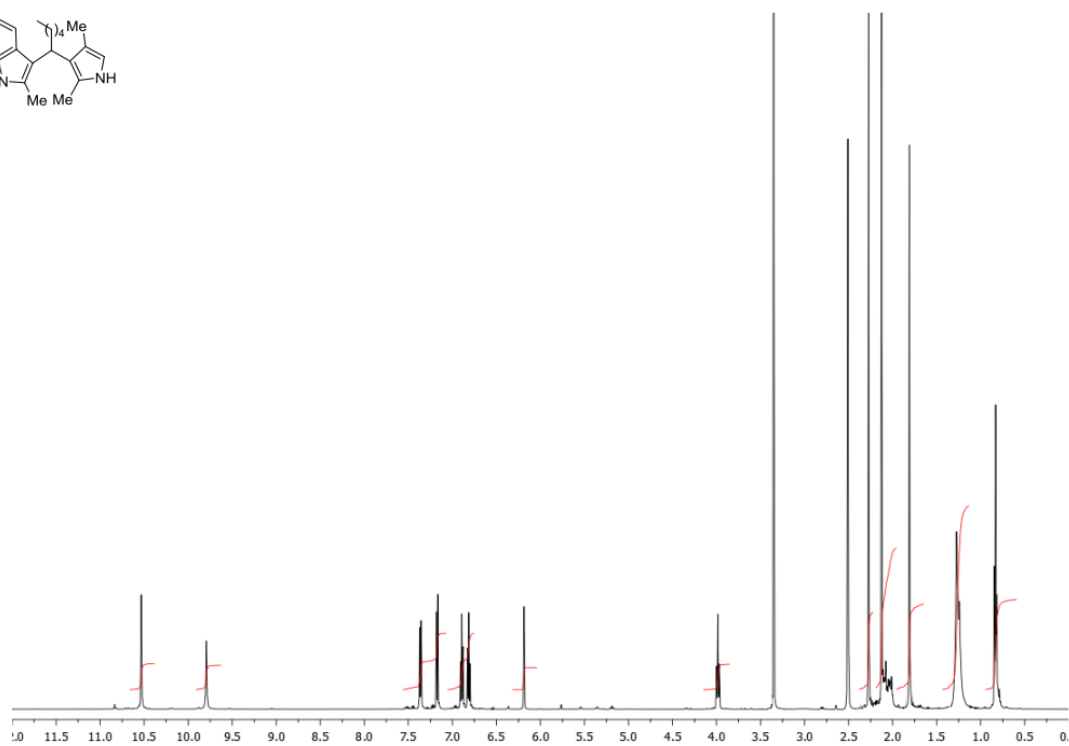
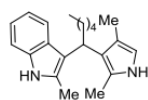
¹³C NMR Compound **140b**.

135.74
130.55
127.88
123.26
122.79
120.55
119.72
119.48
117.97
115.27
110.61
105.19

35.59
33.45
31.85
28.07
22.63
14.45
13.35
12.36
11.45



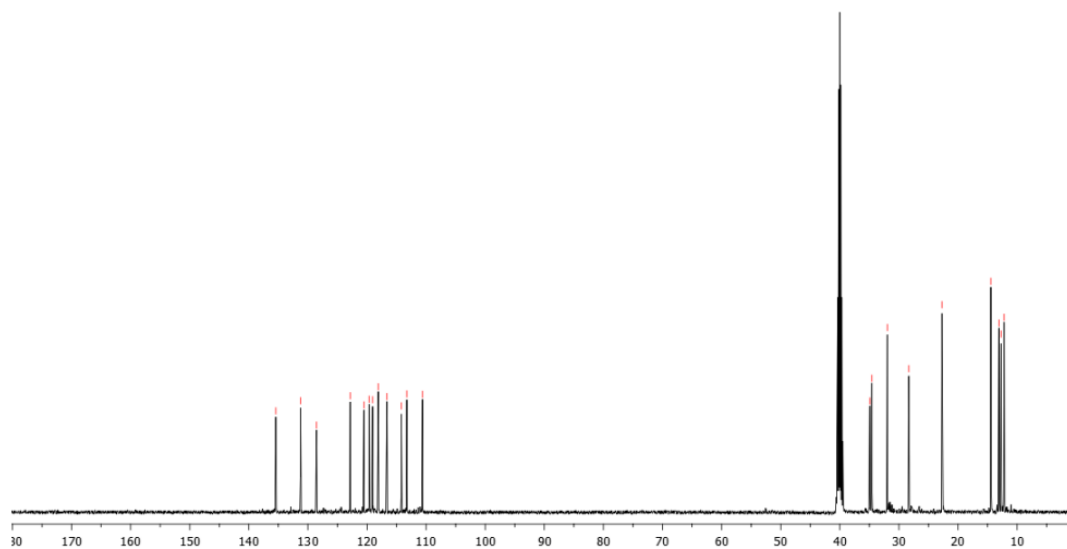
¹H NMR Compound **140c**.



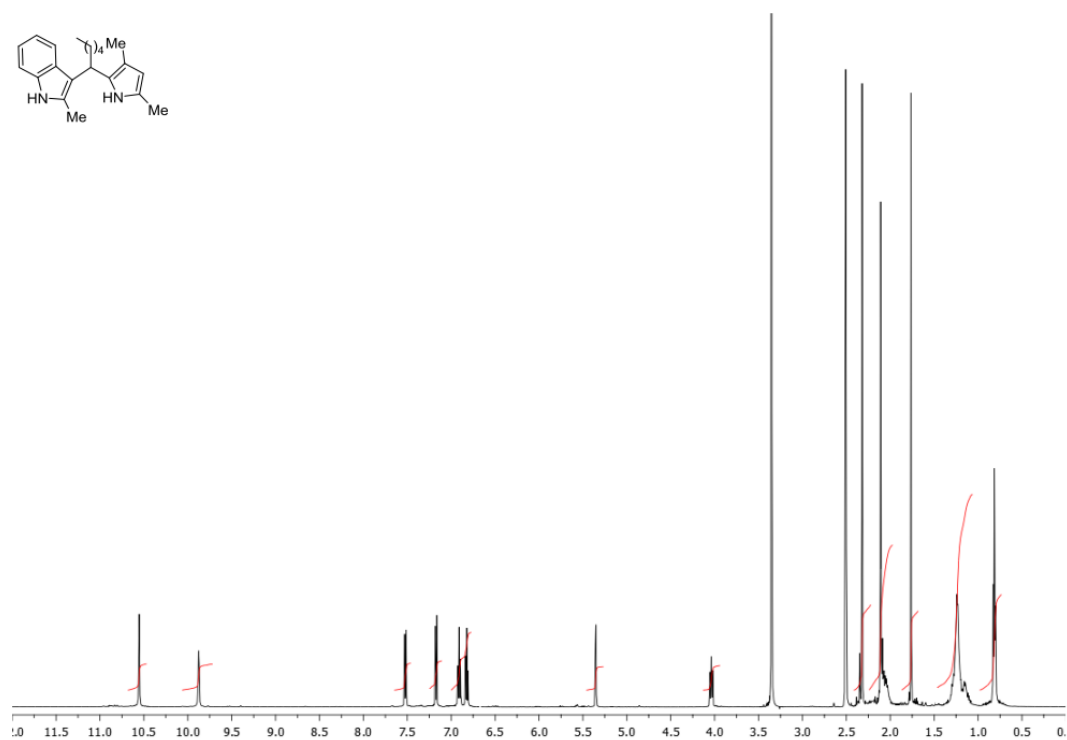
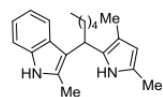
¹³C NMR Compound **140c**.

135.44
131.25
128.54
122.84
120.52
119.62
119.05
118.09
116.63
114.19
113.27
110.61

34.93
34.60
31.96
28.33
22.72
14.45
13.08
12.74
12.19



^1H NMR Compound **140d**.



^{13}C NMR Compound **140d**.

135.64
131.06
129.33
127.73
123.69
119.92
119.12
118.15
113.55
112.01
110.62

33.68
33.34
31.74
27.92
22.58
14.43
14.35
13.35
12.31
11.84

